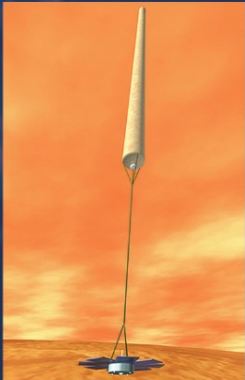


Scientific Ballooning



*Technology and Applications of
Exploration Balloons Floating in the
Stratosphere and the Atmospheres
of Other Planets*

Nobuyuki Yajima / Naoki Izutsu
Takeshi Imamura / Toyoo Abe



Springer

Scientific Ballooning

Nobuyuki Yajima • Naoki Izutsu
Takeshi Imamura • Toyoo Abe

Scientific Ballooning

Technology and Applications of Exploration
Balloons Floating in the Stratosphere
and the Atmospheres of Other Planets



Springer

Nobuyuki Yajima
Institute of Space
and Astronautical Science
1-18-42 Teraodai
Tamaku
214-0005 Japan
yajima-n@jcom.home.ne.jp

Naoki Izutsu
Institute of Space
and Astronautical Science (ISAS)
3-1-1 Yoshinodai
Sagamihara, Kanagawa
229-8510 Japan

Takeshi Imamura
Institute of Space
and Astronautical Science (ISAS)
3-1-1 Yoshinodai
Sagamihara, Kanagawa
229-8510 Japan

Toyoo Abe
Japan Meterological Agency
Aerological Observatory
1-2 Nagamine
Tsukuba, Ibaraki
305-0052 Japan

Cover photo: High-speed flight demonstration through free fall from a balloon at high altitude. This experiment was performed at ESRANGE, Kiruna, Sweden in 2003, conducted by the National Aeronautical Laboratory of Japan and the National Space Development Agency of Japan (now they are merged into Japan Aeronautical Exploration Agency). The balloon operations were carried out jointly by the CNES and the Sweden Space Cooperation (courtesy of the National Aerospace Laboratory of Japan).

ISBN: 978-0-387-09725-1 e-ISBN: 978-0-387-09727-5

DOI: 10.1007/978-0-387-09727-5

Library of Congress Control Number: 2008944012

KIKYU KOGAKU - Seisoken oyobi Wakusei Taiki ni Ukabu Kagaku Kikyu no Gijutsu by Nobuyuki Yajima, Naoki Idutsu, Tsuyoshi Imamura, and Toyoo Abe
Copyright © 2004 by Nobuyuki Yajima, Naoki Idutsu, Tsuyoshi Imamura, and Toyoo Abe
All rights reserved.
Original Japanese edition published by Corona Publishing Co., Ltd.

This English edition is published by arrangement with Corona Publishing Co., Ltd., Tokyo in care of Tuttle-Mori Agency, Inc., Tokyo

© Springer Science+Business Media, LLC 2009

All rights reserved. This work may not be translated or copied in whole or in part without the written permission of the publisher (Springer Science+Business Media, LLC, 233 Spring Street, New York, NY 10013, USA), except for brief excerpts in connection with reviews or scholarly analysis. Use in connection with any form of information storage and retrieval, electronic adaptation, computer software, or by similar or dissimilar methodology now known or hereafter developed is forbidden.
The use in this publication of trade names, trademarks, service marks, and similar terms, even if they are not identified as such, is not to be taken as an expression of opinion as to whether or not they are subject to proprietary rights.

Printed on acid-free paper

springer.com

Frontispiece



Frontispiece 1 Balloon launch at the Sanriku Balloon Center, ISAS. (At the stage when gas is being injected into the balloon. The section protected by red film laid out on the ground also belongs to the main part of the balloon)



Frontispiece 2 Balloon commencing its ascent



Frontispiece 3 Balloon launch scene. (Location: Lynn Lake, Manitoba, Canada; Launch: NASA/NSBF) (courtesy of the High Energy Accelerator Research Organization, Japan)



Frontispiece 4 Balloon launch at Showa Station in Antarctica (1998). (courtesy of the Center for Atmospheric and Oceanic Studies, Tohoku University, Japan)



Frontispiece 5 Indoor inflation test of a super-pressure balloon based on a three-dimensional gore design



(a) Sanriku Balloon Center (courtesy of the ISAS)



(b) NSBF, USA (courtesy of NASA/NSBF)



(c) Aire-sur-l'Adour base, France (courtesy of CNES)



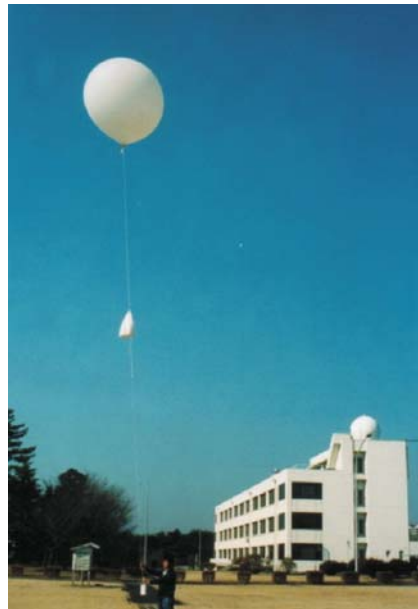
(d) Kiruna, Sweden (courtesy of Esrange, SSC)



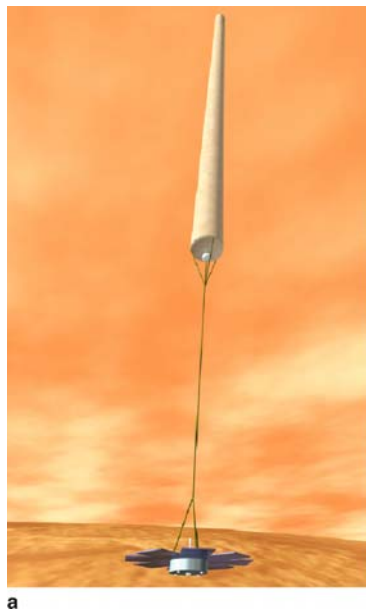
(e) Hyderabad, India (courtesy of TATA Institute of Fundamental Research)
Frontispiece 6 Launch sites of various countries



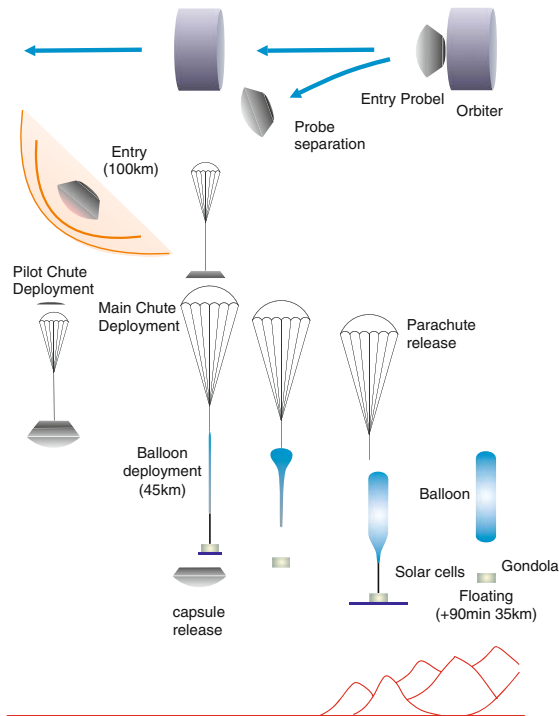
Frontispiece 7 High-speed flight demonstration through free fall from a balloon at high altitude. (courtesy of the National Aerospace Laboratory of Japan)



Frontispiece 8 Scene of the flight of a rawinsonde at the Aerological Observatory (Tsukuba, Japan). (Direction finding equipment has been installed in the dome on the roof of the government building, and this automatically tracks the rawinsonde and receives its signals)

**a**

(a) Artist's illustration

**b**(b) Entry and inflation sequence
Frontispiece 9 Low-altitude, cylindrical Venus balloon

Foreword

The balloons that are the subject of this book are balloons that transport payloads ranging from several hundred kilograms up to several tons into the earth's stratosphere. Specifically, they are stratospheric balloons that are used for scientific observations and for the development of space technology and balloons that are used for aerological observations. These balloons attain flight altitudes that are more than three times those of passenger planes. The density of the atmosphere at these altitudes is less than 1% that at the earth's surface. In addition, as part of planetary exploration, this book includes planetary balloons sent to float over other planets that have atmospheres, such as Mars and Venus. The general term used to describe these sorts of activities is *scientific ballooning*.

Although the flights of stratospheric balloons used for various scientific observations and technological experiments do not take place in the void of space, stratospheric balloons may be placed in the same fields as rockets and satellites, namely space science and technology. This, of course, goes without saying for planetary balloons that are transported into outer space on space vehicles. Organizations that conduct research and development and that launch and perform operations with this type of scientific ballooning are usually associated with each country's meteorological organizations and space research and development organizations.

Stratospheric balloons are giant pressurized membrane structures that float in the thin atmosphere of the stratosphere. Their volumes range from a few tens of thousands of cubic meters up to several hundred thousand cubic meters. Their flight characteristics are governed by complex relationships of fluid dynamics and thermodynamics. For planetary balloons, various atmospheric conditions that differ from those on the ground also come into effect. Consequently, performing systematic engineering design and analysis is a prerequisite for constructing and launching balloons. Aerological knowledge of the atmosphere is indispensable for conducting a flight. Such a foundation also ensures safety and reliability during flights. The aim of this book is to systematically describe the engineering aspects associated with scientific ballooning.

As for the structure of this book, Chap. 1 chronicles the adventure-story-like early stages of manned scientific ballooning. It also summarizes developments that

gave rise to modern scientific ballooning since the 1940s, which is a technological line of demarcation, and describes the characteristics of these developments. Chapter 2 presents the geometric design problems of balloons, ballooning methods, and flight dynamics during flight, which are the common fundamentals for stratospheric ballooning and planetary ballooning. To provide details concerning balloons that fly in the stratosphere, Chap. 3 first gives an overview of the composition and movement of the earth's atmosphere where balloons fly and then describes how balloons are launched and how their flights are controlled. In addition, the materials used for balloon membranes and their manufacturing processes are described. Chapter 4 presents the atmospheric characteristics of each planet in regard to planetary ballooning. Actual examples of balloons that have flown in Venus' atmosphere are then introduced, and the possibilities of various ballooning techniques and scientific observations are mentioned. Chapter 5 describes future aspects of scientific ballooning.

In the writing of this book, Dr. Yajima and Dr. Izutsu were responsible for the engineering aspects of stratospheric ballooning as a whole, Dr. Imamura covered the earth's atmosphere, and Mr. Abe covered aerological observations that make use of rubber balloons. In addition, Dr. Izutsu wrote about the overall engineering aspects and individual balloon technologies in regard to planetary balloons, and Dr. Imamura covered planetary atmospheres and scientific observations. Finally, Dr. Yajima handled the overall coordination.

Stratospheric ballooning in its modern-day form was active in both observation and experimentation in the infancy of space exploration. This activity continues even today, so that its current significance has in no way diminished. One example is the planetary balloon that has already floated over Venus. Nevertheless, we know of no publication that systematically describes the technology associated with scientific ballooning. The authors hope that this book will deepen interest and understanding in this field and that it will contribute even slightly to the further development of scientific ballooning.

We are deeply grateful to the editing committee for accepting this book as one of the volumes of the "Space Engineering Series" and for the helpful suggestions we received regarding its content. We thank Professor Takao Nakagawa of the Institute of Space and Astronautical Science for his valuable advice regarding the effects of the atmosphere remaining above balloons during space observations in the stratosphere. In addition, we express our heartfelt thanks to the many people who cooperated during the course of writing this book. We also thank the people at Corona Publishing for their kind assistance from the planning stage through to publication.

December 2003

The Authors

Preface to the English Edition

This book was first published in Japanese in March 2003 as one of the volumes of the “Space Engineering Series” by Corona Publishing, a publisher of science and technology books in Japan. Up to this point, there has been no book published that systematically covers the technology pertaining to scientific ballooning in the same way that this book does. Moreover, the content of the book is intended to cover scientific ballooning being carried out throughout the world, not just within Japan. As a result, many friends have recommended that we publish the book in English and broaden our target readership. Fortunately, we were able to obtain a Grant-in-Aid for Publication of Scientific Research Results from the Japan Society for the Promotion of Science (JSPS), and this has enabled the publication of this book in English to become a reality. The authors hope that this book will contribute to the future development of scientific ballooning worldwide.

We thank Forte, Inc. for its cooperation in translating this book into English. We express our gratitude to Corona Publishing for graciously agreeing to publish this book in English and accommodating our requests in various ways. We are deeply grateful to the JSPS for their support in its publication.

Nobuyuki Yajima (on behalf of all the authors)

Please note that the names of some space organizations have changed recently (see later). In this book, however, the names of organizations and facilities used are those that were correct at the time of the writing the Japanese language edition of this book.

1. In 2003, the Institute of Space and Astronautical Science (ISAS) and the National Aerospace Laboratory were integrated into the Japan Aerospace Exploration Agency (JAXA) and became the Institute of Space and Aeronautical Science (ISAS) and the Institute of Aerospace Technology (IAT) of JAXA, respectively.
2. In 2005, Sulphur Springs Balloon Plant of Raven Industries, Inc., the balloon manufacturing plant of US, changed to the Sulphur Springs Aerospace Balloon Engineering and Manufacturing Facility of Aerostar International (the parent company of Raven Industries).

3. In 2006, the National Scientific Balloon Facility (NSBF) of NASA was renamed as the Columbia Scientific Balloon Facility (CSBF) in remembrance of the Space Shuttle Columbia disaster.

Preface to Series

A long time has elapsed since the phrase “space age” was first coined. Commencing with the rockets of Tsiolkovsky and Goddard, over 40 years have passed since the launch of the first artificial satellite Sputnik. These days, approximately 100 large rockets for artificial satellites are launched a year, and 1,600 satellites orbit Earth for various missions.

Although the first practical use made of the means of transport (rockets) was space research, space industries subsequently arose, such as satellite communications and remote sensing. Initially, the situation was such that transporting even minimal equipment into space was just barely possible, but now artificial satellites are constantly increasing in size, or alternatively, smaller equipment is being launched at more frequent intervals. In addition, long-duration manned missions have become possible with the Space Shuttle and space stations. Moreover, construction of a space station founded on international cooperation continues. In addition, space tourism and the development of resources on other celestial bodies continue to be discussed as real possibilities. To make these concepts a reality, new reusable space transport vehicles will be necessary, and in addition, the laws and insurance pertaining to space will need to be improved. The realm of space-related activities has suddenly expanded. Perhaps the true space age is only just beginning.

To make such space activities possible, space systems have to be created. Space systems may be described as “systems within systems,” and high levels of complexity and optimization are rigorously pursued. In fact, systems consist of many basic technologies, and the teams that implement them are formed by bringing together graduates of aerospace engineering, electrical engineering, materials engineering, and other such fields. Particularly for mission planners and satellite designers, it is no exaggeration to say that it is essential to have insight into all of these basic technologies. Moreover, the technological fields associated with space activities may be categorized into fundamental technology areas (such as rockets, artificial satellites, space stations, and space measurement and navigation) and areas of practical application (such as satellite communications, remote sensing, and uses of zero-gravity). To make use of these space systems, a broad range of knowledge and technologies is required.

This “Space Engineering Series” consists of separate specialized volumes, and covers these broad-ranging basic technologies. Furthermore, these volumes are written by specialists who are active at the forefront of their fields. In Japan, many instruction manuals and individual books on technology have so far been written, but there has been no plan for providing an overall description of space technology

from these technological and theoretical viewpoints. For that matter, there is almost no precedent to be found anywhere in the world.

Our hope is that those who intend to construct rockets or artificial satellites and launch them into space, those who intend to use satellites for communications, remote sensing, or other applications, those who wish to study space itself, and those who desire to travel into space will consult each volume from their own viewpoint. In addition, we hope that these volumes will prove useful to specialist technologists, system designers, and students who are enthusiastic about these fields.

July 2000

*Tadashi Takano
Editing Committee Chairman*

Contents

1	Introduction	1
1.1	History of Ballooning	1
1.1.1	Advent of Balloons	1
1.1.2	First Uses for Scientific Observation	3
1.1.3	The Age of Modern Scientific Ballooning	5
1.2	Overview of Balloons	9
1.2.1	Stratospheric Balloons	9
1.2.2	Rubber Balloons	11
1.2.3	Planetary Balloons	12
1.3	Remarkable Characteristics of Scientific Ballooning	12
References		14
2	Engineering Fundamentals of Balloons	15
2.1	Buoyant Force and Attainable Altitude of Balloons	15
2.1.1	Principle of Buoyancy	15
2.1.2	Effect of Buoyancy from a Gas	16
2.1.3	Attainable Altitude	17
2.2	Balloon Configurations	19
2.2.1	Historical Background and Overview of Problems	19
2.2.2	Natural-Shape Balloon Concept	24
2.2.3	Expansion of Design Concepts for Balloons with Load Tape	34
2.3	Balloon Systems	44
2.3.1	Zero-Pressure Balloons	45
2.3.2	Super-Pressure Balloons	48
2.3.3	Special-Purpose Balloons	51
2.4	Motion of Balloons	53
2.4.1	Balloon Flight Model	55
2.4.2	Vertical Motion of Balloons	58
2.4.3	Horizontal Motion of Balloons	65
2.4.4	Balloon Heat Balance	66
References		74

3 Stratospheric Balloons	77
3.1 The Earth's Atmosphere	77
3.1.1 The Composition of the Atmosphere	77
3.1.2 Vertical Structure	78
3.1.3 Hydrostatic Equilibrium	79
3.1.4 Meridional Distribution of Temperature	82
3.1.5 Meridional Distribution of Zonal Winds	83
3.1.6 Waves in the Atmosphere	86
3.2 Balloon System Configurations	90
3.2.1 Balloon Configurations	90
3.2.2 Suspension System	93
3.2.3 Basic On-Board Equipments	98
3.2.4 Optional Equipments	101
3.3 Ground Facilities	104
3.3.1 Launch Site	104
3.3.2 Communication Facilities	105
3.3.3 Other Facilities and Equipments	109
3.4 Launch and Flight	110
3.4.1 Acquisition and Use of Meteorological Data	110
3.4.2 Injection of Lifting Gas and Balloon Launch	115
3.4.3 Flight Control	122
3.4.4 Flight Control Apparatus	125
3.4.5 Flight Termination and Payload Recovery	130
3.4.6 Long-Duration Flight Technology	131
3.4.7 Flight Safety and Security	135
3.5 The Manufacture of Balloons	137
3.5.1 Film Materials	137
3.5.2 Design	141
3.5.3 Manufacturing Process	142
3.5.4 Structural Strength	146
3.5.5 Quality Control	149
3.6 Rubber Balloons Used for Meteorological Observations	151
3.6.1 Outline of Meteorological Rubber Balloons	151
3.6.2 Ascent Speed of Rubber Balloons	154
3.6.3 Achievable Altitudes of Rubber Balloons	155
3.7 Utilization of Balloons	156
3.7.1 Scientific Observations	156
3.7.2 Engineering Experiments	161
3.7.3 Routine Meteorological Observations	163
References	171
4 Planetary Ballooning	173
4.1 Atmospheres of Planets	173
4.1.1 Atmospheres of Terrestrial Planets	173
4.1.2 Atmospheres of Jovian Planets	176

4.2	Background of Planetary Ballooning	177
4.2.1	Characteristics of Planetary Balloons	177
4.2.2	History of Planetary Ballooning	178
4.2.3	Peculiarities of Planetary Balloons	178
4.3	Examples of Planetary Balloons	179
4.3.1	Venus Balloons	179
4.3.2	Mars Balloons	188
4.3.3	Other Balloons	190
4.4	Scientific Observations Through Planetary Ballooning	190
4.4.1	Photographic and Spectroscopic Observation of Planetary Surfaces	191
4.4.2	Meteorological Observation	191
4.4.3	Measurement of Atmospheric Components	191
4.4.4	Measurement of Remnant Magnetism	192
4.4.5	Observation of Lightning and Radar Exploration	192
	References	192
5	The Future of Scientific Ballooning	195
5.1	Future Trends in Balloon Technology	195
5.1.1	Payload Weight, Flight Duration, and Flight Altitude	195
5.1.2	Long-Duration Balloon Flight Technology	196
5.1.3	Control of Flight Path	196
5.1.4	Applications to Information Networks	196
5.1.5	Planetary Balloons	197
5.2	Future Trends in Balloon Applications	198
5.2.1	Increasing the Scale of Experimental and Observation Systems	198
5.2.2	The New Role of Balloons in the Satellite Era	198
5.3	Effects of Balloon Technology on Other Fields	200
5.3.1	Linkage with Airship Technology	200
5.3.2	Applications to Space Structures	200
5.3.3	Applications to Ground Structures	201
	References	202
	Table Talk 1: How Archimedes Demonstrated the Existence of Buoyant Force	18
	Table Talk 2: Another Natural-Shape Balloon Formulation	43
	Table Talk 3: Balloon Recovery in Japan is Hard Work	136
	Table Talk 4: Leave it up to the Wind when Flying, Leave it up to the Feet when Manufacturing	150
	Table Talk 5 Tateno Aerological Observatory: Making a Mark on History	170
	Table Talk 6: Where Research is Presented	201
	Appendices	205
	Abbreviations	209
	Index	211

Chapter 1

Introduction

Abstract This chapter begins by chronicling the adventure-story-like early stages of manned scientific ballooning. It then summarizes the developments that led to the rise of modern scientific ballooning since the 1940s, which represents a technological demarcation line. This chapter also introduces the various worldwide organizations that conduct scientific ballooning in their respective countries. A brief summary of scientific ballooning is then given through introductory descriptions of the following chapters.

1.1 History of Ballooning

Humankind first escaped from the ground and became able to fly freely to high altitudes in the atmosphere by using balloons. In the following pages, we will summarize the history of ballooning from its advent to its current status, focusing on the use of balloons for scientific applications. For the overall history of balloons, we refer the reader to the literature [1–3], although some references are a bit dated.

1.1.1 Advent of Balloons

The large, unmanned, hot-air balloon that the Montgolfier brothers (J. M. and J. E. Montgolfier) successfully tested in public in Annonay in the south of France on 5 June 1783 is regarded as humankind's first balloon. From the facts that its volume was 700 m^3 and that it attained an altitude of approximately 2,000 m, we can gauge that it was a large-scale balloon (Fig. 1.1) [4].

The brothers were born into a household of paper wholesalers, and it is reported that they were highly interested in science and read many science-related books. Because they had this foundation, after conceiving of the hot-air balloon,

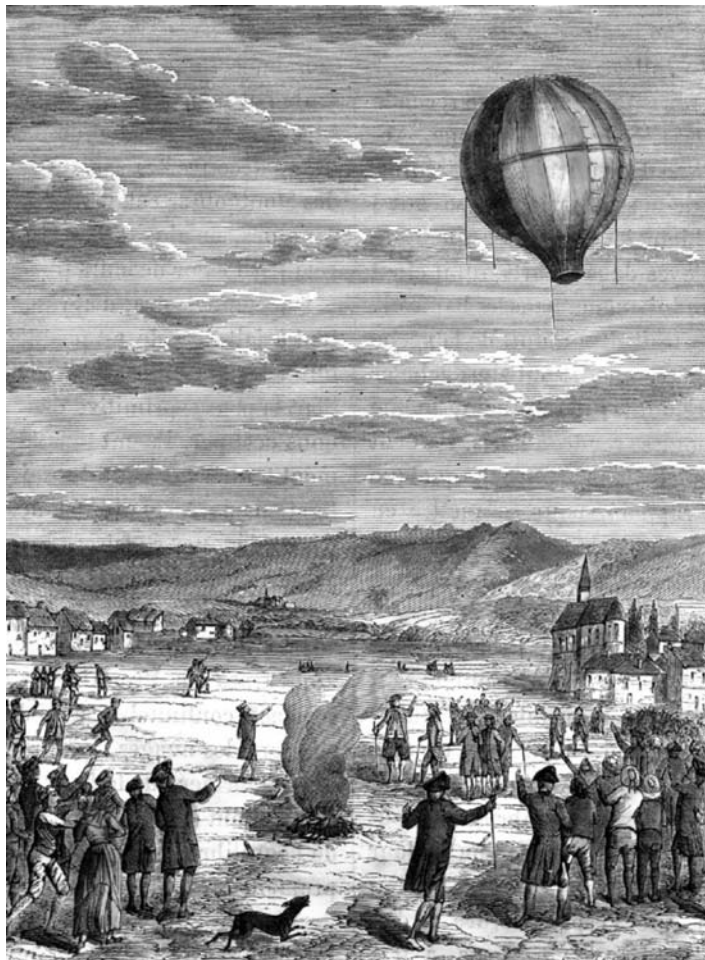


Fig. 1.1 Public experimental flight of the world's first full-scale hot-air balloon by the Montgolfier brothers (5 June 1783) (courtesy of Saburo Ichiyoshi)

they systematically pursued their research and, commencing with small-scale models, they conducted trials involving successively larger balloons. It is interesting that this approach is consistent with that adopted by the Wright brothers, who 120 years later made the first successful airplane flight, and who conducted their work based on a scientific process; for example, they designed the wings by using wind-tunnel testing.

Following the success at Annonay, the Montgolfier brothers succeeded in front of a large number of spectators, which included Louis XVI, in Paris on September 19, and on November 21. In the first flight, small animals were placed on board, and they then accomplished a manned flight with two human passengers on board.

during the second flight. These steps closely resembled the process of development in preparing to send men into space 170 years later, when flights were first conducted with monkeys and dogs on board.

The principle of buoyancy itself was already understood in the pre-Christian era, and the phenomenon of the ascension of air heated by a fire has been observed constantly in everyday life ever since humankind first used fire in primitive times. From this commonplace phenomenon, however, it seems that the impressive advancement of European society at the time of the Industrial Revolution was required for people to conceive of a balloon that a human could ride and then to actually build and fly.

A gas balloon that employed hydrogen as the buoyancy medium was first flown successfully in Paris on 27 August 1783, by J. A. César Charles, a scientist at the French Academy of Sciences. This was a little less than three months after the Montgolfier brothers. A successful manned flight, similar to that of the hot-air balloon, was subsequently conducted on December 1 of that same year. (Fig. 1.2).

Hydrogen had previously been discovered in 1766 by H. Cavendish of Britain, and it was already known to be lighter than air. The Montgolfier brothers also considered using hydrogen gas in their balloons, but they abandoned this approach since manufacturing a balloon membrane to seal in the hydrogen was more difficult than manufacturing one for a hot-air balloon. Charles solved this problem by making the balloon fabric from silk and paper and then coating it with rubber.

In contrast to the Montgolfier balloon, the bottom of which was open, the balloon tested by Charles was a closed, sealed-gas balloon. Therefore, as the balloon gained altitude, the pressure across the membrane increased, so that eventually the balloon would burst. Hence, the first flight finished in a shorter time than anticipated. Consequently, an exhaust valve was installed for the manned flight to circumvent this rise in pressure. Charles's gas balloon included technology that has been passed down even to the balloons of today; specifically, it incorporated detailed measures for ensuring the air tightness of the membrane, guaranteeing its strength and controlling its pressure.

1.1.2 First Uses for Scientific Observation

Once the feasibility of flying balloons had been demonstrated, the activity quickly captured the public's imagination. Attention focused on amusements and adventures with manned balloons at exhibitions, and in addition, a great deal of interest and effort was devoted to long-distance flights, such as over transoceanic distances. Even in Japan, in 1890, a British aviator performed demonstrations on a large scale by parachuting from a balloon.

But then, there were some people who looked askance at these trends and thought that balloons could be used more effectively for scientific observation. First, they tried to discover how the atmosphere changes with altitude by flying as high as possible. On 24 August 1804, a mere 21 years after the first balloon flight, the French

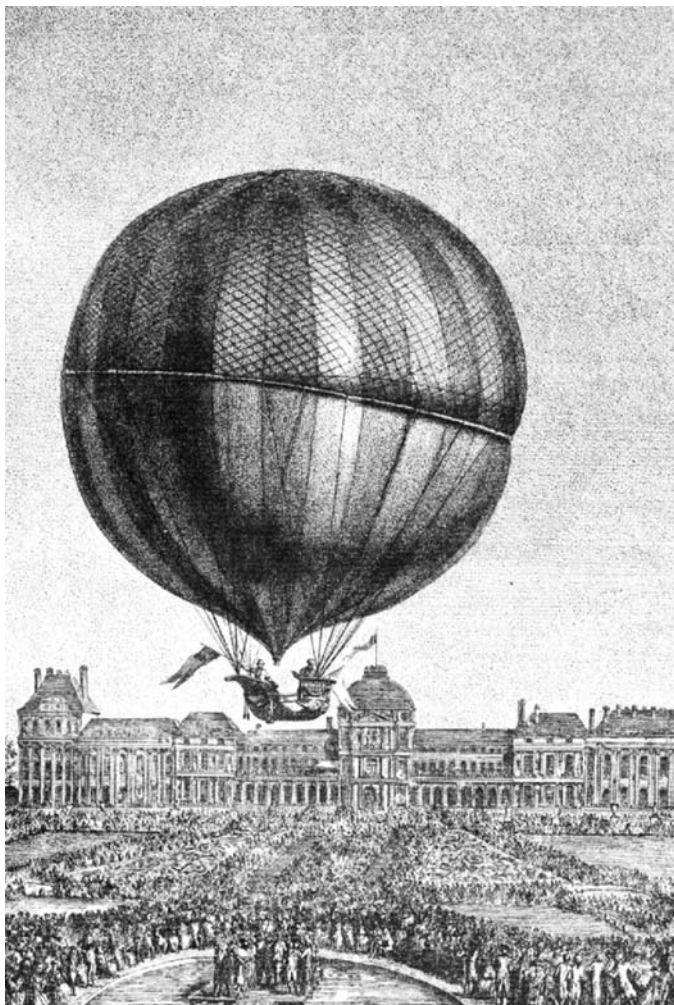


Fig. 1.2 First manned flight of Charles' hydrogen gas balloon (1 December 1783) (courtesy of Saburo Ichiyoshi)

scientist J. L. Gay-Lussac ascended to a height of nearly 8,000 m, with a barometer, a thermometer, and a hygrometer on board. In 1862, the British scientist J. Glaisher attained an altitude of 10 km.

These manned flights were done without any protection against the thin atmosphere at high altitudes. Since the balloons ascended higher than Mt. Everest in less than an hour, this was enough to cause loss of life, making these tests only a step away from being reckless adventures. These exploits also revealed the intensity of the desire that the people of that era had to explore the unknown. On the basis of these pioneering works, at the end of the nineteenth century, the usefulness

of ballooning for scientific observation was accepted by academic institutions, for example, by the Society of Arts in the Royal Academy [5].

The experiment that is regarded as the first step toward full-fledged use of balloons in astrophysics is the observation of cosmic rays carried out by V. F. Hess of Austria in 1912. Hess ascended to 5,000 m, carrying a simple ion chamber, and measured how the number of cosmic rays varied with altitude. On the basis of these observations, the term *cosmic rays* was coined, testifying to the fact that these rays came from space. Hess was awarded the Nobel Prize in 1936 for this achievement. This test was also significant as it demonstrated that true space could be observed unimpeded by the atmosphere by ascending to high altitudes.

Reaching the stratosphere, which represented a milestone in scientific ballooning, was achieved in a flight by A. Piccard of Switzerland in 1931, in which he attained an altitude of 15.8 km. This manned flight was not as reckless as those of the pioneering days, since he employed a small spherical airtight cabin made of aluminum [6].

Another noteworthy development occurred in 1938, when R. H. Upson of the United States suggested a new balloon shape design that later came to be termed the *natural-shape balloon*. It was clear that by this stage, ballooning had already attained the status of modern scientific ballooning, which is described in the next section.

1.1.3 The Age of Modern Scientific Ballooning

The scientific ballooning of today is founded on new technologies, such as shape design concepts, configuration, balloon membrane materials and their adhesives, and the introduction of reinforcing methods that use high strength fibers. Balloons based on these new technologies are classified as modern scientific balloons.

The most significant technological advancement was the development of low-density polyethylene film in the early 1930s by the British chemical company, Imperial Chemical Industries (ICI). By using this film (which is thin, lightweight, tough, and has good elongation characteristics), substantial reductions in the balloon's own weight were achieved, and it became easy to reach altitudes of 30 km or higher. However, the temperature of the atmosphere when passing through the tropopause near an altitude of 12 km is -70°C . The development of a film that did not lose its flexibility even at such a low temperature was an important, early challenge [7].

In the 1940s, systematic research was conducted under the auspices of the U.S. Navy, the University of Minnesota, and other universities, and balloons were put to practical uses, such that they could almost be considered the prototypes of modern balloons. Not only were balloon films developed during this period, but also were the principal technologies of zero-pressure balloon systems that are equipped with a venting duct to prevent a pressure increase on the film and fiber reinforcement methods that use load tape. Progress in electronics, which was advancing concurrently, enabled the realization of wireless communications devices that could be mounted

on a balloon. These devices were lightweight, compact, and highly reliable, and they were able to communicate over long distances. As a result, it became possible to conduct unmanned, long-duration flights of large balloons.

Some of the most enthusiastic proponents of the practical applications of these new balloons for scientific observations were astrophysicists, especially researchers measuring cosmic rays. As mentioned previously, in the early days, Hess, Piccard, and others started making measurements on manned flights of particle rays coming from space. Since it was known that the atmosphere attenuated cosmic rays, it was desirable to perform these measurements at as high an altitude as possible.

A device called an emulsion chamber was conceived in the early 1950s as a way to perform such measurements. In this device, a large-format, dry photographic plate with a sensitive compound coated on its surface is attached to a metal plate; when it is developed after exposure, the traces left by cosmic rays become visible. By investigating these traces collected on the film, a great deal of information can be obtained, including the type and energy of the cosmic rays. If this means could be used, a large amount of measurement data could be collected without being restricted by the limited data transmission capability of the telemetry technology of the time. The longer the flight duration is, the more information is recorded by the film. Because these measurements could be made using unmanned balloons, the demand to develop large, lightweight balloons suddenly increased. In the early stages, the researchers who measured cosmic rays developed balloons themselves. However, due to the above-mentioned synergistic effects of the systematic technology development effort by the United States and other countries and the demands on the observers, in 1960, a 1.8-ton payload was mounted on a balloon having a volumetric capacity of $300,000 \text{ m}^3$, and it reached an altitude of 30 km.

The development of electronic technology made it possible to introduce not only communications technology but also control technology, and even in fields requiring a high degree of measurement technology, applications for large balloons moved into top gear. For example, in the field of astronomical observation, in the latter half of the 1950s, with the Smithsonian Observatory and other institutions playing a central role, a 30-cm-diameter solar telescope, Stratoscope I, was launched with the aim of precisely imaging solar activity, and it succeeded in obtaining detailed close-up images of the surface structure unimpeded by atmospheric turbulence. Johns Hopkins University also launched a similar measuring instrument. On the basis of these successes, development started on a large astronomical telescope, Stratoscope II, which had a 0.9-m-diameter aperture and a gross weight of 3.6 tons, and which incorporated precision tracking control, in the early 1960s [8] (see Fig. 1.3). Its concept and telescope design are reminiscent of a prototype of the large general-purpose telescope satellite, the Hubble Space Telescope, which is in orbit today.

In addition, balloons have been put to use in “rockoon” experiments in which small rockets have been suspended from balloons to supplement the flight capabilities of sounding rockets and in experiments where a pilot wearing a space suit ascended to the stratosphere as preparatory experiments for manned space flights [9].

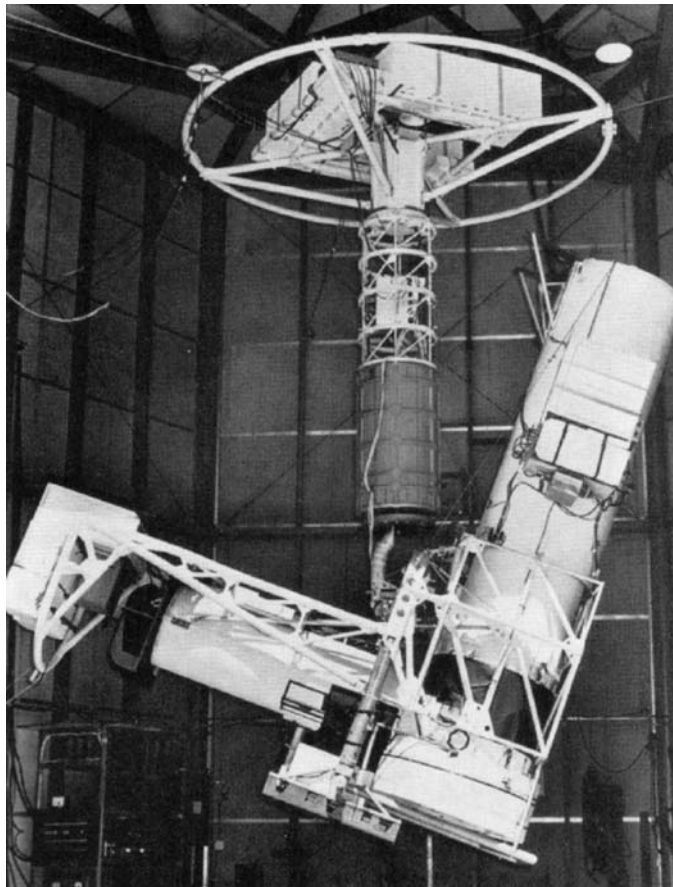


Fig. 1.3 The Stratoscope II balloon-borne large astronomical telescope (courtesy of the Harvard Smithsonian Center for Astrophysics)

1.1.3.1 Establishment of Organized Promotional Systems

In response to the impressive developments in scientific observation and engineering experiments that have employed balloons as mentioned earlier, organizational preparations have advanced in parallel for the systematic carrying out of research, development, and flight operation of scientific balloons [10].

In US, the National Scientific Balloon Facility (NSBF) was established by the National Science Foundation (NSF) in Boulder, Colorado, as a base for large balloons in 1962, and the National Center for Atmospheric Research (NCAR) was charged with managing it. Within the NCAR, one department was established to develop balloon technology. This department inherited the results of research done since the 1940s and commenced a program of systematic research and development.

In 1963, the launch base was relocated to the Palestine, Texas, in the expansive ranching area in middle of the state, which was well suited for balloon flights, and a large permanent launch site was completed in 1973 (see Frontispiece 6(b)). In 1982, its administration was transferred to the National Aeronautics and Space Administration (NASA), and management of facilities was changed to New Mexico State University, where it continues to this day. A balloon research department was established within NASA at the Wallops Flight Facility (WFF) of the Goddard Space Center, and in addition to pursuing research, it is charged with the management of sponsored research at universities, research institutes, and the like.

Over roughly the same period, France has also been establishing a framework for serious scientific balloon experimentation. In 1963, a full-fledged balloon base was constructed at Aire-sur-l'Adour in the south of France as a facility under the control of France's Centre National d'Etudes Spatiales (CNES) (see Frontispiece 6(c)). At the same time, a balloon department was established within the CNES research laboratories in Toulouse. In 1966, the Gap-Tallard balloon base was opened at the base of the Alps. Subsequent French scientific ballooning has assumed the mantle of European scientific ballooning, and alongside US, it continues to make active efforts.

In Japan, observation of cosmic rays using polyethylene balloons commenced in the mid-1950s led by cosmic-ray researchers from Kobe University, Rikkyo University, Osaka City University, and elsewhere. The first flight was carried out in 1954 using a balloon developed by researchers at Kobe University. Subsequently, systematic research and launch testing of balloons was pursued from 1956 under the auspices of the Institute for Nuclear Study, University of Tokyo [11]. In addition, from 1956 to 1961, rockoon testing was performed, in which rockets were launched from balloons under the leadership of the Institute of Industrial Science (IIS), University of Tokyo (See Sect. 3.7.2.3).

In 1964, on the basis of the advanced scientific sounding rocket and satellite research carried out at the IIS, the Institute of Space and Astronautical Science (ISAS) was established as a research institute affiliated with the University of Tokyo. Two years later, a balloon-engineering department was established to perform scientific ballooning at this institute. Subsequently, after temporary experimental sites at Taiyoumura, Ibaraki Prefecture, and Haranomachi, Fukushima Prefecture, a permanent balloon base, Sanriku Balloon Center (SBC) was opened in 1971 at Sanriku-cho, Iwate Prefecture, which continues to this day [12] (see Frontispieces 1 and 6(a)). In addition, in cooperation with the National Institute of Polar Research (NIPR), scientific balloon launches are also performed at the Showa Base as part of Antarctic observation operations (see Frontispiece 4).

In India as well, there was the first successful launch of a polyethylene balloon in 1959 by Osmania University, which is in the city of Hyderabad in the southern part of the Deccan Plateau. In 1969, a permanent balloon base was opened on the outskirts of this city under the TATA Institute of Fundamental Research (TIFR) (see Frontispiece 6(e)). Subsequently, because of its proximity to the Equator, this base has been used not only for research in India, but also by researchers from around the world for measurements that require such a geographical location.

The southern hemisphere is also useful for balloon experiments because of its geographical conditions. For example, the observable regions of space differ from those of the northern hemisphere; in particular, it is possible to observe the center of the galaxy. In Brazil, balloon observations have been attempted since the 1960s, and full-fledged scientific ballooning has been pursued since the end of the 1980s under the auspices of Brazil's space research institute, the Instituto Nacional de Pesquisas Espaciais (INPE). In Australia, there is a facility for launching large balloons near the airport located on the outskirts of the city of Alice Springs, which is near the center of the continent. It has been under the control of the University of New South Wales since 1980 and has been used not only by Australia, but internationally.

In China, a balloon department was created in 1979 within the Cosmic Ray Department of the Institute of High Energy Physics belonging to the Chinese Academy of Sciences, and it is pursuing scientific ballooning in cooperation with the Institute for Atmospheric Science.

1.1.3.2 Research Activities on Planetary Ballooning

The first research paper proposing planetary balloons (i.e., balloons that float over other planets that have atmospheres) was presented at a balloon-related scientific conference in the early stages of space development. It was given just after the launch of the world's first artificial satellite in 1957.

In 1963, a detailed review of balloons to Mars and Venus was published in a technical report by Raven Co., a balloon manufacturing company. Three papers were subsequently presented on Mars balloons at a scientific balloon symposium held in US in 1964 [13–15]. In addition, in 1967, NASA prepared a detailed research report discussing the possibility of a Venus balloon [16].

However, the actual realization of such balloons was delayed for a long time. In 1985, there was a joint project for Vegas 1 and 2 between the former Soviet Union and France. Since then, no other planetary balloon projects have been approved, but a large amount of research has been performed and many proposals have been advanced.

At the ISAS, expandable Venus balloons that use membranes [17] thin metal sphere Venus balloons [18], and the like have been proposed since the latter half of the 1980s, and fundamental research is continuing.

1.2 Overview of Balloons

1.2.1 *Stratospheric Balloons*

Balloons used for scientific observation and technological experimentation that rise to the stratosphere are referred to as stratospheric balloons, scientific balloons, or large balloons. They are classified as unmanned free balloons under civil aviation regulations.

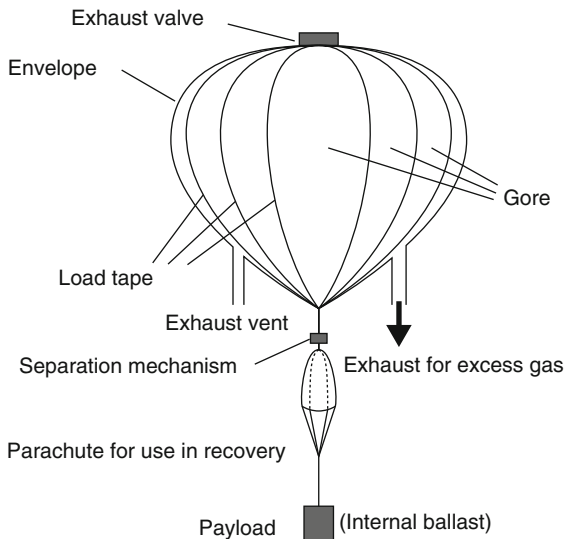


Fig. 1.4 Balloon in flight

A schematic diagram of a scientific balloon system during flight is depicted in Fig. 1.4. The main section, which is made out of a thin polyethylene film, is a sack (referred to as an envelope). This envelope is constructed by vertically connecting the spindle-shaped constituent units, which are cut from a long roll of film; these constituent units are called gores. High-tensile-strength fibers, which are referred to as load tapes, are used for reinforcement. They are inserted at periodic intervals along the join lines of the gores and extend from the bottom to the top of the balloon.

The envelope is filled with hydrogen or helium gas, which is lighter than air; this gas is referred to as the buoyant gas or the lifting gas. On the ground, it has a buoyant force of approximately 12 N/m^3 . The photograph in Frontispiece 1 shows the stage when gas is injected into the balloon. On the ground, the gas enters only the top portion of the envelope, and the remainder of the envelope is uninflated. Frontispiece 2 shows the appearance of a balloon commencing its ascent when only the top portion has been filled with gas. The orange and white spotted pattern at the midpoint is the parachute, and the main part of the balloon continues directly above this.

The buoyant force imparted for ascent is called the free lift. Since atmospheric pressure decreases as the balloon ascends, the gas within the envelope expands. Because it is assumed that the balloon will not expand by stretching, the balloon reaches its ceiling altitude by expanding to its previously manufactured maximum volume.

A balloon equipped with a venting duct at its bottom is called a zero-pressure balloon. After the balloon has expanded to its maximum volume, the lifting gas that generates the free lift overflows from the venting duct, so that the balloon subsequently remains at a constant altitude. Balloons that do not have the venting duct and

whose lifting forces are constrained by an increase in the pressure differential with the outside air are called super-pressure balloons. Scientific balloons commonly attain altitudes of 30 km or higher in the stratosphere, where the atmospheric density is 1/100 or lower than that at the earth's surface.

An exhaust valve is placed at the top of the balloon to control the exhaust of the lifting gas in the envelope. A recovery parachute and payload are suspended from the bottom of the balloon. The weight of large payloads may exceed 1 ton. In addition to the instrumentation required for scientific experiments, common equipment is carried on board payloads such as telecommunications equipment (e.g., telemeters and command units), flight control equipment, ballast for controlling the balance with buoyant forces, and batteries for the power source, etc. Data output from the on-board equipment is transmitted to the ground base by a telemeter during the flight. Also, a receiver in the payload receives operation command signals from the ground base.

The payload is equipped with an external thermal protection cover and a landing shock absorber and is suspended from the balloon. This flight-ready payload is also referred to as a gondola, which is a traditional term used in ballooning.

Essentially, balloons are at one with air currents; that is, balloons are blown by the wind and float passively. Because of this, it is essential to have a detailed knowledge of the weather conditions prior to launch. When a flight is terminated, a separation mechanism is actuated, and the payload descends to the ground (or sea) by parachute, where it is recovered.

1.2.2 Rubber Balloons

The raw material for meteorological rubber balloons is natural rubber latex. It exhibits superior elongation characteristics to those of any chemically synthesized material, and it can stretch more than 500% in one direction. These characteristics derive from the fact that rubber is a polymer in which the isoprene molecules are aligned lengthwise in a chain-like structure, and the molecules have a long chain structure with a countless number of bends when no external force is applied; they are in a condition like a loose fuzzball that is not rigidly clumped together. When an external force is applied to the rubber, the fuzzball is stretched, and it turns into a state where it is completely stretched lengthwise in a chain. When the external force is released, the rubber reverts to its original state. This behavior is very different from that of metals, which expand and contract due to deformation of their crystal structure.

When sulfur is added to rubber (a process referred to as vulcanization), the sulfur forms crosslinks between adjacent long chains, and this enhances the elastic deformation properties of the rubber. In particular, uniform biaxial elongation properties are produced. Rubber balloons exploit these properties of rubber.

A rubber balloon is injected with gas when it is on the ground until it is partially inflated, and it then starts to ascend being nearly spherical in shape. The expansion

of the rubber membrane depends on the $-2/3$ power of the pressure; thus, when the balloon reaches an altitude of about 30 km in the stratosphere, the surface area of the rubber membrane increases by a factor of 22 since the atmospheric pressure at this altitude is about 1/100 that on the ground. The balloon bursts at its expansion limit, thus terminating the flight. As described in detail in Sect. 3.6, the size of rubber balloons is limited by the manufacturing method, so that payloads of no greater than about 10 kg can be suspended from these balloons.

Rubber meteorological balloons were already in practical use in the 1920s, and they have been used up to the present without any fundamental modifications. They are inexpensive and easy to handle when launched. Rubber balloons are indispensable for worldwide stationary meteorological observations performed simultaneously at multiple points throughout the world.

1.2.3 Planetary Balloons

Differing from balloons used on earth, a planetary balloon is transported to the target by a space craft. Lifting gas injection and floatation are both entirely performed by automated systems. The form of the balloon is designed based on the properties of the planet's atmosphere, the floating altitude, and the scale and capabilities of the balloon.

1.3 Remarkable Characteristics of Scientific Ballooning

The advantages of using scientific balloons to perform scientific observations or technological experiments over using rockets and satellites are summarized below.

- (1) *Low cost:* On the basis of a rough estimation of the basic costs of the main balloon and common equipment (excluding the on-board scientific observation instrumentation), the outlay required for a balloon experiment is at least a factor of 10 lower than that required for a small sounding rocket, at least a factor of 100 lower than that required for a large rocket and a small satellite, and at least a factor of a 1,000 lower than that required for a large satellite. Since the launch facilities are particularly basic, its operation and maintenance costs are also substantially lower.
- (2) *Able to mount heavy, bulky payloads:* Even for ascents of 30 km or higher into the stratosphere, balloons are able to carry payloads in excess of 1 ton. Moreover, in contrast with satellites, which are transported in the restricted space of nose cones of rockets, balloons permit a lot of flexibility in the external shape of experimental equipment. Although it depends on the capabilities of the balloon launch system, it is possible to launch objects that are 5 m or more on the side. Currently, the Space Shuttle is the only other way to transport such bulky equipment into space without folding it up.

- (3) *Recovery and reuse of the payload:* Since the observational instrumentation and experimental equipment mounted on a balloon can return to earth by parachute and be recovered, the same equipment can be used multiple times, resulting in significant cost benefits. This is advantageous when it is desired to collect consistent data using the same equipment and when it is desired to perform better observations and experiments by making improvements to the recovered payload. In addition, in cases when the large quantity of observational data makes it impossible to transmit all of the data during the flight, loading a high-capacity data recorder and reading the data after recovering the recorder is a possible solution.
- (4) *Short preparation time:* The mechanical vibrations during launch and the ambient environmental conditions during flight for a balloon are not as severe as those of a sounding rocket or satellite. As a result, instrument development can be completed in a shorter period after planning. In some cases, the on-board equipment can be fabricated and tested by the prototyping department of a university or research laboratory or by the researchers themselves.
- (5) *High flexibility in launch site selection:* Since balloon facilities are relatively small scale, balloons may be launched not only from standard mid-latitude regions, but also from locations such as near the geographic and magnetic north and south poles and equatorial regions. This means that balloon experiments may be performed at locations suited to the physical requirements for the objectives of the observation.
- (6) *“In-situ observations” of the upper atmosphere:* Only balloons are capable of performing “in-situ observations” of the atmosphere at altitudes of 30–40 km in the stratosphere. Aircraft cannot reach these altitudes, and sounding rockets pass through them in a short time. Atmospheric observations from an orbiting satellite are limited to remote sensing measurements made from a long distance.
- (7) *Good operability during flight:* With the exception of special long-distance flights, in conventional balloon experiments, balloons fly where it is possible to directly communicate with the ground base. Consequently, stable reception of telemetry data and detailed command operations are possible throughout the entire flight. In contrast, in the case of a medium-altitude satellite at an altitude of approximately 500 km, the contact period with a single ground station is 10–15 min at the very longest.
- (8) *Pilot experiments for space technologies:* Scientific balloons are used not only for scientific observations of space, but also for research and development of rocket and satellite technology. For example, in the first stage of development of a space vehicle that returns to the earth from orbit, an experiment may be conducted into investigating its high-speed flight characteristics by dropping a model from balloon altitude and allowing it to free fall at high speed.
- (9) *Means to develop the next generation of researchers:* These days, it is widely recognized that fostering and securing students and young researchers who are interested in space science and technology is a critical issue. Balloon experiments are highly valuable for such a purpose. Everyone who participates in a balloon experiment can be involved in many different kinds of activities at every

stage of the project. Usually the participant is involved in the development of on-board systems from its design and development to the final test and launch. However, with satellites there is little such opportunity, since the project is usually large-scale and expensive, and consequently tasks are performed in narrow areas of specialization.

By their very nature, the above comparisons are not applicable to planetary balloons. Rather, it is important to compare the various means for planetary exploration, such as landers and rovers; such a review is given in.

References

1. Cottrell, L.: Up in a Balloon, S.G. Phillips Inc., New York (1970)
2. Jackson, D.: The Aeronauts, Time-Life Books, Virginia (1980)
3. Kirscher, E.J.: Aerospace Balloons - from Montgolfiere to Space-, Aero Pub. Inc. Pennsylvania (1985)
4. Gillispie, C.C.: Montgolfier Brothers and the Invention of Aviation 1783–1784, Princeton University Press, New Jersey (1983)
5. Bacon, J.M.: The Balloon as an Instrument of Scientific Research, Royal Society of the Arts, Vol. 47, Issue 2413, 277–285, Bell & Sons, London (1899)
6. Piccard, A.: Ballooning in the Stratosphere, National Geographic Society, Washington, 355–385 (1933)
7. Nelson, J.R.: Balloon Film Specifications, Proc. 6th AFCRL Sci. Balloon Symp., 329–333, (1970)
8. Schwarzschild, M.: Astronomical Photography from the Stratosphere, Smithsonian Institution, (1964)
9. Rayan, C.: The Pre-Astronauts, Manned Ballooning on the Threshold of Space, Naval Institute Press, Maryland (2003)
10. Bawcon, D.: International Survey of Scientific Ballooning Support Organizations, AIAA Int. Balloon Technol. Conf. AIAA-91-3677-CP, 149–157 (1991)
11. Nishimura, J. et al.: On the Natural Shape of Plastic Balloon, Proc. of the 5th Int. Symp. on Space Technol. and Sci., 446–450 (1963)
12. Yajima, N., Hirosawa, H., Nishimura, J.: Scientific Ballooning in Japan, Indian J. of Radio and Space Phys., Vol. 20, June & August, 206–208 (1991)
13. Strong, J.: Water in the Atmospheres of Planets, Proc. 1964 AFCRL Sci. Balloon Symp., 337–340 (1964).
14. Davis, M.H., Greenfield, S.: The Mars Balloon -Feasibility and Design, Proc. 1964 AFCRL Sci. Balloon Symp., 341–352 (1964)
15. Greenfield, S.M., Davis, M.H.: Balloons for the Scientific Exploration of Mars, Proc. 1964 AFCRL Sci. Balloon Symp., 353–364 (1964)
16. Frank, R.E., Baxter, J.F.: Final Report, Buoyant Venus Station Feasibility Study, NASA CR-66404–66409, (1967)
17. Akiba, R., Hinada, M., Nakajima, T.: Simulation Study of Venus Balloon System, 43rd Congr. of the Int. Astronaut. Fed., IAF-92-0559, (1992)
18. Nishimura, J., et al.: Venus Balloon at Low Altitudes, AIAA Int. Balloon Technol. Conf., AIAA-91-3654-CP, 12–19 (1991)

Chapter 2

Engineering Fundamentals of Balloons

Abstract Balloons are giant membrane structures that float in the thin atmosphere. This chapter first presents the geometric design problems for the balloon body. Specifically, the shape of axisymmetric natural-shape balloons is discussed, and this design concept is then extended to superpressure balloons that are reinforced by load tapes. Throughout this discussion, current progress in research on design concepts that dramatically enhance balloon strength is explained in detail. The dynamics of a balloon flight are governed by a complex combination of fluid dynamics and thermodynamics. A mathematical model that describes the motion of a balloon is derived. This model includes the effects of the aerodynamical forces acting on the balloon, and of the gas temperature variation caused by thermal conduction and radiation between the balloon and surrounding atmosphere, the sun, the ground, and outer space. The ascent, descent, and the lateral motion of balloons are then explained in detail.

2.1 Buoyant Force and Attainable Altitude of Balloons

2.1.1 Principle of Buoyancy

The fact that balloons float in the atmosphere is founded upon the principle of buoyancy discovered by Archimedes in the third century B.C. It states that “an object submerged in a fluid experiences an upward force that is equal to the weight of the same volume of fluid” [1]. This phenomenon can be explained as follows.

As shown in Fig. 2.1a, a rectangular solid is lowered into a fluid. According to Pascal’s law, the object is subject to pressure from the fluid pressing on its surfaces in directions normal to its surfaces. The pressures on the sides are counterbalanced, so that the pressures acting on the upper and lower surfaces p_1 and p_2 are given by

$$p_1 = \rho g z_1, \quad (2.1)$$

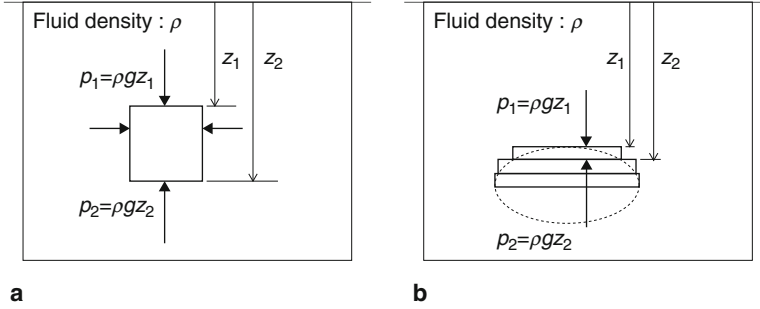


Fig. 2.1 Principle of buoyancy

$$p_2 = \rho g z_2, \quad (2.2)$$

where z_1 and z_2 are the respective depths of the upper and lower surfaces, ρ is the fluid density, and g is the acceleration due to gravity. Hence, if we take the area of the upper and lower surfaces to be S and the volume of the rectangular body to be V , the total sum of forces F in the upward direction that is imparted to the rectangular solid by the fluid is given by

$$F = p_2 S - p_1 S = \rho g(z_2 - z_1)S = \rho gV. \quad (2.3)$$

The same result can be obtained for an arbitrarily shaped body by summing thin horizontal slices (Fig. 2.1b) and applying (2.3) to each plate.

2.1.2 Effect of Buoyancy from a Gas

Consider the increase in the upward force if a buoyant gas of volume V is injected into a balloon. If we take ρ_a and ρ_g to be the densities of the external air and the internal buoyant gas, respectively, the increase in upward force acting on the balloon ΔF becomes

$$\Delta F = (\rho_a - \rho_g)gV. \quad (2.4)$$

The $\rho_a gV$ term on the right-hand side is the buoyant force from Archimedes' principle, and $\rho_g gV$ is the weight of the gas inside the balloon.

Thus, the contribution of the gas to the upward force is given by the difference between the density of the external air and that of the internal buoyant gas. For this reason, in subsequent descriptions, $\Delta \rho gV$ is referred to as the effective buoyant force and it is a function of the difference in the densities $\Delta \rho = \rho_a - \rho_g$.

2.1.3 Attainable Altitude

Balloons float to an altitude at which the buoyant force equals the total weight of the balloon system. Here the total weight of the balloon system includes the weight of the injected buoyant gas. The weight prior to charging with gas (i.e., the weight of the total system minus the weight of the buoyant gas) is referred to as the weight of the balloon system. If the definitions given in the above section are used, the balloon will float to an altitude at which the weight of the balloon system equals the effective lifting force.

Figure 2.2 shows the relationship between the attainable altitude and the mass of a balloon system for various balloon volumes. In this figure, the broken lines indicate different membrane thicknesses, and the solid lines represent different balloon volumes. The value on the horizontal axis at the intersection point of a solid and a broken line indicates the mass of the main balloon made from a membrane having the thickness indicated by the broken line. However, since the masses of balloons having the same volume may differ a little according to their precise specifications, the values given in this figure are simple approximations. For reference, open circles indicate the masses of some actual balloons.

If the balloon volume is specified, the mass of the balloon system can be determined from the desired attainable altitude. The total mass that can be carried is given by the difference between the total mass of the balloon system and the mass of the main balloon. In addition, the altitude given by the value on the vertical axis for the intersection point represents the maximum altitude that can be achieved if the balloon were to ascend with no payload attached. This demonstrates that it is important to lighten the mass of the main balloon in order to reach high altitudes.

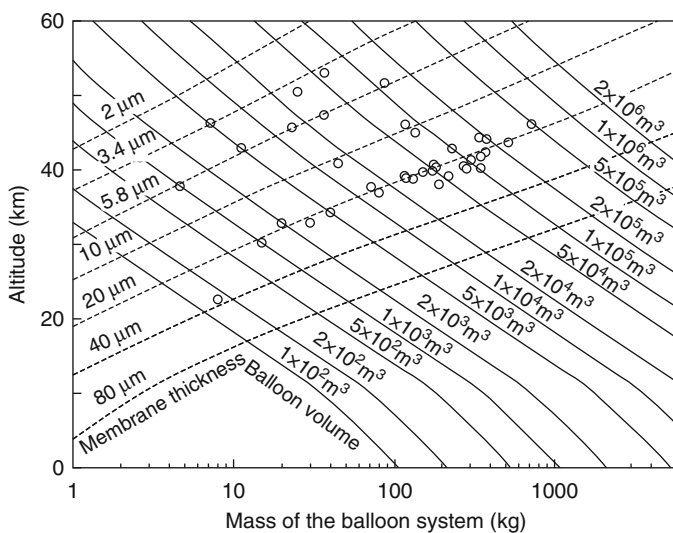


Fig. 2.2 Mass of the balloon system and attainable altitude

The polyethylene film used in scientific balloons is typically about $20\text{ }\mu\text{m}$ thick. For the case when a $100,000\text{-m}^3$ balloon ascends to an altitude of 35 km, the total mass of the balloon system would be about 730 kg; subtracting the balloon mass (230 kg) from this value gives 500 kg as the total mass that can be carried. Although the balloon volume varies depending on payload weight and desired attainable altitude, the volumes generally used lie between a few thousand and a few hundred thousand cubic meters. The biggest operational balloon is a $1 \times 10^6\text{ m}^3$ balloon used by NASA, which is able to carry an approximately 4-ton payload up to an altitude of 37 km. Another balloon is a $1.7 \times 10^6\text{ m}^3$ balloon, which is able to carry a 700-kg payload up to an altitude of 49 km.

Polyethylene films with thicknesses of $6\text{ }\mu\text{m}$ or less are used in balloons designed to carry light payloads to high altitudes. These balloons carry payloads of 100 kg or less, and they are chiefly used for investigating special weather phenomena, for performing atmospheric and space observations, and for checking wind direction and wind speeds in advance in regions near or above 40 km when conducting high-altitude balloon experiments [2]. The ISAS attained a record altitude of 53 km using a $60,000\text{ m}^3$ balloon made of a $3.4\text{-}\mu\text{m}$ -thick film and loaded with a light payload of about 5 kg [3].

Table Talk 1: How Archimedes Demonstrated the Existence of Buoyant Force

Balloon specialists should pay homage to the life of Archimedes, since ballooning is completely dependent on the principle of buoyancy, which he discovered.

So, how was it possible to demonstrate the existence of a buoyant force back in the third century B.C.? This is an interesting question. Fortunately, Archimedes' writings have been translated into many languages [1]. The fact that such ancient writings have been preserved is a miracle in itself and drives home their relevance to the scientific fields of Western civilization.

The proof of the buoyant force may be found in volume one of Archimedes' book entitled "On Floating Bodies," which contains two postulates and nine theses. The basis of this proof is that when the same substance as the fluid is placed in a fluid, it will neither sink nor float. That is, theses three and seven form the basis, which state that a substance becomes lighter by an amount equal to the weight of the substance immersed. Subsequently, a proof is given by citing examples and refining the principle. Of course, viewed from the perspective of modern science, it does not constitute a rigorous proof. However, one impressive point is the fact that a definition of a fluid is presented as the initial postulate (i.e., an assumed axiom). Since buoyancy is a phenomenon that occurs within fluids, Archimedes went through the very proper step of first defining a fluid. If the properties of a fluid had been pursued and extended to Pascal's theorem, then Archimedes' proof of buoyant forces would have been more complete. Next, it is necessary to demonstrate the basis for Pascal's definition (actually, this has been omitted in the present book as well).

Another surprise is found in thesis two, which states, "the fluid's surface assumes a form having the same center as the earth." It is thought it was already known in

the Greek period that the Earth was round. However, the fact that they knew that the surface of water is round suggests that they may have been one step away from discovering the concept of universal gravitation.

2.2 Balloon Configurations

2.2.1 Historical Background and Overview of Problems

With the exception of metal shell balloons that are designed to float in high-temperature and high-pressure environments such as Venus, balloon envelopes are generally made from flexible film (membranes), particularly the envelopes of stratospheric balloons. With the exception of rubber balloons, the increase in volume resulting from stretching of the film can be assumed to be negligible. Thus, the envelopes are manufactured from a lightweight, thin film in its fully expanded shape.

The shape design problem considers what the most appropriate balloon shape is. The following three points must be taken into account:

1. The transmission of the load of the suspended payload to the film should be distributed as uniformly as possible.
2. The balloon strength should be maximized in a way that minimizes the tensile force and that ensures that the tensile force is uniformly distributed on the film that is subject to pressure.
3. Maintaining the relationship of points (1) and (2) even when the shape of the balloon changes due to expansion during ascent.

In the 150 years from the first flight of balloons to the end of the 1930s, the shapes of balloons were not really studied theoretically and systematically in a way that took into account the three points stated above. The sphere was the most frequently used shape since it is best able to withstand pressure. Analyses in scientific books started with such an assumption (e.g., [4]). Other balloons having different shapes were also tried; these included balloons that were slightly deformed at the base of the sphere and long cylinders with hemispheres on the top and bottom.

The first step toward modern scientific ballooning was the concept of the natural-shape balloon proposed by R.H. Upson, which is presented in detail in Sect. 2.2.2. Other shapes are briefly described to demonstrate the superiority of his proposed shape over other shapes.

2.2.1.1 Spherical Balloons

If the weight and buoyant force of the membrane are neglected, the spherical shape gives rise to a uniform biaxial tension in the membrane over the entire surface of the pressurized balloon. For a tension T , a pressure on the membrane P , and a radius r , we have

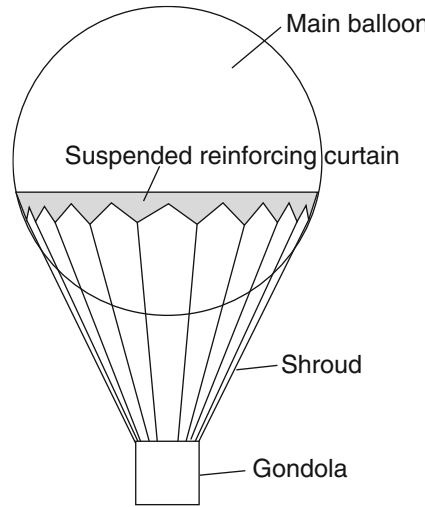


Fig. 2.3 Classical method for suspending a payload. Multiple ropes (called a shroud) are hung from the cloth that is installed like a curtain a little below the balloon's equator, and the payload is suspended at the lowest point. The balloon of Piccard mentioned in Sect. 2.1.1 followed this design

$$T = \frac{rP}{2}. \quad (2.5)$$

At first glance, it might appear that a spherical balloon minimizes the load on the membrane and is the optimal shape for a pressurized balloon. It also has the smallest surface area for a given volume, thus complying with the demand to minimize the weight.

However, there are several problems associated with spherical balloons. The first problem is that there is no single point for suspending a heavy load, since the entire surface of the balloon consists of a thin, uniform membrane. Consequently, the bottom of the balloon has to be locally reinforced, or a net needs to be draped over the upper half of the balloon as shown in the illustrations of classic balloons shown in Figs. 1.2 and 2.3. Alternatively, a curtain is attached around the equatorial line, and multiple ropes (called a shroud) are hung from this area; a payload is then suspended from the ends of the ropes, which has the effect of distributing the load.

The second problem is that on the ground and during ascent the balloon is only partially expanded, and thus its shape differs from a perfect sphere. During these times, the tension in the membrane will be nonuniformly distributed. For these reasons, spherical balloons are useful only for small balloons with light payloads.

2.2.1.2 Cylindrical Balloons

A cylindrical balloon is the one in which the central section of the envelope forms a long cylinder and the upper and lower ends are closed off in some form. They are useful for cases when it is easy to form a cylinder out of the membrane (or when the

membrane is initially formed into a thick tube). The circumferential tensile forces that act on the cylindrical section in the circumferential direction are given by the product of the pressure differential on the membrane and the radius of the cylinder. The sum total of the tensions acting parallel to the cylinder's axis is given by the product of the pressure and the cross-sectional area of the cylinder.

The longer and narrower the shape is, the greater the pressure resistance becomes; however, the volume to surface area ratio becomes worse. In a large stratospheric balloon, in contrast to a spherical balloon, the weight of the balloon itself is large and this is a disadvantage. However, this shape is suitable when there is a large lifting force per unit volume, such as in the high-density, low-altitude atmosphere of Venus.

2.2.1.3 Tetrahedral Balloon

A balloon constructed in the shape of a regular tetrahedron is called a tetrahedral balloon (Fig. 2.4). Because it lacks rotational symmetry, at first it appears to be an unnatural shape for a balloon. But since it has features such as a flat top and a bottom that converges to an acute angle, in some major points it resembles natural-shape balloons that are discussed later. Its shape consists of a cylinder with a length that is equal to half the circumference multiplied by $\cos 30^\circ$, and both ends may be closed off in directions orthogonal to each other.

As a result, since small balloons are easy to manufacture, they are used as auxiliary balloons at CNES for suspending a gondola on the ground (Fig. 2.4). Refer to Sect. 3.4.2 for details on the launch method.

2.2.1.4 Natural-Shape Balloons

Spherical balloons, cylindrical balloons, and tetrahedral balloons all assume their designed geometries only when they become fully inflated after ascent. When they are injected with gas on the ground, only a portion of their top section is inflated. R.H. Upson noticed that in the partially inflated section, there are a large number of folds parallel to the longitudinal axis, as can be seen in Fig. 2.5. This is because there is excess film in the circumferential direction. That is, because the length of the film in the longitudinal direction is constant irrespective of the state of expansion, no tension is generated in the film in the circumferential direction. Upson formulated a balloon shape by assuming only a longitudinal tension. He published a seminal paper on this concept in 1939 [5]. Upson obtained the idea for a natural-shape balloon by observing that a large number of folds are formed parallel to the longitudinal axis due to the excess film in the balloon.

If only an infinitesimal amount of excess film remains in the circumferential direction at full inflation, a balloon shape can be formulated that maintains the same type of shape from partial inflation through to full inflation. Subsequently, this proposed shape (which came to be known as the natural-shape balloon) played a major role in advancing ballooning from an era of trial and error to an era of scientific research.



Fig. 2.4 Tetrahedral balloons being used by CNES. (in this example, two tetrahedral balloons are being used.) (courtesy of CNES)

However, although the formula expressing the shape has a simple form (see later discussion), it cannot be solved analytically. Upson was only able to achieve a similar form through using an approximation. Attempts were made in the 1940s to determine a solution by using an analog computer to draw the balloon shape with a pen recorder; this work was done at the University of Minnesota, which was one of the driving forces behind balloon development in US. In the early 1960s, Smalley at the NCAR systematically derived accurate balloon shapes for various conditions by performing numerical calculations using a digital computer, which had reached a usable stage. These solutions were applied extensively to designing actual balloons [6].

The natural balloon shape, which was first formulated by Upson and then practically realized by Smalley, is a completely rotationally symmetrical body made only of film. At around the same time, fiber reinforcement technology, which involves vertically inserting bundles of high-strength reinforcing fibers (called load tapes) at fixed intervals, started to be applied in the construction of large balloons (Fig. 1.4).

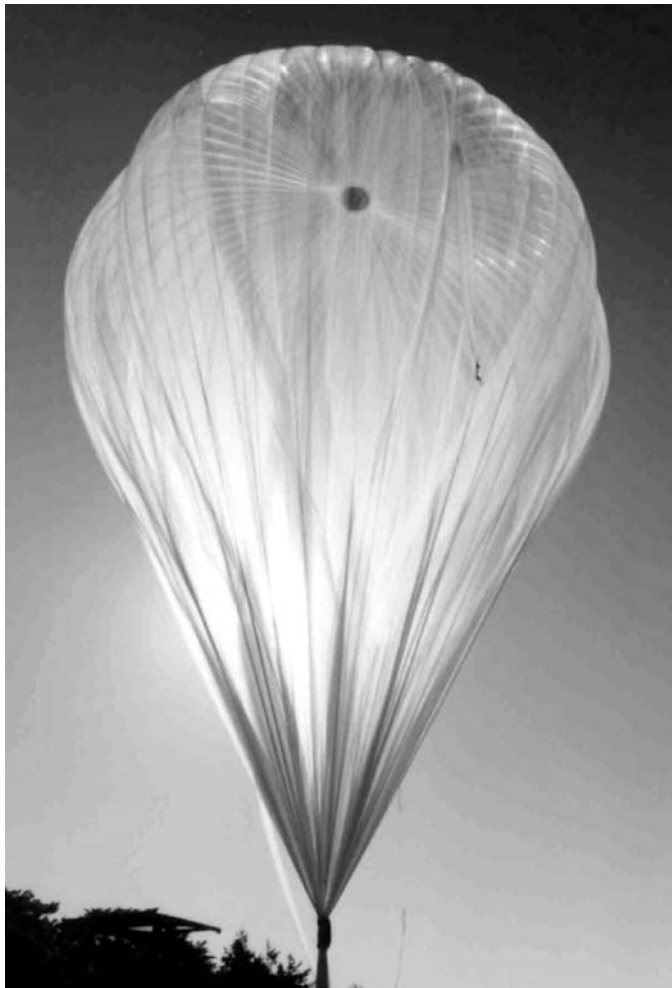


Fig. 2.5 Top of a balloon partially inflated on the ground

This technology increases the envelope's resistance to pressure, enabling heavier payloads to be suspended. In this case, because localized distortions in the film form between adjacent load tapes, the lateral cross section of the envelope is not a perfect circle (Fig. 2.19) and the balloon shape is no longer rotationally symmetrical. Naturally, the film tension is not uniaxial in the meridional (i.e., longitudinal) direction, but it is biaxial in the both the circumferential and meridional directions. However, the overall balloon shape can be viewed as being approximately the natural shape. As a result, problems arising from differences between actual balloons with and without load tapes were disregarded, and were not fully elucidated.

In 1998, two of the authors of this book (N. Yajima and N. Izutsu) reexamined the shape design problem starting from its fundamentals, and they proposed the

“three-dimensional (3D) gore design concept” [7]. This concept involves intentionally forming bulges having small local radii between adjacent load tapes. In this concept, the distinction between the roles of the load tape and the film are well defined, namely the load tape receives all of the forces in the meridional direction, and the film receives the forces generated by the pressure as an uniaxial tension in the circumferential direction. Since only a uniaxial tension is generated in the film, this concept both inherits and advances Upson’s concept, and enables a consistent understanding of the balloon-shape design problem, both for cases when a load tape is present and when it is absent.

Moreover, this concept can be used to optimize the tension generated in the film to a small constant amount that is independent of the balloon volume. A super-pressure balloon, which requires a high resistance to pressure, becomes feasible by applying this extended natural balloon shape design concept, since a balloon can be made by rational design making use of a thin, lightweight film if necessary. The 3D gore design concept solves a longstanding issue of how to construct a practical super-pressure balloon. In the following section, we give a detailed mathematical description of the natural-shape balloon concept, which represents the foundation of balloon shape design.

2.2.2 Natural-Shape Balloon Concept

As the shape a in Fig. 2.6 shows, at the time of launch a balloon is partially inflated with the lifting gas only in one section. As it ascends into the sky, it expands in the manner shown by the shape b, and ultimately becomes the fully inflated shape c in the figure when it attains its level flight altitude.

In this section, we determined the shape of balloons made of film, the stretching of which is small enough to be ignored, and the process by which these balloons expand in the manner described above. In the first stage in this section, no load tape is inserted for reinforcement, and an axisymmetric (i.e., rotationally symmetrical) shape is considered. A description extending to balloons that do have load tape is presented in Sect. 2.2.3.

2.2.2.1 General Expression where there is Biaxial Tension

Generally, only biaxial tensile stresses are considered to act on thin films such as those in balloons, and other stresses (i.e., compressive and shear stresses) can be disregarded. Thus, we first formulate the shape for the case when biaxial forces act in the film as a generalization for determining the natural-shape balloon described in the previous section.

As shown in Fig. 2.7, the balloon film can be represented by the curved surface formed when curve C is rotated around the A-axis. The origin for curve C having an axis of rotation A is set to be the base or nadir of the balloon P_1 , and its endpoint

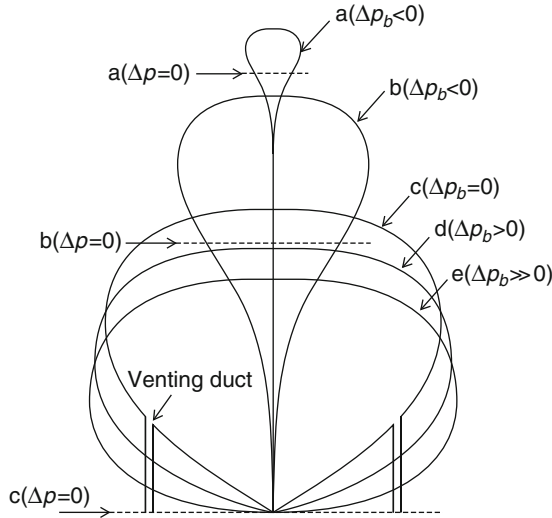


Fig. 2.6 The typical shapes of balloons categorized as a natural-shape balloon. Shape a and b show partial inflation; shape c shows full inflation of a zero-pressure balloon; shape d and e show instances when the balloon internal pressure is greater than the surrounding atmospheric pressure (super-pressure balloon). The dotted lines at $\Delta p = 0$ indicate the heights at which the pressures inside and outside the balloon are the same

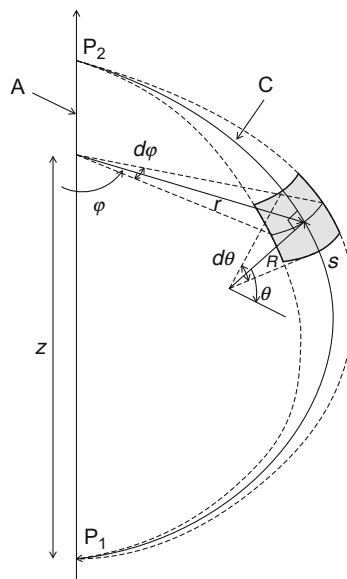


Fig. 2.7 Definition of the surface element on the balloon envelope that is formed by rotating curve C around axis A

is the apex of the balloon P_2 . The length from P_1 along the curve C is represented by s . The overall length of curve C is designated as the length of the balloon and is represented by ℓ_s . The radius of curvature of curve C is denoted by R , the angle formed by the line tangent to curve C and the axis of rotation is denoted by θ , and the distance from curve C to the axis of symmetry A is denoted by r . In addition, as shown in the figure, the height from P_1 at the base of the balloon to each point on curve C is represented by z . The height of point P_2 (i.e., the distance $P_1 - P_2$) is referred to as the height of the balloon. In addition, the maximum value of r is represented by r_{\max} , and the value for $2r_{\max}$ is called the balloon diameter.

The angle in a plane perpendicular to the rotational axis A is φ , and the dynamic balance for surface element $rd\varphi R d\theta (= rd\varphi ds)$ depicted in Fig. 2.7 is considered. The tension per unit length acting on this section of element (Fig. 2.8) is represented by T_θ over surfaces of constant φ and by T_φ over surfaces of constant θ . The actual mass per unit area of balloon film is taken to be w_e , and the difference between the internal pressure of the balloon and the surrounding atmospheric pressure is Δp (Δp is defined to be positive when the internal pressure is higher than atmospheric pressure). Thus, balancing equations for the z direction and the r direction gives (2.6) and (2.7), respectively.

$$(T_\theta + \frac{dT_\theta}{2})(r + \frac{dr}{2})d\varphi \cos(\theta + \frac{d\theta}{2}) - (T_\theta - \frac{dT_\theta}{2})(r - \frac{dr}{2})d\varphi \cos(\theta - \frac{d\theta}{2}), \quad (2.6)$$

$$-rd\varphi w_e ds - rd\varphi \Delta p ds \sin \theta = 0$$

$$(T_\theta + \frac{dT_\theta}{2})(r + \frac{dr}{2})d\varphi \sin(\theta + \frac{d\theta}{2}) - (T_\theta - \frac{dT_\theta}{2})(r - \frac{dr}{2})d\varphi \sin(\theta - \frac{d\theta}{2}), \quad (2.7)$$

$$-2T_\varphi ds \sin \frac{d\varphi}{2} + rd\varphi \Delta p ds \cos \theta = 0$$

where g is the acceleration due to gravity.

Rearranging (2.6) and (2.7) by eliminating the higher-order terms yields the following.

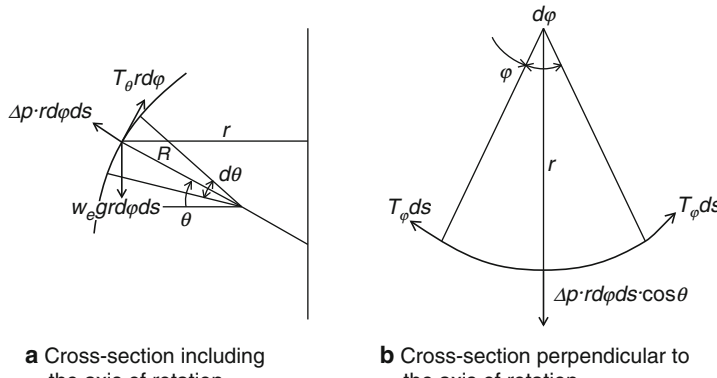


Fig. 2.8 Tension and pressure acting on a surface element of the balloon: **a** Cross-section including the axis of rotation; **b** Cross-section perpendicular to the axis of rotation

$$\frac{d(rT_\theta)}{ds} \cos \theta - rT_\theta \sin \theta \frac{d\theta}{ds} - rw_{eg} - \Delta pr \sin \theta = 0, \quad (2.8)$$

$$\frac{d(rT_\theta)}{ds} \sin \theta + rT_\theta \cos \theta \frac{d\theta}{ds} - T_\varphi + \Delta pr \cos \theta = 0. \quad (2.9)$$

Further rewriting (2.8) and (2.9) gives the following.

$$rT_\theta \frac{d\theta}{ds} = T_\varphi \cos \theta - rw_{eg} \sin \theta - \Delta pr, \quad (2.10)$$

$$\frac{d(rT_\theta)}{ds} = T_\varphi \sin \theta + rw_{eg} \cos \theta. \quad (2.11)$$

At the same time, if the density of the atmosphere and the density of gas inside the balloon are denoted by ρ_a and ρ_g respectively, Δp can be expressed as

$$\Delta p = \Delta p_b + (\rho_a - \rho_g)gz. \quad (2.12)$$

Here, Δp_b is the pressure difference at the base of the balloon $P_1(s = r = z = 0)$.

If the height at the point where $\Delta p = 0$ is set to z_b , (2.12) becomes

$$\Delta p = (\rho_a - \rho_g)g(z - z_b) \quad (2.13)$$

and (2.10) becomes

$$rT_\theta \frac{d\theta}{ds} = T_\varphi \cos \theta - rw_{eg} \sin \theta - b_g(z - z_b)r, \quad (2.14)$$

where b_g represents the effective buoyant force per unit volume (the net upward force) produced by the difference in the densities of the surrounding atmosphere and the lifting gas. That is

$$b_g = (\rho_a - \rho_g)g. \quad (2.15)$$

In addition,

$$\frac{dr}{ds} = -\sin \theta, \quad (2.16)$$

$$\frac{dz}{ds} = \cos \theta \quad (2.17)$$

are found from geometrical considerations. At the same time, the geometric surface area S and volume V for the object formed from the curved surface generated by rotating curve C around the A axis may be determined by

$$\frac{dS}{ds} = 2\pi r, \quad (2.18)$$

$$\frac{dV}{ds} = \pi r^2 \cos \theta. \quad (2.19)$$

2.2.2.2 Formula Describing the Natural-Shape Balloon

In Upson's concept as described in Sect. 2.2.1.4, there is excess film in the φ -direction in the shape of the balloon in the process of becoming fully inflated. In this condition, folds or wrinkles form parallel to the meridian, and there is no tension in the φ -direction of the film across these folds or wrinkles. Consequently, by setting $T_\varphi = 0$ in (2.14) and (2.11), the following two equations that describe the vertical cross-section of a natural-shape balloon can be obtained.

$$rT_\theta \frac{d\theta}{ds} = -rw_{eg} \sin \theta - b_g(z - z_b)r, \quad (2.20)$$

$$\frac{d(rT_\theta)}{ds} = rw_{eg} \cos \theta. \quad (2.21)$$

If it is assumed that there is an infinitesimal excess in the film in the φ -direction even when the balloon is fully inflated, these equations can be used for all stages, from the gas being injected into the balloon at launch through to full inflation.

We set $-F_1$ to be the force in the z -direction acting at the base of the balloon P_1 (downward force from the payload suspended from the bottom of the balloon), and we set $-F_2$ to be the force in the z -direction acting in the same way at the apex of the balloon P_2 (generally, $F_1, F_2 \geq 0$).

Here, the dimensionless length λ is defined as

$$\lambda = \left(\frac{F_1 + F_2}{b_g} \right)^{\frac{1}{3}}, \quad (2.22)$$

and the following dimensionless parameters are defined.

$$\tilde{r} = \frac{r}{\lambda}, \tilde{z} = \frac{z}{\lambda}, \tilde{z}_b = \frac{z_b}{\lambda}, \tilde{s} = \frac{s}{\lambda}, \tilde{\ell}_s = \frac{\ell_s}{\lambda}, \tilde{R} = \frac{R}{\lambda}, \quad (2.23)$$

$$\tilde{T}_\theta = \frac{T_\theta}{b_g \lambda^2}, \quad (2.24)$$

$$\tilde{S} = \frac{S}{\lambda^2}, \quad \tilde{V} = \frac{V}{\lambda^3}. \quad (2.25)$$

Equations (2.20) and (2.21) may be written as follows.

$$\tilde{r}\tilde{T}_\theta \frac{d\theta}{d\tilde{s}} = -k\Sigma_e \tilde{r} \frac{d\tilde{r}}{d\tilde{s}} - (\tilde{z} - \tilde{z}_b)\tilde{r}, \quad (2.26)$$

$$\frac{d(\tilde{r}\tilde{T}_\theta)}{d\tilde{s}} = k\Sigma_e \tilde{r} \frac{d\tilde{z}}{d\tilde{s}}, \quad (2.27)$$

where

$$k = (2\pi)^{-\frac{1}{3}}, \quad (2.28)$$

where Σ_e is the dimensionless film weight, and it is an important similarity parameter defined by

$$\Sigma_e = \frac{w_e g}{kb_g \lambda} \quad (2.29)$$

that characterizes the shape of the balloon. That is, because Σ_e is the only shape parameter in (2.26) and (2.27), shapes having the same value of Σ_e will result in similarly shaped balloons. In addition, (2.16) to (2.19) can be written as follows.

$$\frac{d\tilde{r}}{ds} = -\sin \theta, \quad \frac{d\tilde{z}}{d\tilde{s}} = \cos \theta, \quad (2.30)$$

$$\frac{d\tilde{S}}{d\tilde{s}} = 2\pi\tilde{r}, \quad \frac{d\tilde{V}}{d\tilde{s}} = \pi\tilde{r}^2 \frac{d\tilde{z}}{d\tilde{s}}. \quad (2.31)$$

2.2.2.3 Significance of the Natural-Shape Balloon

As will be described in the next section, the radius of curvature becomes infinite and the surface becomes flat at the apex of the balloon. Consequently, in the partially inflated state during ascent, there is no part of the film where there is a shortage of length in the circumferential direction. Consequently, the balloon maintains a reasonable shape from ascent until full inflation.

As noted above, the reason why it is possible to calculate the shape with the circumferential tensile force $T_\phi = 0$ as a constraint condition is because of the unique properties of the film material (i.e., the membrane). That is, in general an extremely thin and flexible membrane has no resistance to bending and no compressive forces in axially symmetric balloon shapes, as specified as a formulation assumption. If the length along the meridian line of the balloon envelope is constant and if it is assumed that there is some film slightly in excess of the required amount in the circumferential direction, there will be wrinkles generated parallel to the meridian line, and there will be no circumferential film tension perpendicular to these wrinkles. This is an important precondition for realizing natural-shape balloons.

This model is theoretically realized by neglecting stretching of the film; it is a statically determinate problem in structural mechanics, and it has the characteristic that it can be treated by considering shape and film extension separately.

2.2.2.4 Natural-Shape Balloons having Zero or Negative-Pressure Differential at the Base

The Case of Zero-Pressure Differential at the Base

The example below shows the case when $F_2 = 0$. First, treating the total length of the balloon \tilde{l}_s as a constant, shapes with a pressure differential of 0 at the base of the

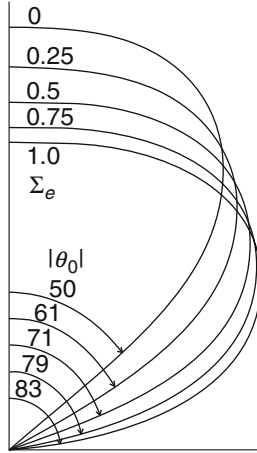


Fig. 2.9 Changes in the cross-sectional shape of a natural-shape balloon. The changes in the angle θ_0 at the base of the balloon are shown as a function of the similarity parameter Σ_e

balloon ($\tilde{z}_b = 0$) as determined by changing the similarity parameter Σ_e are shown in Fig. 2.9. This is obtained by determining θ_0 by repeated computation from the initial conditions

$$\tilde{r} = \tilde{z} = \tilde{S} = \tilde{V} = 0, \quad \tilde{r}\tilde{T}_\theta = \frac{1}{2\pi \cos \theta_0} \quad (\tilde{s} = 0), \quad (2.32)$$

which when integrated becomes

$$\tilde{r} = 0 \quad (\tilde{s} = \tilde{\ell}_s) \quad (2.33)$$

by assuming a θ_0 value for the angle θ at the computational starting point $\tilde{s} = 0$ based on the given parameter Σ_e .

At the apex of the balloon (i.e., at $\tilde{s} = \tilde{\ell}_s$) the radius of curvature is infinite, and the balloon is flat. The condition $\tilde{z}_b = 0$ (i.e., at the base of the balloon P₁ the pressure differential, $\Delta p_b = 0$) can be easily satisfied by setting the bottoms of venting ducts (which are installed in the lower part of the balloon (see shape c in Fig. 2.6) and are open at the bottom to the atmosphere) at the same height as the base of the balloon. This form of balloon is categorized as a zero-pressure balloon and it will be described in detail in Sect. 2.3.1.

Here, smaller Σ_e values indicate the fully inflated condition of a balloon that has a heavy payload compared with the film weight. The major difference in shape caused by differences in Σ_e is the angle at the base of the balloon. This relationship is depicted in Fig. 2.9. This relationship implies that shape varies with payload mass even for balloons having the same volumes and made from the same film.

The Case of Negative-Pressure Differential at the Base (Partial Inflation)

Next, we determine the shape during ascent. By taking the value of Δp_b to be negative (i.e., letting \tilde{z}_b be positive) this case can be determined in a similar way to those cases previously shown by the shape a and b in Fig. 2.6. Since there are the two parameters θ_0 and \tilde{z}_b in this calculation, the two convergence conditions in the iterative calculation are given in (2.33) and the fact that the volume \tilde{V} is a prescribed value determined from the total mass and altitude of the balloon.

Since there is excess balloon film in this case, it is necessary to note that w_e is not a constant value, rather it depends on the distance from the base s . More specifically, we first determine the circumferential length ℓ_φ for each section of the balloon in its fully inflated shape.

$$\ell_\varphi(s) = 2\pi r. \quad (2.34)$$

Then w_e is also a function of s , and

$$\frac{\ell_\varphi}{2\pi r} w_e \quad (2.35)$$

may be substituted for w_e in (2.20) and (2.21).

2.2.2.5 Natural-Shape Balloons with a Positive Pressure Differential at the Base

When There is a Finite Pressure Differential at the Base

Next, we consider enclosed balloons without venting ducts where the pressure at the base of the balloon is greater than the surrounding atmospheric pressure. In other words, we consider the case when $\Delta p_b > 0$ ($z_b < 0$). The shape is determined by the procedure described in Sect. 2.2.2.4, and as Δp_b increases from 0, the balloon becomes oblate in shape, and is referred to as a pumpkin balloon (see the shape d in Fig. 2.6).

When the Pressure Differential at the Base is Infinite

At sufficiently high pressure differentials (i.e., when balloon internal pressure can be regarded as being independent of height) the force due to the weight of the film may be ignored, and the balloon reaches the limit shape shown by the shape e in Fig. 2.6. This shape is obtained by replacing $\tilde{z} + \tilde{z}_b$ by the constant value \tilde{z}_b in (2.26) and (2.27) and setting $\Sigma_e = 0$, and it is described by the following two equations.

$$\tilde{T}_\theta \frac{d\theta}{d\tilde{s}} = \tilde{z}_b, \quad (2.36)$$

$$\frac{d(\tilde{r}\tilde{T}_\theta)}{d\tilde{s}} = 0. \quad (2.37)$$

The shape determined analytically from these equations is also the shape that has the maximum volume based on the constraint that the length of the meridian line is constant.

Here, (2.37) implies that the total value of \tilde{T}_θ in the cross section of fixed height \tilde{z} is constant, being independent of \tilde{z} . Consequently, if we consider the equatorial region where \tilde{r} is a maximum ($\tilde{r} = \tilde{r}_{\max}$), because it is symmetrical about the equator, the total value of tension for this section may simply be considered to be balanced with the force acting on this cross section due to the pressure differential inside and outside the balloon (here a constant value). In short,

$$2\pi\tilde{r}\tilde{T}_\theta = \pi\tilde{r}_{\max}^2(-\tilde{z}_b), \quad (2.38)$$

or expressed another way

$$\tilde{r}\tilde{T}_\theta = -\frac{\tilde{z}_b}{2}\tilde{r}_{\max}^2. \quad (2.39)$$

Accordingly, substituting (2.39) into (2.36) gives

$$\frac{d\theta}{d\tilde{s}} = -\frac{2\tilde{r}}{\tilde{r}_{\max}^2}. \quad (2.40)$$

This equation is called Euler's elastica [8]. This shape can be used to approximate the shape of super-pressure balloons. The radius of curvature along the meridian in the equatorial section of this balloon is half the radius \tilde{r}_{\max} in the horizontal direction in the same section of the balloon.

$$\tilde{R} = \frac{d\tilde{s}}{d\theta} = \frac{\tilde{r}_{\max}}{2} \quad (\tilde{r} = \tilde{r}_{\max}). \quad (2.41)$$

2.2.2.6 Film Tensile Force and Singularity

The film tension \tilde{T}_θ determined as above and the change with film position $\tilde{s}/\tilde{\ell}_s$ of the total value $2\pi\tilde{r}\tilde{T}_\theta$ are shown in Fig. 2.10. This corresponds with the shapes during inflation shown by the shape a to c in Fig. 2.6. The situation is depicted in which the tension \tilde{T}_θ abruptly increases near the top and bottom of the balloon. In addition, one can see that the tension increases as the balloon approaches full inflation.

Figure 2.11 shows the change in the tension distribution for the values of the parameter Σ_e shown in Fig. 2.9. This shows that when Σ_e is small, the total tension around the circumference is almost constant at an arbitrary height \tilde{z} , but as Σ_e increases, the ratio of the tension generated at the top of the balloon to that generated near the bottom increases due to the effect of the film's own weight. The stress per unit length at the apex and base becomes infinite in the same manner as for the case of a pressurized balloon, which was described in the previous section.

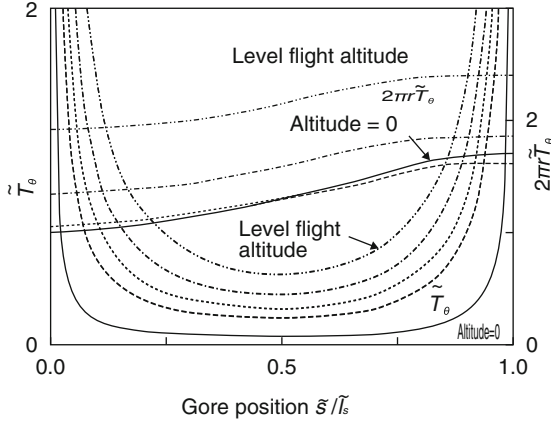


Fig. 2.10 Variation with altitude of the tension as a function of gore position. The *right axis* shows the total tensile force at a given gore position

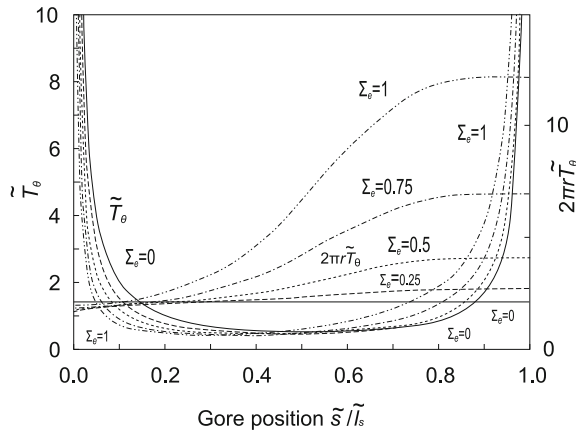


Fig. 2.11 Effect of Σ_e on the tension as a function of gore position. The *right axis* shows the total tensile force at a given gore position

The balloon model presented above is strictly mathematical, and, as such, it is not suitable for actual application in its current form. Because the circumferential length is zero at the apex and the base of the balloon, the film tension T_θ in the meridional direction becomes infinite, making it impossible to suspend a payload from the balloon.

In gore designs of early balloons, the cylinder end section or the taper-tangent end section was used for actual gore patterns (Fig. 2.12) to ensure that the circumferential length did not become zero. In other words, they were constructed so that folds or wrinkles were produced in the meridional direction at the top and

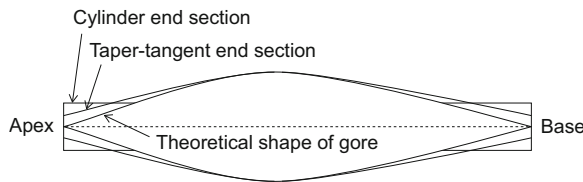


Fig. 2.12 Gore shapes that reinforce by increasing the amount of top and bottom film

bottom. As an extreme example, if both ends of a cylinder having a length equal to that of the balloon's meridional lines are tied, the length in the circumferential direction will be constant independent of the balloon height; hence, if the weight of the film is neglected, the circumferential tension will be constant, and will be independent of location. A load tape system was developed as a smarter design to solve this problem. The behaviors of balloons that have load tapes are discussed in the next section.

2.2.3 Expansion of Design Concepts for Balloons with Load Tape

2.2.3.1 Load Tape

With the exception of when light payloads of at most a few kilograms (such as radiosondes) are suspended, transmitting the concentrated load of a payload as a distributed load to the film is in a major problem in balloons that carry heavy devices ranging from a few hundred kilograms to in excess of 1 ton.

The load tape systems employed in typical scientific balloons made of polyethylene film involve the vertical insertion of reinforcing fibers along the sealing lines of adjacent gores. The fibers are strong and have a sufficiently low extensibility compared with that of the film. The payload is suspended from the point where all the load tapes concentrate at the base. This is a smart configuration that transmits and distributes the payload weight to the film (Fig. 1.4).

Such a system is highly compatible with the shapes of original natural-shape balloons in which only the meridional length is regarded as a constraining condition and where only meridional stress is present. It is well suited to manufacturing processes that make balloons by joining gore boundaries by heat-sealing. In addition, since the load tape bears all of the meridional tension, the advantage of this system is that the film stresses at both the apex and bottom of the balloon do not become infinite as in the description in Sect. 2.2.2.

2.2.3.2 Design of Natural-Shape Balloons with Load Tape (3D Gore Design Concept)

Returning to the starting point, we consider a method for extending the Upson's natural-shape balloon concept to balloons with load tapes. His basic concept involves producing only uniaxial film tension assuming no stretching of the film.

Here we try to design a balloon in which a gore forms a bulge with a small circumferential local radius between adjacent load tapes. At the bulge, we first assume that the meridional gore length is long enough that wrinkles are produced in the film in the circumferential direction, or, equivalently, there is no meridional tension. It is further assumed that the gore width is the length of the curved bulge in the circumferential direction. That is, by applying the same analogy as the original natural-shape balloon model of Sect. 2.2.2, the meridional tension on the film is $T_\theta = 0$, and tension T_ϕ is produced only in the circumferential direction.

Assuming such a configuration (Fig. 2.13b), the forces in the meridional direction are supported by only N strands of load tape, and only uniaxial tension is generated in the film, similar to the situation for original natural-shape balloons having no load tape. However, the direction of the tension is 90° to that for the case when there is no load tape (Fig. 2.13a), and it is in the circumferential direction. As a result, the circumferential film tension transfers to the load tapes and pulls them outward. The load tape curvature is defined by this pull up force and load tape tension.

If considered this way, since only uniaxial tension is present in the film, the statically determinate problem is applicable even to balloons that have load tape [9]. The circumferential tension in the film depends on the local radius of curvature R_ϕ at the location, and it is expressed simply as

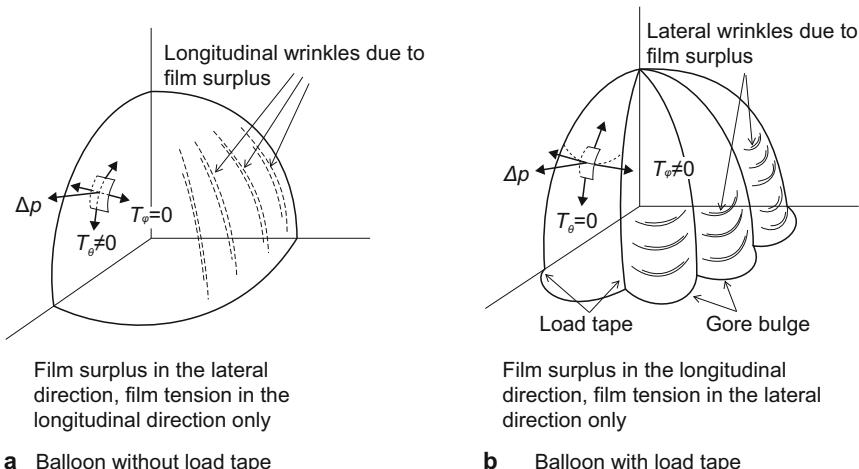


Fig. 2.13 Relationship between reinforcement and film tension resulting from load tape (partial diagrammatic view of upper quarter section): **a** Balloon without load tape (Film surplus in the lateral direction, film tension in the longitudinal direction only); **b** Balloon with load tape (Film surplus in the longitudinal direction, film tension in the lateral direction only)

$$T_\varphi = \Delta p R_\varphi, \quad (2.42)$$

where Δp is the difference between the internal and external pressures.

The radius of curvature R_φ may be selected independently of balloon size, and its minimum value is about half the length of the widest part of the spacing between adjacent load tapes. In other words, the radius of curvature R_φ governed by the number of load tapes N and the equatorial radius (i.e., the maximum circumferential radius) r_{\max} of a balloon without load tape is given by the following equation,

$$\frac{R_\varphi}{r_{\max}} \geq \frac{\pi}{N}. \quad (2.43)$$

Thus, the radius of curvature R_φ may also be reduced to a few tenths of r_{\max} .

In addition, as will be discussed later, the load tape spacing is determined by the width dimension of the film material, which is packaged in a rolled condition at the time of manufacture. Therefore, to manufacture larger balloons, the number of load tape strands is just increased, while the spacing remains the same. According to (2.42), the film tension T_φ is independent of the balloon's size. This remarkable property is very different from that of conventional balloons, and is the key to being able to dramatically increase the pressure resistance of large balloons.

At the same time, the sum total of the tension T_ℓ applied to the load tape is also independent of balloon height. It is the product of the cross-sectional area at the balloon equator and the pressure differential Δp and is given by

$$NT_\ell = \pi r_{\max}^2 \Delta p. \quad (2.44)$$

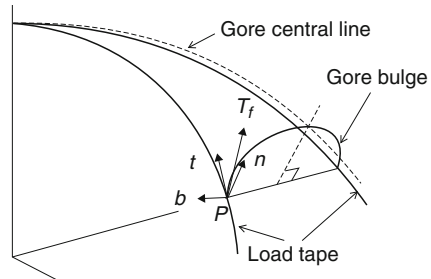
From a different viewpoint, this tension is produced by the circumferential tension in the film pulling the load tape outward, and the tension generated in the film due to the pressure differential Δp is transferred as the load tape tension.

The 3D gore design concept is considered able to combine the functions of load tape and film to optimize the specific characteristics of both. A balloon structure based on this 3D gore concept is ideal for a natural-shape balloon having load tape, and it is an appropriate extension of the original natural-shape model to the case when load tape is inserted. As mentioned at the beginning of this section, to realize such a balloon it is necessary to construct a 3D shape so that each gore forms a bulge having a specific small local curvature [10].

2.2.3.3 Relationship to the Shape of Natural-Shape Balloons without Load Tape

The shapes of a balloon obtained by the 3D gore design concept and a balloon without load tape (which is considered in detail in Sect. 2.2.2) essentially share the following points.

Fig. 2.14 3D gore cross-sectional shape and the direction of tension transferred to the reinforcing tape from the film



1. Inserting high-tensile-strength, low-extensibility load tapes along the meridian is consistent with the assumed conditions for a natural-shape balloon in which the meridional length is regarded as constant.
2. The meridional tension and the perpendicular force of the load tape, which determines its curvature, are both approximately proportional to those on the surface element of a balloon model without load tapes as described in Sect. 2.2.2. Then the load tape curvature is almost the same as the shape of the original natural-shape balloon.

Point (2) can be explained as follows. A segment of an infinitesimally wide strip is assumed to lie across the bulge between adjacent load tapes. The projected cross section of the strip is the product of the width and the load tape spacing. The force that pulls the load tape outward is equal to the product of this projected cross section of the small strip and the pressure exerted on the film. The meridional tension imparted to the load tape is equal to the product of the load tape spacing and the meridional film tension exerted on the surface element of a balloon model without load tapes, as shown in Fig. 2.7.

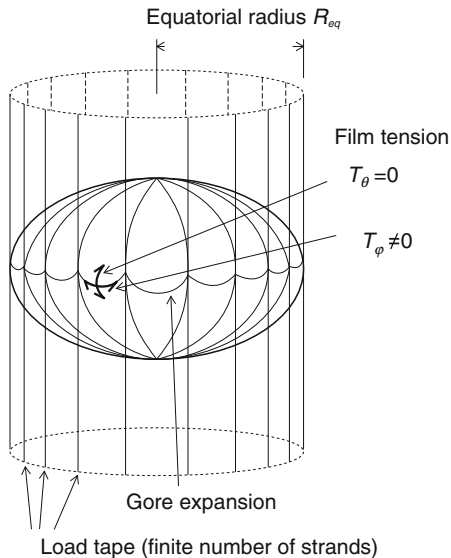
The slight difference between the two shapes is as follows. As shown in Fig. 2.14, a section orthogonal to the central line above the overhanging gore, and Cartesian coordinates \mathbf{t} , \mathbf{n} , and \mathbf{b} are applied to the point P where this section intersects the load tape. \mathbf{t} and \mathbf{n} are normal to the tangent to the load tape. Because the gore section is not orthogonal to the load tape, the gore section tension T_f has not only a component in the \mathbf{n} direction, but also a component in the \mathbf{t} direction, and this deviates from the original natural shape without load tape.

This deviation is caused by the fact that the balloon is partitioned by a finite number (N) of strands of load tape. In large balloons where N is 100 or more, this difference can be neglected, but in small balloons this difference in shape has to be considered during design. The formulation is a little complicated, and we refer the reader to literature [10].

2.2.3.4 Implications of Reinforcement with Load Tape

Figure 2.15 shows a highly pressurized balloon reinforced by N strands of load tape by means of the 3D design concept. In unfurling the load tape at the apex and the bottom, it becomes arrayed like a cylindrical birdcage as shown in the figure. At

Fig. 2.15 Case of a finite number of load tape strands



this point, if the number of load tape strands is increased by a factor of n , the local radius of bulge curvature in the circumferential direction becomes $1/n$ due to film overhang, and hence, the tension decreases by $1/n$ in the same way. At this point, the quantity of load tape material is assumed to be the same, and one strand of tape is split vertically into n strands. In so doing, the tension and strength per strand of load tape both become $1/n$, and the load is uniform.

Furthermore, by repeating the same process, if n is increased to infinity, the film circumferential tension will tend to zero, and the load on the infinite strands of load tape will remain constant. If this balloon is unfurled, the infinite strands of load tape form an array in a cylindrical shape as shown in Fig. 2.16. That is, the infinite strands of load tape mutate into the film-like strong envelope material of the balloon, and the infinitely thin film functions as a gas barrier.

Consider the difference between two balloons: a balloon constructed by the cylinder as the limits of the above-mentioned 3D gore design concept and a balloon constructed by tying the top and bottom of a cylinder made only of film (Fig. 2.17). In the balloon made out of only film, since the amount of film in the circumferential direction is constant at every location, the film tension is also constant. The point of distinction is whether the material that makes up the envelope is film or high-tension fibers.

For a pressure vessel, the weight of the envelope generally decreases in inverse proportion to the specific strength of the envelope material, if the maximum pressure is kept the same. The specific strengths of the balloon film materials with good biaxial homogeneous characteristics are in the range of 3×10^3 to 6×10^3 m. By contrast, since a polymer fiber consists of long molecules aligned parallel to the fiber's axis, a high uniaxial specific strength can be obtained. Table 2.1 gives the specific strengths of representative high-strength polymer fibers, and they vary by about a factor of a

Fig. 2.16 Case when number of load tape strands tends to infinity

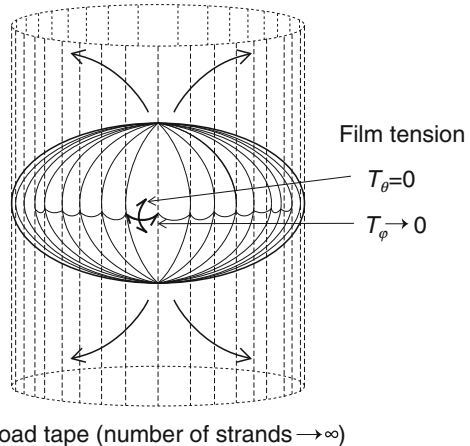


Fig. 2.17 Balloon made as a cylinder consisting just of film

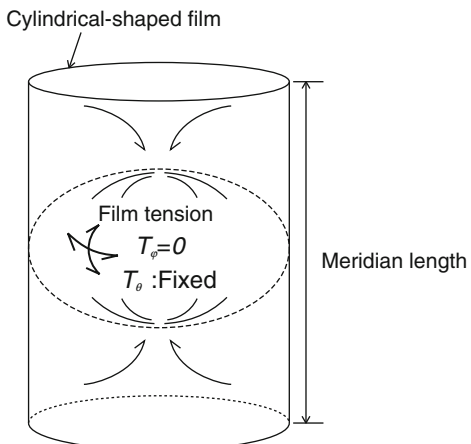


Table 2.1 Specific strengths of representative high-strength fibers and balloon-use film

Material name	PBO	Aramid	High-strength polyethylene	Polyethylene film for balloon use
Specific strength ($\times 10^3$)	380	200	350	3–6

100 compared with polyethylene film for balloon use. An envelope constructed from these polymer fibers, under the constraint that the balloon weight remains constant, will have greater strength than a balloon made with polyethylene film according to the ratio of specific strengths.

The strength of a balloon reinforced with a finite number of strands of load tape is intermediate between the strengths of these two typical balloons (i.e., the film envelope and polymer fiber envelope). The 3D gore design concept offers the most effective reinforcement for balloons with load tapes.

More specifically, if we take R_{eq} to be the equatorial radius of curvature of the balloon constructed as a cylinder shown in Fig. 2.17, the film meridional tension T_θ when the pressure differential Δp is applied is given by

$$T_\theta = \frac{\Delta p R_{\text{eq}}}{2}. \quad (2.45)$$

At the same time, for the balloon shown in Fig. 2.15, if the bulge is assumed to be semicircular, the maximum-value local radius on the equator $R_{\varphi,\text{max}}$ is given by

$$R_{\varphi,\text{max}} = R_{\text{eq}} \sin \frac{\pi}{N}, \quad (2.46)$$

And the film circumferential tension T_φ is

$$T_\varphi = \Delta p R_{\varphi,\text{max}}. \quad (2.47)$$

The ratio of the two tensions $K = T_\theta / T_\varphi \approx N/2\pi$ is the ideal reinforcement improvement rate from load tape. For example, if $N = 100$, then $K = 16$, and for $N = 200$, $K = 32$.

2.2.3.5 How to Construct a Balloon that has No Film Tension in the Meridional Direction

We consider how to make a gore having a 3D bulge from a planar film without elongating the film, so that, as in the description given in Sect. 2.2.3.2, the meridional tension $T_\theta = 0$ and the gore has a constant circumferential radius of curvature R_φ . As shown in Fig. 2.18, the width and length of the gore are made larger than that of conventional gore. At this point, the gore width of each part has a length that enables it to form a bulge of a specified radius of curvature R_φ between the adjacent load tapes. Here, if we make a planar gore, so that the centerline length of the gore is equal to that of the bulge, the length of the gore edges becomes longer than the load tape. Consequently, when manufacturing a balloon, the gore edges are joined to the relatively short load tape by gathering the edges. The excess film is then left in the meridional direction of the gore as circumferential wrinkles. At this juncture, by appropriately controlling the shortening proportion, a bulge that swells in a specified 3D shape can be formed from a planar-shaped gore. This process is similar to the 3D cutting procedures used for tailoring and dressmaking [11]. A model balloon with a volume of $3,000 \text{ m}^3$ was manufactured and tested to verify the 3D gore design concept.

The photograph in Frontispiece 5 shows an indoor full inflation test of the balloon.

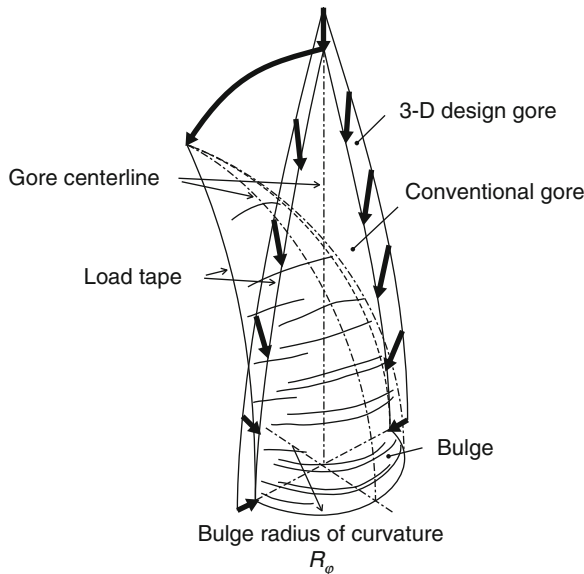


Fig. 2.18 Balloon-manufacturing method for the 3D gore design concept. A gore with a bulge is produced by attaching a gore that is larger than a conventional gore to the load tape by shortening (indicated by the *thick arrows*). This process is similar to the 3D cutting procedures used for tailoring and dressmaking

2.2.3.6 Problems with Conventional Balloons with Load Tape

In the design concept for a conventional balloon having load tape, N strands of load tape are attached at equal intervals to the surface of the natural-shape model having no load tape, as described in Sect. 2.2.2.2. The centerline length of the balloon gore is the meridian of the balloon, and the gore width is $1/N$ of the circumferential length. At the balloon manufacturing stage, the gores are joined to each other along their edges with load tapes.

In this manufacturing method, the length of the centerline of the gore is clearly shorter than the length of the junction line (i.e., the gore edge line). In the state where there is no pressure exerted and no extension in the film, the cross-sectional shape of the balloon becomes a polygon, as shown by line c in Fig. 2.19, and the load tapes are located at the vertices. In this state, the load tape subjected to the payload weight cannot be outwardly raised by film tension, and this configuration does not produce a balloon. Consequently, in an actual balloon, the gore must swell slightly outside the load tape due to its elasticity, as shown in Fig. 2.19b.

In this case, the gore must stretch not only in the circumferential direction, but also in the meridional direction. As biaxial elongation is required, the actual gore bulge due to the film's elasticity is further constrained. As a result, the circumferential radius of curvature near the centerline of the gore is not much smaller than the envelope radius, because the meridional stretching is required there and the tension

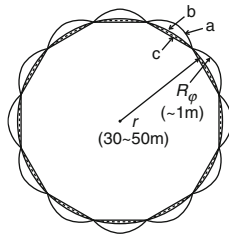


Fig. 2.19 Traverse cross-sectional diagram of a balloon envelope. Line c shows the normal gore cross-section. During full inflation, the shape bulges in the manner indicated by line b due to stretching of the film, and the radius of curvature near the gore centerline becomes about the same as the radius of circumferential curvature r of the balloon. Line a shows the swelled out position resulting from the 3D gore design concept, and the film in this case is not stretched

is generated in the meridional direction as well. This fact means that all the meridional forces are supported by both this film tension and the load tape tension. This phenomenon is not consistent with the design concept that the entire meridional force of the envelope should be supported by the load tape assembly having a high uniaxial tensile strength.

In addition, to utilize film extension for the realization of a balloon is different in principle from the Upson's natural-shape balloon model introduced in Sect. 2.2.2, and it is no longer a statically determinate problem. Accurate analysis of the biaxial film tension produced in this way is not straightforward, and finite element methods require numerical computation that extends to the case of flexible film materials having nonlinear properties. However, as an approximate estimate, the film tension at the burst point by pressurization is roughly the same as the tension on a sphere of the same volume. That is, with the 3D gore design concept, the film tension is proportional to the local radius of the bulge. In contrast with conventional balloons, the film tension is approximately proportional to the equatorial radius of the balloon. The observed burst pressures in flight-testing also support the same result.

With zero-pressure balloons (Sect. 2.3), the pressure differential applied is very small. In addition, the film deformations of a flat balloon gore are very small and are achievable due to the good elongation properties of polyethylene films used for balloons. As a result, while such a critical problem has not become evident in zero-pressure balloons, it is a major obstacle for realizing super-pressure balloons, in which the pressure differentials are particularly high.

A flight test of the 3,000-m³-volume balloon shown in Frontispiece 5 was performed, and Fig. 2.20 shows photographs by an industrial television (ITV) camera installed in the payload looking up from underneath the balloon with a specified pressure differential after reaching the maximum altitude. In the enlarged photograph of Fig. 2.20b, the circular arc can be seen to bulge between the reinforcing tapes in accordance with the design idea of the 3D gore design concept [12]. Figure 2.21 shows a conventional shape for reference, but the differences are distinct in that the outer circumference is approximately circular, and there is no bulge between the load tape.

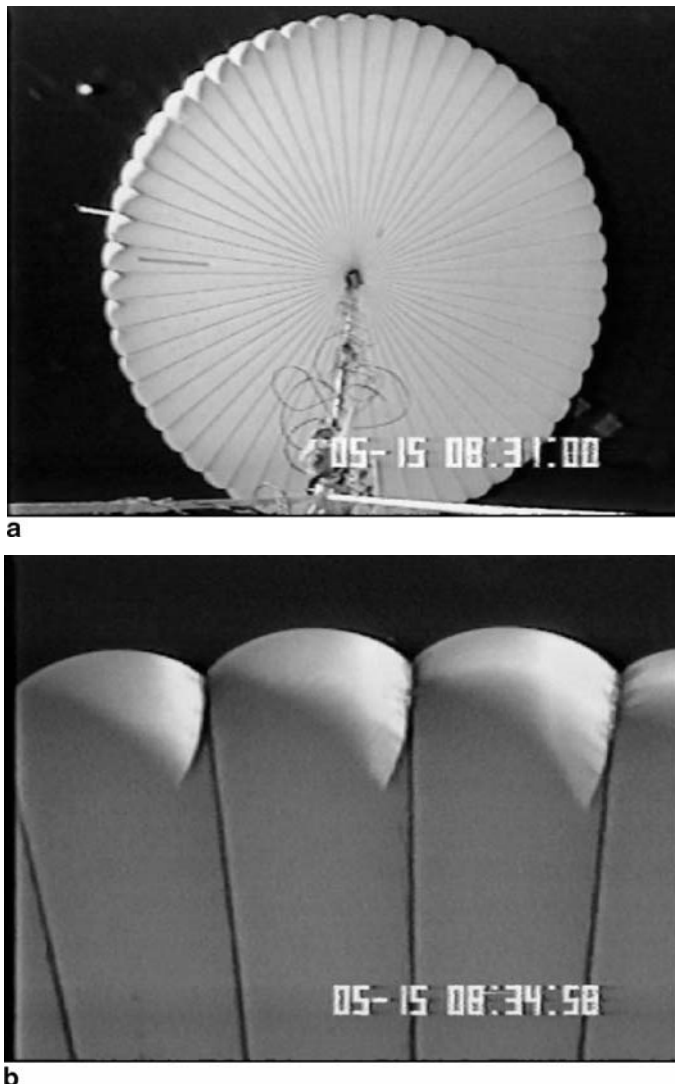


Fig. 2.20 Super-pressure balloon in flight. The bulges between the load tapes resulting from the 3D gore design concept are readily apparent: **a** Photograph of entire balloon; **b** Enlarged photograph

Table Talk 2: Another Natural-Shape Balloon Formulation

Dr. Jun Nishimura (former ISAS Director), who made profound contributions to scientific ballooning in Japan, worked independently on the formulation of a natural-shape balloon using variational methods. The variational method, based on certain constraining conditions, involves solving for extreme values of given functions (maximum or minimum value), and it is described in detail in physics textbooks.

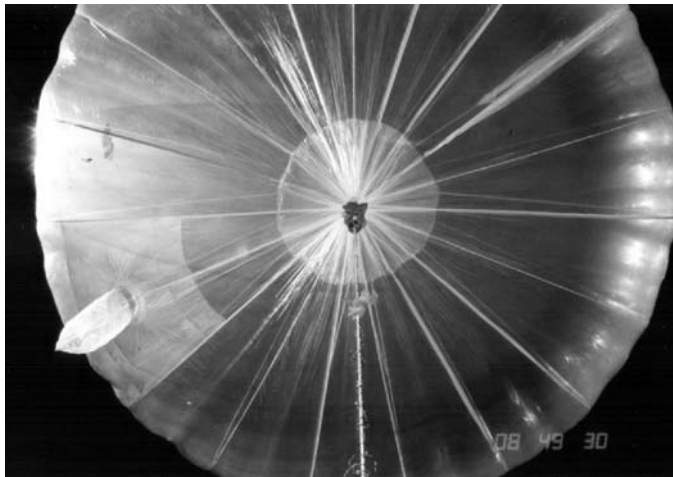


Fig. 2.21 Photograph looking up at a conventional balloon during ascent. Bulging ventilating duct just before exhaust is readily apparent

Dr. Nishimura assumed the two constraining conditions of constant meridional length and constant volume and determined the balloon shape as a function of the minimum potential energy of the buoyant force (the buoyant force point of action goes to the highest position). Although his approach differs from that of Upson, the results obtained were in agreement with the formula for a natural-shape balloon derived by Upson described in Sect. 2.2.2. Mathematically, it is the so-called “elegant solution” (i.e., the one having the simplest derivation).

Incidentally, why did the results of Upson, who determined the shape from the equilibrium of the forces acting on a surface element on the envelope, agree with the results of the variational method, which appears to be a completely different approach? There is a hint in the variational method constraint condition of keeping the meridional length constant. Here, the circumferential length has not been included as a constraint. That means the length is unrestricted. In other words, by considering the fact that there is excess film in the circumferential direction in the balloon in a partially inflated state, the condition that the meridional film tension is zero as conceived by Upson is incorporated as an initial assumption in the variational method.

Combining these two solutions, makes it easier to understand the fundamental properties of natural-shape balloons. More specifically, the balloon shape that generates tension in the film only in the meridional direction is also the shape in which the buoyant force produces the smallest potential energy.

2.3 Balloon Systems

In this section, we give an overview of the construction and functions of some representative balloon systems. Detailed in-flight characteristics for these systems are described in Sect. 2.4.

2.3.1 Zero-Pressure Balloons

Since zero-pressure balloons minimize the pressure on the balloon film, they opened the way to realizing large balloons constructed from thin, lightweight films. The half-century or so of modern scientific ballooning can be called the era of the giant zero-pressure balloon.

2.3.1.1 Construction

As mentioned in Sect. 2.2, zero-pressure balloons have a venting duct at the base of the balloon. After the balloon attains full inflation, if the lifting gas expands further it will overflow to the outside via the vent hole. Zero-pressure balloons are so termed because the internal–external pressure differential of the balloon is zero at the balloon base. Because the inside of the balloon is connected to the outside air through the venting duct, this type of balloon is also referred to as a balloon open to the air.

In reality, the venting hole is located a little higher up than the balloon base, and a duct is suspended from this hole to the base. In this configuration, the position of the venting hole is equivalent to the base. Since the ducts are constructed from the same flexible thin film as the balloon film, when the pressure in the base of the balloon exceeds that of the outside atmosphere, the duct is pushed open from the inside and forms a cylindrical shape, allowing the vent gas to flow smoothly through it. The photograph in Fig. 2.21 shows a venting duct in its inflated, venting state.

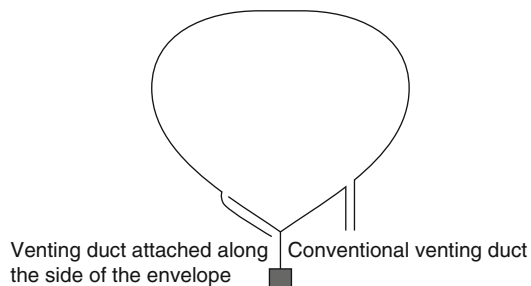
When the pressure differential is negative, the ducts are depressed down, thus preventing air flowing into the balloon. Consequently, the venting duct also functions as a check valve for one-way flow.

Ordinarily, the venting duct installed in the envelope hangs down naturally. However, if the balloon descends rapidly, there is a possibility that the bottom edge of the duct will float upward because of the air stream flowing on the side of the envelope. If this happens, the equivalent position of the vent hole will have been moved to a higher location; the lifting gas will be vented until the pressure differential at that position becomes zero. This reduces the buoyant force, and the balloon's descent may not terminate. Therefore, in cases when the flight plan includes a rapid descent, the venting duct is attached along the side of the envelope, as shown in Fig. 2.22.

2.3.1.2 Sustainability of Constant Altitude

After achieving its fully inflated condition, a balloon continues to ascend, maintaining the same volume while venting the lifting gas. Soon afterwards, the ascent stops at the altitude at which the buoyant force equals the weight of the total balloon system, and the balloon enters its level flight condition. In actual fact, the balloon continues to ascend even after the free lift becomes zero due to its momentum. If the temperature difference between the lifting gas and atmosphere is neglected, there

Fig. 2.22 Venting duct configurations



will be insufficient buoyant force due to excessive venting. After the balloon attains its maximum altitude, it will reverse direction and commence descending, and it will be unable to stop this descent.

As the details will be described in Sect. 2.4, however, essentially the temperature of the lifting gas during ascent is lower than that of the atmosphere because of the effect of adiabatic expansion. If ascent does stop, the gas temperature will increase to atmospheric temperature. This will compensate the reduction in the lifting force due to excessive venting, enabling the balloon to achieve a level flight.

On the one hand, under level flight conditions, if the buoyancy increases for some reason and the balloon starts to ascend again, lifting gas flowing from the venting duct will reduce the buoyancy, and the balloon will maintain a constant altitude. On the other hand, if the buoyancy decreases, the balloon will start to descend. If this occurs, its buoyancy will not recover since the increase in atmospheric pressure will reduce the volume of the balloon, and consequently the balloon will continue to descend.

In other words, if the temperature difference between the atmosphere and the lifting gas is ignored, zero-pressure balloons will have an automatic stabilization point when they ascend, but they will not have a stabilization point when they descend.

2.3.1.3 Altitude Compensation at Sunset

An important characteristic of zero-pressure balloons is the so-called sunset effect. As these balloons have a stable altitude only as they ascend, when the sun sets and they cease to absorb radiation from the sun, the temperature of the buoyant gas falls, buoyancy decreases, and the balloon can no longer maintain its altitude. If the internal balloon gas temperature decreases from T_g [K] by an amount ΔT_g [K] with the setting of the sun, the rate of buoyancy reduction due to contraction of the buoyant gas will be $\Delta T_g/T_g$.

The gas temperature of conventional polyethylene balloons flying over the earth's middle latitudes drops 15–25 K after the sun sets. Assuming the daytime gas temperature to be about 230 K, the reduction in buoyancy is about 7–10% of the total buoyant force. The weight of the payload must be reduced to compensate for this reduction in the buoyant force; this is done by dropping ballast with the aim of main-

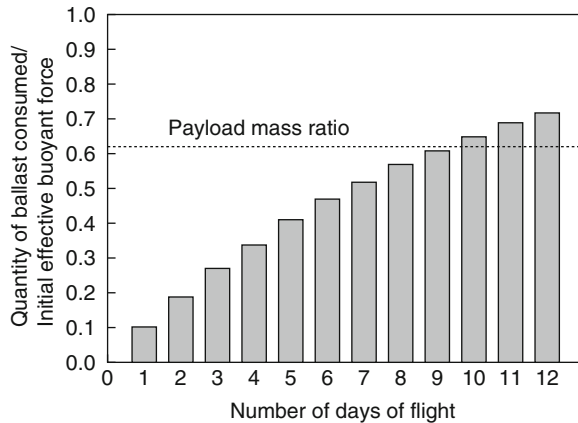


Fig. 2.23 Compensating for sunset and the number of flight days possible

taining the nighttime altitude. The gas temperature increases when the sun rises, and because the buoyancy recovers by an amount equivalent to the weight of the ballast dropped at sunset the previous day, the balloon starts to ascend again, and lifting gas is vented. At the next sunset, ballast is again dropped, and the cycle repeats. Since the total system mass m_t decreases with the dropping of ballast, the amount of ballast that needs to be dropped each day also decreases in proportion with the total system mass.

Let K_B represent the proportion of the quantity of ballast to drop each day to compensate for sunset relative to the total balloon system mass m_t . The total ballast consumption m_B for a flight of n days is then given by

$$m_B = m_t K_B \sum (1 - K_B)^{n-1}. \quad (2.48)$$

Figure 2.23 shows an example of how the total ballast consumption increases with the number of flight days, when K_B remains constant at 10% during an n -day flight. This example is for the case of a balloon with a volume of 100,000 m³ flying in the stratosphere at an altitude of 31.2 km (atmospheric pressure: 10 hPa).

Assuming a standard atmosphere, the effective buoyancy force during level flight is approximately 12,850 N (refer to Appendix 1, “Standard Atmosphere Table”). The mass of the balloon for this volume is in the vicinity of 230 kg, and the inclusion of a parachute and other common equipment increases this figure to about 500 kg. Thus, the payload mass is about 810 kg, and it accounts for 62% of the initial effective buoyancy. Even if the entire payload were ballast, the number of flight days could not exceed 9 days according to Fig. 2.23.

2.3.1.4 Pressure Exerted on the Film

We denote the atmospheric pressure at the flight altitude as p_a and the density difference between the air and the lifting gas as $\Delta\rho$. If the temperature difference between

the lifting gas and air is ignored, the interior–exterior pressure differential Δp at a height z from the base of the balloon can be expressed as

$$\Delta p = \Delta\rho g z = \Delta\rho_0 g z \frac{p_a}{p_{a0}}, \quad (2.49)$$

where $\Delta\rho_0$ and p_{a0} are the differential gas density and the atmospheric pressure on the ground, respectively, and g is the acceleration due to gravity. Since $\Delta\rho_0$ is approximately 1.0kg/m^3 , p_{a0} is 10^5Pa , and the balloon height is approximately 100 m. Thus, even for fully inflated large balloons, the interior–exterior pressure differential at the zenith is very small, being about only 1% of the atmospheric pressure p_a at the float altitude.

2.3.2 Super-Pressure Balloons

As this type of balloon does not require ballast to be jettisoned to maintain its flight altitude, long duration flights are unaffected by the sunset effect. Consequently, since the beginning of modern ballooning in the 1950s, many development projects have been carried out, and attempts at practical applications have been made. Although a high pressure resistance is required, the major aim of many trials was to develop strong lightweight balloon films to satisfy this requirement.

However, it is extremely difficult to practically produce a film that is able to withstand pressure differentials that are several factors of ten greater than those of zero-pressure balloons with only a few-fold increase in the weight of the film. The development of a super-pressure balloon has remained a subject of active research in balloon engineering for the past half-century or so. A fundamental solution to this problem is the “3D gore design concept,” which is described in Sect. 2.2. Specifically, it is a shape design approach that attempts to find ways to reduce the tension produced in the film.

2.3.2.1 Construction

Unlike zero-pressure balloons described in Sect. 2.3.1, super-pressure balloons do not have a venting duct. That is, super-pressure balloons are closed to the outside atmosphere. The two exceptions to this are safety valves that operate automatically to release unexpected high pressures and/or exhaust valves that are opened and closed by remote operation from a ground base to control the buoyancy.

In principle, because the free-lift portion of the buoyant gas is not vented from the balloon, in order to stop the ascent of the balloon, the expansion of the free-lift portion of the gas must be constrained by the balloon film, and the pressure differential with the outside air will increase by this amount. Even when the diurnal change in the lifting gas temperature is considered, the pressure differential is about

20% of the atmospheric pressure at flight altitudes. Although the absolute value of this pressure differential may not appear to be very high in the low-pressure stratosphere, it is about 20 times higher than the pressure differential at the apex of a zero-pressure balloon, and for large-volume stratospheric balloons made from thin film, it is not a simple matter to withstand such pressures.

2.3.2.2 Sustainability of Constant Altitude

The free lift $\tilde{f}m_t g$ is imparted to a balloon system having a total mass m_t , and the balloon expands while ascending. Here, \tilde{f} represents the free lift ratio, which is defined as (free lift)/(total weight of balloon system) (see Sect. 2.4.2.2 for a more detailed explanation). As shown in Fig. 2.24, at an altitude of z_1 (balloon volume: V_{b1} , atmospheric pressure: p_{a1} , atmospheric density: ρ_{a1}) the pressure differential at the balloon base is zero (this is the zero-pressure balloon condition, State 1). The balloon's shape at this time corresponds to that shown by the shape c in Fig. 2.6, as described in Sect. 2.2. At this point, if the pressure gradient between the base and the apex of the balloon is ignored, the balloon's internal pressure p_{b1} will be the same as p_{a1} . After this, the pressure at the base increases as it gains altitude, and the shape of the balloon changes to the pumpkin shape depicted by the shape d to e in Fig. 2.6. Then, at an altitude of z_2 (balloon volume: V_{b2} , atmospheric pressure: p_{a2} , atmospheric density: ρ_{a2} , State 2) it attains its maximum altitude, and stops ascending.

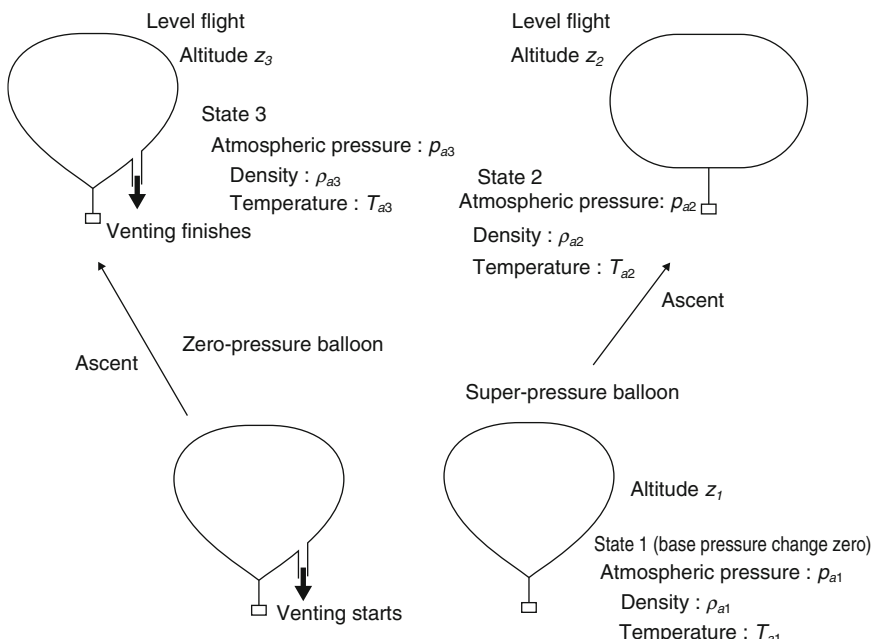


Fig. 2.24 Diagram showing balloon states

Subsequently, in the vicinity of this altitude, the volume of the balloon may be considered to be approximately constant. If the balloon climbs to an altitude higher than z_2 , the air density decreases, and the buoyancy diminishes. Conversely, if its altitude decreases, its buoyancy will increase. In other words, in contrast to a zero-pressure balloon, a super-pressure balloon is stable in both the ascending and descending directions. Since it is not necessary to drop ballast to maintain altitude, long-duration flights become possible.

2.3.2.3 Pressure Exerted on the Film

The relationships between buoyancy, total balloon system mass, and balloon internal pressure in States 1 and 2 are given by

$$(1 + \tilde{f})m_t \frac{T_{g1}}{T_{a1}} = V_{b1}\rho_{a1}, \quad (2.50)$$

$$m_t = V_{b2}\rho_{a2}, \quad (2.51)$$

$$\frac{p_{b1}V_{b1}}{T_{g1}} = \frac{p_{b2}V_{b2}}{T_{g2}}, \quad (2.52)$$

where T_{a1} , T_{a2} , T_{g1} , and T_{g2} are the atmospheric temperatures and lifting gas temperatures for States 1 and 2, respectively. In these two states, if the gas temperature and atmospheric temperature are equal, the balloon's internal pressure $p_{b2,0}$ and its pressure difference with atmospheric pressure $\Delta p_{b2,0}$ at level flight are both simply determined by the atmospheric pressure p_{a2} and the free lift ratio \tilde{f} as expressed by the following equations.

$$p_{b2,0} = p_{a2}(1 + \tilde{f}), \quad (2.53)$$

$$\Delta p_{b2,0} = p_{a2}\tilde{f}. \quad (2.54)$$

When there is a difference between the buoyant gas temperature and the atmospheric temperature, the internal pressure p_{b2} and the internal–external pressure difference Δp_{b2} are given by

$$p_{b2} = p_{a2}(1 + \tilde{f}) \frac{T_{g2}}{T_{a1}}, \quad (2.55)$$

$$\Delta p_{b2} = p_{a2} \frac{T_{g2}\tilde{f} + (T_{g2} - T_{a1})}{T_{a1}}, \quad (2.56)$$

Here, since the altitudes for States 1 and 2 are close, the respective atmospheric temperatures T_{a1} and T_{a2} can be treated as being equal. More specifically, the term $(T_{g2} - T_{a1})$ in the above equation is approximately equal to the temperature difference between the gas and the atmosphere for State 2, (i.e., $\Delta T_g = T_{g2} - T_{a2}$). At night, the gas temperature T_{g2} falls more than the atmospheric temperature T_{a2} . When $\Delta p_{b2} < 0$, the pressurization conditions as a super-pressure balloon are lost, and the balloon becomes a zero-pressure balloon and loses its altitude stability in the

downward direction. This boundary temperature $\Delta T_{g,\text{lim}}$ is derived by substituting $\Delta p_{b2} = 0$ into (2.56) as follows.

$$\Delta T_{g,\text{lim}} = -T_{a2} \frac{\tilde{f}}{1 + \tilde{f}}. \quad (2.57)$$

Since the atmospheric temperature in the stratosphere is about 230 K, when \tilde{f} is 8%, $\Delta T_{g,\text{lim}}$ will be -17 K.

The gas temperature T_{g2} rises due to irradiation by the sun's rays. The phenomenon in which Δp_{b2} becomes greater than $\Delta p_{b2,0}$ is called superheating, and it governs the balloon's design strength.

2.3.3 Special-Purpose Balloons

2.3.3.1 Dual-Balloon Systems

Super-pressure balloons described in Sect. 2.3.2 attempted to maintain a constant flight altitude by keeping a large balloon in a pressurized condition. Figure 2.25b and c depict dual-balloon systems, which are compound systems that combine a small super-pressure balloon and a large zero-pressure balloon, in which the volume of the zero-pressure balloon is K_v times greater than that of the super-pressure balloon. The small super-pressure balloon is used for controlling the altitude, while the large zero-pressure balloon is used for lifting the payload.

Systems that have been proposed include a tandem balloon, in which the balloons are situated above and below the payload (Fig. 2.25b), and a double-envelope

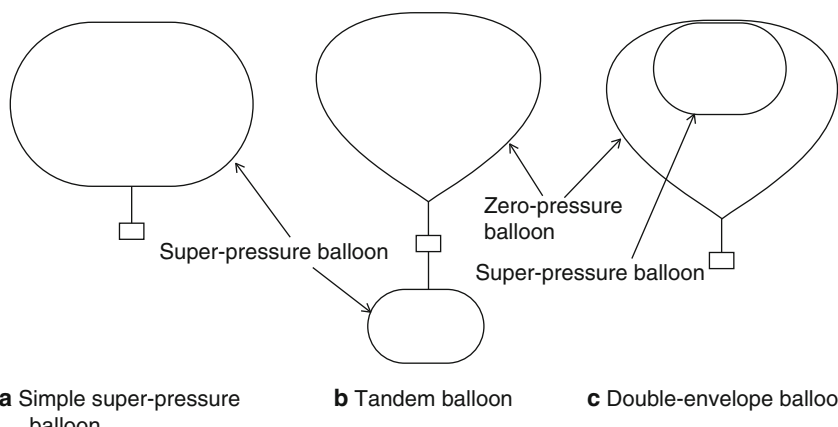


Fig. 2.25 Dual-balloon systems: **a** Simple super-pressure balloon; **b** Tandem balloon; **c** Double-envelope balloon

balloon (Fig. 2.25c). The former of these balloon designs has been tried by NASA, and it was named the Sky Anchor system [13].

In this balloon system, the reduction in the buoyancy of the zero-pressure balloon caused by the sunset effect is compensated by the increasing buoyancy of the super-pressure balloon as the flight altitude decreases. In other words, it differs from a simple super-pressure balloon in that it requires an altitude offset to maintain a stable flight altitude.

The pressure differential Δp of the super-pressure balloon increases to compensate for the change in the buoyancy of the large-volume, zero-pressure balloon. As shown in (2.58), the pressure differential Δp is a factor of K_v larger than that of a simple super-pressure balloon described by (2.54).

$$\Delta p = K_v p_a \tilde{f}. \quad (2.58)$$

In addition, the altitude offset Δz is given by

$$\Delta z = H_0 \ln \frac{p_{\min}}{p_{\max}}, \quad (2.59)$$

where p_{\max} and p_{\min} are the atmospheric pressures at the upper and lower altitude, respectively, and H_0 is the atmospheric scale height (Sect. 3.6.1). Figure 2.26 shows the relationship between the balloon volume ratio K_v and the altitude offset Δz for three different values of the buoyancy variation associated with the changes in gas temperature caused by the presence or absence of irradiation by sunlight.

The buoyant forces should be appropriately distributed between the two balloons, so that the zero-pressure balloon attains a state of zero pressure differential at the ceiling altitude. If we denote the buoyant forces of the zero-pressure balloon and the super-pressure balloon to be F_z and F_s , respectively, we obtain

$$F_z = m_t g - F_s, \quad (2.60)$$

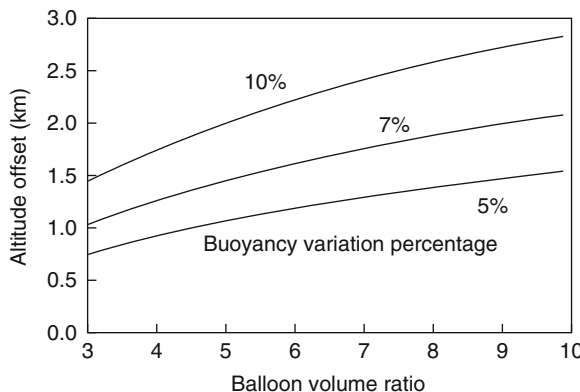


Fig. 2.26 Balloon volume ratio and diurnal variation in the flight altitude. The parameter in the figure is the ratio of diurnal buoyancy variation to total buoyancy

$$F_s = K_v m_t g \tilde{f}. \quad (2.61)$$

In this balloon system, the system weight of the super-pressure balloon can exceed its buoyant force, since the super-pressure balloon must be weighed down by the zero-pressure balloon to a certain degree to control the flight altitude in the manner described above. Thus, it is possible to avoid the strict constraint that the large simple super-pressure balloon must be made from a sufficiently lightweight film to enable it to reach the stratosphere while carrying a heavy payload. This permits a heavy film to be used for the envelope material, extending the range of films that can be used. Consequently, an improvement in the super-pressure balloon's manufacturability and reliability can be anticipated.

An additional advantage of this dual-balloon system is improved flight safety. Even if the super-pressure balloon bursts, the balloon system will not fall immediately because of the buoyancy of the zero-pressure balloon.

2.3.3.2 MIR Balloon

This is a balloon in which the optical properties of the balloon film have been designed in such a way that the buoyancy fluctuation associated with the presence or absence of solar radiation is minimized. Its development has been pursued since the 1970s by CNES, and it is referred to as a MIR balloon (Montgolfière Infrarouge, French for “infrared Montgolfier”). By enhancing the reflectivity of the upper half of the balloon, the increase in the buoyant gas temperature due to solar radiation is reduced, and by enhancing the infrared absorption of the lower half, the infrared energy radiated from the earth is absorbed reducing the drop in the gas temperature during the night. Although this balloon can transport only a light payload, and its diurnal altitude fluctuation can be as large as about 10 km, it has been able to perform long duration flights [14].

2.4 Motion of Balloons

In this section, we describe a flight model to illustrate the motion of balloons. To determine the motion of a balloon and its behavior during flight, it is necessary to model the temperature changes of the lifting gas inside the balloon, in addition to determining the forces acting on the balloon. To simplify the treatment, the balloon is treated as a point mass when considering the forces acting on the balloon. Pressure gradients within the balloon are ignored, and deformation or rotation of the balloon is not considered. However, when the effects of drag and pressure on the balloon are introduced to improve the accuracy of the model, it will be necessary to consider pressure gradients within the balloon and to take the balloon shape into account.

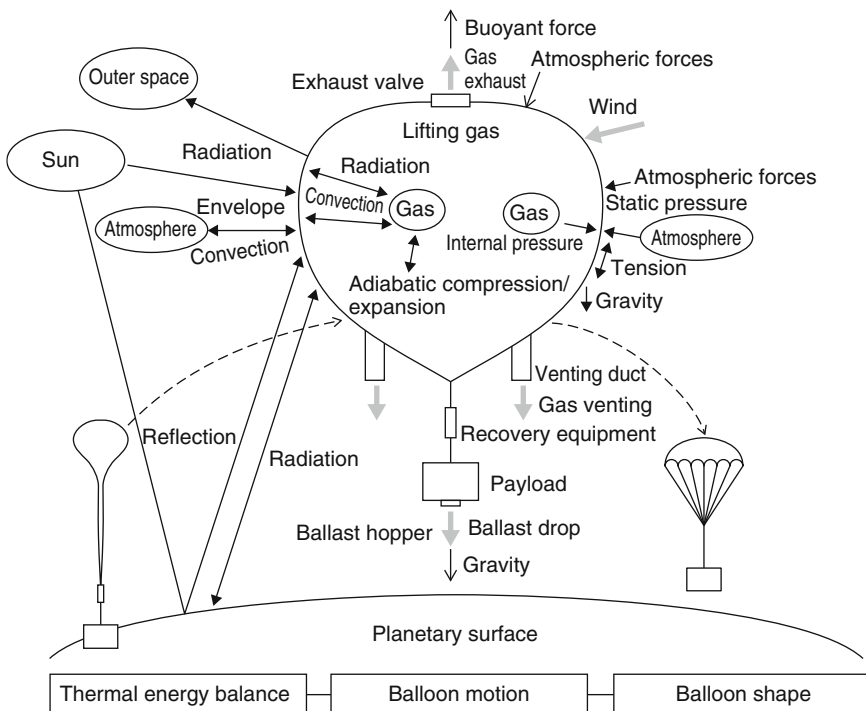


Fig. 2.27 Forces acting on a balloon and heat transfer into and out of a balloon

As shown in Fig. 2.27, the principal forces acting on the balloon are buoyancy, gravity, and the forces associated with the motion of the balloon and the relative motion of the atmosphere (subsequently, forces associated with the planet's atmosphere will be referred to as aerodynamic forces).

In addition, when taking the balloon shape into account, while there are internal and external pressure differences and tensions created within the envelope that vary with location on the balloon's surface, the impact of these fluctuations on the balloon's motion is small, and hence, they are not considered.

The following factors cause temperature changes in the balloon envelope and the lifting gas:

Adiabatic expansion and compression associated with

1. The aerodynamic force vector \mathbf{F} acting on the balloon is expressed in terms of the relative wind velocity ambient atmospheric pressure changes due to the upward and downward motion of the balloon.
2. Convective heat transfer between the atmosphere and the envelope and between the lifting gas and the envelope.
3. Radiative heat transfer between the lifting gas and the sun, planet (earth), and space.
4. Radiative heat transfer between the envelope and the sun, planet (earth), and space.

The horizontal component of the balloon's speed and its speed relative to that of atmospheric winds are considered to be small.

First, in Sect. 2.4.1, we introduce a model that describes the balloon motion. Then, in Sect. 2.4.2, we give general expressions for the vertical motion of a balloon. We consider horizontal motion in Sect. 2.4.3, and the heat energy balance that critically affects the balloon motion in Sect. 2.4.4.

2.4.1 Balloon Flight Model

Consider the coordinate system depicted in Fig. 2.28, in which the z -axis is vertical and the x - and y -axes are orthogonal to the z -axis. Unit vectors parallel to the x -, y -, and z -axes are represented by \mathbf{i} , \mathbf{j} , and \mathbf{k} , respectively. In addition, the balloon's position is denoted by (x_b, y_b, z_b) , its velocity vector is represented by \mathbf{v}_b with components (v_{bx}, v_{by}, v_{bz}) , and the wind velocity vector by \mathbf{v}_w with components (v_{wx}, v_{wy}, v_{wz}) .

\mathbf{F} has two components, namely, the drag force F_D that acts parallel to the relative wind vector, and the side force F_Y that acts perpendicular to the relative wind direction. More specifically,

$$F_D = \frac{1}{2} \rho_a |v_w - v_b|^2 C_D A_b, \quad (2.62)$$

$$F_Y = \frac{1}{2} \rho_a |v_w - v_b|^2 C_Y A_b, \quad (2.63)$$

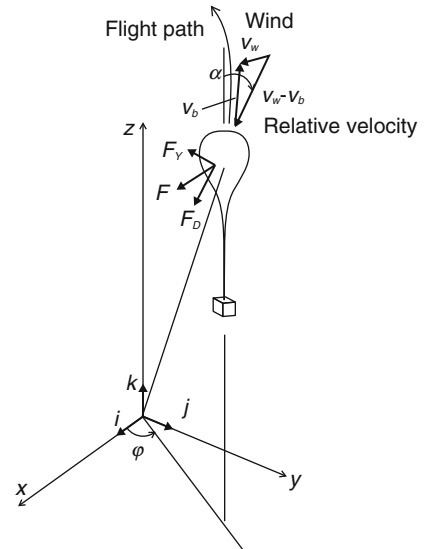


Fig. 2.28 Definition of coordinate system and aerodynamic forces acting on the balloon

where A_b is the standard area when calculating aerodynamic forces; this value is equal to the maximum cross-sectional area perpendicular to the balloon's axis and may be obtained by calculating the shape of the balloon. In addition, ρ_a is the atmospheric density.

The angle between the balloon's relative velocity vector $\mathbf{v}_b - \mathbf{v}_w$ and \mathbf{k} is defined as the balloon's angle of attack α . C_D denotes the effective drag coefficient and C_Y is the effective side force coefficient, and these depend on the angle of attack α , the balloon shape, and the Reynolds number Re_b defined by the following equation

$$Re_b = \frac{\rho_a D_b |\mathbf{v}_w - \mathbf{v}_b|}{\mu_a}, \quad (2.64)$$

where D_b is the balloon's diameter, and μ_a is the coefficient of viscosity for air. The Reynolds number of the balloon Re_b is about 10^6 – 10^7 on the ground and about 10^4 – 10^6 at flying altitudes, depending on the magnitude of the buoyant force. Since a balloon is a membrane structure, it deforms slightly when it is acted on by aerodynamic forces, which modifies its drag coefficient and side force coefficient. In this case, however, deformation of the balloon by aerodynamic forces will be negligibly small. In the case of a 10-m-diameter balloon, for example, the internal–external pressure differential at the top of the balloon due to static pressure is about 100 Pa on the ground, whereas, the dynamic pressure on a balloon ascending at 5 m/s is an order of magnitude smaller, being about 15 Pa. In addition, the coefficients C_D and C_Y also include the air resistance originating from the uninflated lower part of the balloon. For large balloons that are usually used in the earth's stratosphere, C_D near the ground is of the order of 0.3.

If we take φ to be the angle between the vector \mathbf{i} and the vector obtained by projecting vector $\mathbf{v}_w - \mathbf{v}_b$ onto the xy plane, and if we take F_x , F_y , and F_z to be the respective components in the x , y , and z directions of the aerodynamic force \mathbf{F} acting on the balloon, we obtain

$$F_x = (F_D \sin \alpha + F_Y \cos \alpha) \cos \varphi, \quad (2.65)$$

$$F_y = (F_D \sin \alpha + F_Y \cos \alpha) \sin \varphi, \quad (2.66)$$

$$F_z = -F_D \cos \alpha + F_Y \sin \alpha. \quad (2.67)$$

At this point, for a balloon of mass m_b , a payload of mass m_p suspended from the bottom of the balloon, and ballast of mass m_c loaded therein, the balloon system mass (or the gross system mass) m_G is given by

$$m_G = m_b + m_p + m_c. \quad (2.68)$$

In addition, for lifting gas of mass m_g , the total balloon system mass m_t including the mass of the lifting gas is defined by

$$m_t = m_G + m_g. \quad (2.69)$$

The mass m_v is equal to the sum of m_t and the added mass determined by the direction of acceleration.

$$m_v = m_t + C_m \rho_a V_b. \quad (2.70)$$

Here the balloon's added mass coefficient C_m varies depending on the direction of the balloon's acceleration. For a sphere, it is 0.5, whereas for a zero-pressure balloon, vertical component of C_m varies from about 0.4 when the balloon is launched to 0.65 when the balloon has fully expanded. Conversely, the horizontal component of C_m decreases from 0.65 at the balloon launch to 0.4 when the balloon has expanded [15].

Based on the above, the equations of motion for the balloon are given as follows.

$$m_v \frac{d^2 x_b}{dt^2} = F_x, \quad (2.71)$$

$$m_v \frac{d^2 y_b}{dt^2} = F_y, \quad (2.72)$$

$$m_v \frac{d^2 z_b}{dt^2} = (\rho_a V_b - m_t)g + F_z. \quad (2.73)$$

If we assume an ideal gas, the atmospheric density ρ_a is expressed by

$$\rho_a = \frac{M_a p_a}{R T_a}, \quad (2.74)$$

where p_a is the atmospheric pressure, T_a is the atmospheric temperature, M_a is the average molecular weight of air, and R is the gas constant. If we assume that the lifting gas is an ideal gas, the balloon volume V_b can be expressed as

$$V_b = \frac{m_g R T_g}{M_g p_g}, \quad (2.75)$$

where M_g , T_g , and p_g are the lifting gas' molecular weight, temperature, and pressure, respectively. In a zero-pressure balloon, p_g and p_a can generally be considered to be equal. For a volumetric venting rate e_1 from the venting duct installed in the bottom part of the balloon and a lifting gas volumetric exhaust rate e_2 from the exhaust valve installed in the apex of the balloon, the mass balance for the lifting gas is

$$\frac{dm_g}{dt} = -\rho_g (e_1 + e_2), \quad (2.76)$$

or equivalently,

$$\frac{dm_g}{dt} = -\frac{p_g M_g}{RT_g} (e_1 + e_2), \quad (2.77)$$

where

$$e_1 = c_1 A_1 \sqrt{\frac{2\Delta p_1}{\rho_g}}, \quad (2.78)$$

$$e_2 = c_2 A_2 \sqrt{\frac{2\Delta p_2}{\rho_g}}, \quad (2.79)$$

where A_1 is the total cross-sectional area of the venting duct and A_2 is the total opening area of the exhaust valve. c_1 and c_2 are the respective flow rate constants that vary with number and shape and are equal to the product of the flow contraction coefficient and the rate coefficient. In addition, Δp_1 and Δp_2 indicate the pressure differentials between the lifting gas and the surrounding atmosphere at the end of the venting duct and at the opening of the exhaust valve, respectively.

The balloon system mass is reduced by dropping of ballast. The mass drop rate for the ballast is e_3 . More specifically,

$$\frac{dm_c}{dt} = -e_3. \quad (2.80)$$

To determine the lifting gas temperature T_g , it is necessary to consider the heat flow into and out of the balloon. If the heat that flows into the balloon envelope and the lifting gas are denoted by q_e and q_g , respectively, the envelope temperature T_e and the lifting gas temperature T_g can be expressed by the following two heat transfer equations:

$$m_e c_e \frac{dT_e}{dt} = q_e, \quad (2.81)$$

$$m_g c_{pg} \frac{dT_g}{dt} = q_g + V_b \frac{dp_g}{dt}, \quad (2.82)$$

where m_e is the mass of the envelope (which is different from the mass of the balloon m_b), c_e is the specific heat of the envelope, and c_{pg} is the specific heat of the lifting gas at constant pressure. By using (2.75) and the following equation

$$dp_a = -\rho_a g dz, \quad (2.83)$$

which expresses the relationship between the atmospheric pressure and density described in Sect. 2.3.1.3, (2.82) may be rewritten as [16]

$$m_g \frac{dT_g}{dt} = \frac{q_g}{c_{pg}} - \frac{g M_a m_g T_g}{c_{pg} T_a M_g} \frac{dz_b}{dt}. \quad (2.84)$$

The first term on the right-hand side is the heat influx to the lifting gas, and the second term is the effect of adiabatic expansion (or compression). Further details about the above-mentioned q_e and q_g are given in Sect. 2.4.4.

2.4.2 Vertical Motion of Balloons

At this point we describe a basic flight in which a balloon ascends and floats.

2.4.2.1 Stable Floating Condition

When a balloon is in a stable floating condition at a certain altitude, (2.73) is the equation for simple static balance.

$$(\rho_a V_b - m_t)g = 0. \quad (2.85)$$

Treating the atmosphere as an ideal gas, this equation may be rewritten as follows by using (2.74) and (2.75).

$$\frac{m_t}{m_g} = \frac{M_a p_a T_g}{M_g p_g T_a}. \quad (2.86)$$

If we define the ratio of the molecular weights of the gasses \tilde{M} here as

$$\tilde{M} = \frac{M_a}{M_g}, \quad (2.87)$$

an equation describing the general floating condition of a balloon is obtained from (2.86) as follows

$$\frac{m_t}{m_g} = \tilde{p}_g^{-1} \tilde{T}_g \tilde{M}, \quad (2.88)$$

where \tilde{p}_g and \tilde{T}_g are the lifting gas pressure and temperature dimensionalized by the pressure and temperature of the surrounding atmosphere, respectively.

$$\tilde{p}_g = \frac{p_g}{p_a}, \quad (2.89)$$

$$\tilde{T}_g = \frac{T_g}{T_a}. \quad (2.90)$$

In super-pressure balloons, $\tilde{p}_g > 1$, whereas in zero-pressure balloons and in partially inflated balloons, ordinarily $\tilde{p}_g = 1$, but even in the floating condition, the gas temperature and the surrounding atmospheric temperature are generally different. The floating condition for this kind of zero-pressure balloon is expressed by

$$\frac{m_t}{m_g} = \tilde{T}_g \tilde{M}. \quad (2.91)$$

If the lifting gas pressure and temperature are equal to the pressure and temperature of the surrounding atmosphere respectively, this simplifies to

$$\frac{m_t}{m_g} = \tilde{M}. \quad (2.92)$$

2.4.2.2 Motion in the Vertical Direction

The equation for motion in the vertical direction (2.73) can be rewritten as follows

$$\left(m_t + C_m m_g \tilde{M} \frac{\tilde{T}_g}{\tilde{p}_g} \right) \frac{d^2 z_b}{dt^2} = \left(m_g \tilde{M} \frac{\tilde{T}_g}{\tilde{p}_g} - m_t \right) g + F_z, \quad (2.93)$$

and if $\tilde{p}_g = 1$, this becomes

$$(m_t + C_m m_g \tilde{M} \tilde{T}_g) \frac{d^2 z_b}{dt^2} = (m_g \tilde{M} \tilde{T}_g - m_t) g + F_z. \quad (2.94)$$

Here the first term on the right-hand side expresses the net upward force of the buoyant force excluding gravity, and this is referred to as the free lift. This force changes during the flight depending on the relationship between the atmospheric temperature and the lifting gas temperature and on changes in the balloon's volume.

The ratio of the free lift divided by the acceleration due to gravity to the total balloon system mass including the lifting gas is denoted by \tilde{f} .

$$m_g \tilde{M} \tilde{T}_g - m_t = \tilde{f} m_t. \quad (2.95)$$

In particular, the free lift when leaving the ground is expressed by $\tilde{f}_0 m_t g$. When the balloon is leaving the ground, it is generally acceptable to consider the atmospheric temperature and the lifting gas temperature to be equal so that

$$m_g \tilde{M} - m_t = \tilde{f}_0 m_t. \quad (2.96)$$

2.4.2.3 Balloon's Rate of Ascent and Free Lift

When a balloon ascends at a constant speed in still air (free lift is positive), (2.94) becomes

$$(m_g \tilde{M} \tilde{T}_g - m_t) g + F_z = 0. \quad (2.97)$$

If we make use of the expression

$$V_b = m_g \frac{\tilde{M} \tilde{T}_g}{\rho_a}, \quad (2.98)$$

the balloon's rate of ascent is given by the following expression

$$v_{bz}^2 = 2 \frac{m_g \tilde{M} \tilde{T}_g - m_t}{\rho_a C_D A_b} g. \quad (2.99)$$

If the shape of the balloon can be approximated by a sphere, (2.99) becomes

$$v_{bz}^2 = 4 \left(\frac{2}{9\pi} \right)^{\frac{1}{3}} \frac{g}{C_D} \left(\frac{m_t}{\rho_a} \right)^{\frac{1}{3}} \frac{(1 + \tilde{f}) \tilde{T}_g - 1}{(1 + \tilde{f})^{\frac{2}{3}} \tilde{T}_g^{\frac{2}{3}}}. \quad (2.100)$$

The velocity when the balloon leaves the ground $v_{bz,0}$ may be obtained by setting $\tilde{T}_g = 1$

$$v_{bz,0}^2 = 4 \left(\frac{2}{9\pi} \right)^{\frac{1}{3}} \frac{g}{C_D} \left(\frac{m_t}{\rho_a} \right)^{\frac{1}{3}} \frac{\tilde{f}_0}{(1 + \tilde{f}_0)^{\frac{2}{3}}}. \quad (2.101)$$

In stratospheric ballooning, the fraction of free lift is usually expressed by the ratio of free lift to the balloon's system mass m_G . Hence, we introduce f , which is defined by

$$\tilde{f}m_t = fm_G. \quad (2.102)$$

This f is termed the free lift rate. Unless indicated otherwise, the free lift rate usually refers to free lift rate when leaving the ground, f_0 . Furthermore, there is the following relationship between f_0 and \tilde{f}_0 .

$$f_0 = \frac{\tilde{f}_0 \tilde{M}}{\tilde{M} - \tilde{f}_0 - 1}. \quad (2.103)$$

The following relationship holds when lifting gas is not vented,

$$f = \frac{\tilde{f} \tilde{M} \tilde{T}_g}{\tilde{M} \tilde{T}_g - \tilde{f} - 1}. \quad (2.104)$$

By making use of the free lift rate, the following equation can be used to express the balloon's rate of ascent instead of (2.100).

$$v_{bz}^2 = 4 \left(\frac{2}{9\pi} \right)^{\frac{1}{3}} \frac{g}{C_D} \left(\frac{m_G}{\rho_a} \right)^{\frac{1}{3}} \frac{(1+f) \tilde{M} \tilde{T}_g - (f + \tilde{M})}{(\tilde{M} - 1)^{\frac{1}{3}} [(1+f) \tilde{M} \tilde{T}_g]^{\frac{2}{3}}}. \quad (2.105)$$

The velocity when leaving the ground $v_{bz,0}$ is obtained by setting $\tilde{T}_g = 1$ in (2.105).

For a stratospheric balloon, Fig. 2.29 shows the relationship between the free lift rate on the ground f_0 and m_G for different values of the balloon rate of ascent v_{bz} . The lifting gas is assumed to be helium and the drag coefficient of the balloon C_D is assumed to be 0.3. As m_G increases, f_0 decreases. During balloon ascent, the temperature of the lifting gas decreases due to adiabatic expansion. Since the second term on the right-hand side of (2.84) expresses this temperature change caused by adiabatic expansion (which becomes adiabatic compression during descent), the change in T_g attributable to only adiabatic expansion is expressed by

$$\frac{dT_g}{dz} = - \frac{g \tilde{M} \tilde{T}_g}{c_{pg}}. \quad (2.106)$$

Using this equation, we consider the hypothetical case of ascent from a state in which there is no difference between the atmospheric temperature and the lifting gas temperature ($\tilde{T}_g = 1$). By calculating the change in helium gas temperature with altitude, the temperature drop with altitude is found to be -13.7 K/km. In the same way, the temperature drop with altitude due to atmospheric adiabatic expansion for dry air is -9.8 K/km. The actual tropospheric temperature drop with altitude is low at -6.5 K/km, but this is due to the effects of water vapor (see Sect. 3.1.2 for a detailed explanation of changes in atmospheric temperature with altitude).

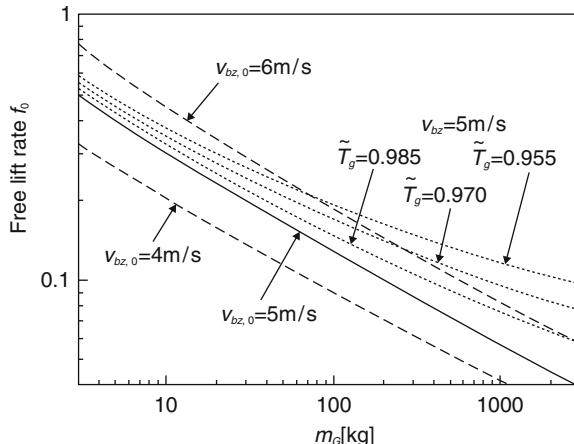


Fig. 2.29 Relationship between the balloon system mass and the free lift rate required to obtain a specified rate of ascent. The solid line and the dashed lines show the case when $\tilde{T}_g = 1$

In other words, based just on the effect of adiabatic expansion of the atmosphere and the lifting gas, the difference in the temperature drop with altitude is -7.2 to -3.9 K/km, and left this way, the temperature difference will increase with ascent. In reality, however, the lifting gas is warmed by convective flow with the atmosphere and by radiation. In addition, if the temperature of the lifting gas decreases, the buoyant force and rate of ascent will also decrease, counteracting the effects of adiabatic expansion. Because of these factors, the lifting gas temperature usually remains a few degrees below the atmospheric temperature when a balloon ascends.

By introducing this temperature drop, the free lift rate required for a certain balloon ascent speed (5 m/s) is indicated by the dotted line in Fig. 2.29. As for the lines shown in Fig. 2.29, at their respective ground conditions $\tilde{T}_g = 0.985$ corresponds to $T_g - T_a = -4.3^\circ\text{C}$; $\tilde{T}_g = 0.970$ corresponds to $T_g - T_a = -8.6^\circ\text{C}$, and $\tilde{T}_g = 0.955$ corresponds to $T_g - T_a = -13^\circ\text{C}$.

Ordinarily, the ratio of the heat loss due to adiabatic expansion to the heat influx by convective and radiative heat transfers increases as the cube root of the balloon volume. Therefore, if m_G increases, the increase in the free lift rate necessary to compensate the buoyancy loss caused by the temperature drop in order to obtain the required rate of ascent will become larger.

In fact, the free lift rate necessary to obtain a rate of ascent of 5 m/s in Fig. 2.29 is approximately equal to the curve shown at $\tilde{T}_g = 0.985$ when m_G is small, and it approaches the line $\tilde{T}_g = 0.970$ as m_G becomes larger. In other words, the lifting gas temperature for a normal balloon is about 5°C below the temperature of the surrounding atmosphere, and for large balloons exceeding 1 ton, it is more than 7°C lower.

As (2.100) shows, if the free lift rate does not change, the balloon rate of ascent is proportional to the $-1/6$ power of the atmospheric density, and it increases with altitude. In actual fact, however, the free lift rate due to adiabatic expansion given

above decreases in normal ascent. Consequently, there is no marked change in the rate of ascent for large balloons. This is because if the rate of ascent increases, the buoyancy decreases due to the increase in the temperature drop rate caused by adiabatic expansion resulting in a drop in the rate of ascent.

On the one hand, however, for the case when the reduction in the atmospheric temperature with height is very high (as when passing through the tropopause (see Sect. 3.1.2), for example), the rate of ascent decreases considerably due to the sudden increase in the temperature difference between the atmosphere and lifting gas. For details, refer to Sect. 2.4.4. On the other hand, in the case of small high-altitude balloons whose ratio of the volume at full expansion to that on the ground is around 1,000, after they clear the tropopause, the tendency for the rate of ascent to increase with altitude becomes stronger.

2.4.2.4 Balloon Floating Altitude

The line denoted a in Fig. 2.30 represents the variation in the atmospheric density with altitude. The horizontal axis is the logarithm of density. If we assume that for a balloon that is ascending the temperatures of the lifting gas and the atmosphere are the same ($\tilde{T}_g = 1$), the balloon density ρ_b , which is defined by the following equation, is smaller than ρ_a by the amount of free lift, and the balloon ascends along the line labeled “b” in the figure.

$$\rho_b = \frac{m_t}{V_b} \quad (2.107)$$

The altitude at which the internal pressure of the balloon and the atmospheric pressure are equal is called the pressure altitude, and this point is regarded as State 1.

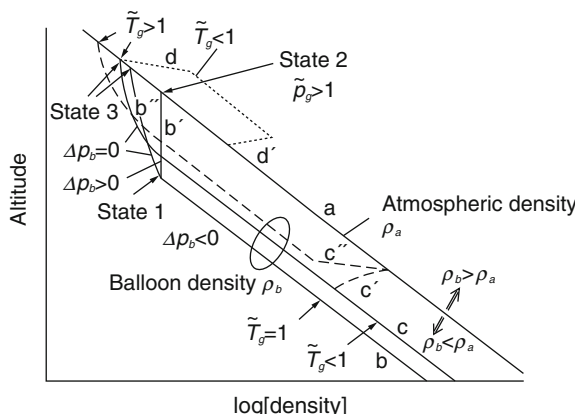


Fig. 2.30 Relationship between atmospheric density and balloon density when a balloon ascends and descends

On the one hand, for balloons such as super-pressure balloons that do not vent gas, the balloon continues to ascend still further from State 1, until the balloon density and the atmospheric density are equal. This point is called State 2. On the other hand, in the case of a zero-pressure balloon, ascent continues further from State 1 at constant V_b while venting the free-lift portion of lifting gas and maintains a constant altitude after $\rho_b = \rho_a$. The altitude at this point is called the density altitude, and it is regarded as State 3.

The density altitude when the lifting gas temperature and the atmospheric temperature are equal is called the isothermal density altitude, and it is determined by

$$\rho_{a3} = \frac{m_G \tilde{M}}{V_{b\max}(\tilde{M} - 1)}, \quad (2.108)$$

where $V_{b\max}$ is the balloon's maximum volume. However, usually, the lifting gas temperature is different from the atmospheric temperature, and the actual achievable altitude is given by

$$\rho_{a3} = \frac{m_G \tilde{M} \tilde{T}_g}{V_{b\max}(\tilde{M} \tilde{T}_g - 1)}. \quad (2.109)$$

Next, during the ascent stage after leaving the ground until reaching State 1, at which the venting of lifting gas begins, the following equation holds

$$\rho_a = \frac{m_t}{V_b} (1 + \tilde{f}_0) \tilde{T}_g. \quad (2.110)$$

This means that if $\rho_a > \rho_b$, i.e., $\tilde{T}_g > 1/(1 + \tilde{f}_0)$, the balloon ascends, and if $\rho_a < \rho_b$, i.e., $\tilde{T}_g < 1/(1 + \tilde{f}_0)$, the balloon starts to descend. Usually, because $\tilde{T}_g < 1$ during ascent, the balloon ascends along line c, which lies closer to line a than to line b in Fig. 2.30.

The altitude of State 1 is

$$\rho_{a1} = \frac{m_t}{V_{b\max}} (1 + \tilde{f}_0) \tilde{T}_g = \frac{m_G}{V_{b\max}} \frac{1 + f_0}{\tilde{M} - 1} \tilde{M} \tilde{T}_g. \quad (2.111)$$

For super-pressure balloons that do not vent gas, if the internal balloon gas pressure p_g is greater than the atmospheric pressure p_a , in other words, if

$$\frac{\tilde{M}(1 + f_0)\tilde{T}_g}{\tilde{M} + f_0} > 1, \quad (2.112)$$

then the achievable altitude will be nearly independent of the lifting gas temperature and will be given by

$$\rho_{a2} = \frac{m_G}{V_{b\max}} \frac{\tilde{M} + f_0}{\tilde{M} - 1}. \quad (2.113)$$

Table 2.2 Differences in pressure altitude and density altitude

Density	$f_0 = 0.1$	$f_0 = 0.3$		
	$\tilde{T}_g = 1$	$\tilde{T}_g = 0.95$	$\tilde{T}_g = 1.05$	$\tilde{T}_g = 0.95$
ρ_{a1}	1.276	1.213	1.340	1.433
ρ_{a2}	1.176	1.176	1.176	1.208
ρ_{a3}	1.160	1.170	1.152	1.170

When the lifting gas temperature drops (such as at night) in cases where the decrease in the internal pressure with the temperature drop is larger than the pressure proportion equivalent to the free-lift gas, the balloon is no longer a super-pressure balloon and has become a zero-pressure balloon.

As an example, Table 2.2 shows, for a stratospheric balloon, how the altitude (atmospheric density) changes for the cases when $f_0 = 0.1$ and $f_0 = 0.3$ in States 1–3. The atmospheric density (and hence the altitude) for each state may be determined by multiplying the values shown in the table by $m_G/V_{b\max}$. Specifically, if we assume that $m_G/V_{b\max} = 0.0073$, then for the case where $f_0 = 0.1$ and $\tilde{T}_g = 1$, the altitude difference between States 1 and 3 will be about 530 m, and the altitude difference between States 2 and 3 will be about 190 m. If the free lift rate becomes larger, for $f_0 = 0.3$ and $\tilde{T}_g = 0.95$, the altitude difference between States 1 and 2 will be about 1,300 m.

Usually, a balloon enters a level flight with a low temperature $\tilde{T}_g < 1$, and subsequently, because the gas warms, and the temperature rises during the day, the temperature becomes $\tilde{T}_g > 1$, and the balloon climbs slightly and once again enters a level flight; this is indicated by line c in Fig. 2.30. In Table 2.2, \tilde{T}_g changes from 0.95 to 1.05.

2.4.2.5 Upward Motion Operation

Line c in Fig. 2.30 shows the case where ascent is stopped by forcibly exhausting gas through the exhaust valve during ascent. When ballast is subsequently dropped and the balloon climbs again (shown by line c in Fig. 2.30), the final float altitude increases. On the other hand, when the lifting gas temperature drops at night, the balloon starts to descend as indicated by line d in Fig. 2.30. The descent stops if ballast is jettisoned since the balloon density decreases as shown by line d in Fig. 2.30.

2.4.3 Horizontal Motion of Balloons

As shown in (2.71) and (2.72), balloon motion in the horizontal direction is governed by the aerodynamic forces produced by the difference between the velocity of the

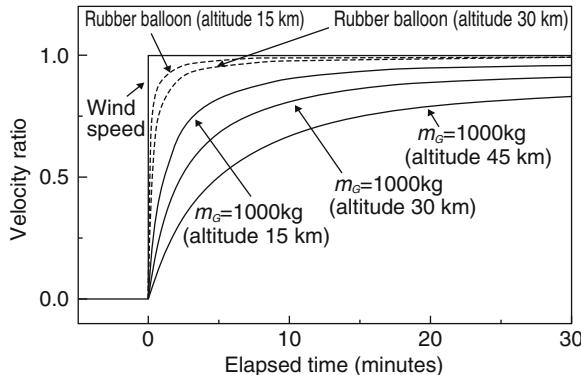


Fig. 2.31 Balloon motion when there is a step change in the speed of the surrounding wind

balloon in the horizontal plane and the wind velocity. If the wind velocity does not vary with time and location, this difference in velocity gradually disappears, and ultimately, the balloon moves at the same speed as the surrounding winds. However, since the wind varies with location, altitude, and time, as well as fluctuating abruptly, the horizontal motion of the balloon is not necessarily the same as the movement of the surrounding atmosphere. In particular, because a balloon at a high altitude has an extremely large volume, it is necessary to account for the slow response of the balloon to changes in the wind.

As a simple example, Fig. 2.31 shows how the speed of a balloon changes with time when the wind speed of the surrounding air changes suddenly by 2 m/s. For comparison, the motion of a radiosonde rubber balloon used in upper atmosphere observations (Sect. 3.6) is also shown.

The time required for a suddenly produced difference between the wind's velocity and the velocity of a small rubber balloon to diminish to 25% of its initial value is approximately 20 s at an altitude of 15 km, and even at an altitude of 30 km it is about 40 s. By contrast, the time required for a balloon having a balloon system mass of 1,000 kg is approximately 3 min at an altitude of 15 km and about 7 min at an altitude of 30 km, and this time extends to 15 min at an altitude of 45 km. While this is an extreme example, it is normal for balloons having diameters in the tens of meters or larger to require several minutes to acquire almost the same velocity vector as that of the surrounding wind. This means that a balloon ascending at 5 m/s will have ascended several kilometers by the time it changes direction.

2.4.4 Balloon Heat Balance

In this section, we describe the balloon heat balance that determines the temperature of the lifting gas. In other words, we determine q_e and q_g in (2.18) and (2.82). In the following description, “atmosphere” refers to the planetary atmosphere in which the balloon is flying, and “ground surface” means the ground surface of the planet.

As shown in Fig. 2.27, in addition to absorbing solar radiation, the envelope and lifting gas of a balloon flying in the atmosphere emit long-wavelength radiation into space and to the ground surface. In addition, the ground surface and atmosphere reflect part of the solar radiation energy, and along with infrared radiation from the ground surface, this radiation is partially absorbed by the balloon envelope and lifting gas. The reflection from the ground surface varies greatly depending on latitude, the condition of the ground surface, and whether or not there are clouds. In addition, there is heat transfer resulting from convective flow between the envelope and atmosphere and between the envelope and lifting gas. The radiative heat transfer between the envelope and lifting gas may be neglected since the temperature difference between them is small.

2.4.4.1 Envelope and Lifting Gas Heat Transfer

Here, we approximate the balloon as being spherical for simplicity, and denote its effective cross-sectional area as A_e , and its effective surface area as S_e . The heat flow into the balloon's envelope q_e and lifting gas q_g are given by the following equations, respectively

$$q_e = \tilde{\alpha}_e I_0 (A_e + F_{bs} a_s S_e) + \tilde{\epsilon}_e \sigma S_e (F_{bs} T_s^4 - T_e^4) + \tilde{\epsilon} \sigma S_e (T_g^4 - T_e^4) + h_{ge} (T_g - T_e) + h_{ae} (T_a - T_e), \quad (2.114)$$

$$q_g = \tilde{\alpha}_g I_0 (1 + a_s) S_e + \tilde{\epsilon}_g \sigma S_e (T_s^4 - T_g^4) + \tilde{\epsilon} \sigma S_e (T_e^4 - T_g^4) + h_{ge} (T_e - T_g), \quad (2.115)$$

where I_0 is the solar constant, and it is corrected depending on the altitude and the solar altitude, a_s is the reflectance of the ground surface (albedo), and it varies depending on the location of the balloon, the time, and whether or not there are clouds. $\tilde{\alpha}_e$ is the effective solar absorptivity and $\tilde{\epsilon}_e$ is the effective infrared emissivity of the envelope; $\tilde{\epsilon}$ is the effective emissivity between the envelope and lifting gas; and $\tilde{\alpha}_g$ is the effective solar absorptivity and $\tilde{\epsilon}_g$ is the effective infrared emissivity for the lifting gas. T_s denotes the effective temperature of the ground surface viewed from the balloon, and it varies depending on the altitude, whether it is daytime or nighttime, and the cloud conditions. h_{ge} and h_{ae} are the convective heat transfer coefficients between the lifting gas and envelope and between the envelope and atmosphere, respectively. σ is the Stefan-Boltzmann constant. In addition, F_{bs} is the shape factor from the balloon to the planet, and it is 0.5 for a sphere.

If we consider the reflections from the balloon's interior, the effective emissivity and the effective absorptivity of the envelope and lifting gas can be determined using the following equations [16]

$$\tilde{\alpha}_e = \alpha_e \left(1 + \frac{\tau_e (1 - \alpha_g)}{1 - r_e (1 - \alpha_g)} \right), \quad (2.116)$$

$$\tilde{\varepsilon}_e = \varepsilon_e \left(1 + \frac{\tau_{ei}(1 - \varepsilon_g)}{1 - r_{ei}(1 - \varepsilon_g)} \right), \quad (2.117)$$

$$\tilde{\varepsilon} = \frac{\varepsilon_e \varepsilon_g}{1 - r_{ei}(1 - \varepsilon_g)}, \quad (2.118)$$

$$\tilde{\alpha}_g = \frac{\alpha_g \tau_e}{1 - r_e(1 - \alpha_g)}, \quad (2.119)$$

$$\tilde{\varepsilon}_g = \frac{\varepsilon_g \tau_{ei}}{1 - r_{ei}(1 - \varepsilon_g)}, \quad (2.120)$$

where τ_e is the solar transmissivity of the envelope, τ_{ei} is the infrared transmissivity of the envelope, r_e is the solar reflectivity of the envelope, r_{ei} is the infrared reflectivity of the envelope, α_e is the solar absorptivity of the envelope, α_{ei} is the infrared absorptivity of the envelope, ε_e is the infrared emissivity of the envelope, α_g is the solar absorptivity of the lifting gas, and ε_g is the infrared emissivity of the lifting gas.

In reality, until the balloon is fully inflated, there is excess envelope (film) in the lower part of the balloon in the circumferential direction, and there are areas that overlap each other. As a result, the thickness differs depending on the location, and these equations become more complicated.

By using Nu_a and Nu_g to denote the Nusselt numbers for the atmosphere and the lifting gas, respectively, and the λ_a and λ_g to denote the thermal conductivities of the atmosphere and lifting gas, respectively, the convective heat transfer coefficients can be expressed by

$$h_{ge} = \frac{Nu_g \lambda_g}{D_b}, \quad (2.121)$$

$$h_{ae} = \frac{Nu_a \lambda_a}{D_b}, \quad (2.122)$$

where D_b is the balloon diameter.

The Nusselt number for the atmosphere for natural convection is given by

$$Nu_a = 2 + 0.589(Gr_a Pr_a)^{1/4} / [1 + (0.469/Pr_a)^{9/16}]^{4/9}, \quad (2.123)$$

$(Pr_a \geq 0.7, Gr_a Pr_a \leq 10^{11})$

and for forced convection, it is given by [17, 18]

$$Nu_a = 2 + 0.03 Pr_a^{0.33} Re_b^{0.54} + 0.35 Pr_a^{0.36} Re_b^{0.58}. \quad (2.124)$$

If we consider the presence of natural convection within the balloon, the Nusselt number for the lifting gas is determined by [18]

$$Nu_g = 0.54(Gr_g Pr_g)^{1/4} \quad (Gr_g Pr_g < 2 \times 10^7), \quad (2.125)$$

$$Nu_g = 0.135(Gr_g Pr_g)^{1/3} \quad (Gr_g Pr_g > 2 \times 10^7), \quad (2.126)$$

where Gr_a and Gr_g are the Grashof numbers for the atmosphere and lifting gas, respectively, and Pr_a and Pr_g are the Prandtl numbers for the atmosphere and lifting gas, respectively.

With this, the equations describing balloon motion are complete. If (2.71) to (2.73), (2.114), and (2.115) are solved for specified initial conditions, it is possible to derive the balloon's behavior. In the next section, we look at the example of a stratospheric balloon over the earth and present a number of examples of calculations.

2.4.4.2 Ascending Motion

The two curves shown in Fig. 2.32 are a comparison of typical calculations for the cases of stratospheric balloons launched during the day and at night. The appropriate initial buoyancy is provided so that the average rate of ascent is about 5 m/s, and no ballast is dropped to correct the speed during flight.

The balloon ascends into the troposphere at roughly constant speed. When past the tropopause the atmospheric temperature drop ceases, and in due course it rises with altitude (refer to Sects. 3.1.2 and 3.1.3 for a detailed explanation of the structure of the stratosphere), but the temperature of the lifting gas continues to fall due to adiabatic expansion. Consequently, the temperature difference between the atmosphere and the lifting gas grows larger, and this results in a substantial drop in buoyancy. As the figure shows, the balloon's rate of ascent falls off in this vicinity. However, during the day, since there is sunlight, this temperature drop is gradually eliminated compared with that at nighttime as shown in Fig. 2.33a, and the temperature difference does not become much larger.

In addition, the aerodynamic forces in the vertical direction acting on a balloon are proportional to the balloon's cross-sectional area, and the buoyancy is proportional to the balloon's volume. Consequently, as the altitude increases, the upward

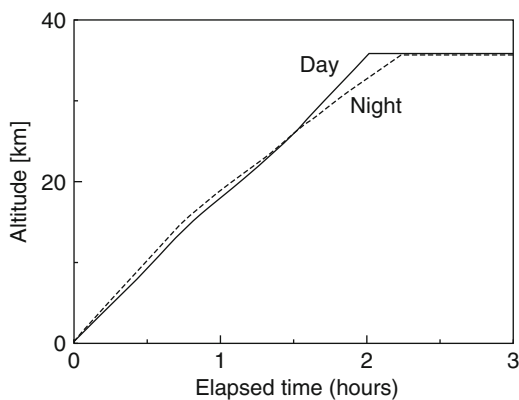


Fig. 2.32 Ascent of a zero-pressure balloon. Difference between balloons launched at day and night

Difference between balloons launched at day and night

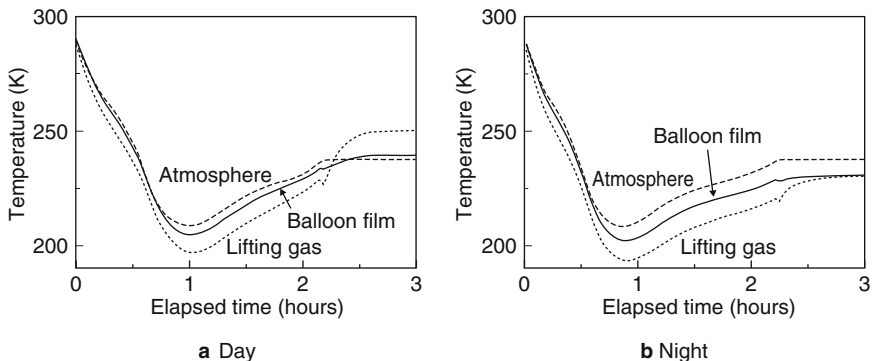


Fig. 2.33 Changes in atmospheric temperature, balloon film temperature, and lifting gas temperature. **a** and **b** correspond to day and night in Fig. 2.32, respectively: **a** Day; **b** Night

force increases in proportion to the third power of the balloon volume. This means that the rate of ascent increases in proportion to the 1/6-power of the balloon's volume. On the one hand, because of the combined effects of this and of sunlight, a balloon that slows down in the tropopause will start to gradually accelerate.

On the other hand, if a balloon ascends at night, since there is no supply of thermal energy from sunlight, as shown by the temperature changes in Fig. 2.33b, the temperature difference that begins in the tropopause does not diminish much. As a result, the balloon's rate of ascent beyond the tropopause does not increase very much. Hence, if there are cold clouds below, the slowing effect may be too large, and the balloon's rate of ascent may drop off greatly. Consequently, to avoid such excessive slowing, the free lift at night is often made larger than that during the day. In the calculation for the nighttime case shown in Figs. 2.32 and 2.33b, the free lift rate was increased by approximately 2% compared with that in the daytime.

2.4.4.3 Behavior Near the Float Altitude

Figure 2.34 is an enlargement of part of the altitude changes shown in Fig. 2.32. As shown in the figure, while the venting of the free-lift portion of the lifting gas starts a little below the float altitude, because the lifting gas temperature is lower than the atmospheric temperature, the balloon finishes venting and attains the float condition at an altitude lower than the isothermal density altitude. Subsequently, in accordance with the warming of the lifting gas, the balloon oscillates up and down a number of times and comes to rest at its final float altitude.

Venting of lifting gas is carried out a number of times in response to this oscillation. In the daytime case, because solar radiation induces a large increase in the temperature of the lifting gas, this up-and-down motion is usually small. However, these flight situations undergo various changes under different conditions. In the example shown in the figure, in the daytime case, the oscillation is small because the lifting gas temperature increases over the interval that gas is vented and the rate of

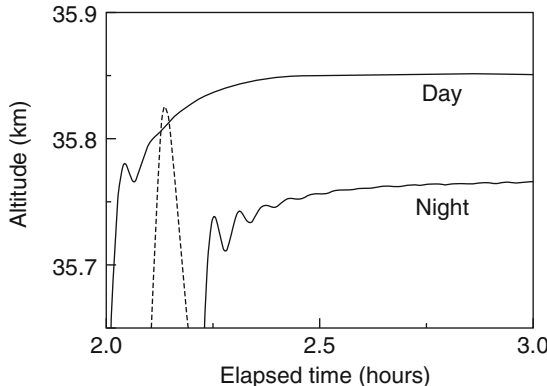


Fig. 2.34 Enlargement of Fig. 2.32 in the vicinity of where the at-float altitude is attained. The balloon reaches its level flight altitude by changing altitude up and down a few times as shown by the *solid line*. Venting of the lifting gas occurs 2–3 times in response. The *dashed line* shows the calculation results for the hypothetical case in which it is assumed that there is no temperature drop due to adiabatic expansion. Since the balloon ascends beyond its level flight altitude due to its inertial motion, there is excessive venting, and the balloon starts to descend after reaching its maximum altitude

ascent drops. However, the oscillations repeat in the nighttime example, since a long time is required for heat exchange with the atmosphere.

If there is no drop in gas temperature during ascent, and if we assume that $\tilde{T}_g = 1$ at all times, after the balloon reaches the float altitude, the balloon will ascend to a higher altitude due to inertial motion, and because lifting gas will be excessively vented, the balloon will commence to descend at a rate of approximately 1 m/s (as shown by the dashed line in Fig. 2.34).

2.4.4.4 Infrared Radiation Effects

Figure 2.35 shows the inflow and outflow of heat to the balloon film (envelope) and lifting gas term-by-term for the two calculations shown in Figs. 2.32 and 2.33.

It shows that, in contrast to the effect of adiabatic expansion, which remains approximately constant from immediately after launch until just before reaching float altitude, the quantity of absorbed radiation heat, while initially very small, gradually becomes larger as the altitude increases, and it exceeds the heat produced by adiabatic expansion. In particular, the absorption and radiation in the infrared region are shown to become even larger than the absorbed solar energy.

In the balloon's float condition, the energy absorbed from the sun, the infrared absorption from the ground, and the infrared radiation radiated to space are in equilibrium. In the float condition, provided the temperature does not change, the quantity of infrared radiation essentially does not change. However, if the condition under the balloon changes, the amount of infrared absorbed is expected to change greatly.

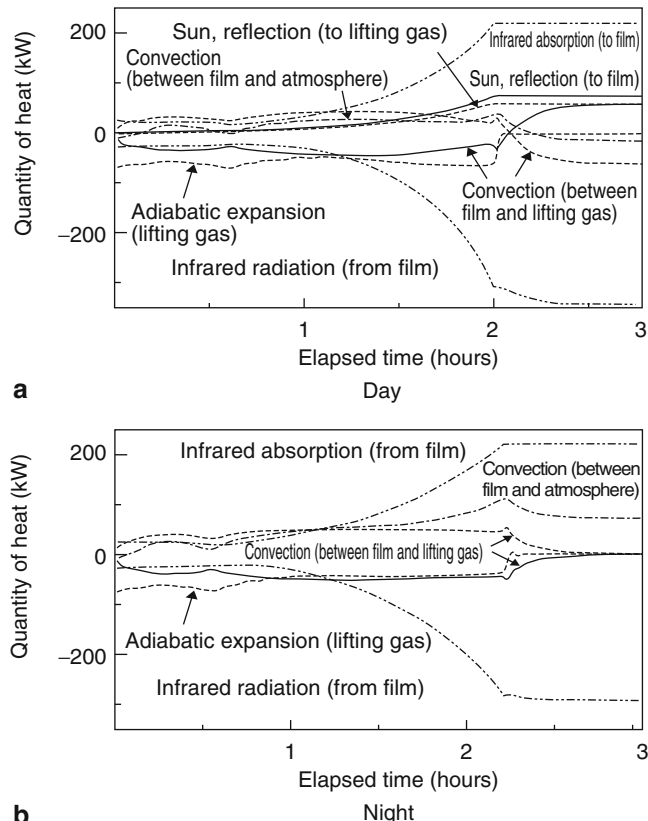


Fig. 2.35 Heat going into and out of balloon film and lifting gas. Figures **a** and **b** correspond to day and night in Fig. 2.32, respectively: **a** Day; **b** Night

A typical example of this is the difference between when there are no clouds under the balloon and when the area under the balloon is covered with cold clouds.

In the daytime, even if the area below the balloon is covered with clouds and the quantity of infrared radiation from below is reduced, since the reflection of solar radiation from the clouds compensates this decrease, the quantity of heat absorbed by the balloon film and lifting gas does not change greatly. Thus, the flight usually maintains a stable altitude. In contrast, since there is no solar radiation at night, if the area below is covered with cold clouds, the amount of infrared absorption drops off, and this is related directly to a drop in the balloon film's temperature.

Figure 2.36 shows calculation examples for this extreme case. In a period of 30 min, a balloon travels from a location where there are no clouds to a location where the area below the balloon is completely covered by clouds. The condition that the effective temperature T_s drops by 20°C continues for a while, as shown by the hatched region in the figure. In this kind of extreme case, the balloon loses substantial buoyancy and starts to descend. The final rate of descent reaches

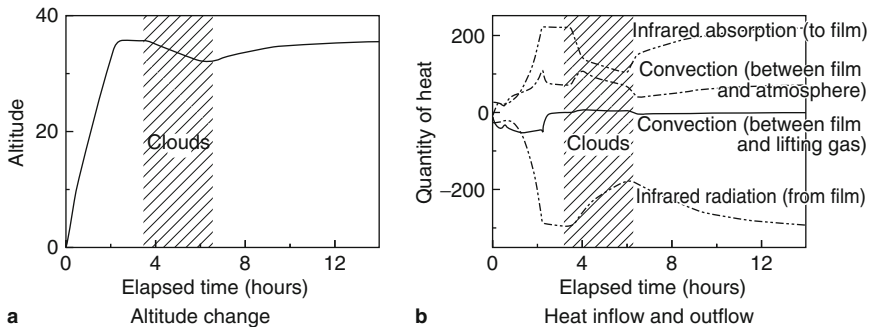
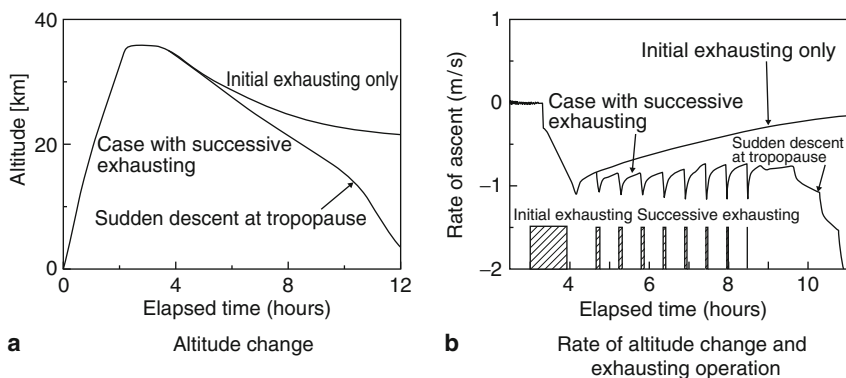


Fig. 2.36 Calculation results for a case where the area below the balloon is covered with cold clouds: **a** Altitude change; **b** Heat inflow and outflow



Successive exhausting is required to descend at a fixed rate.

Fig. 2.37 Simulation results for descending from a float condition by opening the exhaust valve. Successive exhausting is required to descend at a fixed rate: **a** Altitude change; **b** Rate of altitude change and exhausting operation

0.3–0.4 m/s. However, if the clouds disappear and the infrared absorption is restored, the balloon stops descending, gradually turns around and starts to ascend again, but the speed of altitude recovery can be seen to be very slow, being about 0.1–0.3 m/s.

2.4.4.5 Descending Motion

To vary the altitude of a balloon that is in a level-flight condition, ballast is dropped to ascend, and lifting gas within the balloon is exhausted by opening the exhaust valve installed in the apex of the balloon to descend.

When descending by exhausting lifting gas from the exhaust valve, in contrast to the case for ascending, the temperature of the lifting gas increases due to adiabatic compression. Consequently, although it is assumed that a given rate of descent can be obtained by exhausting the required amount of gas to lose a certain amount of buoyancy, as the results of numerical simulations shown in Fig. 2.37 demonstrate,

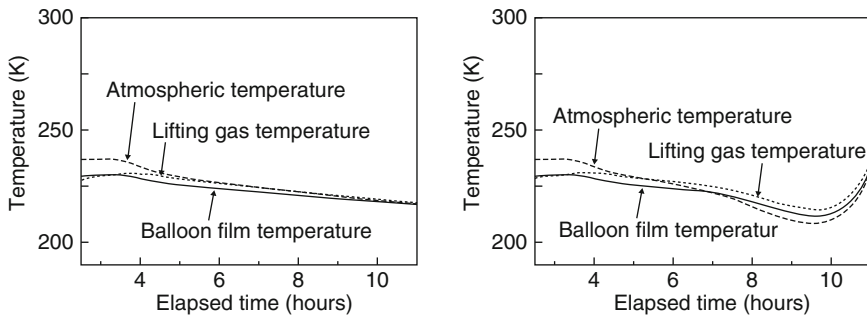


Fig. 2.38 Changes in atmospheric temperature, balloon film temperature, and lifting gas temperature. Figures **a** and **b** correspond, respectively, to the case when there is initial exhausting only and the case where successive exhausting is performed as shown in Fig. 2.37a, **b**

with just an initial exhausting, the gas temperature increases and the rate of descent declines, and ultimately, the descent may stop. The temperature change at this time is shown in Fig. 2.38a.

Consequently, successive exhausting is required to make the balloon descend at a constant rate. Since the valves normally used are not able to control the flow rate, exhausting is continued intermittently as shown in the bottom part of Fig. 2.37b in order to maintain an approximately constant rate of descent. The temperature of the lifting gas at this time rises above that of the surrounding atmosphere as shown in Fig. 2.38b.

The phenomena described above occur at altitudes higher than the tropopause. Since the temperature of the atmosphere rises when the flight altitude falls below the tropopause, it becomes difficult to stop the balloon's descent because the rate of descent rapidly increases even if the successive exhausting is terminated, as the example of successive exhausting shown in Fig. 2.37 demonstrates.

References

1. Archimedes, H.T.L. (ed): *The Works of Archimedes*, Dover Publications, New York, (2002)
2. Markhardt, T.: Recent Developments in the Use of Thin-Film Polyethylene Balloons for Meteorological Applications, AIAA Int. Balloon Technol. Conf., AIAA-91-3691-CP, 215–216 (1991)
3. Yamagami, et al.: Development of the Highest Altitude Balloon, *Adv. Space Res.*, Vol. 33, No. 7, 1653–1659, (2004)
4. Prandtl, L., Tiejens, O.G., (Translated by Rosenhead, L.): *Fundamentals of Hydro-and Aeromechanics*, McGraw-Hill, New York, (1934)
5. Upson, R.H.: Stress in a Partially Inflated Free Balloon -with Note on Optimum Design and Performance for Stratosphere Exploration, *J. Astronaut. Sci.*, Vol. 6, No. 2, 153–156 (1939)
6. Smalley, J.H.: Determination of the Shape of a Free Balloon, AFCRL-65-92, (1965)

7. Yajima, N.: Survey of Balloon Design Problems and Prospects for Large Super-Pressure Balloons in the Next Century, *Adv. Space Res.*, Vol. 30, No. 5, 1183–1192 (2002)
8. Smalley, J.H.: Development of the e-Balloon, *Proc 6th AFCRL Sci. Balloon Symp.*, 167–176 (1970)
9. Yajima, N.: A New Design and Fabrication Approach for Pressurized Balloon, *Adv. Space Res.*, Vol. 26, No. 9, 1357–1360 (2000)
10. Yajima, N., et al.: Three Dimensional Gore Design Concept for High-Pressure Balloons, *J. Aircr.*, Vol. 38, No. 4, 738–744 (2001)
11. Yajima, N., Izutsu, N.: Super-Pressure Balloon and Method of Manufacturing the Same, US Patent No. 6290172, (2001)
12. Izutsu, N., et al.: Flight Demonstration of a Superpressure Balloons by Three-Dimensional Gore Design, *Adv. Space Res.*, Vol. 30, No. 5, 1221–1226 (2002)
13. Smith Jr., J.H.: Development of Sky Anchor Balloon System, *Proc. 10th AFCRL Sci. Balloon Symp.*, 81–101 (1978)
14. Pommereau, J.P., et al.: First results of a Stratospheric Experiment Using a Montgolfiere Infra-Rouge (MIR), *Adv. Space Res.*, Vol. 5, No. 1, 27–30 (1985)
15. Anderson, W.J., Shah, G.N., Park, J.: Added Mass of High-Altitude Balloons, *J. Aircr.*, Vol. 32, 285–289 (1995)
16. Carlson, L.A., Horn, W.J.: New Thermal and Trajectory Model for High-Altitude Balloons, *J. Aircr.*, Vol. 20, 500–507 (1983)
17. Incropera, F.R., de Witt, D.P.: *Introduction to Heat Transfer*, John Wiley & Sons, New Jersey, (1990)
18. Kutateladze, S.S., Borishanskii, V.M.: *A Concise Encyclopedia of Heat Transfer*, Pergamon Press, Oxford, (1966)

Chapter 3

Stratospheric Balloons

Abstract To provide details concerning stratospheric balloons, this chapter first presents a brief summary of the composition of the earth's atmosphere and air movement within the atmosphere. Up-to-date meteorological data both prior to launch and during the flight are essential for ensuring safety during a flight, as are forecast predictions. Collection of upper-air data obtained by objective analysis and numerical prediction is described. The utilization of these data for numerically simulating balloon flight paths is also mentioned. Next, common on-board instruments used for balloon flight control are described. We then explain how balloons are launched and how their flights are controlled. The facilities for balloon launching and radio tracking of balloons are introduced. In addition, the materials and manufacturing processes for balloon membranes are presented. Rubber balloon technology for meteorological observation is also described. Typical examples of balloon utilizations in various science and technology fields are mentioned at the final section.

3.1 The Earth's Atmosphere

3.1.1 *The Composition of the Atmosphere*

In this section, we give an overview of the structure and movement of the earth's atmosphere, the medium in which balloons fly. See reference [1, 2] for a detailed explanation concerning meteorology.

The principal constituents of the earth's atmosphere are shown in Table 3.1. Although the atmosphere also contains water vapor at a few percent or less, it has not been included in the table since its level varies greatly with time and location. With the exception of water vapor, the composition of air remains largely the same up to an altitude of around 80 km. Nitrogen accounts for approximately 80% of the atmosphere, and it is thought to have been present since the early period of the earth's formation. Oxygen makes up approximately 20% of the earth's atmosphere, and it is

Table 3.1 Atmospheric composition of the troposphere

Constituent molecule	Volumetric ratio (%)
Nitrogen (N_2)	78.08
Oxygen (O_2)	20.95
Argon (Ar)	0.93
Carbon dioxide (CO_2)	0.035
Neon (Ne)	0.0018
Helium (He)	0.00052

believed to have been formed from water and carbon dioxide through photosynthetic reactions in green plants. The fact that the earth's atmosphere principally consists of nitrogen and oxygen, which both have higher molecular weights than helium, is an advantage for flying balloons.

Although the quantities of carbon dioxide and water vapor are very small, they have a large impact on the structure of the atmosphere through the greenhouse effect. More specifically, the earth's surface absorbs solar energy causing it to warm up and to radiate energy into space as infrared radiation. Carbon dioxide and water vapor then absorb a portion of this infrared radiation, thereby trapping energy in the atmosphere. As a result of this mechanism, the temperatures at the earth's surface and in the lower atmosphere are several tens of degrees Celsius higher than what they would be if no carbon dioxide or water vapor were present.

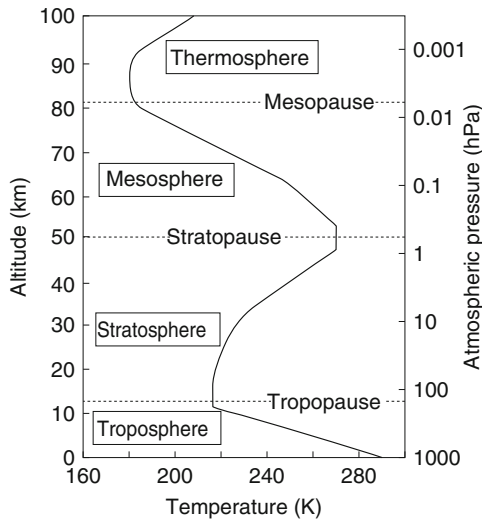
3.1.2 Vertical Structure

For the sake of convenience, the atmosphere can be classified into a number of layers on the basis of the temperature variation with altitude as shown in Fig. 3.1. Starting from the ground, these layers are termed the troposphere, the stratosphere, the mesosphere, and the thermosphere.

The troposphere is approximately 16-km thick in equatorial regions and approximately 8-km thick in high-latitude regions. It is a region in which air is frequently mixed vertically. The majority of meteorological phenomena, including high and low-pressure systems and typhoons, occur in the troposphere. The temperature in the troposphere decreases with altitude, because the air at low altitudes is warmed by the above-mentioned greenhouse effect. Convection and other atmospheric motion transport heat upward, which also greatly affects the temperature distribution. The upper boundary of the troposphere is called the tropopause, and above this is the stratosphere.

The stratosphere extends to an altitude of approximately 50 km, and it is the region in which the temperature increases with altitude. Since the upper reaches of the stratosphere contain warm air, it is difficult for the kind of convective movements that take place in the troposphere to occur in the stratosphere. This kind of tempera-

Fig. 3.1 Temperature variation with altitude and division of regions



ture distribution is created by the fact that ozone, which is present in minute amounts in the stratosphere, absorbs solar ultraviolet radiation and warms the air in the upper part of the stratosphere. Ozone (O_3) is formed by the photodissociation of molecular oxygen (O_2) into atomic oxygen (O) and the subsequent combination of molecular oxygen and atomic oxygen. As shown in Fig. 3.2, ultraviolet radiation having a wavelength shorter than 320 nm, which does not reach the troposphere, strongly penetrates the stratosphere and gives rise to this kind of photochemical reaction. The fact that there are high levels of ultraviolet radiation in the stratosphere needs to be borne in mind when selecting suitable materials for balloons. The stratosphere contains only a few parts per million (ppm) of water vapor, making it extremely dry compared with the troposphere. The upper boundary of the stratosphere is called the stratopause, and above this is the mesosphere.

The mesosphere is the region between approximately 50 and 80 km in which the temperature decreases with altitude. Above this, there is the thermosphere, where the temperature once again increases with altitude. The air in the thermosphere is warmed as a result of nitrogen and oxygen molecules absorbing solar ultraviolet radiation.

3.1.3 Hydrostatic Equilibrium

The two vertical axes of Fig. 3.1 represent altitude and pressure. They clearly show that the atmospheric pressure decreases with altitude, but how was the atmospheric pressure distribution determined? Taking S to be the area at the base of a vertical air column in the atmosphere as shown in Fig. 3.3, consider a mass of air within the column between altitudes z and $z + \Delta z$. If we denote the pressure at altitude z as p and the pressure at altitude $z + \Delta z$ as $p + \Delta p$ (where $\Delta p < 0$), the upward force

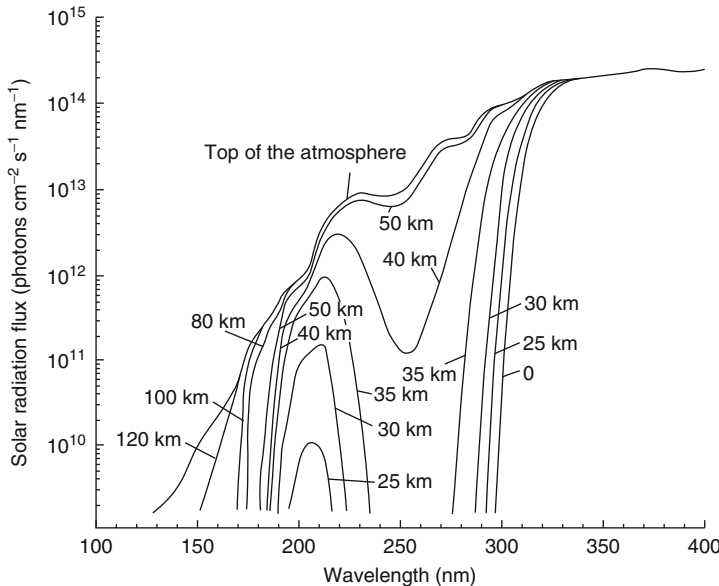
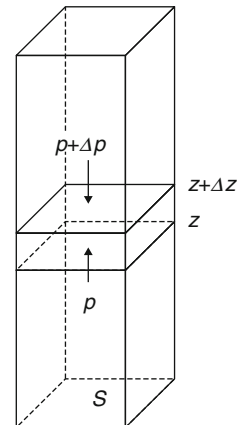


Fig. 3.2 Solar radiation intensity spectra at various altitudes [Source: Matsuno, T. and Shimazaki, T.: Atmosphere of the Stratosphere and Mesosphere, Atmospheric Science Lecture Series (in Japanese), University of Tokyo Press (1981)]

Fig. 3.3 Forces acting in the vertical direction on the upper and lower surfaces of a mass of air



resulting from the difference in atmospheric pressure acting on the upper and lower surfaces of the air mass is $-S\Delta p$. At the same time, if we take g as the acceleration due to gravity and ρ as the mass density of air, the gravitational force $g\rho S\Delta z$ acts on this mass of air in the downward direction. The force due to the pressure difference and the force due to gravity are generally in equilibrium in the atmosphere, and this gives rise to the relationship

$$-S\Delta p = g\rho S\Delta z. \quad (3.1)$$

If we consider the limit as Δz becomes small, we obtain the following relationship

$$\frac{dp}{dz} = -g\rho, \quad (3.2)$$

which shows that pressure decreases with altitude. This relationship is known as hydrostatic equilibrium.

Next, we introduce the equation of state for ideal gas:

$$p = \rho RT, \quad (3.3)$$

where R is the gas constant, and its magnitude is determined by the composition of the gas. For dry air on earth, $R = 287 \text{ JK}^{-1} \text{ kg}^{-1}$.

$$\frac{dp}{dz} = -\frac{gp}{RT} \quad (3.4)$$

is obtained from (3.2) and (3.3). If we denote the pressure at the earth's surface as p_0 , the above equation leads to

$$p(z) = p_0 \exp \left(- \int_0^z \frac{1}{H(z')} dz' \right), \quad (3.5)$$

where

$$H(z) = \frac{RT(z)}{g} \quad (3.6)$$

is a quantity called the scale height, which has the dimension of length. The scale height in the earth's troposphere and stratosphere is about 6–8 km.

If we assume that the temperature T does not vary with altitude, and we designate H_0 as the scale height at this time, (3.5) becomes

$$p(z) = p_0 \exp \left(-\frac{z}{H_0} \right), \quad (3.7)$$

and it can be seen that the atmospheric pressure decreases by a factor of $1/e = 0.368$ with an increase in altitude of H_0 . In addition, the atmospheric density ρ becomes

$$\rho(z) = \rho_0 \exp \left(-\frac{z}{H_0} \right) \quad (3.8)$$

in the same manner. At this point, if we integrate both sides of this equation from $z = 0$ to ∞ , we obtain

$$\int_0^\infty \rho(z) dz = \rho_0 H_0. \quad (3.9)$$

The left-hand side of (3.9) represents the vertically-integrated atmospheric mass that is present above the unit area of the earth's surface, and the right-hand side

represents the mass of the air column with atmospheric density ρ_0 and height H_0 . In other words, the scale height is the height of an air column when the vertically-integrated atmospheric mass is expressed as an air column having the same density as that at the earth's surface.

3.1.4 Meridional Distribution of Temperature

In this section, we describe the atmospheric temperature distribution in the north-south direction. The amount of solar radiation (incident sunlight) varies greatly in the north-south direction, in contrast to the case in the east-west direction, where it is averaged out by the earth's rotation. Consequently, air temperatures vary much more in the north-south direction than in the east-west direction. Here, we attempt to estimate the amount of solar radiation that a unit area on earth receives in one day. At the vernal and autumnal equinoxes, the amount of solar radiation is greatest in the equatorial regions where the sun passes directly overhead, and it is smallest in the polar regions, where the height of the sun is low. In contrast, near the solstices, the amount of solar radiation averaged over one day reaches a maximum at the summer pole because the sun shines throughout the night (notwithstanding its low height), and the amount of solar radiation is zero at the winter pole because of the polar nights.

Figure 3.4 shows how the atmospheric temperature varies with latitude and altitude. The figure depicts the case when it is winter in the northern hemisphere, but the case for the opposite season is approximately the same except that the left and right sides are exchanged. The trend for the solar radiation described above is reflected well in the temperature distribution in the stratosphere. On the one hand, in the stratosphere, the highest temperature is observed at the pole in the summer hemisphere, and the lowest temperature is observed at the pole in the winter hemisphere.

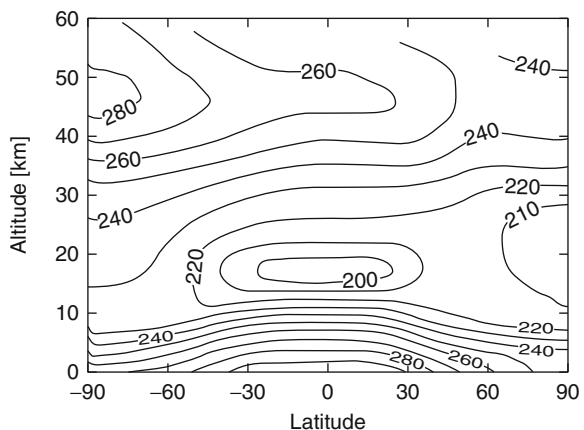


Fig. 3.4 Latitude-altitude distribution for monthly-averaged temperatures [K] in January. Average values for 1992–2002. (Figure prepared using data from the UK Meteorological Office (UKMO))

On the other hand, in the troposphere, the equatorial region is warmest, and the polar regions are coldest irrespective of the season. This is because the oceans with their large heat capacity store heat in summer and release heat to the atmosphere in winter, and that sunlight is effectively attenuated by clouds, aerosols, and the atmosphere itself at high latitudes. By contrast, at altitudes of 15–20 km near the tropopause, the temperature is lowest in the equatorial region. This is because the ground and ocean surface temperatures are high in the equatorial region, causing convection to extend to higher altitudes than at other latitudes, so that the tropopause is at a higher altitude. Adiabatic expansion that occurs during the course of upward advection extending to this high tropopause produces a low tropopause temperature in the equatorial region.

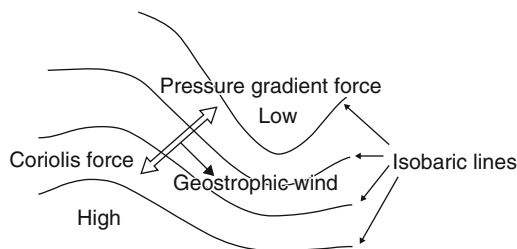
Moreover, the temperature distribution described above is not determined merely by the energy balance at each latitude. Within the atmosphere, there are slow currents that exchange air both vertically and in the north-south direction. This phenomenon is known as meridional circulation. By transporting heat in the troposphere from the equatorial region to high latitudes, and by transporting heat in the stratosphere from the summer hemisphere to the winter hemisphere, the meridional circulation ensures that the north-south temperature variation is small. The speed of the north-south winds associated with the meridional circulation are of the order of a few meters per second or less, and because this is lower than the wind speeds associated with mean zonal winds and atmospheric waves (which are described in Sects. 3.1.5 and 3.1.6), they are difficult to extract from daily meteorological data.

3.1.5 Meridional Distribution of Zonal Winds

Wind does not blow in a straight line from a high-pressure area to a low-pressure area because of the apparent force generated by the earth's rotation, known as the Coriolis force. As a simple explanation of the Coriolis force, one may consider throwing a ball horizontally over a rotating disk. The ball would appear to curve laterally to a person riding on the disk. That is, a force appears to act perpendicular to the direction the ball flies; this apparent force is the Coriolis force. In the northern hemisphere, the Coriolis force is oriented to the right of the wind direction, while in the southern hemisphere it is oriented to the left. Its magnitude is proportional to the product of the wind speed and the sine of the latitude. In large-scale wind systems in mid-latitude regions, as shown in Fig. 3.5, winds blow largely parallel to isobaric lines indicating that the pressure gradient force from high to low-pressure areas, and the Coriolis force in the opposite direction are approximately equal to each other; this type of wind is termed a geostrophic wind. In the northern hemisphere, winds blow so that the high-pressure areas are on the right side of the wind vector, and in the southern hemisphere, they blow so that low-pressure areas are on the right side of the wind vector.

In addition, while winds in the upper troposphere and the stratosphere may predominantly be considered geostrophic winds, winds near the earth's surface can-

Fig. 3.5 Relationship between pressure gradient force and Coriolis force in a geostrophic wind (for the northern hemisphere)



not be considered geostrophic. This is because frictional forces cannot be ignored. These operate near the earth's surface, and act in addition to the Coriolis force and pressure gradient force. If the resultant of these three forces is considered, winds blow at an angle from high-pressure areas to low-pressure areas. The altitude range over which ground friction is effective varies with topography and season, and typically it is 1–2 km. Furthermore, even at high altitudes at which friction can be ignored, small-scale horizontal structures on the scale of a few hundred kilometers or less may not consist of geostrophic winds.

3.1.5.1 Troposphere

Figure 3.6 shows the distribution of the monthly mean zonal winds with latitude and altitude for each season. In the troposphere, because temperatures are high in the equatorial region and low in the polar regions, high-pressure areas are produced in the equatorial region, and low-pressure areas are produced in the polar regions. As a result, from the relationship of geostrophic winds, westerly winds (i.e., blowing toward the east) known as prevailing westerlies are produced near the mid-latitude tropopause. Although seasonal variations in the troposphere are small compared with the stratosphere (described in the next section), prevailing westerlies are strongest in winter in both hemispheres.

Particularly strong parts of prevailing westerlies are known as jet streams, and they consist of the subtropical jets that occur in the vicinity of 30° latitude and polar front jets at higher latitudes. Since subtropical jets vary little with time and space, they are clearly observable even in mean monthly data such as that shown in Fig. 3.6. By contrast, because polar front jets occur over a wide region from the middle latitudes to the poles and vary strongly over time, they are not apparent in Fig. 3.6. During winter in the northern hemisphere, the subtropical jet and polar front jet unite in the vicinity of Japan, causing the wind speeds to intensify so that they may exceed 100 ms^{-1} .

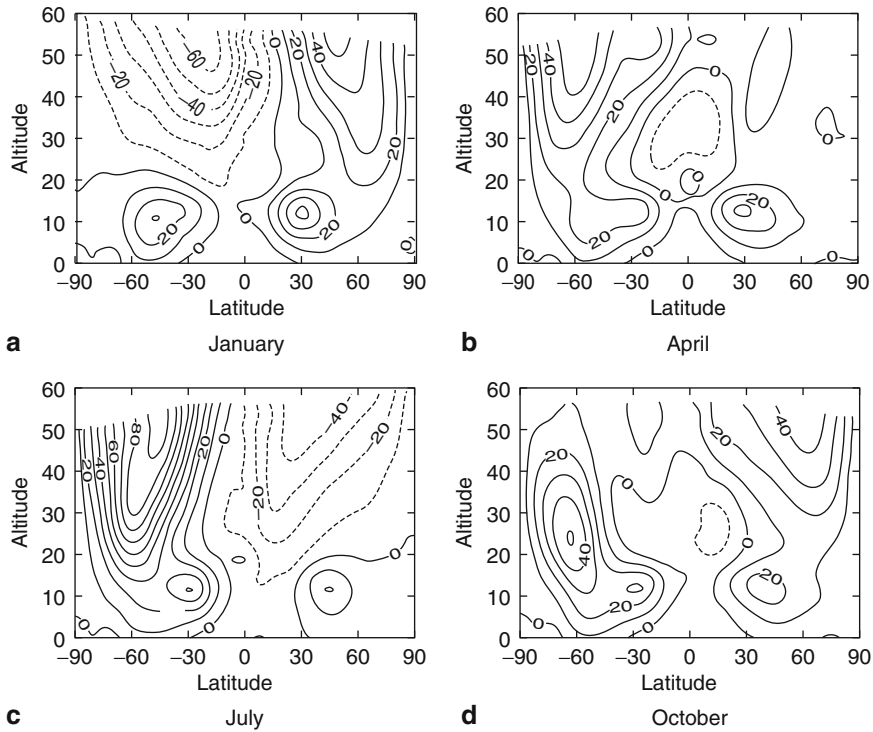


Fig. 3.6 Latitude-altitude distributions of monthly mean (for 1992–2002) zonal winds for each season. Units are m/s. Solid lines represent regions of westerly winds (i.e., blowing toward the east), and dashed lines indicate regions of easterly winds (i.e., blowing toward the west) (UKMO data are used in the preparation of figures): **a** January, **b** April, **c** July, **d** October

3.1.5.2 Stratosphere

As Fig. 3.4 reveals, in the stratosphere, there is a pronounced difference in the temperature between the summer and winter hemispheres; specifically, its temperatures are high in the summer polar region and low in the winter polar region. As a result, the pressure decreases from the summer pole to the winter pole in both hemispheres, and from the relationship of geostrophic wind, easterly winds are produced in the summer hemisphere, and westerly winds in the winter hemisphere. In spring and autumn, because the temperature is highest at the equator, high-pressure regions are produced in the equatorial region, and low-pressure regions are produced in the polar regions in the same manner as in the troposphere. Consequently, westerly winds are generated in both hemispheres.

Figure 3.7 shows the seasonal progression of zonal winds in the stratosphere at an altitude of approximately 30 km. At latitudes higher than 30° in the northern hemisphere, during the transition between the winter westerly winds to the summer easterly winds, the region of the easterly winds expands from higher to lower latitudes. In the skies over Japan (northern mid-latitude), while there is some an-

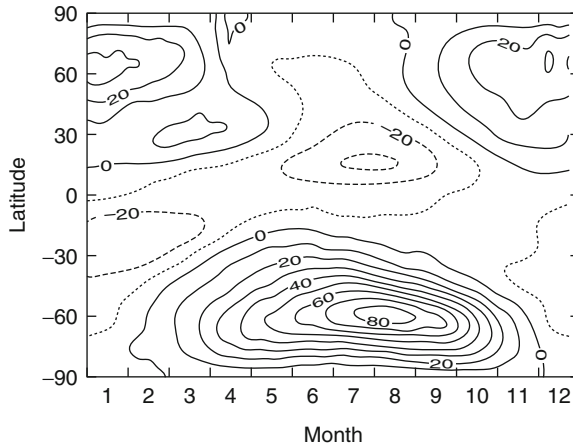


Fig. 3.7 Seasonal variation in zonal-mean zonal winds at various latitudes at the 10-hPa surface (altitude approximately 30 km). Units are m/s. *Solid lines* indicate regions of westerly winds, and *dashed lines* indicate regions of easterly winds. The values were obtained by averaging mean weekly data for the period 1992–2002. (UKMO data was used in the preparation of this figure)

nual variation, the wind direction generally changes in mid May, and the easterly winds peak in late July. These easterly winds deteriorate from about July in the polar region, and the easterly wind component weakens from the higher latitudes. The easterly winds revert back to westerly winds in about mid September.

Although not shown in the figure, a phenomenon known as the quasi-biennial oscillation occurs in the equatorial stratosphere below the 15° latitude. This phenomenon involves the approximately annual alternation of easterly winds and westerly winds, and has the characteristic that both easterly and westerly winds commence at high altitudes and then descend to lower altitudes. The maximum wind speed occurs at an altitude of approximately 25 km, and the amplitude of the fluctuations in this region is about 25 m s^{-1} . This cycle has a period of about 2–2.5 years (26 months on average). The quasi-biennial oscillation is thought to be induced by zonal acceleration resulting from the combination of atmospheric waves having eastward momentum and those having westward momentum.

3.1.6 Waves in the Atmosphere

Up until this point we have focused on structures averaged in the zonal direction, but zonally inhomogeneous structures are also important for balloon operations. For example, the prevailing westerlies that can be seen in daily high-altitude weather maps usually move in a zigzag direction, and various wave motions are associated within them.

3.1.6.1 Troposphere

Figure 3.8 shows the pressure distribution in the upper troposphere for one particular day. Altitude contours are drawn for the 300-hPa pressure surface. Since the atmospheric pressure decreases monotonically with altitude, high altitudes in the figure may be considered to have high pressures, and low altitudes may be considered to have low pressures. From the relationship of geostrophic wind, wind blows in westerly (eastward) direction while zigzagging roughly along contour lines; also, the narrower the interval between contours is, the stronger the wind is.

The isobaric lines are considerably distorted from being circular. Along a given latitudinal band, pressure troughs (contour lines distorted to the south) and ridges (distorted to the north) appear repeatedly, indicating the presence of waves in the atmosphere. Some waves have horizontal wavelengths of 10,000 km or more and are visible in the monthly average, while others have wavelengths of a few thousand kilometers and fluctuate over a period of several days, and these are simultaneously superimposed. The former are created by large-scale geographic effects such as the distribution of continents and oceans. The latter are termed baroclinic waves, and they transport heat toward high latitudes by exchanging warm air on their low-latitude side with cold air on their high-latitude side. Baroclinic waves are accompanied by low and high-pressure systems on the ground, and they are responsible for changes in daily weather.

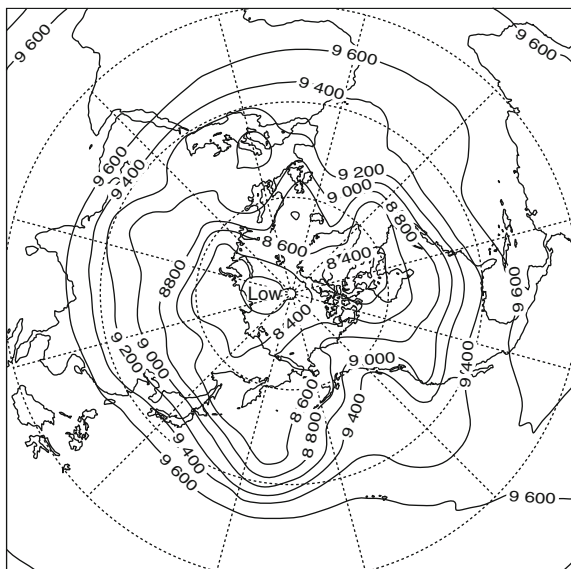


Fig. 3.8 Altitude contour lines for 300-hPa surface (altitude approximately 9 km) on 15 January 2002. Units are meters. Interval for longitude and latitude contours is 30° (UKMO data are used in preparation of the figure)

3.1.6.2 Stratosphere

In the stratosphere, waves having long wavelengths are significant. Figure 3.9a shows the pressure distribution for a particular day in winter in the northern hemisphere. The isobaric lines that encircle the low-pressure systems that cover the North Pole are greatly distorted, and there is a high-pressure system in the vicinity of Alaska. This sort of structure is created by waves known as planetary waves, which are generated in the troposphere and subsequently propagate to the stratosphere. Because planetary waves propagate vertically only in westerly winds, they are present in the stratosphere in winter when westerly winds blow, but they do not occur in summer when easterly winds blow.

Since there are no planetary waves, the pressure distribution in the northern hemisphere in summer shown in Fig. 3.9b is nearly concentric. In addition, pressure distributions in the southern hemisphere in winter are approximately concentric circles. The reason for this is considered to be that it is difficult to excite planetary waves in the southern hemisphere because the topography there is less rugged than that in the northern hemisphere.

Changes in planetary wave activity in the northern hemisphere winter often cause great disorder in the stratosphere. A particularly large-scale phenomenon is sudden warming. Before the occurrence of sudden warming, a low-temperature region that characterizes the winter stratosphere is present at the pole, and westerly winds blow around the low pressure. High pressures then appear at middle latitudes, and encroach into the polar region (like the one shown in Fig. 3.9a). The North Pole eventually becomes a high-temperature region and easterly winds begin to blow around the high pressure. The warming of the polar region starts at higher altitudes and gradually weakens and descends. In conjunction with this, commencing at higher altitudes and progressing down, the wind direction changes from westerly to easterly. However, this condition does not continue for long, and in due course the polar temperature falls and returns to its original state.

In addition to planetary waves and baroclinic waves described earlier, there are small-scale waves known as gravity waves that have horizontal wavelengths ranging from a few kilometers up to a few hundred kilometers and that occur throughout the atmosphere. Gravity waves, the restoring force of which is buoyancy, propagate within stably stratified fluids. They are accompanied by winds that oscillate in the horizontal and vertical directions. Although this type of wave does not appear in weather maps, waves having wind amplitudes of a few meters per second or more are observed on a daily basis in the stratosphere. In general, because their vertical wavelength is a few kilometers or less and their period ranges from a few minutes to a few hours, they cause balloons to undergo oscillatory motion during ascent and during level flight.

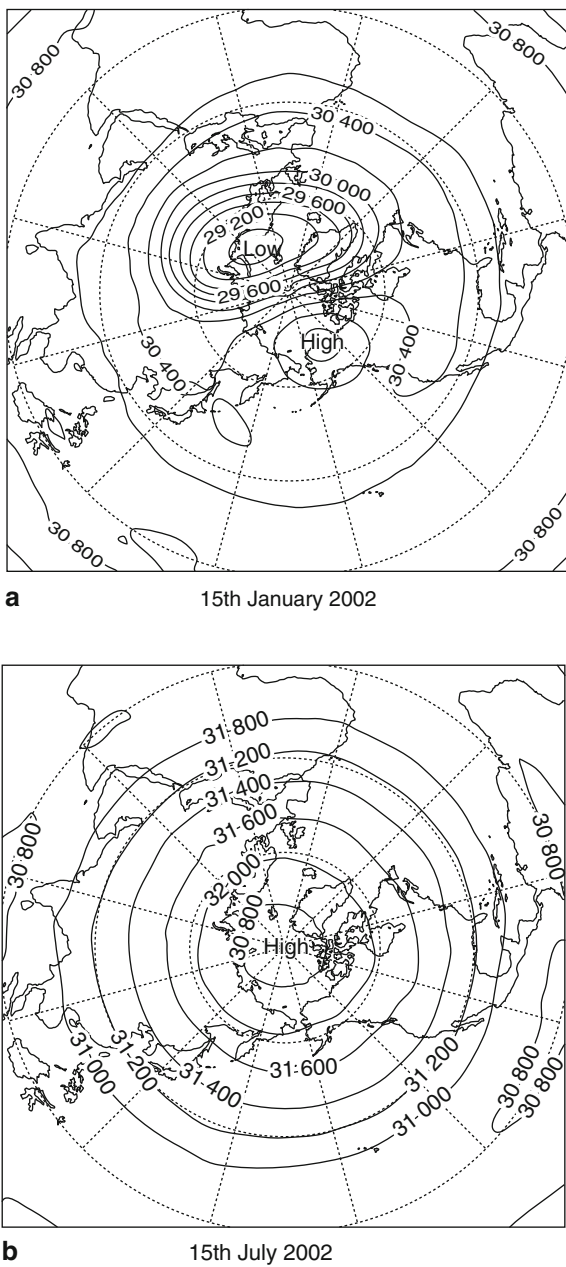


Fig. 3.9 Contour lines for altitudes on the 10-hPa surface (altitude approximately 30 km) (UKMO data are used in the preparation of the figure); **a** 15 January 2002, **b** 15 July 2002

3.2 Balloon System Configurations

3.2.1 Balloon Configurations

Below is a list of equipment essential for flight control and for aeronautical safety and which is installed on stratospheric balloons.

3.2.1.1 Exhaust Valve

An exhaust valve is installed in the apex of the balloon as a control valve for releasing lifting gas to reduce buoyancy. As described in Sect. 3.5.3.2, there is a disk-shaped fitting plate at the balloon apex used for fastening the ends of the load tape and film, and it is also used as the base for mounting the exhaust valve. The valve is opened by an electric motor or solenoid valve, and commands are relayed by remote control or by the signals from an on-board control system that automatically controls the amount of gas.

The main uses of the exhaust valve are:

- (1) To adjust the speed of ascent when it is faster than normal
- (2) To decelerate or stop ascent at an intermediate altitude in accordance with the flight program
- (3) To descend to a lower flight altitude than the level flight altitude

Since the low pressure of the stratosphere means that the exhaust rate is low relative to the total balloon volume, this valve has a large diameter of 30–50 cm. In cases when particularly rapid venting is required, the apex plate may be enlarged, and multiple valves may also be installed. Because of the limited installation space, it is desirable for the valve to be thin and lightweight. It generally consists of a cap on a base with a circular opening in it, like that shown in Fig. 3.10. Gas is vented from the gap created when the cap is raised.

The amount of exhaust gas e_2 from the exhaust valve is determined by (2.79). Since it is difficult to precisely measure the actual flow rate under the equivalent condition of the stratosphere, the following procedure is adopted to specify the characteristics of the exhaust valve. Normally, the actual exhaust flow rate is measured on the ground (i.e., at a pressure of 1 atm) and the flow rate constant c_2 , which is the product of the flow contraction coefficient and the velocity coefficient, is determined experimentally. Since the exhaust flow rate on the ground $e_{2,0}$ is proportional to the square root of the pressure differential inside and outside the balloon, it is given by

$$e_{2,0} = c_2 A_2 \sqrt{\frac{2(\rho_{a0} - \rho_{g0})g}{\rho_{g0}}} \sqrt{h_0}, \quad (3.10)$$

where ρ_{a0} and ρ_{g0} are the densities of air and the lifting gas on the ground, respectively, and h_0 is the height from the point where there is no internal and external pressure differential to the balloon apex.



Fig. 3.10 Exhaust valve installed in the apex of a balloon

Table 3.2 Exhaust valve performance

Balloon system mass (kg)	Rate of buoyancy reduction (Ns^{-1})			
	Ground	Altitude (20 km)	Altitude (30 km)	Altitude (40 km)
100	6.1	0.58	0.16	0.046
250	7.1	0.67	0.19	0.054
500	8.0	0.75	0.21	0.061
1,000	9.0	0.85	0.24	0.068

If $e_{2,0}$ is determined, the amount of exhaust gas at a different altitude can be found using the following equation.

$$e_2 = e_{2,0} \left(\frac{p_a}{p_{a,0}} \right)^{1/6}. \quad (3.11)$$

From this equation, the buoyancy lost per unit time by venting the lifting gas is proportional to the ratio of the atmospheric pressure at that altitude to that on the ground raised to the 5/6-power as expressed by the function below.

$$\frac{dB}{dt} \propto e_{2,0} \left(\frac{p_a}{p_{a,0}} \right)^{5/6}. \quad (3.12)$$

Consequently, the time required to lose the same amount of buoyancy at an altitude of 35 km is, for example, about 70 times that on the ground.

The performance of the exhaust valve used at the ISAS is shown in Table 3.2.

3.2.1.2 Ballast Hopper

To provide for the need to reduce the load carried during flight, ballast and its jettison equipment is carried on board. Since the ballast hopper is the only means available for restoring or increasing climbing power, it is crucial for controlling balloon flight. It is installed in the bottom part of the payload or separately at some point along the suspension line.

To be able to freely adjust the weight jettisoned, a high-density material such as sand or iron particles is stored in a hopper, and there is a small-diameter discharge valve in the base of the hopper. Like the exhaust valve, the discharge valve is electrically actuated, and it is operated by remote radio command and/or by an on-board automatic altitude control system. Since ballast discharge from the discharge valve resembles sand falling in an hourglass, the weight discharged is roughly proportional to the length of time the valve is open, irrespective of the flight altitude.

3.2.1.3 Balloon Destruct Device

When a balloon flight is completed, the gondola is separated from the balloon, and it descends by parachute as described in Sect. 3.2.2. At this time, because it is dangerous to allow the balloon to continue to fly intact, it is customary to also destroy the balloon at the same time and allow it to fall to earth.

Figure 3.11 shows the standard method for constructing a balloon destruct device. It involves attaching a strong tape in an inverted V shape to the film (tear panel) near the apex of the balloon envelope extending fine destruction cord from the top of the V, and after making a temporary joint at the balloon apex, passing the rope along the balloon base and securing it to the top of the parachute. When this rope is pulled in synchronization with the dropping of the parachute, the balloon film starts to tear along the tearing rope and in this way the balloon is destroyed. In this configuration, the rope for tearing the envelope apart and a portion of the film remain attached to the top of the parachute. If there is a possibility that this may negatively influence the parachute's performance, a separate cutter may be installed along the length of the rope.

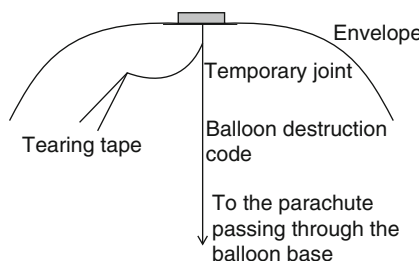


Fig. 3.11 Balloon destruct device. When the payload is dropped by parachute, the envelope is ripped apart by the pulling action of the balloon-destruction cord

3.2.1.4 Equipment for Ensuring Aviation Safety

Although the ceiling altitude of stratospheric balloons is higher than the flight altitude of aircraft, during ascent and descent, balloons pass through altitudes that aircraft fly at. For these periods, the equipment list below is installed (either on the balloon itself or in its vicinity) as safety measures with respect to aircraft.

Radar Reflector

Installation of a 200–2,700-MHz radio wave reflector to reflect radar waves transmitted by aircraft is prescribed in the rules of the International Civil Aviation Organization (ICAO). Normally, a corner reflector constructed of thin, lightweight plates having 50-cm-long sides is installed near the base of the balloon. Alternatively, the same effect may be achieved by adding radar-reflective fibers, which may be incorporated in the load tape that is attached longitudinally on the balloon.

Flashing Light

This light enables aircraft pilots to identify a balloon, and it is attached near the balloon base or on the gondola.

In addition, an aircraft transponder, which is a standard piece of on-board equipment on aircraft, may be installed on large balloons. This equipment is described under basic on-board equipment in Sect. 3.2.3.

3.2.2 Suspension System

Figure 3.12 shows a typical arrangement for suspending the payload and related systems from a balloon. In general, the bottom part of the balloon base fitting is a ring-shaped metal fastener (described in Sect. 3.5.3.2), and the suspension system is connected at this point.

Starting from the top of the balloon system, the principal constituents of the suspension system are the separation mechanism, parachute, suspension line, and loaded on-board systems such as observational equipment. However, in systems loaded as shown in the figure, common equipment, such as communications equipment for controlling balloon flight and ballast jettison equipment, and the observational equipment are sometimes divided into two parts and suspended in separate gondolas. Therefore, the structure of the on-board system components is not fixed.

In Japanese balloons, generally everything is housed together with the observational equipment in a single gondola. NASA puts electronic equipment for controlling the balloon in a separate small gondola, and at CNES, all general equipment is placed in a separate gondola from the observational equipment. Russian systems

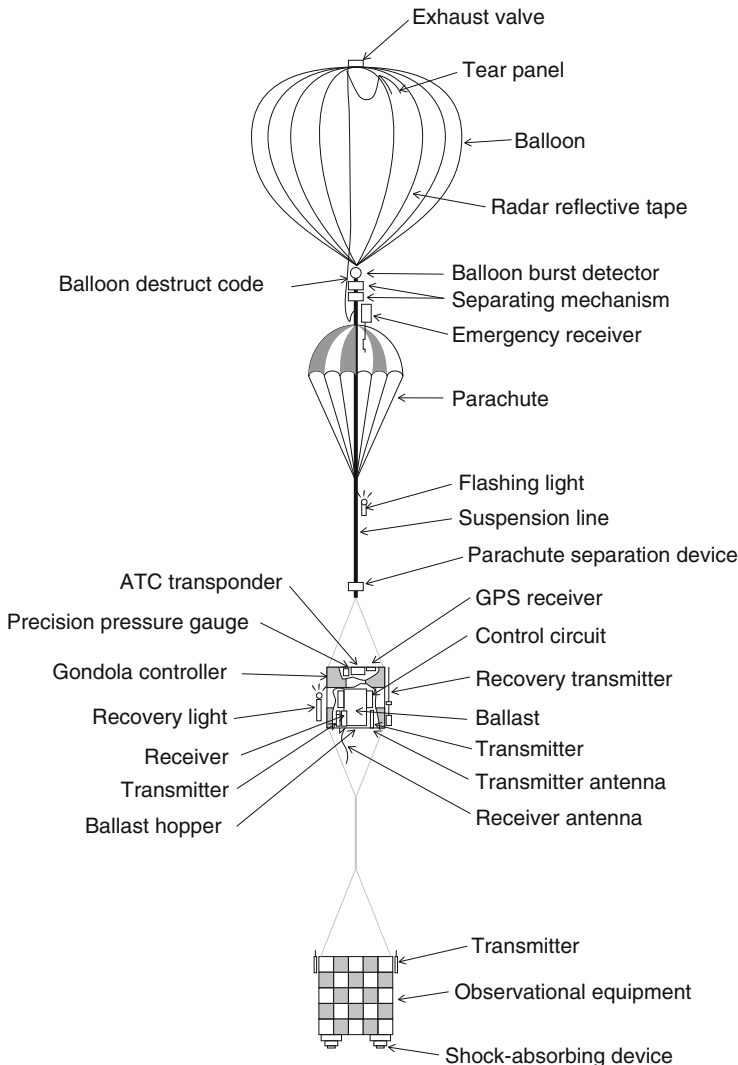


Fig. 3.12 The typical configuration of a system for suspending a payload from a balloon

attach a horizontal bar to the lowest tier of the suspension system and laterally suspend multiple gondolas packed for each individual objective.

High-tensile nylon ropes are used as suspension lines in the case of the comparatively light loads carried at the ISAS. NASA, which frequently has multiton payloads, uses two-wire or four-wire-construction strong steel wires. CNES normally employs two-ply construction belts.

3.2.2.1 Separating Mechanism

This is a mechanism for separating the suspension line from the balloon above the parachute when a flight is terminated. In ISAS, the suspension line in this section is a single rope, and a rope cutter, in which a cutting blade is pushed out by a pyro device, is placed along the rope as shown in Fig. 3.13.

Figure 3.14 shows a system in which steel wire is used as the suspension line employed by NSBF in US. This figure shows a redundant configuration that uses two cutters to increase its reliability. The sections on both the balloon side and the on-board equipment side are held between anchoring blocks and are fixed with the wire rope, and this rope is cut using a pyro-cutter. This mechanism is highly reliable, because after cutting there is complete separation without any mechanical entanglement.

As described in the section on safety and security (Sect. 3.4.7), since the separation mechanism is a key device for safely terminating balloon flights, it is desirable to assure high reliability through redundancy and/or other measures.

In an emergency situation, such as when a balloon suddenly bursts and starts to descend, it is necessary to actuate the separation mechanism as soon as possible and to switch to parachute descent. If this process is delayed, there is a risk that the burst balloon will cover the parachute, so that the parachute will not deploy if it separates, and that the gondola will free fall. To avoid such a dangerous situation, in the US and Europe, a balloon burst detector consisting of a load sensor is installed in the

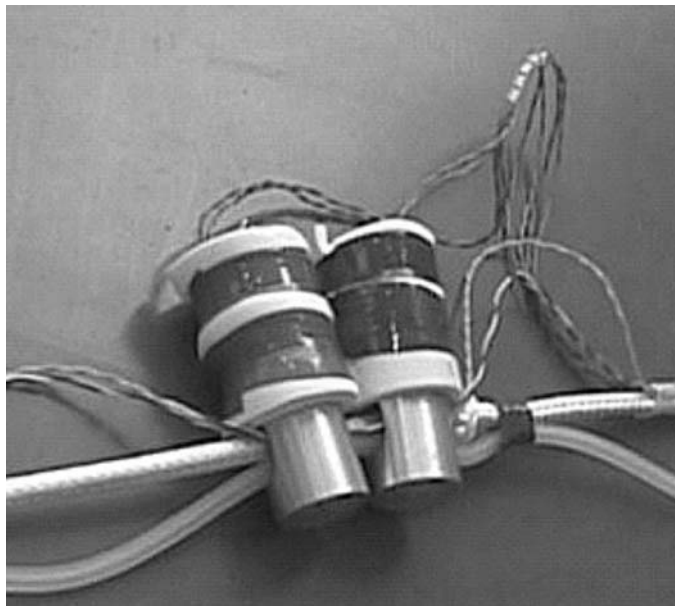


Fig. 3.13 Rope cutter: This figure shows a redundant configuration that uses two cutters to increase its reliability

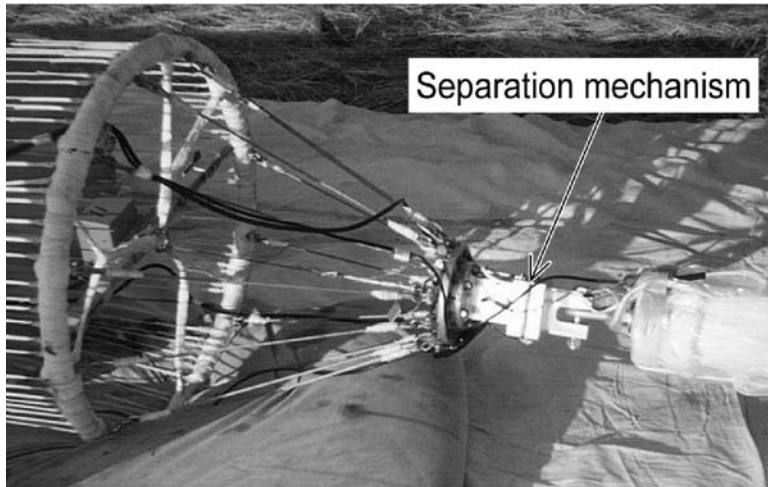


Fig. 3.14 NBSF separation mechanism. The *left side* is the top of the parachute. The *right side* is the balloon base (courtesy of NASA/NSBF)

upper part of the separation mechanism, and if a sudden loss in balloon buoyancy is detected, the separation mechanism is promptly actuated.

This separation mechanism, which includes systems such as the command system that sends trigger signals to it (Sect. 3.2.3), is also referred to as the flight termination device.

3.2.2.2 Parachute

Unlike in aircraft applications, the parachute for balloon use is not normally packed, rather it is installed in an extended condition along the suspension system, as shown in Fig. 3.12. Consequently, after separating from the balloon, the parachute deploys smoothly with no unpacking. There are cases in which the parachute suspension line and riser are used as a part of the suspension line. In this case, however, if the applied load is lost on separation and free fall occurs for a few seconds, there is the risk that the suspension line may contract, causing the canopy to deform, and hindering parachute deployment. As a result, the suspension line may be independently inserted through the center.

Parachutes having flat circular canopies are frequently used. However, slotted parachutes, cross parachutes, and the like are also used to reduce payload swinging during descent and to ensure a safe landing.

If we let m_p represent the payload mass including the parachute (parachute system mass), $C_{Dp}A_p$ represent the product of the parachute drag coefficient and effective surface area, and v_p represent the descent velocity, the equation of motion in the vertical direction can be written as

$$\frac{dv_p}{dt} = g - \frac{1}{2} \frac{C_{Dp} A_p}{m_p} \rho_a v_p^2. \quad (3.13)$$

If we designate the descent speed at the ground as v_{p0} , the drag area per unit mass becomes

$$\frac{C_{Dp} A_p}{m_p} = \frac{2g}{\rho_{a0} v_{p0}^2}, \quad (3.14)$$

where ρ_{a0} is the atmospheric density on the ground. A final descent speed of approximately 7 m s^{-1} has been selected, which is common for cargo parachutes. Now, if we assume that the parachute deploys instantaneously t_f seconds after the commencement of free fall, the maximum acceleration produced when deploying the parachute canopy will be given by

$$\frac{1}{g} \frac{dv_p}{dt} = 1 - \frac{g^2 t_f^2 \rho_a}{v_{p0}^2 \rho_{a0}}. \quad (3.15)$$

Because descent starts in the low-density stratosphere, there are approximately 3–5 s of free fall between balloon separation and deployment of the parachute. Accordingly, if we determine the maximum acceleration from (3.15), at an altitude of 30 km or higher, the acceleration will be small at 1 G or less, and at an altitude of approximately 20 km, it will be about 3–4 G. Consequently, the strength of the parachute and suspension system is designed to withstand a deployment shock of approximately 5 G. In actual descent calculations, it is necessary to consider crosswinds that change with altitude and changes in the parachute's drag area.

In the case of a flat landing area with no obstacles, if there are strong ground winds, there is the risk that the parachute may remain open and drag the gondola along the ground causing damage to it. To prevent such a situation, methods may be employed after landing to either completely separate the parachute or to deflate the canopy by cutting part of the riser.

3.2.2.3 Observational and Experimental Equipment

Observational and experimental equipment are installed in the lowest tier of the suspension system. There is no particular prescribed method for doing this, and connecting straps may be attached to suit the objectives. One thing that needs to be considered is the use of a design able to withstand the shock of about 5 G produced when the parachute deploys, which is described in the previous section.

3.2.2.4 Shock-Absorbing Device for Recovery

To protect observational equipment from being damaged by the landing shock, shock-absorbing materials (crush pads) are installed on the bottom of the gondola. Usually, corrugated cardboard having a lightweight honeycomb construction,

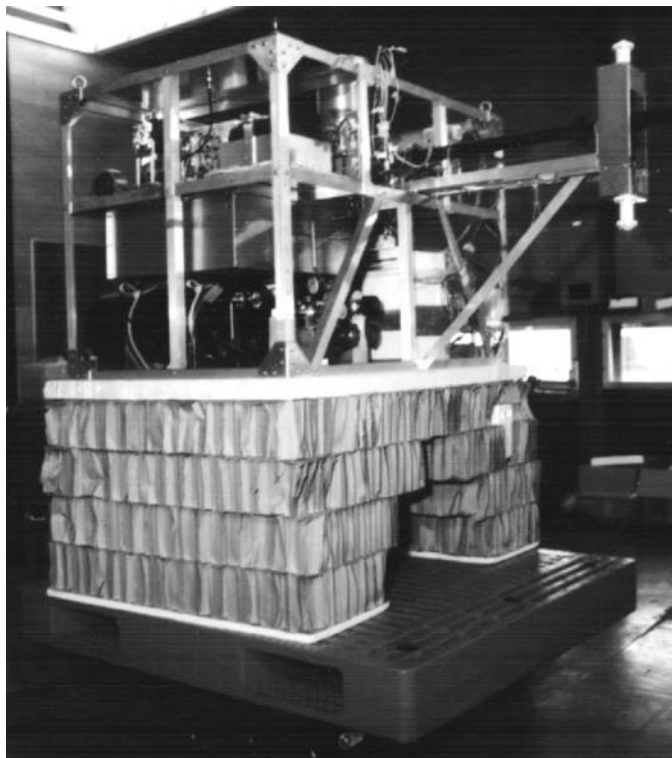


Fig. 3.15 Gondola with material for absorbing the shock of landing installed on its base

specially designed for this purpose, is used by stacking the required number of layers. A photograph showing the exterior view of an observational device with crush pads attached is shown in Fig. 3.15.

3.2.3 Basic On-Board Equipments

Equipment that is commonly mounted irrespective of the flight objectives is referred to as basic on-board equipment.

3.2.3.1 Communication Equipments

Data Transmission System

This is a system for transmitting the operational condition of on-board equipment that regulates and controls the balloon's flight and output data from observational

equipment to the ground station. It is also referred to as a telemeter. In the early days, data methods transmission methods used multiple modulated analog signals in a single multiplex frequency-modulated signal. However, with the progress of electronic technology, digital data transmission methods have been adopted. Such transmission methods essentially use the same functions as those employed in rockets and satellites, but with slightly simpler configurations.

The system consists of a multiplexer, encoder, transmitter, antenna, and power source. The multiplexer scans multiple input signals and the encoder digitizes the multiplexed signal in accordance with uniform rules. The digital data are modulated by a carrier wave and then transmitted to the ground base by the transmitter. In general, data for regulating and controlling the balloon flight and that for scientific observations are transmitted by independent devices each having its own transmitter. However, in some cases involving simple experiments, the two devices have been combined in the same system.

Command Acquisition and Execution System

This is a system that receives command signals from the ground station and decodes and executes the command. The form of the command may be turned on/off by relay contact or serial data (Fig. 3.16). As was the case with the above-mentioned data transmission system, this communication equipment has the same function as that used in rockets and satellites. The functional content is largely separated into commands for controlling the balloon flight and commands for controlling the mounted observational equipment.

The principal commands that control the balloon flight are buoyancy control by dropping ballast and opening and closing the exhaust valve and operations for terminating the balloon flight and for dropping the observational equipment by parachute. An important function for both concerns the safety and reliability of the balloon flight.

Since high reliability is required for the execution of flight termination, system redundancy is often employed. At the ISAS, a small command receiver for flight termination is installed independently on the balloon base. The same capabilities are included in the main command receiver, which is part of the on-board equipment, and in a totally redundant system it is actualized for the flight termination command.

3.2.3.2 Positioning System

This is a system on the balloon for continuously measuring the current position of the balloon during flight. Ever since global positioning systems (GPSs), which are position location systems that employ satellite data, became available for practical use, they have been the principle means for determining the flight position of balloons. Because a balloon moves slowly, a mounted GPS receiver does not need to be

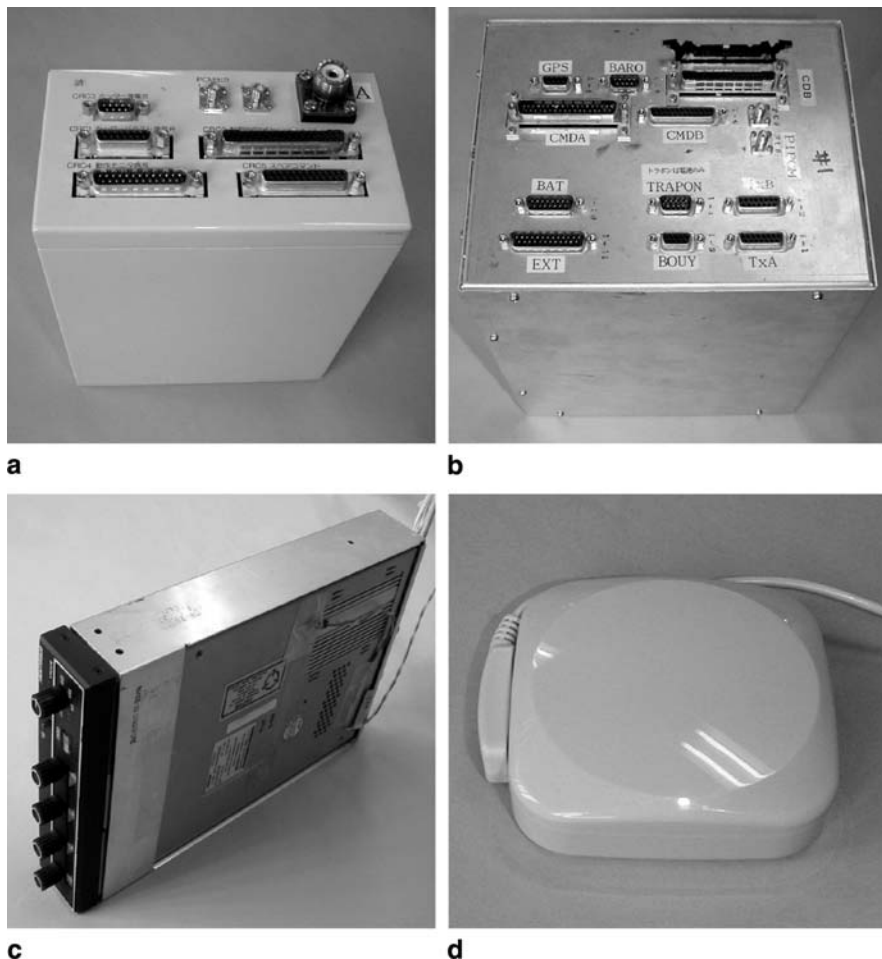


Fig. 3.16 Communication equipment mounted on a balloon system: **a** Command receiver, **b** Data transmission system (telemeter), **c** ATC transponder, **d** GPS receiver

specially designed, and an ordinary, small receiver is sufficient. The output position data are sent to the ground station by the data transmission system.

3.2.3.3 ATC Transponder

The full name for this equipment is Air Traffic Control Radar Beacon System (ATCRBS). It is standard equipment installed in aircraft for air traffic control use. It has an internal transmitting and receiving device, and it is equipped with a pressure altimeter. Each device is assigned an aircraft identification code, known as a Discrete Beacon Code (DBC), and there is a switch to set this.

When the ATC transponder receives an interrogation signal from the Secondary Surveillance Radar (SSR) of the air traffic control system, it sends back its identification code and altitude information. As a result, the position of the balloon is displayed on the air traffic controller's radar screen along with the identification code and altitude, in a similar manner as the information for other aircraft. Consequently, balloons are fully incorporated within air traffic control operations, ensuring safety. The frequencies used are 1,030 MHz (receiving) and 1,090 MHz (transmitting) (Fig. 3.16c).

3.2.3.4 Power Source

Ordinarily for a flight of no longer than 2–3 days, the power source is a primary or secondary battery, although this depends on the power consumption of the on-board equipment. If the flight duration is a week or longer, or when there is a large power consumption, the use of a solar cell system similar to those used on satellites should be considered.

3.2.4 *Optional Equipments*

3.2.4.1 Pointing Control for Observation Instrumentation

In astronomical observation, a control system is required for pointing the observation equipment at a celestial object. This serves the same function as attitude control in astronomy satellites. In the case of a satellite in orbit, the level of disturbance is small in a weightless state, and the variation over time is slow. By contrast, in the case of a balloon, there is pendulum motion around the suspension lines with a rapid cycle having a period of a few tens of seconds, and this poses a hindrance to achieving high-precision control. The fact that the gondola is suspended perpendicular from the gondola allows one axis of the attitude of the observation equipment to be ascertained precisely, making it useful for attitude determination.

The pointing control systems are usually developed in accordance with the needs of each observation, but in some cases basic equipment supplied for a wide range of common uses is provided on the balloon side. One frequently used item is a device for controlling the azimuthal angle around the suspension lines on the main body of the gondola that the observational equipment is mounted on.

The methods for achieving this are:

- (1) Installing a motor part way along the suspension system, and rotating the gondola with the balloon as a platform.
- (2) Generating a torque and rotating the gondola using a momentum exchange device within the gondola (this is similar to satellites).

The apparatus for method (1) is simple, but because it generates torque by twisting the long suspension line, it is difficult to obtain a rapid control response. The same reaction wheel as that employed in satellites is often used as the drive assembly for method (2). As described earlier, the angular disturbance imparted to the gondola is large compared with that imparted to a satellite. The size of the flywheel or the power of the drive motor is increased as the control accuracy required increases. From this point of view, a control moment gyro (CMG) is useful. A CMG is a drive assembly that generates a high torque through the gyro effect. Specifically, it is composed of a gyro that is mounted on a gimbal. The gyro generates a large angular momentum by rotating a large wheel at high rotation rate. The gimbal rotation axes are driven by a motor, and the direction of the large angular momentum vector changes quickly.

To achieve two-axis tracking of observation objects, the following methods have been adopted for rotating the entire body of the observation equipment: (1) The elevation angle of the observation equipment is controlled on the gondola that is azimuthally controlled by the above-mentioned methods, or (2) mounting a two-axis gimbal at the center of gravity of the gondola, in which the observation system is installed. The gondola is suspended from the balloon via the gimbal. The gondola can then freely rotate around the two axes, and a biaxial attitude control system that uses a momentum exchange device drives the gondola. Naturally, the latter method is applicable to large systems.

Figure 3.17 shows an astronomical infrared telescope. It is an example of a system in which the azimuthal angle of the gondola is controlled by a CMG [3], whereas the US Stratoscope II shown in Fig. 1.3 is an example of a system in which biaxial control is achieved using a two-axis gimbal.

3.2.4.2 Lowering of Observation Equipment

The length of the suspension system is usually about 20–30 m, but in cases when the main body of the balloon obstructs observations, it is necessary to increase the distance between the payload and the balloon. However, a suspension system that is too long will hinder launch operations. To overcome this, a small winch is installed in the suspension system, and it is used to slowly lower the gondola by applying a brake [4]. If the working distance is a few hundred meters, it will be necessary to devise a cooling system to dissipate the large amount of heat energy generated by breaking.

3.2.4.3 Environmental Conditions and Preflight Testing

Although the vacuum and radiation environments experienced by a balloon are not as severe as those experienced by a satellite in orbit, the surrounding environment during a balloon flight is far from suitable for the on-board equipment. Solar radiation energy is intense during the daytime, whereas at night there is a cooling



Fig. 3.17 Stellar infrared observation telescope equipped with arc-second-order precision tracking capability (a CMG is used for the drive assembly)

effect due to heat transfer to the low-temperature atmosphere and due to radiation of infrared energy into space.

Therefore, sufficient consideration must be given to the thermal environment. Thermal protection can be provided by coating with white paint or applying urethane foam to instruments normally subject to radiation. The multilayer insulation used on satellites, called thermal insulators, (even a simple form of it) is even more effective.

Preflight operational testing under the atmospheric conditions at ground level is inadequate, making it essential to perform low-temperature testing under reduced pressure at 50 hPa or lower. In addition, because multiple systems are loaded in a narrow space and are in close contact with each other (similar to the situation on a satellite), it is necessary to be careful about mutual electromagnetic interference. In particular, noise generated from digital equipment such as computers may impair

the operation of the telemeter and the command receiver and positioning systems, which may seriously affect flight safety. As a result, it is necessary to carry out careful testing using an adequate management program prior to launch.

3.3 Ground Facilities

3.3.1 *Launch Site*

3.3.1.1 Conditions of Location

To assure safety on the ground and to ensure smooth launch operations, site conditions for a base for launching balloons need to satisfy the following requirements:

1. There should be no densely populated areas or important safety or security facilities in the surrounding area.
2. It should be easy to transport project personnel, equipment and materials, and high-pressure lifting gas to it.
3. The winds near the ground during the test season must be weak with few changes in direction.
4. There should be no large cities or important facilities under the path of the level flight.
5. It must be possible to safely and reliably recover the on-board equipment from the flight termination area.
6. There should be no hindrance to air traffic control operation.
7. It should be a far from any international border.

Although Item 1 is important in case there is trouble at the time of launch, the site must be convenient enough to satisfy Item 2. Item 3 ensures smooth launch operations. Since the east-west component is predominant in winds in the stratosphere where level flight takes place, Item 4 refers to belt-shaped flight zones that also consider fluctuations in the north-south direction. Item 5 is included because it is difficult to recover on-board equipment in mountainous regions or other such terrain. Item 6 arises because balloons transverse the flight altitude of aircraft during ascent and flight termination. Because of the marked increase in civil aviation in recent years, it requires more effort to satisfy this point. Item 7 is a requirement because, just like aircraft, balloons are not permitted to enter another country's airspace without permission. Consequently, this rule does not necessarily apply to a flight based on international collaboration.

To satisfy the above-mentioned conditions, launch sites are established in wilderness areas and in expansive agricultural and livestock regions that have a low population density.

Photographs of the balloon launch sites of Japan (ISAS), the US (NASA/NSBF), France (CNES), Sweden (SSC/ESRANGE), and India (TIFR) are shown in Fron-tispiece 6. The sites in Japan, the US, and France are located at mid-latitudes. The

site in Sweden is in the Arctic Circle (latitude 68° north), while the site in India is located near the equator (latitude 17°23'' north).

3.3.1.2 Site Conditions

The length of large balloons on the ground (including the suspension system for the parachute and other equipment) extends to more than 200 m. The observation system suspended at the bottom needs to be lifted smoothly during balloon launch. As a result, as described in detail in Sect. 3.4.2, the general launch method involves moving the position of the launcher according to the drift of the apex of the balloon by the surface wind, just after the balloon leaves the ground and starts to ascend.

For this reason, it is desirable for the launch field to be spacious and to be several times the total length of the balloon system in at least one direction. In many cases, the ground on which the balloons are placed is cemented, but it is possible to perform adequate experimentation by just spreading a sheet over an uncemented area. There are also cases in which airfields having a limited number of flights are used. A building for assembling and preparing the balloon system, a building for storing payload equipment, and a storage area for various kinds of equipment such as the launcher and gas canisters are required next to the launch field.

3.3.2 Communication Facilities

Facilities to communicate with a balloon during flight are usually established at the launch site or a nearby location. The necessary requirements are the assurance of a broad reception range and stable communication. If a balloon is flown outside this reception range, relay stations are needed along the flight path. In recent years, with the progress in satellite communication technology, advances have been made in establishing direct communication via satellite, eliminating the need for ground stations.

On the one hand, since it is not a good idea to carry a high-power transmitter and large-aperture directional antenna on a balloon, a low-power (i.e., several Watts) transmitter equipped with a nondirectional antenna is generally carried. On the other hand, stable communication within the line-of-sight distance is achieved by using high-gain, large communication antennas on the ground.

3.3.2.1 Line-Of-Sight Distance from the Ground Station

The distance over which direct communication is possible extends to the point that a balloon flying in the stratosphere disappears over the horizon as viewed from the ground station. In brief, considering the earth to be spherical, the line-of-sight distance L_{\max} for the case where the topology is assumed to be locally flat

$$L_{\max} = L_1 + L_2, \quad (3.16)$$

where

$$L_1 = R_{\text{er}} \tan \theta_1, \quad (3.17)$$

$$L_2 = R_{\text{er}} \tan \theta_2, \quad (3.18)$$

$$\theta_1 = \sin^{-1}(R_{\text{er}} + H_g) = \cos^{-1}\left(\frac{R_{\text{er}}}{R_{\text{er}} + H_g}\right), \quad (3.19)$$

$$\theta_2 = \sin^{-1}(R_{\text{er}} + H_{\text{bal}}) = \cos^{-1}\left(\frac{R_{\text{er}}}{R_{\text{er}} + H_{\text{bal}}}\right), \quad (3.20)$$

where R_{er} is the radius of the earth, H_g is the installation height of the ground communication station, and H_{bal} is the balloon flight altitude. L_1 is the straight-line distance from the ground station to the horizon, and L_2 is the straight-line distance from the balloon to the horizon.

L_1 becomes longer the higher the height of the reception antenna installation, and L_2 becomes longer the higher the flight altitude of the balloon. For example, for a base station located at a height of 500 m above sea level and a balloon altitude of 30 km, L_1 is 80 km, and L_2 is 620 km, giving a total of 700 km.

Additionally, on the one hand, as a practical matter, the communication distance is extended due to radio-wave diffraction near the horizon and refraction of radio waves propagating in the atmosphere. On the other hand, communication becomes unstable with distance due to interference with waves reflected from the earth's surface. This effect is quite marked when flying over the ocean since the reflectivity of the ocean's surface is larger than that of land.

3.3.2.2 Balloon Tracking by Communication Antenna

The high-gain antenna of a ground station is naturally a narrow-beam directional antenna. Consequently, to capture the balloon within the beam, it necessary to mount the antenna on a two-axis drive system and control its direction. Usually, one of the following three methods is used to track the balloon.

- (1) Manual tracking: Because a balloon travels slowly, with the exception of immediately after launch near the ground station, high-speed tracking is not necessary; this is in contrast with the case for rockets. Therefore, the antenna is manually pointed in a direction of high receiver sensitivity using a joystick or something similar.
- (2) Automatic tracking: The antenna is automatically pointed in the direction of the strongest radio waves using control technology to drive the antenna mount. Narrow conical scanning of the beam or using multiple slightly offset beams is used to determine the deviation from the direction of strongest reception of radio waves by signal processing. Of course, operating of the receiver and the antenna mount is more complicated and expensive than method (1).

- (3) Use of GPS positioning: As described in Sect. 3.2.3.2, if a GPS receiver is mounted on a balloon, the precise geometrical position of the balloon (latitude, longitude, and altitude) can be determined using satellites. If this positioning information is sent to the ground base by a telemeter, the direction from the antenna to the balloon (elevation and azimuthal angles) can be determined by performing simple calculations using the known ground station positions (latitude and longitude). The antenna can be pointed toward the balloon by controlling the angles on the mount so that they become the same as the calculated angles. The automatic tracking method is the same as that used for (2). However, because the method for determining the antenna orientation direction is more straightforward, and the mount is controlled by a simple angle-setting servo that adjusts to the directed value, the control technology is considerably simpler. The receiver requires no special capabilities, and the system is inexpensive. In addition, it has the advantages that even if the balloon travels long distances, there is no reduction in the precision of determining the angle, and tracking can be performed reliably even with a faint signal up to the limit at which GPS data can be read out.

Figure 3.18 shows the exterior of the communications facility at the Sanriku Balloon Center of the ISAS and the antenna placed in the radome used for telemeter communication that has automatic balloon-tracking capability.

3.3.2.3 Relay Station

In cases when a balloon is flown beyond the line-of-sight range of the ground station, the communication range can be extended by placing relay stations on standby prior to the expected flight path. There are simple stationary relay stations and mobile relay stations transported by motor vehicles. Data received at a relay station are sent to the ground station via modem and/or internet connection. Figure 3.19 shows a vehicle-mounted mobile observation station of the ISAS.

3.3.2.4 Use of Satellite Communications

Long duration flights have been performed that last for a week or longer (these are described later), such as transoceanic flights and flights around the polar regions. In these flights, maintaining continuous communication with the balloon using satellites and conducting balloon control and acquisition of observational data is more effective than establishing relay stations. NASA is already pushing ahead with the use of its Tracking and Data Relay Satellite (TDRS), which is a satellite dedicated to relaying communications with satellites.

The use of Inmarsat, a satellite in geosynchronous orbit that performs commercial maritime and land mobile communication, is also being tested. In Japan, balloon-satellite flight communication testing is being carried out using the ETS-V, a test satellite that performs the same sort of communication [5]. However, because

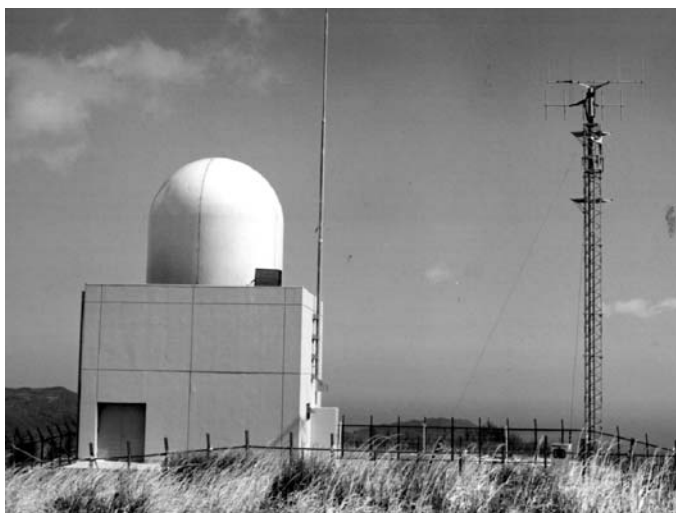
**a****b**

Fig. 3.18 Communication facility at the Sanriku Balloon Center. There is a 3.6-m-diameter parabolic antenna within the radome (courtesy of the ISAS): **a** Communication facility, **b** Parabolic antenna



Fig. 3.19 Mobile observation vehicle equipped with the capability to transmit to and receive from a balloon (courtesy of the ISAS)

of the long distances from the balloon, a large directional antenna is necessary to increase the transmission gain for high-speed data transmission with a satellite in geosynchronous orbit. In addition, a control system is required to point the antenna from the balloon toward the satellite.

There were plans to achieve mobile phone capability by placing multiple satellites in orbits lower than geosynchronous orbit (for example, Iridium). The services necessary to perform communication with this type of system have been put to practical use. In 2002 and 2003, ISAS used the Iridium mobile satellite telephone service for the bilateral data link between the ground station and the balloons that performed the long duration circumpolar flights at Antarctica [6].

In this case, communication is possible by simply connecting a data communication adapter to a mobile phone. However, because balloon-dedicated lines are not guaranteed with commercial communication systems such as mobile telephones, there is concern about the certainty and reliability of communication when flying a large balloon.

3.3.3 Other Facilities and Equipments

Principal facilities other than the above-mentioned are buildings and indoor facilities to aid preparation and tests of the scientific equipment carried by the balloon,

facilities associated with the lifting gas, and facilities to monitor the ground weather. Since the quantity of lifting gas required for a single launch of a large balloon converted to atmospheric pressure is more than $1,000\text{m}^3$, lifting gas is normally compressed into high-pressure cylinders that are charged to about 150 atmospheres or more and stored at the launch site.

Knowledge of the ground weather conditions in the vicinity of the launch site, particularly the wind speed and direction, is essential when launching a balloon. Instruments such as a standard Wilson-type wind speed and wind direction meter are used near the ground. One simple means often employed is to raise a small rubber balloon on a tether line about 100-m long, and by observing its behavior, determine the ground winds up to the height of the balloon. There are also tests being introduced that require a relatively expensive device known as a wind profiler, which transmits radio waves or ultrasound waves upward and observes the two-dimensional profile of the upper atmosphere from the reflected waves.

3.4 Launch and Flight

3.4.1 Acquisition and Use of Meteorological Data

3.4.1.1 Necessity of Aerological Data and the Role of a Meteorological Team in Balloon Experiments

After a balloon has been launched, it moves with the wind in the area it is floating in. As described in detail in Sect. 3.4.3, the flight speed and course can only be varied by changing altitude through the two means of exhausting lifting gas and dropping ballast; this change in altitude may result in the balloon being blown by a different wind from the initial one.

For this reason, current aerological data both prior to launch and during the flight is indispensable for ensuring safety during a flight, as are forecast predictions. To achieve this, the balloon experiment team generally includes a meteorological team. Depending on the situation, meteorological experts may be included in the team or brought in from the outside as advisors. In prelaunch meetings, it is common practice for the meteorological team to describe the ground weather and aerological conditions, and for flight planning and launch decisions to be made based upon this information.

The first task of the meteorological team is to investigate the annual variation in the wind conditions as a function of altitude in the vicinity of the launch site. Figure 3.20 shows the seasonal variations in the winds in the north-east region of Japan where a balloon base is located. This figure illustrates how the altitude distribution of the east-west wind component or the north-south wind component of the respective winds varies with the time of year. In this case, balloons generally fly in the east-west direction. This figure shows that the prevailing westerlies are strong

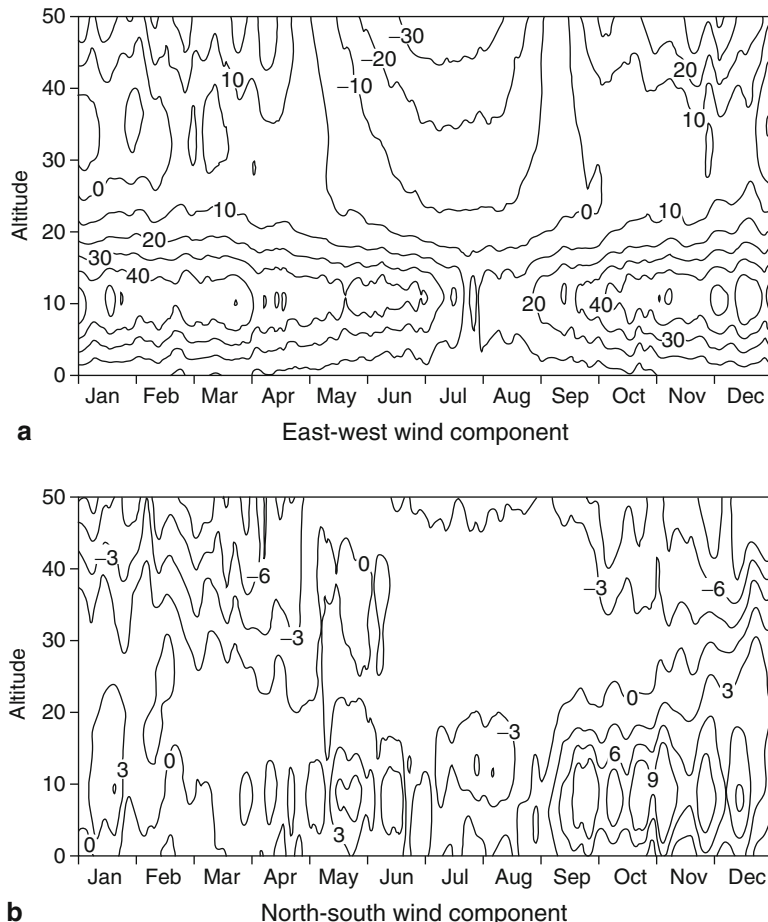


Fig. 3.20 Seasonal variation in winds in the vicinity of the Japanese balloon base (latitude: 39° north). Units are m/s. Westerly and southerly winds are denoted by positive values, and easterly and northerly winds are denoted by negative values. (Figure prepared using data from the UK Meteorological Office (UKMO)): **a** East-west wind component, **b** North-south wind component

during the periods May–June and August–September so that balloons travel toward the Pacific Ocean during ascent. It also shows the winds at float altitude are easterly and are not strong during these the periods. These characteristics make these two periods suitable for long duration flights.

Next, simulations are performed prior to launch to assess whether the various wind conditions at each altitude satisfy the requirements for launching the balloon and for performing scientific observations. In other words, the predicted ascent path during the ascent phase (i.e., after launch, but before the balloon reaches its pre-determined float altitude) will be examined to see whether it lies within the stipulated course bounds described in detail in Sect. 3.4.7. In addition, the winds at float altitude will be assessed to determine whether they are suitable for the planned scientific observations.

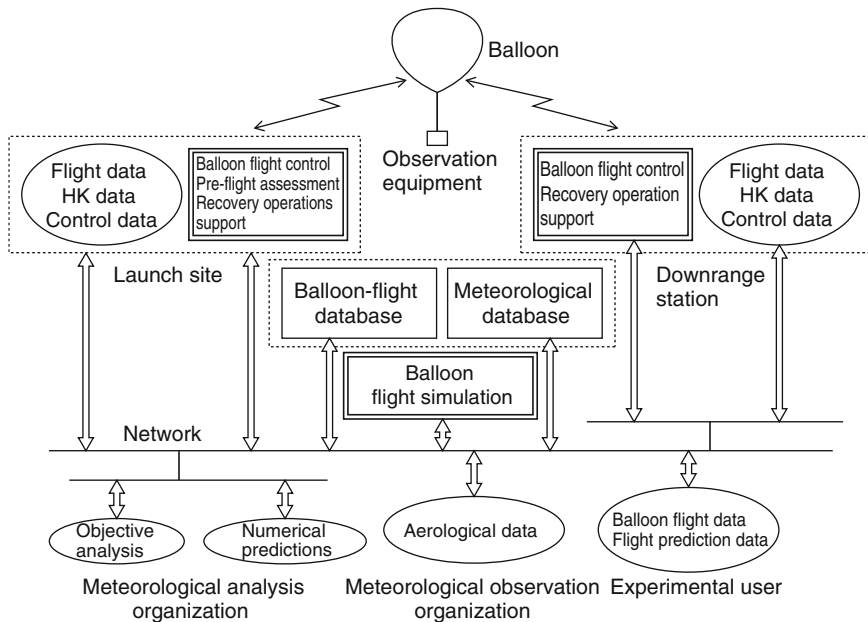


Fig. 3.21 Functional framework for a flight control system

When the balloon reaches float altitude at which scientific observations are performed, the most desirable course needs to be selected by adjusting the balloon's altitude. When the observations have been completed and the gondola carrying the observation equipment is separated from the balloon and descends by parachute, highly accurate course predictions are made to predict the location on the ground or at sea that the gondola will land to enable quick and safe recovery.

The various simulations and assessments performed for each phase as described above are conducted by connecting the launch site, downrange station, recovery station, etc. in a network as shown in Fig. 3.21. Various aerological data, balloon flight data, and on-board equipment housekeeping (HK) data are also acquired via this network. The simulations use both directly observed aerological data (from radiosondes and sounding rockets) and indirectly observed aerological data, such as that from meteorological satellites.

In addition, as a result of the great advances in computers and numerical analysis techniques in recent years, various objective analytical data and various numerical prediction data, which is calculated using the objective data as initial values, can be obtained. Particularly with the recent spread of the Internet and the acceleration of information disclosure, some of this data are made freely available to anyone.

3.4.1.2 Types of Aerological Data

In this section, we present an overview of representative aerological data.

Radiosondes

Radiosondes acquire directly observed data that indicate the actual aerological conditions. They are described in detail in Sect. 3.6. Since they are managed within a worldwide network, measurements are performed simultaneously at several hundred different locations around the world. It should be kept in mind that these data are obtained by measurements taken along the flight path of a rubber balloon. These sort of direct observations are biased toward the heavily populated regions in the northern hemisphere. Furthermore, with the exception of ocean-based weather observation ships, there are almost no observation points over the oceans, so that the locations at which data are collected are limited.

Sounding Rocket Observations

Dropsondes are released from sounding rockets that are launched to altitudes up to approximately 60 km, and as they descend by parachute, they measure the air temperature, wind direction, and speed as functions of altitude. In Japan, launches used to be carried out once a week at Ryori, Ofunato-shi, Iwate Prefecture, but these were discontinued in March 2001.

Doppler Anemometers

These are installed on the ground, and they emit an upward pulse to investigate the variation in wind speed and direction as a function of altitude in the upper atmosphere. These devices are also referred to as wind profilers. There are Doppler sodars based on sound waves, Doppler radars based on radio waves, and Doppler lidars that employ lasers.

Meteorological Satellites

There are geostationary meteorological satellites such as the “Himawari” and polar-orbiting meteorological satellites such as “NOAA.” The temperature and wind speed distribution are measured by remote sensing.

Objective Analysis

The various data measured on the ground, the aerological data described above, and the data from meteorological satellites include spatial irregularities and many other factors that contribute to error. The process of determining the values on a regular grid from these types of data is called objective analysis. Many types of the observed data mentioned above are used in numerical models. Data that have been

adjusted so that it optimally expresses actual atmospheric conditions are referred to as assimilated data. This kind of analysis is performed by many meteorological organizations.

As representative examples, there is the assimilated data released by the British Atmospheric Data Centre (BADC) prepared by the UK Met Office as a part of the Upper Atmosphere Research Satellite (UARS) project. These data extend up to approximately 60 km in a $0.5625^\circ \times 0.375^\circ$, 30-layer grid in the vertical direction and it consists of the daily analysis values at 12:00 UTC. In addition to this, there are analysis values from numerical predictions described next.

Numerical Predictions

Numerical analysis prediction values based on various models and techniques are published. For example, there are the values from the Global Forecast System (GFS) Model of the National Centers for Environmental Prediction (NCEP). As for grids, there are data up to 180 h ahead up to an atmospheric pressure of 1 hPa for a $0.5^\circ \times 0.5^\circ$ grid with a 47-layer vertical resolution. In addition, data from the European Centre for Medium-Range Weather Forecasts (ECMWF) is also well known. In Japan, the Japan Meteorological Agency (JMA) releases data up to an atmospheric pressure of 10 hPa for a $1^\circ \times 1^\circ$ grid with a 17-layer vertical resolution.

Figure 3.22 shows a set of four iso-altitude contour plots at the 10-hPa-atmospheric-pressure layer specially prepared and presented by the Numerical Prediction Division of the JMA at the time when the ISAS was conducting balloon experiments at the Sanriku Balloon Center. In the plots for May shown in Figs. 3.22a and b, the region of dense iso-altitude lines on the high-latitude side has easterly winds because the stratosphere has its summer atmospheric pressure distribution. Conversely, there are westerly winds at lower latitudes. Conditions in which the easterly wind region daily extends southward are clearly observable. The plots for August in Figs. 3.22c and d show the situation in which the effect of the collapse of the Arctic polar vortex shifts from high to low latitudes. That is, while easterly winds remain in the south, they change to westerly winds in the north.

Much of the various numerical data described above is prepared using a technique called Gridded Binary (GRIB), which is one of the standard formats of the World Meteorological Organization (WMO) that highly compresses large amounts of grid meteorological data. By preparing systems that can use this type of data, the data can be applied to regions in other countries, which for the most part are unable to perform experiments and make direct observations.

However, even when using the variety of data described above, it is comparatively difficult from the precision of the data to obtain data that can accurately predict the flight of a balloon at high altitudes. In such cases, independent observations are necessary. It is important to obtain temperature and wind data up to high altitudes, such as by the pre-flight launching of rubber balloons, and to supplement the system operations described above. In these cases, there are also advantages in being able to obtain detailed information about phenomena such as temperature inversion layers.

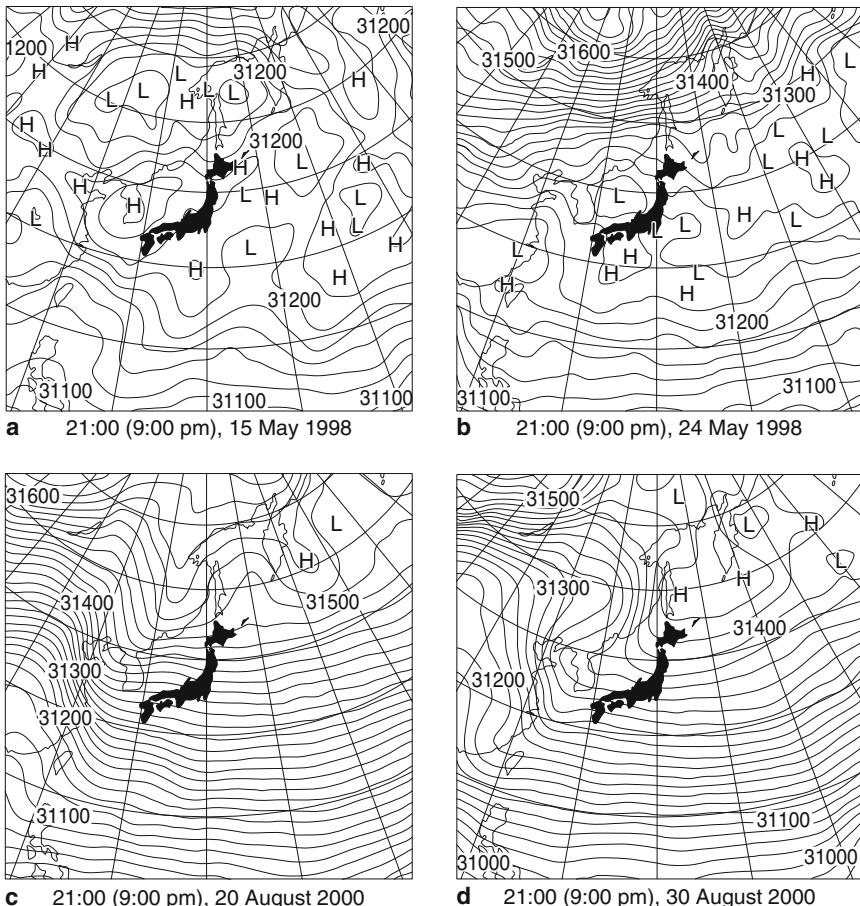


Fig. 3.22 Changes in iso-altitude contour plots at an atmospheric pressure of 10 hPa. (courtesy of Numerical Prediction Division, Japan Meteorological Agency): **a** 21:00 (9:00 pm), 15 May 1998; **b** 21:00 (9:00 pm), 24 May 1998; **c** 21:00 (9:00 pm), 20 August 2000; **d** 21:00 (9:00 pm), 30 August 2000

3.4.2 *Injection of Lifting Gas and Balloon Launch*

3.4.2.1 *Launch Operations*

All of the required lifting gas must be injected into the balloon on the ground prior to launching. This is a major difference from aircraft, which are able to control their propulsion power, and which can stand by with the engine output at a minimum until commencing take off. Consequently, it is important to find a method for restraining a balloon, which has full buoyancy on the ground, and which does not result in the film being damaged in the period between injecting the lifting gas and launching.

At this time, since the top globe of the balloon, which is inflated on the ground, is greatly affected by ground winds, it is important to make sure that it is as low as possible.

If the wind conditions become suitable for launching, the restraints must be released as quickly as possible, and the balloon and the payload must be allowed to ascend smoothly. The requirements for a good launch method are that it should minimize the effect of ground wind fluctuations on the sequence of operations and that it must meet the broad requirements for a safe launch. Here, we focus first on dynamic launching, which is the most widely used launching method worldwide and is the method used by NASA. We then contrast other methods with this method.

The mechanical equipment used and its placement when launching a balloon is depicted in Fig. 3.23 (see also Frontispiece 3 for a photograph of an actual launch). The roller vehicle on the left is equipped with a cylindrical roller that is 0.5–1 m in diameter and about 2 m wide (Fig. 3.24). The buoyant force of the top globe is restrained by this cylindrical roller, which makes contact with a wide area of the film surface to prevent the film from being damaged. At the same time, the uninflated portion of the balloon is stretched along the ground and makes an angle of 90° to the inflated portion. The buoyant force is restrained by securing the terminal of the suspending system to the launcher, as described later. It is a common practice to bind the bottom of the top globe with a wide band (referred to as a collar) so that the injected lifting gas does not expand downward and increase the aerodynamic drag.

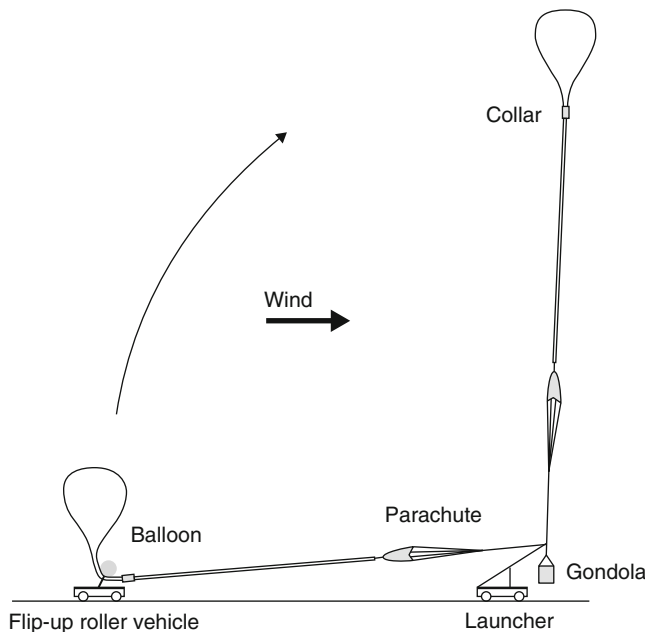
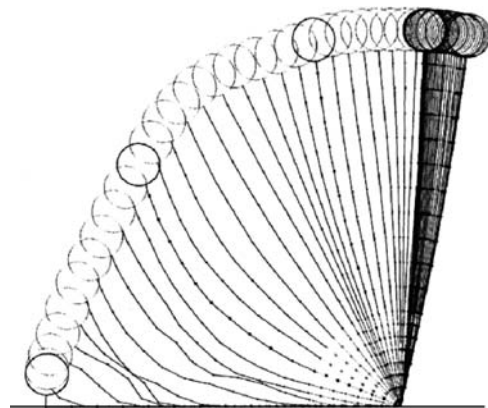


Fig. 3.23 Dynamic launching



Fig. 3.24 Roller section (courtesy of NASA/NSBF)

Fig. 3.25 Balloon ascent process by dynamic launching

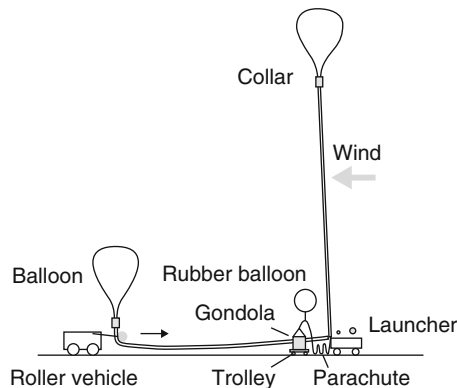


One of the two arms that support the rotating shaft of the cylindrical roller is part of a mechanism that can instantly release the rotating shaft so that the entire roller swings about the other arm while simultaneously rotating about its shaft. This action releases the restraint from the top globe of the balloon, and the balloon ascends while lifting the uninflated portion of the balloon, the parachute, and other components and drifting in the wind.

Figure 3.25 shows computer simulation results of the process by which a balloon that is released from a roller vehicle ascends by tracing out a catenary curve to the launcher.

The launcher shown on the right side of Fig. 3.23 is a wheeled vehicle and has a long arm that suspends and clamps the gondola. When the top globe is released from the cylindrical roller, the launcher moves downwind of the apex of the balloon and releases the gondola; the timing of this process is synchronized so that the gondola leaves the ground smoothly with little shock.

Fig. 3.26 Static launch method carried out at the Sanriku Balloon Center of the ISAS



Launch fields in Japan are narrow, so that static launching is used in which the launcher remains stationary (Fig. 3.26). After gas injection, the roller vehicle gradually advances toward the launcher. The top globe stands up vertically, and eventually the entire balloon is allowed to rise up over the launcher. At the time of launch, when the restraint is released, the positions of the launcher and gondola are adjusted, so that the timing of the launch is coordinated with fluctuations in the ground wind [7]. Since 2003, a balloon-launching method that is similar to the dynamic launching method has been used.

At CNES, the gondola is raised 2–3 m using a separate small auxiliary balloon, as shown in Fig. 3.27a, and it is launched almost simultaneously with the ascent of the main balloon. The two balloons initially ascend in parallel, but when the main balloon becomes higher than the auxiliary balloon, the auxiliary balloon automatically detaches, and the gondola load shifts to the main balloon, as shown in Fig. 3.27b.

3.4.2.2 Balloon Handling on the Ground

Since the film of a balloon envelope is thin and tears easily, the following steps for handling at the launch site are followed to minimize operations that involve artificially moving the balloon.

- (1) Removing the balloon: The transport box is positioned on the field near the roller vehicle. While the box is moved slowly toward the launcher, starting with the top of the balloon, the balloon is removed from the transport box, and stretched lengthwise in a straight line on the field.
- (2) Setting up the launch roller: The top of the balloon is passed under the launch roller, and it is turned back. The length that it is turned back is equal to the length to the part of the top globe that expands when it is injected with lifting gas while on the ground.
- (3) Collar installation: A collar is attached to the bottom part of the top globe so that gas does not go below this point.

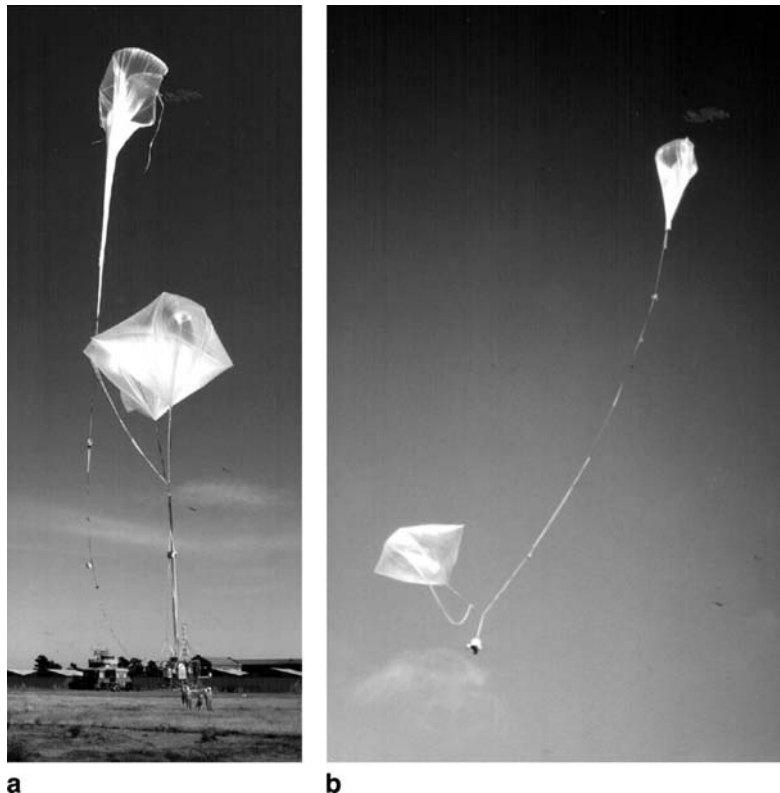


Fig. 3.27 Launch method using an auxiliary balloon (courtesy of CNES)

- (4) Suspending system coupling: The top of the suspending system is attached to the fitting at the base of the balloon.
- (5) Gondola coupling: The bottom of the suspending system is attached to the top of the gondola, which is installed in the launcher.

3.4.2.3 Injection of Lifting Gas

The gas hose is extended for the lifting gas from the high-pressure cylinder, and gas is injected through the inflation tube (see Frontispiece 1). It is desirable for the filling time to be short. In large balloons, inflation tubes come out at two locations, and gas is simultaneously injected through both tubes. Gas injection is generally completed within 1 h.

3.4.2.4 Measuring the Amount of Lifting Gas

The free lift required for a balloon to ascend stably at a constant velocity is just under 10% of the balloon system weight for large balloons. Accordingly, it is desirable for

the buoyancy produced by the gas injected into the balloon to be able to be measured to an accuracy of at least 1%, or ideally, 0.1%.

The easiest and most accurate way of determining the amount of gas injected into a balloon is by subtracting the amount of gas remaining in the high-pressure tank vessel from the initial amount of gas in the tank vessel. Since gas is expelled rapidly from the gas vessel during gas injection, the temperature of the gas within the vessel drops below the external air temperature over time due to adiabatic expansion. Consequently, to measure the amount of gas remaining, it is necessary to not only measure the pressure in the vessel, but also, at the same time, to accurately determine the changing gas temperature. However, because it is difficult to measure the temperature of the gas within the vessel directly, the temperature of the vessel itself is commonly substituted.

When the lifting gas that has been charged into a pressure vessel of volume V_c [m³] at a pressure P [Pa] and a temperature T [K] is completely injected into a balloon, if we denote the pressure and temperature of the atmosphere by p_a and T_a , respectively, the volume of the balloon V_b is given by

$$V_b(P^*, T) = \frac{T_a}{T} \frac{P^*}{p_a} V_c, \quad (3.21)$$

where P^* is the pressure that includes the compression factor α as a correction for the amount the lifting gas deviates from an ideal gas, and the relationship to the actual measured pressure P is

$$P^* = kP, \quad (3.22)$$

$$k = \left(1 + \alpha P \frac{293}{T} \right)^{-1}, \quad (3.23)$$

$$\alpha = 5.03 \times 10^{-4} \text{ (In the case of helium).} \quad (3.24)$$

If we take the pressure and temperature of the gas vessel before injecting lifting gas to be P_1 and T_1 , respectively, and the pressure and temperature at a time during injection to be P_2 and T_2 , respectively, and if we take the density of atmosphere and the density of the lifting gas under atmospheric temperature and atmospheric pressure conditions during injection to be ρ_a and ρ_g , respectively, the mass of the gas m_g and the buoyant force F injected into the balloon at that stage from (3.21) are, respectively, given by

$$m_g = \{V_b(P_1^*, T_1) - V_b(P_2^*, T_2)\} \rho_g, \quad (3.25)$$

$$F = \{V_b(P_1^*, T_1) - V_b(P_2^*, T_2)\} \rho_a g. \quad (3.26)$$

Since the target buoyant force F_f that should be injected into a balloon is usually given by the sum of the balloon system weight before injection and the buoyancy for ascent (free lift), which is proportional to this weight, it is necessary to add the weight of the gas to the injected buoyant force. Consequently, the buoyancy deficit during injection is

$$\Delta F = F_f - (F - m_g g) = F_f - \{(V_b(P_1^*, T_1) - V_b(P_2^*, T_2))(\rho_a - \rho_g)g\}. \quad (3.27)$$

Here the second term on the right-hand side corresponds to the effective buoyancy described in Sect. 2.1.2 In addition, gas densities values reported in data tables are given for standard conditions T_0 and P_0 (usually 273 K and 101,325 Pa). If we assume use of values ρ_{a0} and ρ_{g0} , the gas densities in (3.27) may be converted as follows

$$\rho_a - \rho_g = \frac{T_0}{T_a} \frac{P_a}{P_0} (\rho_{a0} - \rho_{g0}). \quad (3.28)$$

At this stage, the tentative target gas pressure P_f^* at $\Delta F = 0$ is

$$P_f^* = \frac{T_2}{T_1} \left(P_1^* - P_a \frac{T_1}{T_a} \frac{F_f}{V_c(\rho_a - \rho_g)} \right). \quad (3.29)$$

This target pressure P_f^* is estimated by assuming that the vessel temperature remains constant at T_2 , so that it initially has a large error at the start of injection. However, this error is corrected by itself by the following process. The gas pressure and temperature (temperature of the pressure vessel) are detected by sensors and their values are input into a computer. Real-time calculations are performed in accordance with (3.29), based on these most recently obtained data. Then the actual measured temperature T_2 approaches the final temperature as gas injection progresses. Hence, the error in the estimated target pressure P_f^* decreases and eventually approaches zero. If instructions based on this target pressure, which is determined during injection, are given to the personnel responsible for injecting the lifting gas, he/she can easily control the amount of injected gas with good precision.

In addition, since the gas temperature initially decreases during injection due to adiabatic expansion, and the temperature of the gas pressure vessel then decreases, a slight temperature difference is produced between these temperatures from the time delay in the heat transfer between the gas and the vessel. However, a few minutes after completing injection, the temperature of the lifting gas becomes almost the same as that of the vessel since the heat capacity of the lifting gas is small compared with that of the vessel. In this transient period, since the values calculated for the amount of injection gas shift toward having to inject additional gas, if the amount of gas injected does not exceed that indicated by the computer, the buoyancy will approach the correct value. For the same reason, even if the gas vessel temperature and the atmospheric temperature remain different, because the temperature of the vessel changes slowly, it may be treated as having the same temperature as that of the lifting gas, and hence its effect on the amount of buoyancy can be ignored.

3.4.2.5 Providing Free Lift

The initial free lift necessary for the balloon to ascend at the appropriate speed must be determined prior to injecting the lifting gas. This amount is considered under “Balloon ascent speed and free lift” in Sect. 2.4.2.2 and is illustrated in Fig. 2.29.

As is clear from (2.105), when the same free lift ratio f (ratio of the free lift to the balloon system weight) is provided, the ascent speed v_{bz} increases in proportion to the 1/6-power of the balloon system mass m_G . That is, an f causing the same ascent speed will decrease with an increase in m_G .

Normally, an ascent speed of about 5 m s^{-1} is chosen. In this case, according to (2.105), the free lift ratios for balloon system masses of 250, 500, 1,000, and 2,000 kg are 12%, 10%, 8.5%, and 7.3%, respectively. Here, the index for the effect of temperature reduction on the lifting gas due to adiabatic expansion \tilde{T}_g is selected experimentally as being close to 0.98.

More specifically, as mentioned under “Ascending motion” in Sect. 2.4.4.2, the ascending motions of balloons launched at daytime and at nighttime differ considerably. Ascent is also affected by disparities in the variation of the atmospheric temperature with altitude, such as the presence or absence of an inversion layer. An appropriate initial free lift ratio should be determined to minimize the need to correct the ascent speed by venting lifting gas and dropping ballast. Consequently, it is necessary to use the balloon dynamics analysis programs described in Sect. 3.4.1, to perform simulations of the ascent speed by inputting conditions such as upper-atmosphere temperature distribution data at the time of launch and the variation of the solar radiation intensity with time.

3.4.3 Flight Control

The launched balloon is controlled by an operator from an operations console at the ground station, based on data transmitted from the balloon. The main control tasks corresponding to each stage of flight are as follows.

3.4.3.1 Immediately After Launch

This is generally the stage in which the most trouble is experienced during the course of a balloon experiment, and the greatest care must be taken in flight control.

Notification of Concerned Parties

The agencies concerned (including the air traffic authority) are promptly informed of the balloon launch in accordance with preexisting procedures. Depending on these arrangements, close contact may continue until the balloon is higher than the flight altitudes of aircraft.

Balloon Problems

There is a possibility of damaging the envelope due to problems in the preparation stage or shock during launch. Whether to continue the flight or not is decided quickly. If a serious problem is encountered, the safety on the ground is checked, and the flight is aborted immediately.

Adjusting Early-Stage Ascent Speed

If a mistake was made in the amount of gas injected, so that the ascent does not start at the normal velocity, the power of ascent is adjusted by dropping ballast or venting lifting gas from the exhaust valve.

Flight Range Confirmation

When there are populated areas or facilities that must be avoided in the vicinity of the launch site, it must be determined whether or not the flight course lies within the predetermined safety range. If the flight path differs from the forecasted path, appropriate response measures will be taken based on ground wind data.

Checking Operations of On-Board Equipment

It is determined whether the operating conditions of the flight control equipment pose any problems to continuing the flight and whether the operating conditions of the observation instrumentation are such that meaningful observations can be performed. If there is a serious failure, the flight is safely terminated while the balloon can be controlled reliably.

3.4.3.2 Control During Ascent

Ascent Speed Adjustment

Usually, even if the appropriate free lift is provided and the balloon ascends at the normal velocity, the balloon sometimes decelerates when it enters the tropopause where the atmospheric temperature is higher (Sect. 3.4.1), and hence the difference between the atmospheric temperature and the temperature of the lifting gas increases. Even if there is a strong temperature inversion in the troposphere, the ascent will decelerate. This effect is particularly large at night. Since the velocity recovers slowly if ballast is dropped after too much deceleration has occurred, it is important to respond appropriately.

Level Flight at an Intermediate Altitude

This is an operation that temporarily stops ascent at an intermediate altitude below the ceiling altitude when the balloon is only partially expanded. This is done to make adjustments to the flight route or to meet the requirements of the scientific experiments. Since there are no conditions that will ensure the altitude will automatically become constant, this operation requires venting the free lift portion of the lifting gas from the exhaust valve at the appropriate altitude so that the ascent speed becomes nearly zero. It is effective to do this by using the balloon dynamics analysis program that includes the ascent speed control and incorporates the upper atmosphere meteorological data described in Sect. 3.4.1.

3.4.3.3 Altitude Operations at Level Flight Altitude

Maintaining a Level Altitude

As described in Sect. 2.3.1, there is no stable altitude for a zero-pressure balloon in the downward direction. When the area below the balloon is covered by clouds having a low cloud-top temperature (Sect. 2.4.4), infrared radiation from the earth is blocked, and the balloon loses altitude because the temperature of the lifting gas decreases. This effect is particularly large at night. It is sometimes difficult to predict exactly whether clouds are just briefly passing, in which case the balloon's altitude will quickly recover, or if clouds will remain for a long time so that ballasting is necessary. In experimental trials, installation of an infrared sensor on the bottom of the gondola was found to facilitate prediction.

Operation at Sunset

The inevitable variation in flight altitude due to the reduction in the lifting gas temperature that occurs at sunset is described in Sect. 2.3.1. This phenomenon commences when the elevation angle of the sun begins to decrease. The solar radiation passes through a thicker section of the atmosphere and is consequently attenuated more. It becomes significant as the albedo decreases as the sun sets, initially at ground level, and then at the balloon's altitude. The ideal method for compensating for the sunset effect that minimizes ballast consumption is to determine the reduction in buoyancy before the balloon begins to descend and to drop ballast in small amounts. The ballasting operation is then optimized by precisely measuring the balloon's vertical velocity, along with the internal–external gas temperature difference or the pressure differential at the base of the balloon.

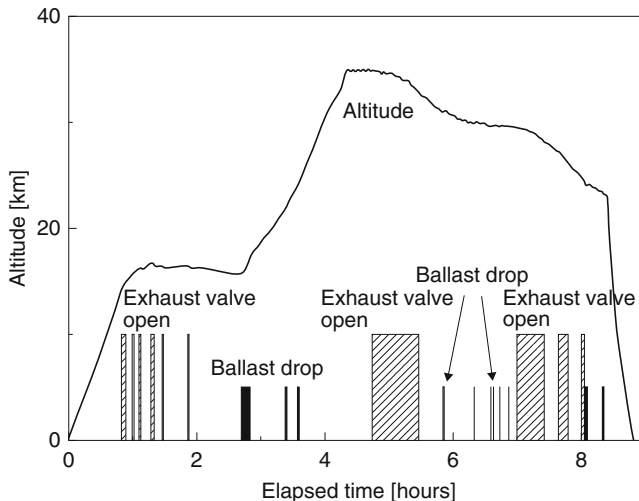


Fig. 3.28 Example of controlling balloon's altitude through venting and dropping ballast

Slow Descent in Flight Altitude

This operation is performed when it is necessary to gradually lose altitude by venting lifting gas from the exhaust valve during a scientific observation. The relationship between the free lift and the descent velocity is essentially the same as that for ascent. However, as described in Sect. 2.4.2, when altitude decreases, the temperature of the lifting gas increases due to adiabatic compression, and the descent velocity becomes slower because buoyancy temporarily recovers. A venting operation that accounts for this kind of dynamics is performed based on analysis of the balloon's motion. Figure 3.28 shows a record of the flight altitude operations performed at the time of a stratospheric air sampling experiment at several altitudes in 2002. It clearly shows the change in the balloon's altitude as a result of venting.

3.4.4 Flight Control Apparatus

3.4.4.1 Flight Location Positioning

As will be described in Sect. 3.4.7, to ensure aeronautical safety during a balloon flight, it is necessary to continuously determine the geographical location of the balloon during the flight and to ascertain its flight path. In addition, from the viewpoint of the scientific objective, determining the location of the balloon is essential for performing observations and experimentation and for recovering the payload. The balloon location is specified as the latitude and longitude directly below the balloon, as well as the sea-level altitude, and it is displayed as a tracking chart in the operations room.

The systems described below are used for location positioning. Out of these, GPS is an extremely effective means for determining the position of a balloon, and it is becoming the current system of choice.

Radio Tracking Systems

If the balloon is tracked by a ground-station directional antenna, the balloon's line-of-sight elevation and azimuth angle can be determined from the angles on the antenna's mount. If the slant range (i.e., line-of-sight distance) to the balloon is known, the balloon's geographical position can be calculated. In regard to the slant range, a sinusoidal wave (e.g., 5 kHz) superimposed on a command radio wave is transmitted to the balloon from the ground station, and on the balloon, this demodulated sinusoidal wave signal is input into the telemetry transmitter and is transmitted back to the ground station. The slant range can be obtained by measuring the delay between the original wave and the returned sinusoidal wave at the ground station.

Since this system is essentially the same as systems used in rockets and artificial satellites, for specific details, please refer to "Radio wave measurements and radio navigation in space", Vol. 1 of the "Space Engineering Series" books [8].

With the radio tracking system, as the balloon's position becomes more distant and the antenna's elevation becomes smaller, positioning errors produced by fluctuations in tracking increase. In addition, because their propagation speed varies as a result of air density changes in the atmosphere, radio waves bend slightly toward the earth's surface. As a result, the distance to the balloon is overestimated, and measurement errors of the balloon's altitude increase.

GPS System

GPS is a high-precision positioning system that uses satellites to cover all regions on the earth. Twenty-four satellites are distributed in orbits and transmit radio waves necessary for positioning. Since a ground-based receiver can simultaneously receive radio waves from at least four satellites, the slant ranges to the satellites can be obtained from the phase difference of the arriving radio waves, and latitude, longitude, and altitude data can be obtained using the principles of triangulation. For further information, refer to many technical books and instruction manuals on this subject, and also the detailed presentation given in the book mentioned above [8].

Since even small GPS receivers designed for personal use are capable of obtaining positioning data with a precision of 1 arcsecond or less for latitude and longitude and of 10 m or less for altitude, they are more than adequate for normal flight control of conventional balloon flights. The only special functions required are those relating to altitude. To prevent them being used for military purposes, altitude data above 10 km are not output from personal receivers. However, this restriction is enforced

only by the software for processing the signal in the receiver, and if measures are taken to circumvent this regulation, positioning can be performed that adequately covers balloon altitudes.

ARGOS System

This is a simple positioning system that is provided as an additional function of the meteorological satellite NOAA. The NOAA satellite travels in a polar orbit and receives radio waves transmitted intermittently from small devices called ARGOS transmitters. The position of an ARGOS transmitter can be pinpointed by determining the amount of Doppler shift in the frequency of the radio waves it receives. At middle latitudes, the satellite only comes in communication contact about once an hour, and its positioning accuracy of several kilometers is not necessarily good for the balloon operation. However, because these transmitters are compact, lightweight, and have a long operation time, they are employed as back-up devices for positioning during flights or for searching when balloon recovery requires a significant time.

Omega System

This was a positioning system used for small ships. Beacon radio waves at a frequency of 10 kHz were transmitted by coastal agencies at eight different locations around the world, and these gave global coverage. The latitude and longitude could be determined by receiving the radio waves using a simple receiver and calculating the phase difference of the radio waves. This system was established in 1975, and it was used for the determining the position of large balloons and meteorological sondes. However, it has become obsolete with the spread of GPS.

3.4.4.2 Flight Path Prediction

Real-time prediction of the direction and speed of the movement of a balloon during a flight is an important task in flight control. In particular, when terminating a flight, the air traffic control authority concerned is usually informed of the final planned termination position about one hour in advance. Since the air traffic control authority concerned tries to inform aircraft within an established range centered on this position, it is important that it should be accurate so that the established range does not deviate from the prediction. This is also true when a balloon is expected to come down close to a national border. As described in Sect. 3.4.1, the same forecasting method is used as that for predicting the flight path prior to launch based on various high-altitude meteorological data, but because the range is restricted and the elapsed time short, high accuracy predictions can be made in a short period of time.

3.4.4.3 Monitoring and Control of Flight Conditions

Flight Termination Safety

The most critical aspects of flight safety management are the operations for terminating a flight. Instructions must be reliably executed, and erroneous actions must not be performed in the absence of instructions. Because the suspended system is separated by pyrotechnics at the termination of a flight, commands are usually given by some sort of two-stage process. For example, the first command causes preparations to be completed for detonating the pyrotechnic device, and a state is produced in which the subsequent command will be accepted for only for a short predetermined period of time. Flight termination actions are only performed if the second command is received during this period. The first command status is confirmed by the ground station through a telemeter, and it is possible to abort on command even if the initiation-ready state was mistakenly activated. This ensures greater safety and certainty.

Control of Buoyancy

During a flight, when buoyancy is controlled by venting lifting gas from an exhaust valve or dropping ballast, situations must be avoided in which it is not possible to guarantee buoyant forces that are sufficiently high to maintain a desired altitude for the remaining flight duration. Consequently, it is important to reliably control the accumulated value for the quantity of lifting gas vented and the corresponding buoyant force as well as the total amount of ballast dropped and the amount of ballast remaining.

Operating Conditions of Internal Instrumentation

In addition to information noted above, information concerning the operating conditions of basic onboard-instrumentation for controlling the flight of the balloon (such as the voltage of the electric batteries, the multipoint working temperature, and the reception command status of the on-board receiver) are displayed via telemetry on the flight-control monitor screen at the ground station, to confirm whether or not a safe flight is being conducted.

Figure 3.29 shows a typical screen shot of such a flight-control monitor screen. In the upper left-hand corner of the screen, critical items for controlling the balloon flight are displayed, such as the balloon location, the command activity display, the quantity of lifting gas vented and the current buoyancy, and the amount of ballast

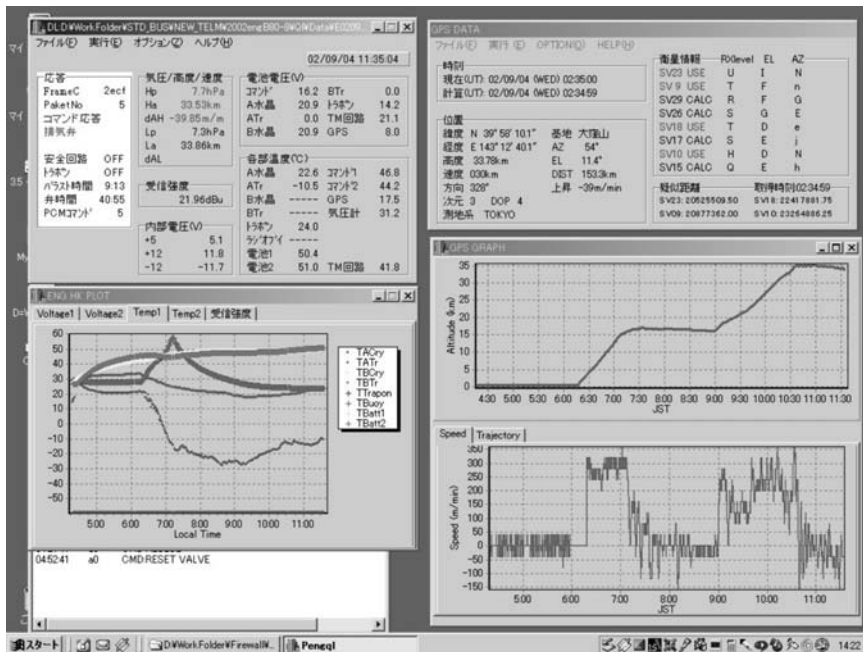


Fig. 3.29 Display screen for data sent from the balloon (excluding observational data)

remaining. In the upper right-hand corner, the operating status of the batteries that power the internal instrumentation and the measured temperatures inside and outside the gondola are displayed.

The screens on the right-hand side are displays of data for confirming the overall operating condition of on-board observation and test instrumentation. Detailed displays of the status of the observational and experimental equipment are usually shown using a system developed by the experimental group, and experimental work that includes command operations is performed independently in a separate room. Critical command information for controlling the balloon flight and operating voltages and temperatures for the on-board equipment are displayed in the upper left-hand corner. In the upper right-hand side is a display of detailed data from the GPS, which is used for tracking the location of the balloon. In the lower part of the screen, on the left is a temperature history at each measurement location, and on the right are the changes in altitude and velocity with time.

In the flight tracking maps, the position directly below the balloon is indicated on a map. In recent years, as detailed computer maps have been prepared, the flight track can be superimposed on a map on a computer screen by using such software. Figure 3.30 shows a typical display of the track display system used at SBC of the ISAS.

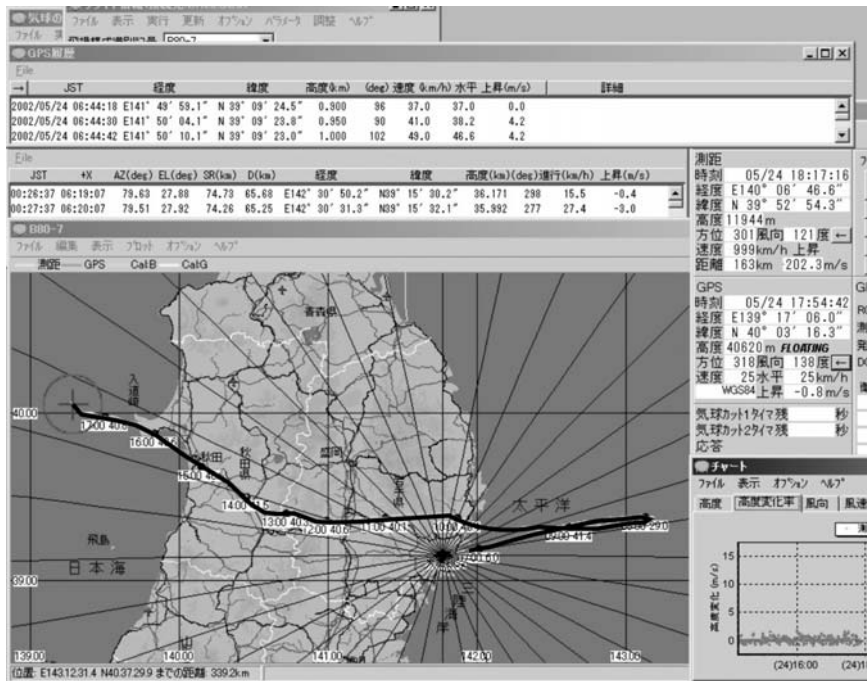


Fig. 3.30 Balloon flight track chart superimposed on the balloon flight control screen map

3.4.5 Flight Termination and Payload Recovery

3.4.5.1 Parachute Descent

To safely recover the payload, it is important to be able to make accurate predictions of the descent route and the landing (splashdown) point after the balloon has commenced descending by parachute from the flight altitude. In addition, information on the geographical features in the vicinity of the predicted landing (splashdown) point must be known, and it must be confirmed that there will be no injury to people or damage to property. Since, in many cases, the decision to terminate the flight must be made in a short amount of time, it is necessary to continually perform these predictive calculations in real time during the course of the flight.

To calculate the predicted parachute descent path, first calculate the speed of descent in the vertical direction, which is determined by the size of the parachute and the density of the air. Next, determine the horizontal travel distance based on the horizontal wind direction and wind speed data for the atmosphere in the 3D grid point from the numerical analysis models provided by meteorological agencies described in Sect. 3.4.1. The landing (splashdown) point is obtained as the integrated value of these calculations.

In the computer maps used for performing recovery on the ground, usually information on regions having a low population density, which are suitable for recovery, is not as detailed as that for urban areas. At the space research base ESRANGE (Frontispiece 6d) of the Swedish Space Corporation (SSC), in addition to information found on conventional maps, detailed maps have been prepared that indicate the location and population all the way down to small villages in regions where balloon experiments are performed. The predicted route of the parachute descent is indicated on the map. This system is valuable when making the decision to transmit the termination command for the balloon experiment [9].

3.4.5.2 Searching and Recovering

It is desirable to locate and recover experimental equipment that has been dropped as soon as possible. Strategies that can be employed for achieving this include continuous transmission of radio signals after landing (or splashdown) to aid in locating the equipment, or intermittently transmitting information on the landing position by installing an on-board ARGOS transmitter as described in Sect. 3.4.4.1.

Low-altitude aerial searches using helicopters and the like are frequently performed. NASA employs a more direct and reliable method that involves visually observing the balloon in flight from a small airplane at the time of flight termination. In this method, the command signal to drop the payload by parachute is sent from the airplane, and the payload is tracked to its landing point.

Although the balloon itself falls separately from the payload, because it has a high aerodynamic drag, it falls near the observation equipment. Since its recovery is an environmental issue, efforts are made to recover it.

3.4.6 Long-Duration Flight Technology

In many cases when performing observations and experimentation by balloon, it is desirable to continue observations for as long as possible. If the balloon can continue to fly for a few months, the cost-benefit performance of the balloon experiment will be equivalent to that of a satellite, which is capable of continuing observations for several years while orbiting the earth. However, the following problems are encountered in long-duration balloon flights.

- (1) The communication range from the ground base will be exceeded because the flight distance becomes long. In addition, there is a risk that the balloon will infringe the territory of other countries by crossing national borders.
- (2) If a zero-pressure balloon is flown at middle latitudes, as described in Sect. 2.3.1, it is necessary to drop ballast equivalent to 7–10% of the total buoyancy per day, which limits the number of days of the flight.

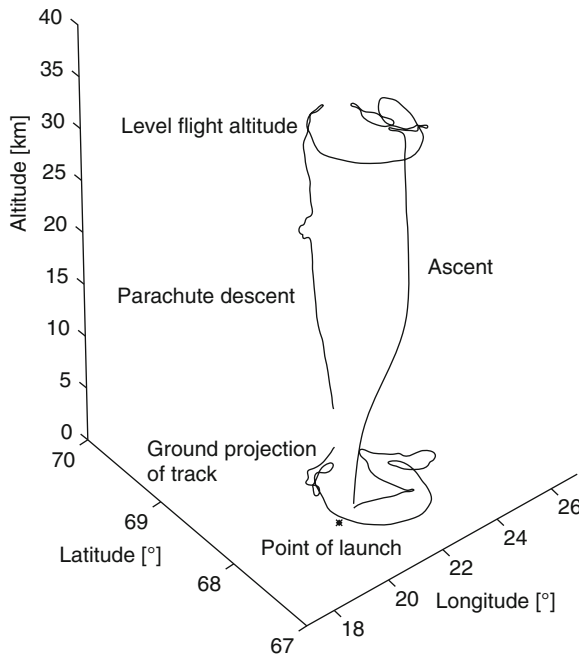


Fig. 3.31 Example of a long-duration flight that exploited the turn-around in the stratospheric wind direction at ESRANGE, Sweden. [Modified from I. Sadourny: “The French Balloon Programme”, Proc. 13th ESA Symp. On European Rocket and Balloon Programmes and Related Research, SP-397, pp.11–16 (1997).]

3.4.6.1 Flights Under Turn-Around Condition

As described in Sect. 3.1, in the stratosphere, westerly winds predominate in the winter season, whereas easterly winds blow in the summer season. Consequently, there are extremely weak winds during the transition period. If a balloon is flown during this period, it can remain within a short distance of the ground base for a long period of time, and the above-mentioned limitation (1) is avoided. Figure 3.31 shows a typical example in which the timing of the turn-around for upper atmospheric winds was skillfully selected at high latitudes (Sweden, ESRANGE, SSC) and which succeeded in remaining almost directly overhead for a period of 40 h.

3.4.6.2 Summer and Winter Flights in Polar Regions

At high latitudes greater than about 80° , the sun does not set in summer, and there is no sunshine in winter. Hence, there is little temperature change in the lifting gas due to fluctuations in the solar radiation, and even using a zero-pressure balloon it is possible to maintain altitude and continue a flight by dropping almost no ballast.

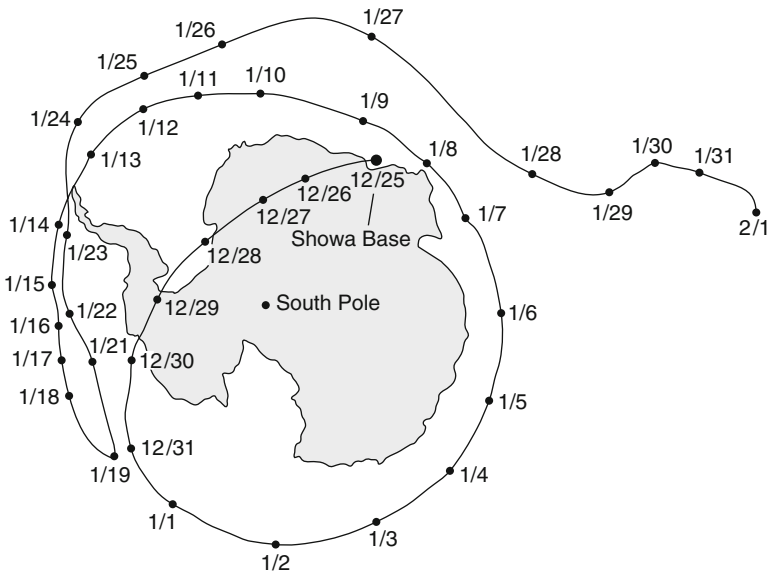


Fig. 3.32 Track chart for a balloon circling the South Pole at Showa Base (1993). Launched on 25th December, the balloon flew and maintained altitude by dropping a very small amount of ballast for 25 days until 19 January. When all the ballast had been dropped on 19 January, the balloon lost altitude, and it encountered wind systems blowing in the reverse direction

In addition, since in the stratosphere, circular winds blow centered on the poles, balloons remain safely within the polar region.

In particular, since the circular winds in summer are more stable than those in winter, as shown in Fig. 3.9, balloons trace out a circle centered on the pole. Such long-duration circumpolar flights are carried out by NASA from the Antarctic McMurdo Base [10], and by Japan from its Showa Base [11]. Figure 3.32 shows an example of a balloon circling around the South Pole that was flown from the Showa Base in 1993.

3.4.6.3 Flights that Make Use of Layers where Winds Blow in Opposite Directions Depending on Altitude

In middle latitudes, such as Japan, as described in Sect. 3.1.5, there are strong westerly winds (called jet streams) in the upper reaches of the troposphere, and the wind direction in the stratosphere in summer is in the opposite direction. In balloon flights at the Sanriku Balloon Center, long-duration flights have been attempted with the names “Boomerang Balloon” and “Cycling Balloon.” For these, the balloons ascend to the region of westerly winds, at which point the exhaust valve is operated. Ascent stops once the free lift portion of gas has been vented, and the balloon drifts east with a high speed. Next, the ballast is discarded when the balloon has traveled

a suitably long distance, and when the balloon ascends again to its stratospheric ceiling altitude, it turns around and returns westward.

The Boomerang Balloon flies in a westerly direction while it continues observation, and the flight is terminated at an appropriate point. The Cycling Balloon is repeatedly caused to descend to altitudes at which westerly winds blow by operation of the exhaust valve, and subsequently it is made to fly to the east.

Since 1972, balloon flights based on these ideas have been carried out at Sanriku Balloon Center of the ISAS to extend flight duration in a limited flight zone [12].

3.4.6.4 Flights Using Super-Pressure Balloons

As described in Sect. 2.3.2, in principle, super-pressure balloons do not need to drop ballast to maintain their altitude. Instead, the limitations for long-duration flights are fatigue and creep deformation of the film resulting from diurnal pressure changes and deterioration due to exposure to ultraviolet radiation. These limitations are related to the problem of selecting the materials for the film and load tape when designing the balloon and setting the strength margins. An additional limitation on long-duration flights is the loss of lifting gas due to it permeating through the film. This limitation can be addressed by improving the gas permeation characteristics of the film. Although polyethylene film can be used for flights on the order of a few weeks, the permeation characteristics of ethylene vinyl alcohol copolymer (EVOH) are several orders of magnitude lower than those of polyethylene. This problem can be further resolved by using EVOH film as one layer of a multilayer structure.

3.4.6.5 Long-Distance, Long-Duration Flights via Normal Flights in Mid-Latitude Regions

The problem that dropping ballast for altitude compensation for the setting of the sun limits the number of flight days in mid-latitude regions was described in Sect. 2.3.1. In the Russia-Nippon Joint Balloon Project (led by Hirosaki University, Russia's Lebedev Physics Institute, and other universities and institutions), the Russian balloon group achieved the maximum flight duration within this limitation [13]. Balloons were launched in summer when easterly winds are predominant in the stratosphere. They were launched from Kamchatka in far east Russia, and their target destination was Moscow, which is located at approximately the same latitude.

This project used 180,000 m³ balloons that flew at an altitude of approximately 35 km. The balloon system mass was 2,080 kg (650 kg of which was due to the balloon itself); within this amount, the largest mass was the ballast (800 kg), and a payload mass was 450 kg (including 230 kg of scientific observation equipment). In July 1995, two balloons were launched, and they achieved flight durations of 5.5 days (5,357 km) and 7 days (7,200 km), respectively. A flight track chart prepared by the Russian side is shown in Fig. 3.33.

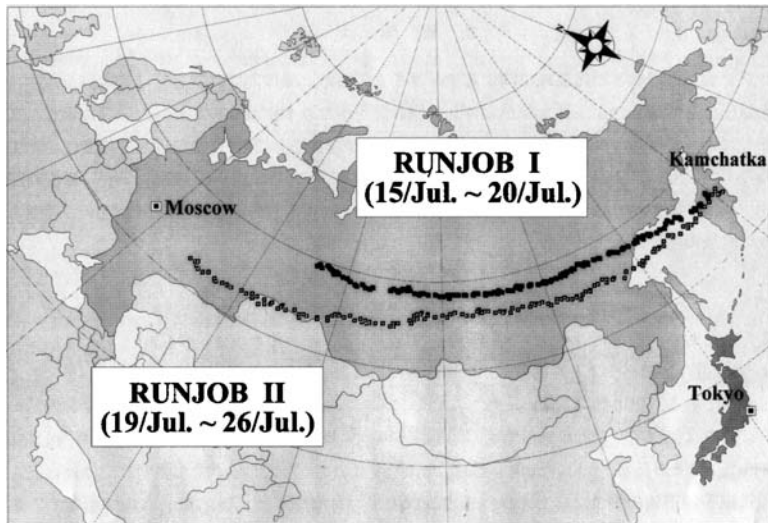


Fig. 3.33 Flight path record for two Kamchatka-to-Moscow long-distance, long-duration flights in the RUNJOB (Russia-Nippon Joint Balloon) Project (July 1995) (courtesy of Hirosaki University)

3.4.7 *Flight Safety and Security*

If an accident were to occur in scientific balloon experiments in which huge-volume balloons are flown that suspend payloads from a few hundred kilograms to over a ton, there is the possibility of causing great damage and injury. Consequently, there is a legal obligation to conform to the regulations listed below. It goes without saying that those performing this kind of work are responsible not just to follow these regulations, but also to ensure the overall safety of the project.

3.4.7.1 Aeronautical Safety and Security

During ascent and at the time of flight termination, scientific balloons pass through altitudes in which aircraft fly. As a result, in regard to regulations relating to air traffic control, the basic regulations for unmanned free balloons are described in Sect. 3.1 “Protection of people and property” (Sect. 3.1.8) of the International Civil Aviation Treaty, Appendix 2 stipulated by the International Civil Aviation Organization (ICAO). In addition, in “Appendix 4 – Unmanned Free Balloons” in the same document, detailed regulations are provided, such as requirements for equipment that should be prepared, items to report when flying, and understanding and reporting requirements for flight positions and routes [14].

Balloon experiments in all countries conform to these regulations. In Japan, after negotiation with the Japan Civil Aviation Bureau and associated aeronautical organizations, this is handled by a flight plan (NOTAM) being issued.

Balloons that are subject to air traffic control are classified as lightweight, medium-sized, or large-sized according to the payload mass and strength of the suspension rope. Lightweight and medium-sized balloons are regulated by only the payload mass and suspension rope strength, and since there are no regulations pertaining to the strength of the balloon itself, these regulations are considered to be concerned with rubber balloons for use in meteorological observation and similar items. Almost all polyethylene-film scientific balloons fall in the large-size category. For details, please refer to Appendix 2.

3.4.7.2 Maritime Safety and Antipollution Measures

In the case of Japan, safety management at sea falls under the jurisdiction of the Japan Coast Guard, and a briefing is given in advance of a balloon experiment. Generally, this briefing considers safety measures and recovery of the payload after splashdown in the ocean. Since 1970, due to the Law Relating to the Prevention of Marine Pollution and Maritime Disaster being passed, recovery of the balloon itself has also become compulsory.

3.4.7.3 Ground Safety and Security

There are no regulations with stipulations pertaining particularly to balloons, but informing and conferring with concerned organizations in advance is within the bounds of common sense. Compared with ascent, when balloons achieve high altitudes they are generally considered to be stable; but even so, it goes without saying that it is desirable to rule out flying in skies over urban areas and areas that have important safety facilities.

Table Talk 3: Balloon Recovery in Japan is Hard Work

One great advantage of balloons is that the payload can be recovered and reused as described in Sect. 3.1.3. In many countries, parachute descents are made in spacious wilderness areas or sparsely populated ranching areas. If the location is suitable, a helicopter flies directly to the spot, lifts the payload by suspending it underneath, and returns in a short time. However, since Japan has no suitable sites, all recoveries are performed at sea. This is where the hardships start.

With limited expenditure, large high-speed ships and the like dedicated to recovery are merely wishful thinking. Ships used for doing harbor work tend to be contracted for recovery. Because these ships are designed for coastal work, they are slow, and they pitch and roll easily in waves. And yet, when near the shore, there is the opportunity to admire the dolphins and seals that come alongside. However, at locations far from the shore, no matter how calm the waves are, large, slow swells pitch the boat up and down. You are seized with the feeling that your stomach is going to fly out of your mouth.

Recovery must be carried out as soon as possible since serious damage can be done to equipment by leaking of seawater. After the sun sets, it is difficult to locate things visually. It is often a race against time. Even so, payload recovery is relatively easy, recovery of the giant main balloon soaked in ocean water is dreadfully hard work.

If the balloon splashes down at a point near the shore, one can understand that things will be easier. However, there are many more ships and fishing facilities. Once a balloon drifted into an offshore fixed fishing net. It was written up in the local newspaper as “When lamenting over a poor catch, a giant catch of a balloon came in.” Such are the difficulties associated with scientific ballooning in Japan.

3.5 The Manufacture of Balloons

3.5.1 Film Materials

3.5.1.1 Film Characteristics

Polyethylene films with thicknesses of about $20\mu\text{m}$ are used for the film material in large zero-pressure balloons that suspend payload having masses ranging from a few hundred kilograms to over a ton. Thin, lightweight films with thicknesses of 6 and $3\mu\text{m}$ have been used for light payload masses of the order of a few kilograms, where the primary objective is to ascend to high altitudes exceeding 40 km.

Mechanical Characteristics

The desired characteristics for a film are adequate strength, high elongation percentage, high tear strength, and a sufficiently low brittleness temperature. This last characteristic is because the balloon must not lose flexibility even when it passes through the tropopause (approximately 10-km thick in middle latitudes), which has the lowest temperature of the upper atmosphere (Fig. 3.4). Recently-developed films are able to withstand temperatures down to approximately -100°C [15].

Typical results for uniaxial tensile strength testing of film are shown in Fig. 3.34. The vertical axis is the stress imparted to the film, and the horizontal axis is the strain in the film. The elastic deformation region, in which the initial length is recovered when tension is released, extends up to point A. The region from point A to point B is the plastic deformation region, in which the initial length is not recovered.

Desired characteristics of a balloon film are that it continues to extend further even after exceeding the elastic limit and that it does not easily rupture. An index of toughness, which can be found by integrating the stress-strain curve, is effective for evaluating balloon films. Table 3.3 shows the characteristics of two typical balloon films at normal temperatures (20°C) and low temperatures (-80°C). A distinguishing characteristic is that the films have high elongation percentages (400% or greater) at low temperatures.

Fig. 3.34 Typical stress–strain curve for balloon film

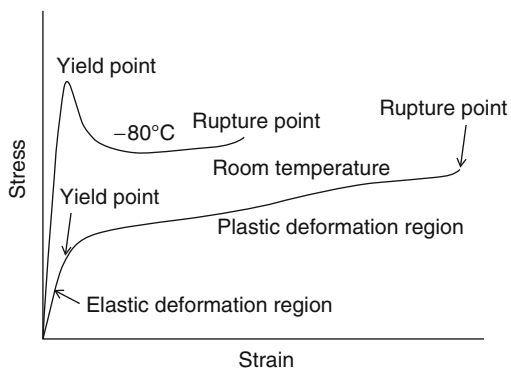


Table 3.3 Balloon film strength characteristics

Film Temperature (°C)	SF373		ASTRO-E	
	20	-80	20	-80
Yield-point strength (Nm^{-1})	200	900	200	900
Yield-point elongation (%)	10	10	10	10
Rupture strength (Nm^{-1})	600	1,100	700	1,120
Rupture elongation (%)	500	450	600	400

Optical Characteristics

The diurnal gas temperature variation within the balloon is related to the optical characteristics of the polymer film as discussed in Sect. 2.4.4. As a brief summary of these characteristics, the index ε/κ is used to estimate the properties of the balloon film, where ε is the visible light absorption coefficient of sunlight and κ is the average infrared absorption coefficient in the wavelength range 7.5–14.5 μm , which is the infrared emission region of radiation from the earth.

The respective infrared transmission characteristics of low-density polyethylene film, high-strength polyester film, and polyvinyl alcohol film are shown in Figs. 3.35a–c [16]. The low-density polyethylene film used in zero-pressure balloons has narrow absorption bands due to CH and CH_2 groups near wavelengths 3, 6.8, and 1.4 μm , but otherwise, it has a constantly high value over almost the entire wavelength region, and it has the distinguishing characteristic of high transparency.

Polyester film and polyvinyl alcohol film used in small super-pressure balloons have higher absorptions in the long wavelength region. Polyvinyl alcohol film, in

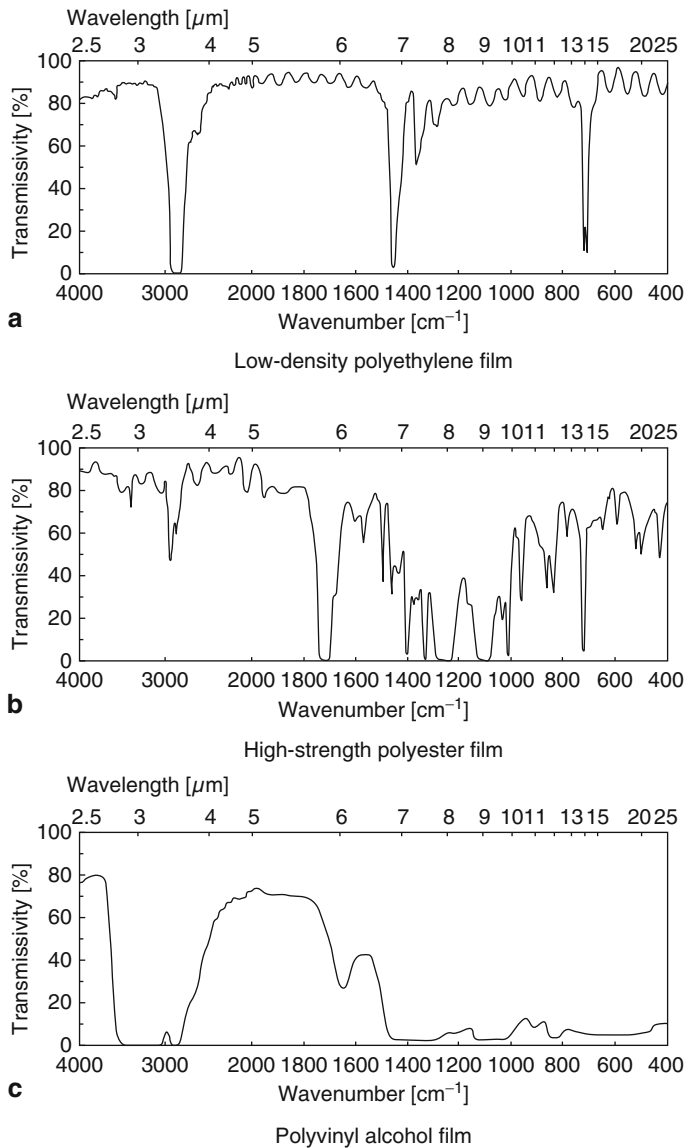


Fig. 3.35 Infrared transmission characteristics of balloon film [Source: Toshiyuki Kiuchi, Toshio Maki: “Simple discrimination of packing materials (plastic films) by their infrared absorption spectra”, Agricultural and Forestry Products Inspection Institute, Investigation and Research Report, 1, pp. 75–92 (1973)]: **a** Low-density polyethylene film; **b** High-strength polyester film; **c** Polyvinyl alcohol film

particular, has strong absorption characteristics over 7.5–14.5 μm, which are closely related to the infrared absorption constant κ . EVOH film, a copolymer of ethylene and vinyl acetate, which exhibits extremely high gas barrier properties, also has similar optical characteristics.

From the characteristics noted above, on the one hand, the infrared absorption coefficients κ for polyethylene film, polyester film and polyvinyl alcohol film are estimated to be approximately 0.2, 0.6, and 0.9, respectively. On the other hand, the absorption coefficients in the visible light region ε for these films are about 0.05, 0.1, and 0.1, respectively. Accordingly, the optical properties indices of these balloon films ε/κ are 0.25, 0.16, and 0.11, respectively. As this index decreases, there is a tendency for the effects of radiation received from the earth at night to become stronger and for the drop in the lifting gas temperature to diminish. At the same time, as shown in the Fig. 2.36 of Sect. 2.4.4.4, when clouds having a low cloud-top temperature cover the earth's surface, the radiation conditions change, and hence, the balloon's flight behavior is also significantly affected.

3.5.1.2 Load Tape

For zero-pressure balloons, high-tensile polyester fibers are used in the reinforcing load tape, which is inserted along the gore bond line. Since these fibers are produced by unidirectional extension, they have exceptional uniaxial tensile strength. The specific strength (tensile strength/density) is usually 100 times or greater than that of the envelope film. Consequently, if used effectively, load tape can efficiently increase balloon strength with a smaller increase in weight than by strengthening the film itself (see Sect. 2.2.3.4 for the effect of reinforcing on balloon strength).

Fibers are secured by sandwiching them between two strips of polyethylene tape that are slightly thicker than the balloon film as is suitable for the balloon manufacturing process (Fig. 3.36). Such material is usually referred to as load tape. The balloon is manufactured by joining the gores together; at the same time this tape is inserted between the two layers of gores.

As for the strength of the load tape, with the exception of special cases, standard materials having rupture strengths of 667 N, 890 N, 1112 N, etc. are commonly used.

Because large forces are exerted on the reinforcing fibers in super-pressure balloons, rope made of high tensile fiber is often used directly. Although it is appropriate to refer to this as a load rope or a load tendon, it is also customarily

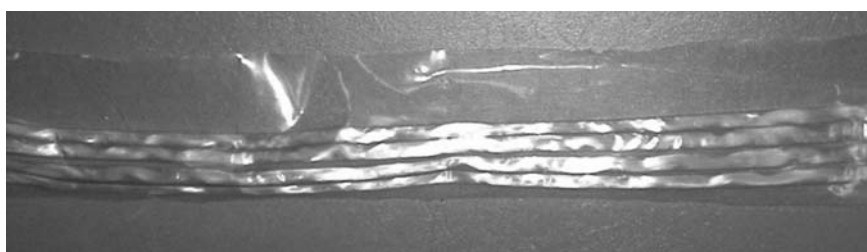


Fig. 3.36 Load tape inserted along the heat seal line of the gores to reinforce the balloon

referred to as load tape without distinction. We also use the term load tape in this book, except where noted.

3.5.2 Design

3.5.2.1 Zero-Pressure Balloons

We give an overview of methods for designing zero-pressure balloons for specified float altitudes and payload masses. The shape of a zero-pressure balloon is determined by solving the six equations of (2.26)–(2.31).

The minimum and maximum payload masses that can be suspended on the designed balloon are specified. The minimum value of the design payload mass is determined by the spread angle of the balloon base, and this depends on the dimensionless film weight Σ_e (similarity parameter, see Fig. 2.9). If a payload lighter than this minimum value is suspended, at full inflation the spread angle will exceed the designed angle, and the circular length of the film in the proximity of the balloon base will be insufficient and the film will become stretched, making it easy to tear.

As will be described in Sect. 3.5.4, the maximum value for the design payload mass is determined by the tension on the film and the strength of the load tape. Tension must be assessed both for serious cases in which a portion of the load tape takes on the full load for the case when the balloon has partially inflated such as during launch operations (Fig. 3.43), as well as at full inflation. In the latter case, the tension is inversely proportional to the cosine of the opening angle of the balloon base (3.30). The general design flow is given below.

- (1) Determine the minimum payload mass $F_{1,\min}$ and the float altitude $z_{b,\max}$ at that time.
- (2) Select the film type and thickness, number of gores, and the type and number of load tape strands.
- (3) Calculate the balloon mass m_b .
- (4) Determine the required balloon volume V_b from the given float altitude.
- (5) Select the overall length of the balloon.
- (6) Calculate the balloon shape, and determine the opening angle of the balloon base at this time by performing iterative calculations.
- (7) Change the overall length of the balloon such that the balloon's volume at this time equals the required volume, and repeat from step (6).
- (8) Assess the load tape and film tension at the base.
- (9) Assess the load tape and film tension at the apex.
- (10) Adjust the film thickness, load tape, and other parameters as necessary.
- (11) Repeat from step (3) until $b_g V_b = (m_b g + F_{1,\min})$ is satisfied, where b_g is the effective buoyant force per unit volume (2.15).
- (12) Determine the maximum payload mass $F_{1,\max}$ that satisfies conditions (8) and (9) and the float altitude at this time.

In practice, errors that occur during manufacturing may be corrected by applying additional film (known as fullness) to the balloon base in the circumferential direction. In addition, the film may be made two or three layers thick for reinforcement at the balloon's apex (Sect. 3.5.4.1), and this complicates the design flow described above.

3.5.2.2 Super-Pressure Balloons

According to the 3D gore system, the basic shape of super-pressure balloons is a pumpkin-like irrespective of the volume. Therefore, the balloon volume can be simply calculated if the radius of the gore overhang R_φ is determined. Accordingly, the film thickness and load tape strength can be determined if the float altitude and the maximum internal–external pressure difference are specified. The balloon mass can subsequently be determined. This calculation is repeated iteratively until the size of the balloon is such that it is capable of floating at the specified float altitude while suspending the given payload.

3.5.3 Manufacturing Process

Although a standard manufacturing process has been established for large zero-pressure balloons, the manufacturing process for super-pressure balloons is still currently in the development stage. Consequently, we give a detailed description of the manufacturing process for zero-pressure balloons, but limit the discussion of super-pressure balloons to just the essential points of the technologies that have been tried. Refer to Appendix 3 for typical specifications of a zero-pressure balloon (i.e., volume, mass of the main body, length, number of gores, etc.)

3.5.3.1 Forming and Joining Gores

The balloon envelope is manufactured by cutting out gores from a long film that has been wound onto rolls into spindle shapes (Fig. 3.37) and thermally joining multiple pieces together lengthwise. The spindle shape is determined by dividing the overall shape of a natural-shape balloon, as determined in Sect. 2.2, lengthwise into N sections of equal width. The raw material film width is approximately 3 m, and since the radius at the largest part of a large balloon can be as great as 50 m, the number of gores can exceed 100.

An example of the sealing process is shown in Fig. 3.38. The heat sealing machine used for balloons is usually called a belt sealer. Two ring-shaped metal belts rotate on an upper and a lower stage, and the edges of two gores are placed one over the other and fed into the space between the belts, which is heated. At this time, the reinforcing load tape is also laid on the sealing line of the gore and this is fed

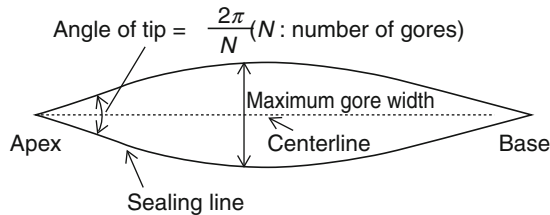


Fig. 3.37 Shape of a gore, which is the structural unit of the envelope in balloon manufacture (the dimension in the length direction has been shortened)

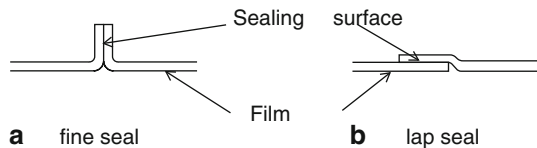


Fig. 3.38 Gore sealing process in the manufacture of a balloon (courtesy of Mr. Loren Seely, Raven Industries, Inc.)

into the space between the belts. Naturally, the belt heat is precisely controlled by a controller.

In the sealing process, the film is placed on a long table and the sealing device moves along the side of the table. The sealing surface adopts a form referred to as

Fig. 3.39 Heat sealing methods for films: **a** Fine Seal; **b** lap seal



a fine seal (Fig. 3.39a). The lap seal system of laying gore edges one over the other and sealing in the manner shown in Fig. 3.39b has the advantage of creating stronger joining, but it is not normally used for balloons, because it is not a simple operation.

In the sealing process for the gore, sealing is performed with the curved gore side running along the straight edge of the table, making it difficult to handle. Winzen Int., Inc. in the US (subsequently purchased by Raven Industries, Inc.) solved the problem by developing the “Stable Table” technique and realized an efficient method for manufacturing balloons [17]. The following procedure gives an overview of this method.

- (1) The shape of a gore is marked on a table. This shape is not symmetrical with respect to the original centerline. One edge is a straight line, and a line is drawn from it at a distance equal to the gore width.
- (2) Two sheets of films are laid out that have not been cut out in the shape of a gore, and they are spread out for the length of the balloon. These two sheets are sealed together along one edge.
- (3) This sealed line is moved to the gore edge line that is marked on the table, and the unbonded film edge of the upper film is turned over toward the edge of the table. The film that lies on the table forms gore pattern while the excess film overhangs the edge of the table.
- (4) A new film is stretched and overlaid over the gore that was moved to the position where the bond line is marked, and the top and bottom films are bonded on a straight line along the table edge. At the same time, any excess film that extends outside the bond line is cut off.
- (5) Step (3) is returned to, and the bond line is moved to the marked position.

In this way, the manufacturing process of the balloon progresses by repeating Steps (3) through (5). Two superior characteristics of this method is that all the seal lines are straight, and that the gore shape can be cut out from the film at the same time as performing sealing. With this method, only the width of the gore shape is the same as the designed value, and because the shape is asymmetric, its appearance looks strange. However, the maximum width of a gore in an actual balloon is about 3 m, whereas large balloons have lengths 100 m or longer, and hence, the disparity in the two shapes is very slight and it can be sufficiently absorbed by the film’s extensibility.

3.5.3.2 Processing of the Apex and Base

At the apex and base of a balloon, the film part of the gore has almost no width, and the load tapes essentially converge. A balloon is constructed by hermetically



Fig. 3.40 Processing of a top fitting (courtesy of Mr. Loren Seely, Raven Industries, Inc.)

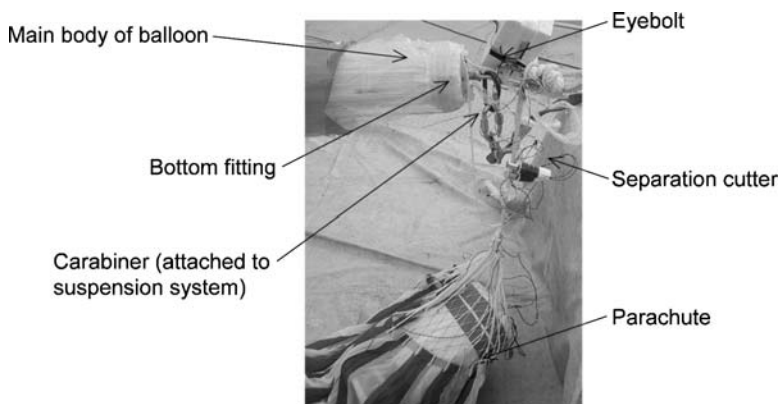


Fig. 3.41 Processing of the bottom fitting

sealing these parts. The balloon apex has a flat shape, and hence the disk plate, which is made from light metal, is handled as the base plate as shown in Fig. 3.40. The upper ends of the gores are fastened between the base plate and the clamping ring plate around the external perimeter. They are held in position by the frictional resistance generated by crimping.

As presented in the section on balloon shape design, because all the tensile forces in the vertical direction are concentrated at the apex, it is important to clamp it sufficiently strongly. Since the strengths of the film and the load tape decrease if the strength of compression is too great, it is necessary to control the strength when clamping. At the bottom fitting, a column-shaped metal clamp fitting made of a lightweight metal is used (Fig. 3.41). The bottom ends of the gores are fastened with rings and clamped. In addition, an eyebolt or similar mechanism is attached to the bottom of the clamping part for fastening the top of the suspension line.

3.5.4 Structural Strength

3.5.4.1 Zero-Pressure Balloon

Balloon Strength

As described in Sect. 2.2.3.6, the film tension in zero-pressure balloons, which are manufactured by conventional methods that differ from the 3D gore design concept, is complexly generated in two axial directions. Its actual strength as a balloon is approximately the same as that of a spherical balloon of the same volume. The point at which the film loads are a maximum is located slightly above the point of maximum radius.

As a typical example, consider the case of a balloon with a volume of $100,000 \text{ m}^3$ in level flight at an altitude of 35 km (atmospheric pressure: 570 Pa, atmospheric density: 0.0085 kg m^{-3}). The radius of the balloon calculated as a sphere is about 30 m. The internal–external pressure differential near the balloon apex is approximately 0.6% of atmospheric pressure according to (2.49), or 3 Pa, and the film tension is about 90 N m^{-1} .

As shown in Table 3.3, since the rupture strength at low temperature of a $20 - \mu\text{m}$ -thick balloon film is approximately $600 - 1,100 \text{ N m}^{-1}$, it has a safety factor of 7–12.

In the case of zero-pressure balloons, from the similarity of the shape, the maximum load exerted on the apex occurs on the ground, where atmospheric pressure is about 100–200 times higher than that in the stratosphere, and the load on the apex is approximately six times greater, since it is proportional to the cube root of the ratio of the atmospheric pressure on the ground to that in the upper atmosphere. However, as for the shape on the ground, because the point of zero pressure differential is located a little above the base, and there is a large quantity of film, the effective safety factor is generally estimated to be a little greater than 2, which is not enough.

Since such a situation applies to only the apex of a gas-filled balloon on the ground, increasing the ground safety factor by strengthening the entire balloon would result in a wasteful increase in weight. Given this factor, the strength of large balloons is increased by using two or three layers of film at the apex only; these multiple layers are called double caps and triple caps, respectively.

Strength Needed in Load Tape

At the base of the balloon, the suspension lines are attached to the load tape that converges at the base, and the payload is suspended. The load of the payload W_p is suspended completely by the load tape. In a fully inflated balloon, if the number of strands of load tape is denoted by N and the spread angle at the base is taken to be θ_n (Figs. 2.9 and 3.42) the load W_r exerted on each strand of load tape is given by

$$W_r = \frac{W_p}{N \cos \theta_n}. \quad (3.30)$$

Fig. 3.42 Transmission of payload load to the load tape

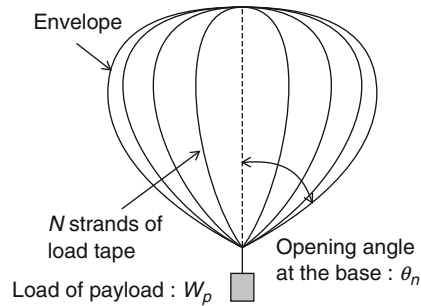
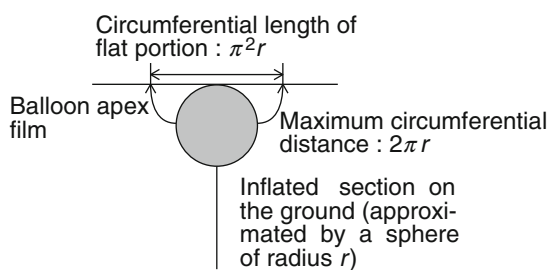


Fig. 3.43 Surplus load tape at the time of inflation on the ground



The load on the load tape is greater when lifting gas is injected into the balloon on the ground than that at the ceiling altitude. The volume of the balloon expansion on the ground is proportional to the ratio of the atmospheric pressure on the ground to the atmospheric pressure at the level-flight altitude, and hence is 1/100 or less. As described in Sect. 2.2.2, because the shape of the apex of a natural-shape balloon is flat, the portion that expands on the ground is the portion that is flat when fully inflated. Accordingly, there is a large surplus of film in the circumferential direction, resulting in longitudinal folds being formed.

We now approximate the shape of a balloon on the ground to a sphere and assume that the apex of the fully inflated balloon forms a flat surface as shown in Fig. 3.43. If the radius of the sphere on the ground is taken to be R_0 , the circumference of the equatorial region will be $2\pi R_0$, and the circumference of the film when in a flat condition corresponding to this region will be $2\pi(2\pi R_0/4)$. Hence, the ratio of these two lengths is $\pi/2 \approx 1.6$. In this region of approximately 60% excess, because the load tape cannot take up forces projecting outwards from the film, slumping and buckling within the balloon occurs, and buoyancy cannot be sustained. Moreover, the weight of the uninflated section also needs to be supported. The total load on the load tape is approximately twice that when the balloon is fully inflated.

3.5.4.2 Super-Pressure Balloons

Below we derive the film and load tape tensions when the pressure differential between the internal gas of the balloon and the atmosphere is given by Δp . As mentioned in Sect. 2.3.2, Δp is equal to approximately twice the product of the

atmospheric pressure at the ceiling altitude and the free lift ratio (i.e., the ratio of the free lift to the total weight of the balloon system). If the free lift ratio is assumed to be 8% and the float altitude is assumed to be the same as that for the above-mentioned zero-pressure balloon, namely 35 km (atmospheric pressure 570 Pa), Δp will be approximately 90 Pa.

Film Tension

If manufactured in accordance with 3D gore design concept, the film tension will be equal to the product of pressure differential Δp and the local radius of the gore. Since the width of the unprocessed film is about 3 m, the radius of curvature produced in the circumferential direction as a result of protrusion between the load tape is about 1 m. Accordingly, the circumferential tension produced in the film is approximately 90 N m^{-1} , which is similar to that for a zero-pressure balloon.

As the float altitude of the balloon increases, the atmospheric pressure in the vicinity of the balloon will decrease, and the tension per strand of load tape and the tension in the film will also decrease. Thus, theoretically even polyethylene film, which is currently used for zero-pressure balloons, is sufficiently strong for super-pressure balloons at the high altitudes usually required for scientific observations.

For example, in the case of a super-pressure balloon using a 20- μm thick polyethylene film, it is possible to float a 500-kg payload at an altitude of 33 km with a balloon having a volume of $100,000 \text{ m}^3$ (Fig. 3.44). If a $200,000-\text{m}^3$ -volume balloon is used, the achievable altitude becomes 36 km. This compares favorably in weight and size to regular zero-pressure balloons that are currently being used extensively. In addition, using the same materials as those used in current zero-pressure balloons, and by making only a few modifications to the manufacturing process, it is easily possible to realize a large super-pressure balloon.

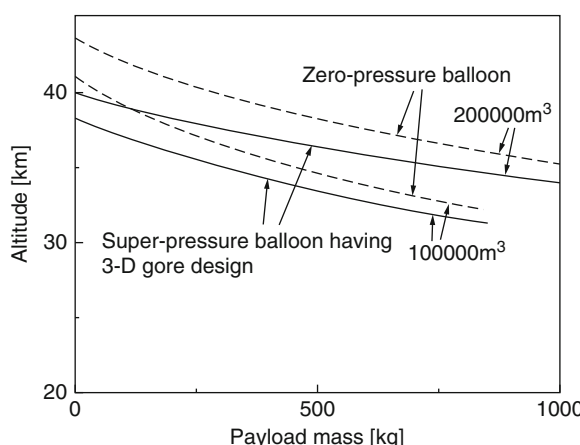


Fig. 3.44 Achievable altitude of a super-pressure balloon

In the case of a simple spherical balloon having a radius of 30 m, for a pressure differential of 90 Pa, the tension would be $1,350 \text{ N m}^{-1}$, which is excessively large to achieve using a lightweight film.

Load Tape Tension

Since the total tensile force acting on the load tape is equivalent to the total longitudinal force generated in the balloon, it is equal to the product of the equatorial cross-sectional area and the pressure differential Δp . In the example given above, the equatorial radius is about 30 m and the number of load tape strands is 100 or greater, so that the tension per strand is 2,600 N or less. Consequently, stranded rope consisting of bundles of high-tensile fibers is used as the load tape.

3.5.5 *Quality Control*

After a balloon has been manufactured and before it is launched, it is not possible to conduct direct quality testing (such as experimental inflation) on the balloon. The balloon is packed in a box and transported to the launch site. It is subsequently removed from the box during launch operations and launched as is. Consequently, the reliability of the balloon depends entirely on quality control during the manufacturing stage. Currently, quality control is generally carried out as described later.

3.5.5.1 Quality Control at the Film Stage

Film thickness variability testing and tensile strength testing at both normal temperatures and low temperatures are performed as film sample tests at the polyethylene film manufacturing plant. In addition, one of the low-temperature property tests involves dropping a steel ball from a fixed height onto a film held at a low temperature; by analyzing the radial tear of the film, the film's biaxial low-temperature strength characteristics can be evaluated. These tests are performed in units of film rolls.

3.5.5.2 Control at the Manufacturing Stage

Film Defect Testing

At the balloon manufacturing plant, the film surface is first examined for defects. When the roll of film is delivered to the factory, it is rewound onto another roll for use in balloon manufacturing, the spread film surface is passed between two polarizing plates, and defects such as pinholes, film scratches, and nonuniformity are detected visually and marked. If large defects are detected, the film is rejected



Fig. 3.45 Strength testing of sealing samples (courtesy of Mr. Loren Seely, Raven Industries, Inc.)

at that point and it is not used in balloon manufacture. If small defects are detected, the film is repaired at the balloon manufacturing stage by applying patches.

Heat Sealing Process Testing

For quality assurance of the heat sealing processing of the film and load tape, the inspector in charge visually examines the sealing line, and counts each defect (such as air bubbles, tucks, and wrinkles) and determines their distribution along the sealing line [18]. If the number of defects exceeds a certain level, the film fails inspection. Furthermore, additional length is prepared at the beginning and end points of the sealing line for use as test samples. After a fixed tension is applied to these test samples (Fig. 3.45), the sealing strength is measured using a tensile tester.

Table Talk 4: Leave it up to the Wind when Flying, Leave it up to the Feet when Manufacturing

The balloon factory of Raven Industries, Inc. in Sulphur Springs, Texas, near Dallas is very long and thin. It could be easily identified even from low-resolution satellite photographs taken in the early stages of satellite imaging. When large balloons having volumes as large as $1,000,000 \text{ m}^3$ are laid out on the ground, they can be as long as 200 m. When space for working is included at both ends, a building about 300-m long is necessary. Long wooden tables are placed within it as shown in Fig. 3.38, and the manufacture of balloons is performed on these tables.

Film rolls are installed on gate-shaped transfer benches positioned between the tables, and the film is spread out over the tables while being pushed along by hand from one end of a table to the other. Next, one side is continuously bonded, the bond line is transferred to the marked location on the table, and a new film is then spread out. This work is very repetitive. One processing operation consists of about five round trips. Since over 200 pieces of film are pasted together to form a balloon, the total round trip distance is close to 400 km. Female workers who make up six-member teams perform this work steadily, and it takes about six weeks to complete. The distance walked per person in one day exceeds 10 km.

3.6 Rubber Balloons Used for Meteorological Observations

3.6.1 *Outline of Meteorological Rubber Balloons*

Rubber balloons are indispensable for observing weather in the upper atmosphere. Sometimes they are used as tracers, and other times they are used to carry meteorological observation equipment into the atmosphere.

Meteorological observations that use rubber balloons as the observation target include pilot balloon (abbreviated as “pibal”) observations used to measure winds in the atmosphere, and balloon observations for detecting clouds. In pilot balloon observations, a small rubber balloon is flown by giving it buoyancy so that it ascends at a specified rate, and observation of the winds in the sky are made by tracking the balloon with a theodolite (an instrument that measures the azimuth angle and elevation angle of a visible object when a telescope is set up so that it can rotate in the horizontal and vertical planes). In cloud detection balloon observations, the cloud base altitude is determined by measuring the time from balloon release until it enters the clouds.

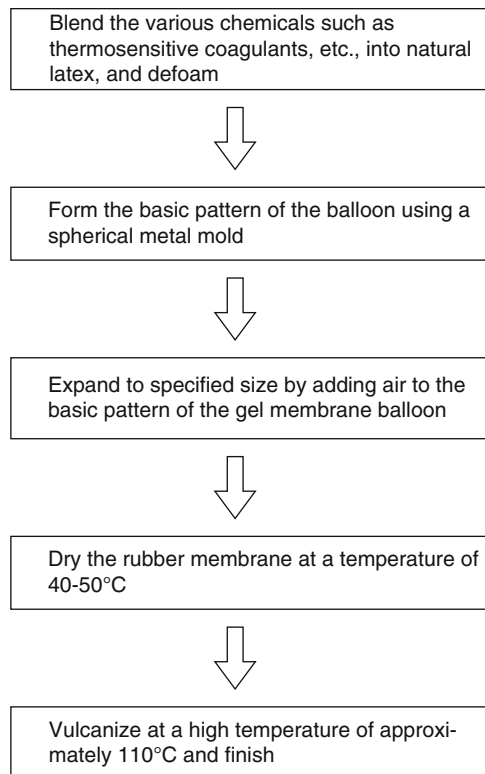
In aerological observations that directly measure pressure, temperature, relative humidity (henceforth “humidity”), wind speed and direction up to altitudes of approximately 30–35 km, rubber balloons are used to lift suspended meteorological instruments (radiosondes). Observational data are transmitted to the observing station via a telemeter. In addition, these balloons are also used as the observation targets for the optical observation of upper-air winds.

Hydrogen gas is used as the lifting gas for balloons.

3.6.1.1 **Manufacture of Rubber Balloons for Meteorological Observations**

Natural rubber latex (referred to below as “latex”) is the principal raw material for rubber balloons used for meteorological observations. Latex is an emulsified secretion obtained from the bark of rubber trees, and it is a type of colloid sol. Rubber (the dispersoid) is dispersed in aqueous solutions of various organic and inorganic

Fig. 3.46 Manufacturing process for rubber balloons



substances (the dispersing medium), and crude rubber is obtained via concentration. The manufacturing process for rubber balloons for meteorological observation is shown in Fig. 3.46.

Since latex does not harden (i.e., form a gel membrane) on its own, vulcanizing agents such as sulfides, zinc oxide, and ammonium salts, vulcanizing accelerators, gelatinizers, antioxidants, dispersants, stabilizers, and the like are blended in. This is known as compound latex. The compound latex is defoamed to ensure that air bubbles do not form in the rubber membrane of the balloon. Zinc oxide and ammonium salt form a zinc ammine complex, and solidification occurs when this is heated, producing a rubber membrane.

The basic pattern of the balloon (the gel membrane) is manufactured using the rotational molding method by placing the defoamed compound latex into a spherical metal mold. In this method, the metal mold containing the compound latex is placed in a tank containing hot water at approximately 80°C, and the mold is rotated and revolved about two orthogonal axes within this tank. By this heating process, the compound latex forms a spherical gel membrane of uniform thickness on the inner walls of the mold, and this spherical shape is the basic pattern for the balloon. This basic pattern is then removed from the mold and allowed to expand to the specified size (until the diameter becomes about six times larger) by blowing air from its

mouth before the gel membrane dries. After drying at a temperature of 40–50°C, it is vulcanized at a temperature of approximately 110°C, and the rubber balloon is completed.

3.6.1.2 Types and Sizes of Rubber Balloons for Meteorological Observations

The size of rubber balloons for meteorological observation is expressed in terms of the balloon's weight. The type of balloon used for aerological observations depends on the weight of the meteorological observation equipment to be carried (i.e., the suspended weight) and the altitude of the observations (achievable altitude: altitude at which the rubber film of the balloon exceeds its expansion limit and bursts) as shown in Table 3.4. This table also gives the values for each balloon of free lift (pure lift) required for the balloon to ascend at the specified rate.

Sixty-gram rubber balloons are used for daytime pibal observations. For balloon observations to determine the height of clouds, even smaller 20-g rubber balloons are used. Two-hundred-gram rubber balloons are used for rawin observations to observe upper-air winds through the use of small, lightweight meteorological instruments and for rawinsonde observations to measure air pressure, temperature, humidity, and upper-air winds up to an altitude of approximately 20 km. Six-hundred-gram rubber balloons are used for rawinsonde observations to measure air pressure, temperature, humidity, and upper-air winds up to an altitude of approximately 30 km, which is the principal altitude for aerological observations. Ozonesonde observations, which measure the vertical distribution of ozone, use 2,000-g rubber balloons

Table 3.4 Standards for principal rubber balloons used in meteorological observations

Balloon classification	Weight (g)	Diameter of mouth-piece (cm)	Suspended weight (g)	Free lift (g)	Achievable altitude (km)	Purpose
60 g	60±4	1.4±0.3	—	146 ^a	>4.0	Pibal observation
200 g	200±12	3.2±0.4	200	1,200 ^b	>14.0	Rawin observation
600 g	600±27	3.2±0.4	300	1,600 ^b	>27.0	Rawinsonde observation
800 g	800±30	3.2±0.4	600	1,800 ^b	>28.0	Rawinsonde observation
1,200 g	1200±50	3.2±0.4	300	1,700 ^b	>33.0	Rawinsonde observation
2,000 g	2000±80	5.0±0.4	1400	2,000 ^b	>27.0	Ozonesonde observation

Excerpt of data from the Japan Meteorological Agency.

^aPure lift for an ascent speed of 200 m min⁻¹.

^bPure lift for an ascent speed of 360 m min⁻¹.

because the observational instruments are heavy. There are also 3,000-g and 4,500-g rubber balloons that are capable of suspending and flying even heavier observational equipment.

3.6.2 Ascent Speed of Rubber Balloons

In the case of pibal observations using 60-g rubber balloons, because no instrumentation to measure altitude is used, the balloon altitude is estimated from the free lift, which is determined by the amount of hydrogen or helium gas used to inflate the balloon. The ascent speed for pibal observations is set at 200 m per minute. For the case of radiosondes, by considering the rate of wind draft to the temperature sensor and the sensor response time, the ascent speed is generally set at 360 m per minute.

If we ignore the increase in the balloon's internal pressure due to the tension of the expanded rubber, the ascent motion of the rubber balloons is essentially the same as the case when the gas temperature and the atmospheric temperature are approximated as being equal in the general ascent motion of an ordinary balloon described in Sect. 2.4.2. Under such a simplification, the ascent speed can be expressed in accordance with the format formulated for meteorological observations, so that it becomes as follows. Denoting the free lift as L , the suspended weight as M , the balloon weight as W , and the density of air and the density of hydrogen at standard conditions as respectively ρ_0 and σ_0 , the ascent speed v is given by

$$v = \frac{KL^{1/2}}{(L+M+W)^{1/3}}. \quad (3.31)$$

Here, if we take the density of the atmosphere at the flight altitude to be ρ , the constant K is given by

$$K = \left(\frac{4\pi}{3}\right)^{1/3} \left(\frac{2g}{C\rho\pi}\right)^{1/2} (\rho_0 - \sigma_0)^{1/3}. \quad (3.32)$$

If the drag coefficient C is known, the constant K can be unambiguously determined. However, because the value varies with the balloon material and shape, it is determined empirically based on data from actual flights. When estimating the ascent speed of a radiosonde (Model RS 2–91 rawinsonde) with a 600-g rubber balloon from (3.31), units of m/min for the ascent speed and units of gram for free lift are used, and the value of $K = 122$ is used.

The relationship between ascent speed and the free lift of a 600-g rubber balloon using this value of K is shown in Fig. 3.47. In this figure, values measured by the Aerological Observatory, Japan Meteorological Agency (Tsukuba) are indicated by dots [19].

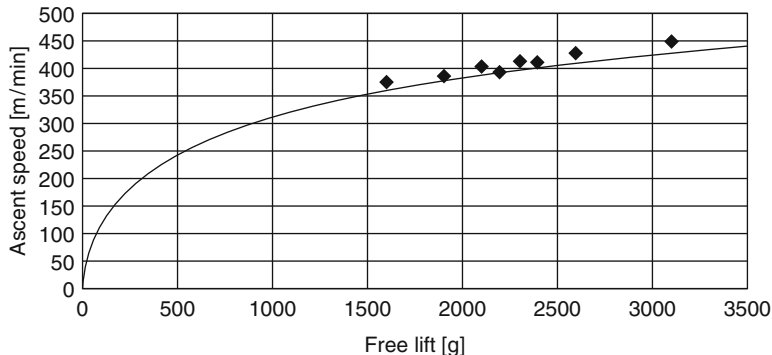


Fig. 3.47 Relationship between free lift (pure lift) and ascent speed of a 600-g rubber balloon

3.6.3 Achievable Altitudes of Rubber Balloons

Balloons, which continue to ascend while expanding, burst when they exceed the expansion limit of the rubber film. This burst altitude (pressure) is referred to as the achievable altitude of the rubber balloon. Since aerological observation terminates with the bursting of the balloon, the achievable altitude of a rubber balloon is an important controlling factor in determining the upper limit of aerological observations. If we assume that the density ρ_b of the rubber film does not change during balloon expansion, the relationship between the maximum burst volume $V_{b,\max}$ and the minimum film thickness of the rubber film d_{\min} is

$$V_{b,\max} = \frac{4\pi}{3} \left(\frac{W}{4\pi d_{\min} \rho_b} \right)^{3/2}. \quad (3.33)$$

The pressure at the maximum volume, i.e., the pressure at the achievable altitude is

$$P_b = \frac{T_b}{T_0} \frac{P_0(L + M + W)}{(\rho_0 - \sigma_0)V_{b,\max}}, \quad (3.34)$$

where T_0 and P_0 are the atmospheric temperature and pressure on the ground, respectively, and T_b is the atmospheric temperature at the balloon's altitude.

The film thickness at the balloon's bursting point determined from observation data from the Aerological Observatory, Japan Meteorological Agency is approximately $3.5\text{ }\mu\text{m}$. The balloon size, achievable altitude (pressure), and film thickness at the balloon's bursting point based on observation data at the Aerological Observatory are given in Table 3.5.

Table 3.5 Balloon size, achievable altitude (pressure), and film thickness at the balloon's bursting point

Balloon size	600 g	800 g	1,000 g	1,200 g	1,500 g
Average free lift (g)	1,600	1,760	1,700	1,700	1,700
Suspended weight (g)	300	410	400	400	410
Achievable pressure (hPa)	8.4	5.9	4.8	4.3	3.1
Estimated film thickness at the bursting point (μm)	3.47	3.33	3.46	3.29	3.45
Average ascent speed (m min^{-1})	375	367	365	364	351

3.7 Utilization of Balloons

3.7.1 Scientific Observations

3.7.1.1 Observations and Experiments that Exploit the Reduction in Atmosphere's Influence

The majority of electromagnetic waves and particles that come from space are absorbed by the earth's atmosphere, and only a very small proportion reaches the earth's surface. Figure 3.48 shows the relationship of wavelength to altitude attenuated to 1/2, 1/10, and 1/100 by the atmosphere. The atmosphere causes almost no attenuation only at wavelengths longer than 0.1 mm in the radio region and in the range 3,800–7,700 Å ($1\text{ nm} = 10^{-9}\text{ m} = 10\text{ \AA}$) of the visible region; in other regions, it causes some attenuation.

Infrared rays are principally attenuated by water vapor that exists in the troposphere. Since the amount of attenuation decreases rapidly at altitudes above 30 km, this is an effective wavelength region for balloon observations. However, radiation emitted by the thin atmosphere itself interferes with observations in the far-infrared region. Far-infrared emissivities in the vicinity of a wavenumber of 65 mm^{-1} at aircraft altitudes (14 km) and balloon altitudes (35 km) are shown in Fig. 3.49 [20].

For ultraviolet rays absorbed by the stratospheric ozone layer, only wavelength regions near visible light can be observed, and observations at balloon altitude is difficult in the region from far-ultraviolet to X-rays, where attenuation by the photoelectric absorption effect of molecules, atoms, and ions is great. Because the amount of attenuation decreases from hard X-rays to γ -rays, the possibilities for observation increase. However, it is desirable for balloons to ascend to as high an altitude as possible.

Figure 3.50 shows one of the major results obtained during the early stages of balloon experimentation carried out in 1968 in Japan. It is a record identifying the position of the X-ray source in Cygnus [21].

In addition, Fig. 3.51 shows a photograph of a far-infrared telescope used to observe the 60 and $160 - \mu\text{m}$ wavelength regions. It is an observation instrument that precisely scans the sky through directional control. The arms at the top of the

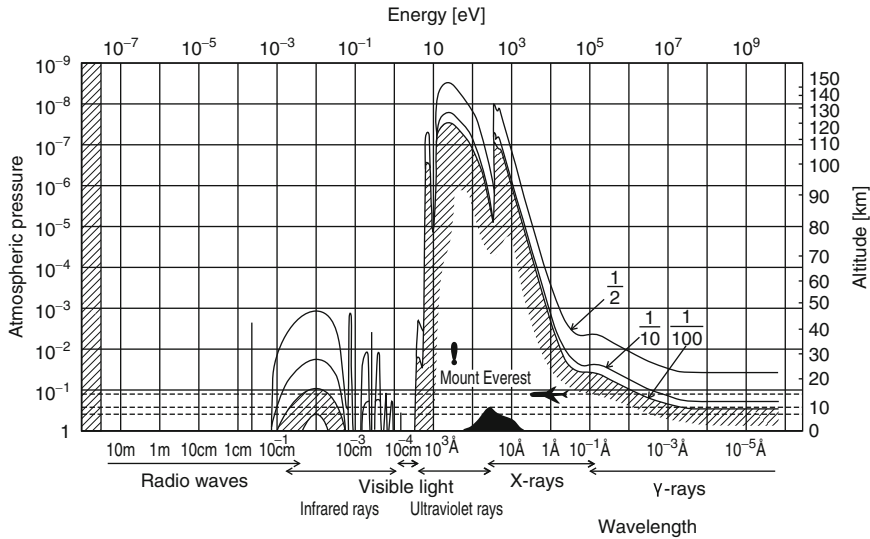


Fig. 3.48 Attenuation of incoming energy by the atmosphere. (Source: Space Engineering Handbook, 2nd Edition, Japan Society for Aeronautical and Space Sciences Compilation (in Japanese), Maruzen, Tokyo (1992))

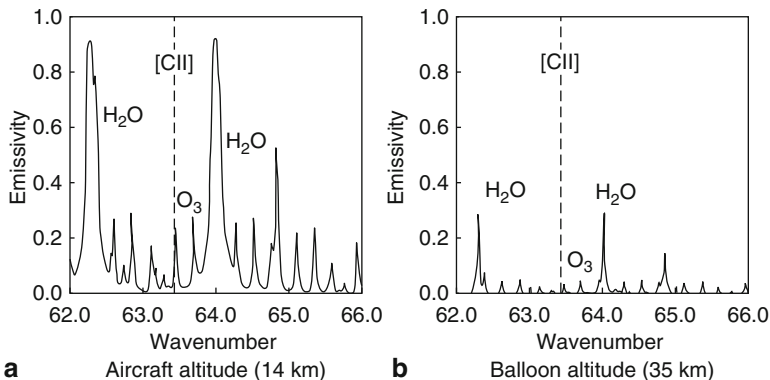


Fig. 3.49 Effect of atmospheric emission in the far-infrared region. (Source: Haruyuki Okuda, “Galactic structure research from [CII] 158 μ m,” 1993 Grant-in-Aid for Science Research (General Research A) Research Results Report (1994)): **a** Aircraft altitude (14 km); **b** Balloon altitude (35 km)

gondola function as a reaction wheel that rotates the instrument in the azimuthal direction.

Observations were performed in Japan, in Texas in the US, and in Alice Springs in Australia in the southern hemisphere, and a detailed infrared map of the entire galactic plane was successfully obtained as shown in Fig. 3.52 [22].

Cosmic rays consist of protons, atomic nuclei, electrons, and the like having high energies that come from space with speeds close to that of light. These are

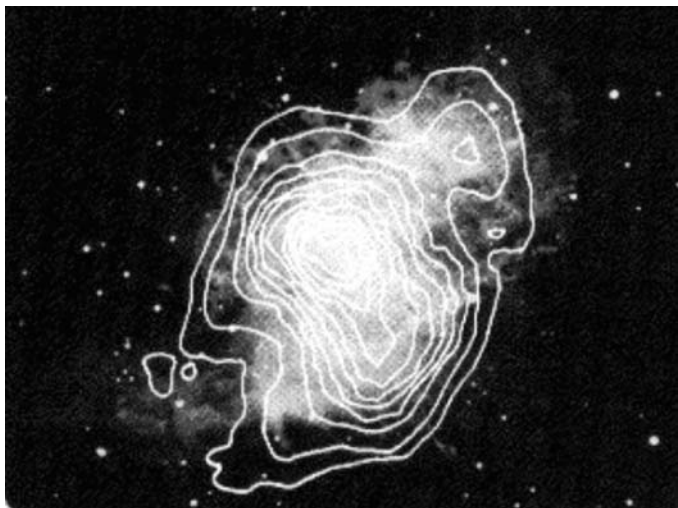


Fig. 3.50 X-ray map of Cygnus. (courtesy of the ISAS)



Fig. 3.51 Far-infrared telescope

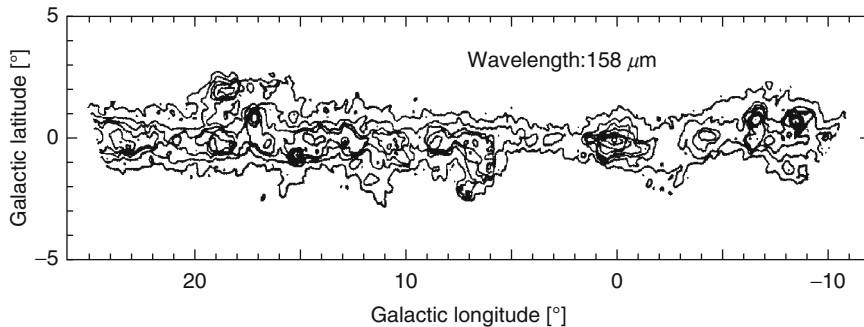


Fig. 3.52 Far-infrared map of the galactic plane (Source: Haruyuki Okuda, “Galactic structure research from [CII] 158 μm,” 1993 Grant-in-Aid for Science Research (General Research A) Research Results Report (1994))

called primary cosmic rays. When cosmic rays enter the Earth’s atmosphere, they collide with and interact with the atomic nuclei of oxygen and nitrogen within air to produce secondary particles such as mesons, and these collide with nuclei in air to further produce secondary particles. The majority of particles at low altitudes are these secondary cosmic rays.

The observations that produced many achievements in the early stages of modern scientific ballooning were from nuclear physics research that investigated these secondary cosmic rays. Balloon experimentations detected many newly discovered elementary particles in the atmosphere, such as positrons and mesons. The experimental results offered many meaningful data for the particle research. With the construction of gigantic accelerators on the ground, this kind of research became obsolete, and was superseded by research into cosmic physics and astronomy that observed primary cosmic rays at higher altitudes.

However, some particles in cosmic rays have high energies that cannot be produced in ground-based accelerators, and so some research topics in nuclear physics still use balloons. The white observation equipment shown in Frontispiece 3 just before launch is an example of a cosmic-ray detector that actively participates on both fronts. As Fig. 3.53 shows, the cosmic-ray detector is installed inside a thin-walled cylindrical superconducting magnet [23]. The main objectives of these observations are to discriminate the charge polarity of particles through their interaction with the strong magnetic field produced by the superconducting magnet and to observe anti-matter that originates from space. (See Frontispiece 3 for the condition at the time of launch.)

3.7.1.2 Observation of the Thin Atmosphere

There is an ozone layer in the stratosphere that absorbs ultraviolet rays, making the existence of life on earth possible. In addition, changes in the concentration of greenhouse gases such as CO₂ in the stratosphere cause changes to the aver-



Fig. 3.53 Cosmic ray observation instrument BESS equipped with superconducting magnet. (courtesy of the High Energy Accelerator Research Organization)

age global temperature. The stratosphere also contributes significantly to the global atmospheric circulation. Starting in the early 1970s, the effect on the ozone-layer concentration of NO_x , which is a constituent of the exhaust gas of supersonic transport (SST) that flew in the stratosphere, became a problem, and there was a high level of public concern.

Figure 3.54 shows the altitude distribution of the ozone density. Since balloons are capable of long-duration flights within the atmosphere, which is a requirement of such observations, they are able to perform high-precision “in-situ” observations.

Figure 3.55 shows a cryosampling system used for observing the components of trace substances in the stratosphere [24]. The air of the stratosphere is collected at 12 different altitudes, and after recovery, the concentration of components is analyzed in detail by using high-precision analytical instruments at collaborating universities and research institutes. To collect analyzable quantities of the thin atmosphere, the collection vessels are cooled with liquid helium. As the air collected partially solidifies, atmospheric air that has been compressed approximately 3,000 times is collected in the vessels at an altitude of 30 km.

In addition to this, devices have been developed to observe the atmosphere by optical and chemical means, and experiments are continuing to be conducted.

Fig. 3.54 Altitude distribution of ozone density.
 (Source: Shimazaki, T.: Stratospheric Ozone, (in Japanese), University of Tokyo Press (1989))

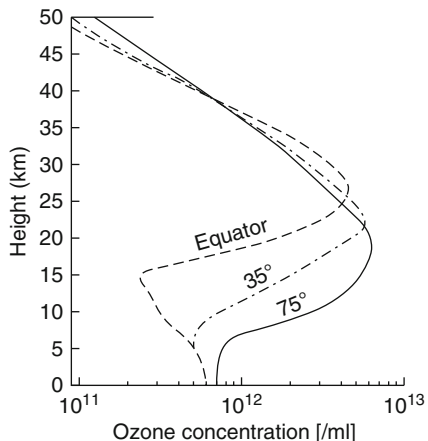


Fig. 3.55 Cryosampling system used to collect air in the stratosphere from 12 different altitudes

3.7.2 Engineering Experiments

3.7.2.1 Experiments at the Stage Prior to Space Application

At balloon altitudes, the radiation from the sun and the earth, the cosmic background microwave radiation at a temperature of 3 K, and the effects of primary cosmic radiation rather closely resemble those of space. In the 1950s, manned balloon experiments were performed using airtight cabins in the US Air Force's Man-High project and the US Navy's Strato-Lab project, marking the first stage of space development.

At the beginning of the 1960s, wearing only a spacesuit from the Mercury project, an astronaut ascended to an altitude of 35 km in an open gondola [25]. In the same period, large balloons were launched from icebreaker vessels and aircraft carriers. With their rapid navigation capability, ships traveled in the downwind direction, and by offsetting the effects of the sea's surface winds, balloons were launched smoothly from spacious decks.

Even today, balloons are used in experiments in the stage prior to development of space technology. For example, if an object is dropped from an altitude of 30 km or higher and is allowed to freefall, it will easily achieve a speed of about Mach 1. Consequently, using this method, preliminary testing of return capsules and space planes reenter the earth's atmosphere from space. Flight testing of an entry capsule penetrating a planetary atmosphere can also be performed. Frontispiece 7 shows a photograph of the experimental equipment prior to launch. This experiment was performed in 2003 as part of high-speed flying vehicle research by the National Aerospace Laboratory (NAL) of Japan and the National Space Development Agency of Japan [26]. The site is ESRANGE in Sweden.

3.7.2.2 Weightlessness Experiments

Free fall from balloon altitudes produces about 30 s of weightlessness. Compared with weightlessness experiments in space using satellites, this is a short period of time, but it has the advantages that the experiments are simple and convenient and the time to recovery is short. Because of the low cost of this technique, it is also used for preliminary testing of plans that will make use of satellites or the space station [27].

3.7.2.3 Launching Rockets from Balloons (Rockoons)

During the early stages of sounding rockets, to increase the achievable altitude, trials to transport a small rocket to a high altitude by suspending it from a balloon and launching the rocket from the balloon altitude were performed. As a rough estimate, a rocket that reaches an altitude of 20 km when launched from the ground will reach 100 km if launched at an altitude of 20 km from a balloon.

This system combines a rocket and a balloon and was named a “rockoon.” Launches were carried out in the US from 1952 using the Deacon rocket. Balloon launches were carried out from icebreakers with the purpose of surveying the earth's magnetic field near the magnetic pole. The project leader was A. Van Allen of the University of Iowa, who is famous for the discovery of the Van Allen radiation belt [28].

Launches continued until the latter half of the 1950s, and in 1957, 36 rockoons were launched as part of the International Geophysical Year (IGY). In addition, this type of observation was carried out to investigate the effect of cosmic rays in preparation for manned space flights.

Even in Japan, the Institute of Industrial Science, University of Tokyo, which pursued the development of a solid-fuel rocket for IGY, showed an interest in rockoons. In 1956, a rockoon research group was established to initiate collaboration between rocket and balloon-scientists. The Japanese Meteorological Agency has also actively collaborated with this group. The initial intent was to launch balloons from ships in the same way as the US, and preliminary testing was carried out using the meteorological observation vessel Ryofu Maru, but because of the ship's capabilities and operational limitations, activities were switched to land launches.

Testing was first carried out in June 1958, when a rocket was successfully launched from a balloon. In June 1961, the Model Sigma II rocket was successfully launched from a balloon at an altitude of 20 km, and reached an altitude of 100 km as planned. The mission also succeeded in performing scientific observations of cosmic rays [29]. Figure 3.56 shows photographs of a rockoon test.

Although rockoons came to be used less frequently because of the improved capabilities of sounding rockets, testing having special objectives has subsequently been carried out. Figure 3.57 shows a photograph of a "Winged Flight Test Vehicle" that the ISAS carried out in 1990. The test vehicle, which was equipped with a booster rocket, was launched from a balloon at an altitude of 20 km, and after achieving an altitude of 80 km, made a reentry flight test at high speed [30].

3.7.3 Routine Meteorological Observations

Aerological observations by suspending and flying meteorological observation instruments on rubber balloons to measure the temperature, relative humidity (referred to below as "humidity"), and wind speed and direction of the upper air are carried out simultaneously on a daily basis worldwide (Frontispiece 8). The measurement data are used as the initial values for numerical prediction models that are the basis for weather forecasting. Numerical prediction models predict the thermodynamic structure of the atmosphere and atmospheric flows based on the laws of physics. They are used to forecast phenomena such as typhoons, low-pressure systems, and the structure, ebb and flow, and movement of fronts. The observation data are also used in weather reports required for the operation of aircraft, in monitoring the earth's environment for climate change and other phenomena, and in research studies on meteorological phenomena.

Meteorological observation equipment consists of the sensors for air pressure, temperature, humidity, and a transmitter to send the measured data to the ground station. This is called a radiosonde. There are various kinds of radiosondes: there is the rawinsonde that measures air pressure, temperature, humidity, wind direction, and wind speed, the rawin that measures air pressure, wind direction, and wind speed, and the ozonesonde that measures air pressure, temperature, amount of ozone, wind direction, and wind speed.

**a****b**

Fig. 3.56 Rockoon test in Japan. (courtesy of the ISAS): **a** Test site and research team members; **b** Sounding rocket suspended from the launcher just prior to launch



Fig. 3.57 The ISAS's Winged Flight Test Vehicle. (courtesy of the ISAS) The vehicle separated from the balloon at an altitude of 20 km, and the booster rocket was ignited. After ascending to 80 km, an atmospheric reentry flight was conducted

3.7.3.1 Aerological Observation Points and Observation Times

Worldwide, there are about 900 weather stations and other types of observation points where aerological observations are performed. Observations are carried out at the same time according to the agreement with the World Meteorological Organization (WMO). Rawinsonde observations are performed at 00:00 and 12:00 GMT, and rawin observations are performed at 06:00 and 18:00 GMT. Ozonesonde observations are performed at 06:00 GMT every Wednesday. The observation data are exchanged internationally through the Global Telecommunication System (GTS), which is a worldwide meteorological communication network, and this information is used throughout the world.

In Japan, the Japan Meteorological Agency (JMA) has 18 observation points and the Defense Agency has two observation points where routine aerological

observations are performed. The JMA also performs observations at four ocean weather ships and at the Antarctic Showa Base.

3.7.3.2 Ground Apparatus Used in Aerological Observations

Radiosondes that ascend mounted on rubber balloons measure changes in air pressure, temperature, humidity, and other factors as variations in capacitance and electrical resistance and transmit this information to the ground via radio. On the ground, equipment such as antennae, receivers, and a computer receive and decode the radio signals and calculate the air pressure, temperature, and humidity of the upper air.

The configuration of the Model JMA-91 aerological observation system currently used by the JMA is shown in Fig. 3.58. This system automatically tracks the direction of incoming radio waves transmitted from the radiosonde, receives the signal from the radiosonde, and determines its azimuth and elevation angles. The balloon position is calculated by using the azimuth and elevation angles and the balloon altitude calculated from the pressure, temperature, and humidity measured by the radiosonde. The wind profile is found from the change in the balloon position. The wind direction is obtained from the direction of balloon drift and the wind speed by dividing the distance moved by the time taken.

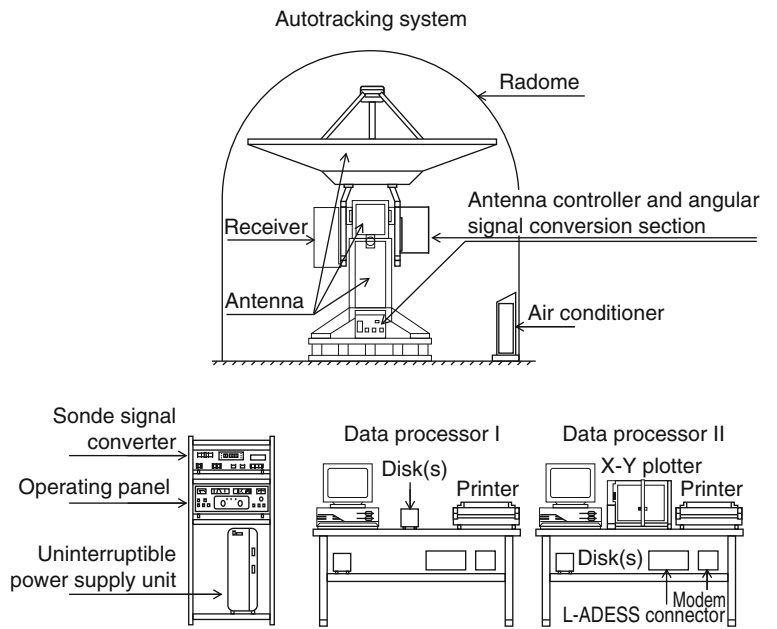


Fig. 3.58 Configuration of the Model JMA-91 aerological observation system. (Source: Aerological Observation Guidelines, (in Japanese), Japan Meteorological Agency)

In addition, there are other systems, such as GPS and LORAN, that make use of radio navigation methods for observing upper-air winds. Since radio navigation methods do not require automatic tracking antenna, the antenna, receiver, and other ground equipment are simpler than those used by automatic tracking systems. Ocean weather ships and others use the GPS system.

3.7.3.3 Rawinsonde

A general view of the Model RS2-91 rawinsonde that the JMA uses in routine observations is shown in Fig. 3.59.

The pressure sensor is an aneroid-diaphragm pressure gauge that is 46 mm in diameter and that uses an iron–nickel alloy. It detects the expansion and contraction of an aneroid cell that occur with changes in pressure as changes in the capacitance between the aneroid cell and electrode plates, and it continuously measures the air pressure. The temperature sensor is a temperature gauge that uses a thermistor and that has a rapid response rate and a very large change in resistance with changes in temperature, and it measures temperature changes as changes in resistance. The humidity sensor is a variable-capacitance humidity sensor that consists of a moisture-sensitive polymeric membrane located between electrodes that detect changes in capacitance between electrodes resulting from changes in humidity. Changes in capacitance or resistance from the pressure, temperature, and humidity sensors are converted to frequency by a CR oscillator and transmitted to the ground. On the ground, altitude is calculated by converting these frequency signals into the physical quantities of pressure, temperature, and humidity; the upper-air winds are calculated from this altitude and the antenna azimuth and elevation angles; temperature, humidity, and upper-air winds up to an altitude of approximately 30 km are thereby obtained. As actual examples of observation data, observations at 09:00, 7 Novem-

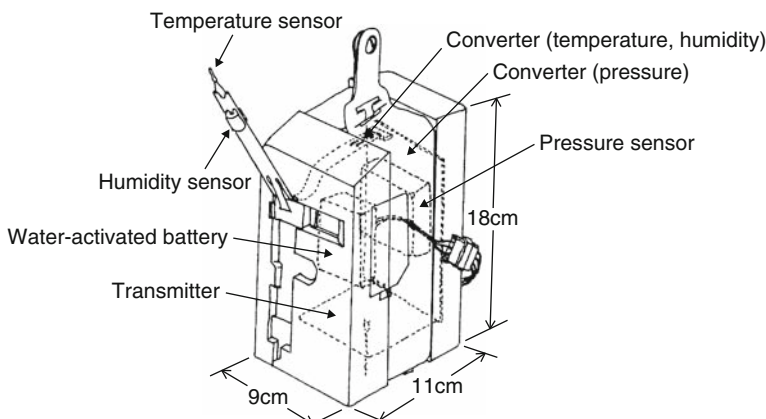


Fig. 3.59 General diagram of the Model RS2-91 rawinsonde. (Source: Aerological Observation Guidelines, (in Japanese), Japan Meteorological Agency)

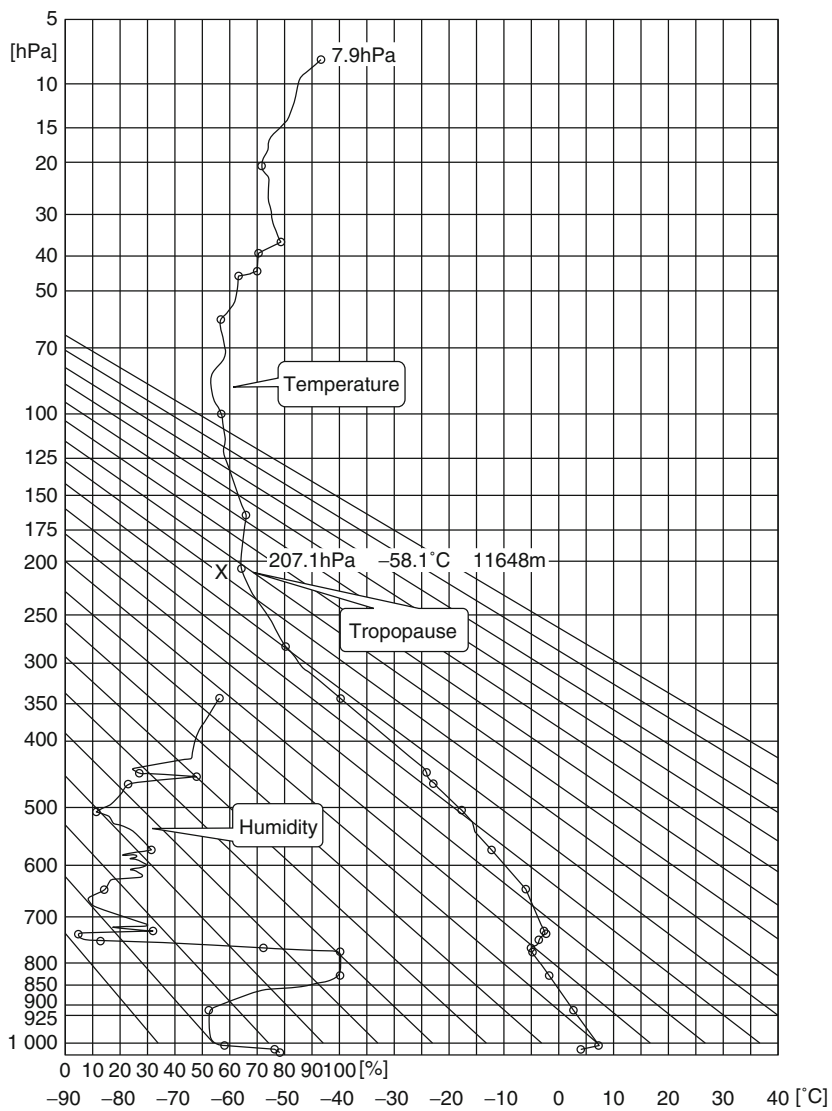


Fig. 3.60 Example of rawinsonde temperature and humidity observations. P-T diagram for 09:00, 7 November 2002 (flight time 08:30) at the Aerological Observatory. The circles indicate points selected by internationally determined standards to reproduce the vertical structure for temperature and humidity, and the symbol “X” indicates the tropopause (selected by international standards as the boundary between the troposphere and the stratosphere)

ber 2002 at the Aerological Observatory are presented in Figs. 3.60 and 3.61. Figure 3.60 is a P-T diagram indicating changes in pressure vs. temperature and pressure vs. humidity, and Fig. 3.61 is an upper-air wind diagram illustrating changes in altitude vs. wind direction and altitude vs. wind speed.

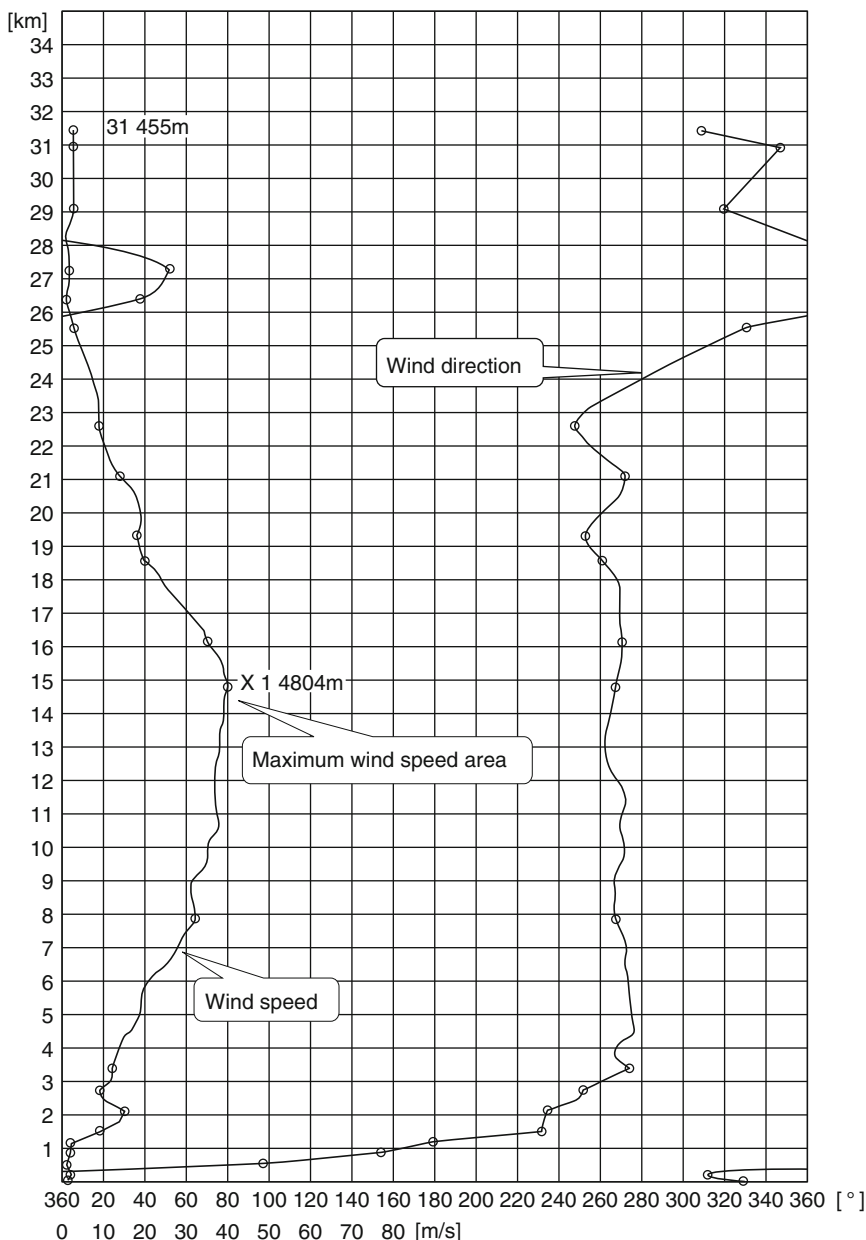


Fig. 3.61 Example of rawinsonde upper-air wind observations. Upper-air wind diagram for 09:00, 7 November 2002 (flight time 08:30) at the Aerological Observatory. The circles indicate points selected by internationally determined standards to reproduce the vertical structure of the wind direction and wind speed, and the symbol “X” indicates the area of maximum wind speed (the point of maximum wind speed with a wind speed of at least 30 ms^{-1} out of the points selected by international standards)

3.7.3.4 Aerological Observation Materials

Aerological observation data are promptly sent as meteorological information in the internationally agreed format during or immediately after observations and are used for weather forecasting both inside and outside the country. In addition, the data are saved on CD-ROM and are made available to the public [31]. There are Japan Meteorological Agency Monthly Reports, Aerological Observation Annual Reports, and Average Year Values (statistics for 1971–2000) on CD-ROM in which Japanese domestic aerological observation data are recorded, and these are available for perusal at weather stations. World aerological observation data including aerological observation data from Japan are released on a Web site belonging to the University of Wyoming in the US.

Table Talk 5: Tateno Aerological Observatory: Making a Mark on History

Aerological Observatory, Japan Meteorological Agency is located at Nagamine, Tsukuba City, Ibaraki Prefecture (36.03°N, 140.08°E, 60 km northeast of Tokyo) (Frontispiece 8). Established in 1920, this was Japan's first aerological observation station. Today, it occupies a block in the modern Tsukuba Science City, and the Tsukuba Space Center of Japan Aerospace Exploration Agency is located in an adjacent block. Originally, however, it was located in the middle of an area of mountain forest and wilderness, and Tateno and Nagamine are both place names from that time.

The first director was Mr. Wasaburo Oishi. He vigorously pursued upper-air observations up to altitudes of about 10 km at this fledgling aerological observatory. The observation method used was pibal observation (Sect. 3.6.1), which tracked rubber balloons with a balloon theodolite. He launched 1,288 balloons during the two-year period from March 1923 to February 1925. As a result of these observations, he discovered the existence of prevailing westerlies at the top of the troposphere that blow strongly in winter (Sect. 3.1.5). This is considered to be a lasting contribution to the history of meteorological research.

This research was published in Aerological Observatory Report No. 1 in Esperanto in 1926. This was interesting since it reflects the great sense of internationalism that pervaded Japan at that time. The title of the report collection was “Raporto de la Aerologia Observatorio de Tateno,” and the title of the thesis was “Vento super Tateno.” It was also published in Japanese in the same year as “Average Winds in the Upper-air of Tateno.”

Subsequently, this research took an unexpected direction. Outside publishing was suppressed as a result of military expansionism, and before long, affairs came under the control of the army. This research was recognized as a meteorological basis for the feasibility of the balloon bomb that was deployed in the final stages of the Pacific War. These balloons, which carried bombs to America in a few days by riding the prevailing westerlies, used a timer to automatically terminate their flight. The time

that was set was determined by measuring the speed of the westerlies. These balloon bombs are described in detail in “Japan’s World War II Balloon Bomb Attacks on North America” by Robert C. Mikesh (published by Smithsonian Institution Press, 1973).

Times change, and at the dawn of postwar scientific ballooning in the 1950s, cosmic-ray researchers struggled valiantly at the Tateno Aerological Observatory with the complete cooperation of the observatory to transport observation equipment using polyethylene balloons. Twenty long years passed before Mr. Oishi’s work on the middle-latitude westerlies received international recognition by the adoption of the term “jet stream” after World War Two. In 2003, to acknowledge Mr. Oishi’s efforts, Dr. J.M. Lewis presented a paper entitled “Oishi’s Observation – Viewed in the Context of Jet Stream Discovery” at the American Meteorological Society, March 2003. On the premises, there is a simple wooden memorial house honoring Mr. Oishi and his pioneering achievements.

References

1. Salby, M.L.: Fundamentals of Atmospheric Physics, Academic Press, California (1996)
2. Matsuno, T., Shimazaki, T.: Atmospheres in the Stratosphere and Mesosphere (in Japanese), Atmospheric Science Lecture Series 3, University of Tokyo Press, Tokyo (1981)
3. Yajima, N., et al.: Attitude Control System for a Balloon-Borne Telescope, Proc. 13th Int. Symp. Space Technol. Sci., 1189–1194 (1982)
4. Matsuzaka, Y., et al.: Development of Balloon-Borne Reel-Down and –Up Winch System, Adv. Space Res., Vol. 5, No. 1, 41–44 (1985)
5. Suzuki, R., Yajima, N.: Balloon System for Data Collection and Command Sending by Means of Geostationary Satellite, Proc. 18th Int. Symp. Space Technol. Sci., 1479–1484 (1992)
6. Saito, Y., et al.: Japanese Polar Patrol Balloon Experiments from 2002 to 2004, Proc. 24th Int. Symp. Space Technol. Sci., 875–880, 2004
7. Akiyama, H., et al., A New Static-Launch Method for Plastic Balloons, Adv. Space Res., Vol. 3, 97–101 (1983)
8. Takano, T., Sato, T., Kashimoto, M., Murata, M.: Radio Instrumentation and Navigation in Space (In Japanese), Corona Publishing Co., LTD, 2000
9. Andersson, L.: A New improved Balloon System at Esrange, Proc. 13th ESA Symp. European Rocket Balloon Program. and Related Res, SP-397, 439–442 (1997)
10. Ball, D.: Long Duration Ballooning in Antarctica –An Operational Perspective, AIAA Int. Balloon Technol. Conf., AIAA-91-3679-CP, 158–164 (1990)
11. Nishimura, J., et al.: Polar Patrol Balloon, J. Aircr., Vol. 31, No. 6, 1264–1267 (1994).
12. Nishimura, J., et al.: Boomerang Balloon, the 10th Int. Symp. Space Technol. Sci., 1253–1257 (1973)
13. Kuramata, S., et al.: Russia Nippon Joint Balloon Experiment -Long Duration Flight from Kamchatka, Proc. 22th Int. Symp. Space Technol. Sci., 1839–1845 (2000)
14. International Civil Aviation Organization (ICAO), International Standards, Rules of the Air, Annex 2, To the convention on international civil aviation, 9th Edition, 1264–1267 (1990)
15. Seely, L.G., Smith, M.S.: Recent Progress in Scientific Balloon Film Research, the 17th Int. Symp. Space Technol. Sci., 1571–1576 (1990)
16. Kiuchi, T.: Simple Discrimination of Packing Materials (Plastic Films) by their Infrared Absorption Spectra, Agricultural and Forestry Products Inspection Institute, Investigation and Research Report, 1, 75–92 (1973) (in Japanese)

17. Smith, M.S.: Operational Evaluation of Recently Developed Balloon Fabrication Methods, AIAA Int. Balloon Technol. Conf. AIAA-91-3670-CP, 101–107 (1991)
18. Seely, L.G., Smith, M.S.: Computer Applications in Scientific Balloon Quality Control, The 17th Int. Symp. Space Technol. Sci., 1577–1582 (1990)
19. Shibue, N., Kamata, H., Abe, T.: The Investigations Concerning Aerological Observation Balloons-The attained altitude, ascending rate, and the quantity of leakage gas- (in Japanese), J. Aerol. Obs., No. 61, 59–68 (2001)
20. Okuda, H., et al.: Large Scale [CII] Line Emission in the Galaxy Observed by Stratospheric Balloons, Infrared Phys. Technol. Vol. 35, No. 2/3, 391–405 (1994)
21. Oda, M.: CygX-1/A Candidate of the Black Hole, Space Sci. Rev., Vol. 20, No. 6, Springer Netherlands, 757–813 (1977)
22. Nakagawa, T., et al.: Far-Infrared [CII] Line Survey of the Galaxy, In: The 2nd Cologne-Zermatt Symp.: The Phys. and Chem. of Interstellar Molecular Clouds, (ed.) Winnewisser, G., Guido, C., Springer-Verlag, Berlin, (1995)
23. Yamamoto, A., et al.: Balloon-borne Experiment with a Superconducting Solenoid Magnet Spectrometer, Adv. Space Res., Vol. 14, No. 2, 75–87 (1994)
24. Honda, H., et al.: Development of Stratospheric Whole Air Sampling System Using LHe as a Cryogen and Its Operation Results for 15 Years, Adv. Space Res, Vol. 33, No. 10, 1797–1805 (2004)
25. DeVorkin, D.H.: Race to the Stratosphere: Manned Scientific ballooning in America, Springer-Verlag (1989)
26. Miyazawa, Y., et al.: HOPE-X High Speed Flight Demonstrator Research Program, Proc. 22nd Int. Symp. Space Technol. Sci., 1367–1373 (2000)
27. Namiki, M., et al.: Microgravity Experiment System Utilizing Balloon, Adv. Space Res, Vol. 5, No. 1, 83–86 (1985)
28. Foerstner, A.: James Van Allen, University of Iowa Press, Iowa (2007)
29. Monthly Journal of the Institute of Industrial Science, University of Tokyo, Special Issue: Rokoon (in Japanese), Vol. 12, No. 1, (1981)
30. Inatani, Y.: Atmospheric Reentry Flight Test of Winged Space Vehicle, AIAA 4th Int. Aerosp. Planes Conf., AIAA-92-5053, (1992)
31. Abo, Y.: Manual of Aerological Observation (in Japanese), Japan Meteorological Business Support Center, (2001)

Chapter 4

Planetary Ballooning

Abstract It is possible to fly balloons above planets that have atmospheres in the same manner as in the Earth's atmosphere. This chapter first presents the atmospheric characteristics of each planet in regard to planetary ballooning. The advantages of using balloons for planetary exploration are mentioned. The technological peculiarities of planetary balloons are described in contrast with balloons that fly in the Earth's atmosphere. Actual balloons that have flown in Venus' atmosphere are described in detail. This chapter also describes the various ballooning techniques that are being investigated for future projects. Subjects for scientific observation by balloons are also mentioned.

4.1 Atmospheres of Planets

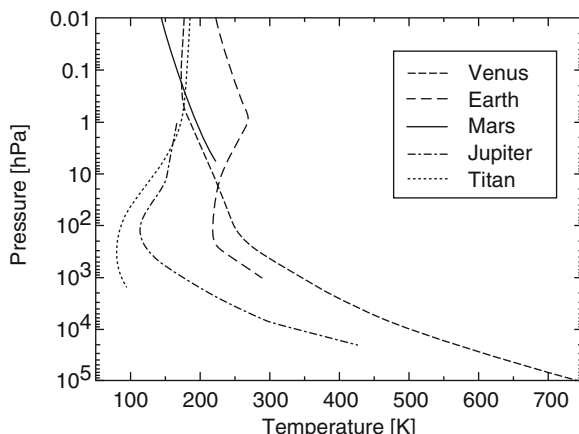
Balloons have been used for a variety of different applications on earth, and in the future it is anticipated that they will be used in various applications with particular emphasis on scientific observations on other planets. On other planets, where it is difficult for humans to travel on the surface, the importance of balloons is enhanced as they are able to ride the atmospheric currents and travel over large distances. Later we give an overview of the characteristics of the planets that have atmospheres and their atmospheric environment. For further details, please refer to literature [1].

4.1.1 Atmospheres of Terrestrial Planets

Table 4.1 compares Earth, Venus, Mars, and Titan (one of the satellites of Saturn), which are all terrestrial planets possessing atmospheres. Figure 4.1 compares the temperatures of these planetary atmospheres with reference to pressure.

Table 4.1 Basic parameters of terrestrial planets

	Earth	Venus	Mars	Titan
Equatorial radius (km)	6,378	6,052	3,397	2,575
Mass (10^{24} kg)	5.97	4.87	0.64	0.13
Gravitational acceleration at the planetary surface (m/s^2)	9.78	8.87	3.72	1.35
Distance from the sun (semi-major axis: 10^8 km)	1.50	1.08	2.28	14.3
Rotation period (earth days)	1.00	243.0	1.03	15.9
Orbital period (earth years)	1.00	0.615	1.88	Same as the rotation period
Principal atmospheric constituents	N_2, O_2	CO_2 (96.5%)	CO_2 (95.3%)	N_2 (65–98%)
Mean surface pressure (hPa)	1,013	92,100	5.6	1,500
Mean surface temperature (K)	288	735	210	94
Planetary magnetism (nT)	5×10^4	None or very weak	Local remnant magnetization	Not detected

**Fig. 4.1** Temperature profiles of the atmospheres of Earth, Venus, Mars, Jupiter, and Titan (a satellite of Saturn). With the exception of Jupiter, the bottom tip of each temperature curve corresponds to the planetary surface

4.1.1.1 Venus

Although Venus is about the same size as Earth, the principal component of Venus' atmosphere is carbon dioxide, whereas the principal components of the earth's atmosphere are nitrogen and oxygen. The pressure at Venus' surface is about 90 times greater than that of Earth, and because of the greenhouse effect generated by the large quantity of carbon dioxide, the temperature at Venus' surface reaches 735 K. Information about Venus' surface and low-level atmosphere is limited due to screening by clouds of concentrated sulfuric acid extending over the entire planet at altitudes between 45 and 70 km (pressure: 2,000–50 hPa), and due to the difficulty of using probes at such high temperatures. On the basis of the results of radar surveys, the planetary surface is thought to have been resurfaced in the comparatively recent past (several hundred million years ago), but direct evidence of current igneous activity has not been obtained up to this point, and the mineral composition is not well understood, although the bulk composition seems to be basalt.

The atmospheric motion of Venus differs greatly from that of the earth, and according to observations, easterly winds prevail over the entire planet. Wind speeds near the planetary surface are a few m/s or less but increase with altitude, reaching 100 m/s at the top of the cloud layer; the atmosphere at these altitudes makes a full circuit around the planet in 4–5 days. Since Venus rotates from east to west and has a period of 243 days, the atmosphere at the altitude of the cloud layer outpaces the planetary surface and has an angular velocity 60 times greater than that of the planet's surface. This high-speed wind is termed super-rotation. The mechanism for super-rotation has not yet been determined, and it is regarded as a major question in meteorology. The Vega Venus Balloon, which was a joint mission principally between the former Soviet Union and France, floated at the cloud layer altitude, and it demonstrated new possibilities for researching the meteorology of Venus. However, meteorological data at lower altitudes are considered to be vital for understanding the phenomenon of super-rotation.

4.1.1.2 Mars

Mars is about half the size of Earth. Like Venus, the principal component of Mars' atmosphere is carbon dioxide, but it is much more rarefied, and the temperature is lower than that on Earth. The planet's surface is dry, so that fine dust is always suspended in its atmosphere. The absorption of sunlight by this dust heats the atmosphere, and this has a large effect on the weather of Mars. Because of the low temperatures in the polar regions, the carbon dioxide that is the principal component of the atmosphere partially freezes, forming dry ice and covers the planet's surface. However, topographical data suggest that there was a period on Mars that was warmer than it is now and that perhaps the liquid, water flowed on the surface. A detailed investigation of the surface topology and mineral composition of Mars is necessary to discover the kind of climate changes that have occurred on Mars.

The large-scale wind systems on Mars are considered to resemble those in the Earth's stratosphere. Specifically, easterly winds predominate in the summer

hemisphere, where the polar region is a high-pressure area, because of the kinetic balance of geostrophic winds, and westerly winds predominate in the winter hemisphere because the polar region is a low-pressure area. In spring and autumn, both hemispheres have westerly winds. In addition, dust storms are a characteristic of the weather on Mars. Large-scale dust storms covering the entire planetary surface occur, but the mechanism of their occurrence is not well understood.

4.1.1.3 Titan

One of the Saturn's satellites, Titan, is larger than the earth's moon (radius: 1,738 km) and Mercury (radius: 2,439 km), and, while it is not a planet, it has a thick atmosphere whose principal component is nitrogen. The mass of the atmosphere per unit area on the surface is about 11 times that on Earth, but because the acceleration due to gravity is small, the atmospheric pressure at the surface is about 1.5 times that of Earth. In addition to nitrogen, the atmosphere also contains methane, which makes up a few percent of the atmosphere. The satellite's surface cannot be observed from above the atmosphere at visible wavelengths since the surface is covered by a thick aerosol of hydrocarbons. The existence of hydrocarbon lakes or seas is suggested from a radar sounding performed by the Cassini spacecraft, but they are currently not well understood. Because it is far from the sun, Titan is an intensely cold world.

Although the motion of the atmosphere is not well understood, according to wind speed distributions measured by an entry probe and inferred from temperature data obtained by remote sensing, the upper-level atmosphere moves in the direction of satellite's rotation at speeds ranging from a few dozen m/s to 100 m/s. But then, the solid component of Titan revolves around Saturn with the same side constantly facing Saturn; its rotational speed at the equator is 12 m/s. These results suggest that significant super-rotation occurs on Titan in the same manner as on Venus.

4.1.2 Atmospheres of Jovian Planets

Jupiter, Saturn, Uranus, and Neptune are classified as Jovian planets and have thick atmospheres consisting mostly of hydrogen and helium. They do not have well-defined solid surfaces, or if they do, they are extremely deep within the planets. The pressures are 100–1,000 hPa in the environs of the ammonia and methane clouds that are visible from the outside, and atmospheric temperatures and pressures increase with depth below this (Fig. 4.1). A characteristic of Jovian planets is that, with the exception of Uranus, the upward heat flow from the interior of the planet is approximately the same as the energy received from the sun.

In regard to atmospheric motion, winds in the outermost layer can be estimated from cloud movement, and it is known that winds in the east-west direction predominate and that the wind speed varies by up to 100 m/s with latitude. However, the

flow characteristics of the atmosphere at lower depths, which accounts for the majority of the atmosphere, are unknown. There are two main possibilities: that the wind system observable in the outermost layer extends continuously down into the depths of the planet, or that the movements on the surface and those at lower depths are independent of each other.

The interior atmosphere of Jupiter was explored directly by a probe released from the US' Galileo spacecraft. Data were acquired until the probe reached a pressure of 22,000 hPa (200 km below the outermost clouds). Strong winds were found to blow even at depths not penetrated by sunlight, and many other results were obtained, such as the atmospheric composition. However, one aspect that should be pointed out is that the probe appears to have been dropped into a special area, referred to as a hot spot. Hot spots are areas where strong outbound infrared radiation is observed, and clouds are thought to be locally thinned in their vicinity. In these observations, water clouds, which were theoretically predicted to exist, were not detected, and the atmosphere was extremely dry. This can be explained if a hot spot is an area of descending flow with little water vapor. The Galileo probe raised many questions regarding how representative the obtained data actually was; it is anticipated that these sorts of questions could be resolved by using a balloon that is able to float over a wide area.

4.2 Background of Planetary Ballooning

4.2.1 Characteristics of Planetary Balloons

It is possible to fly balloons on planets that have atmospheres in the same way as on Earth. A balloon that floats in the atmosphere of a planet other than earth or a satellite of another planet is termed a planetary balloon. The following are achievable by using a planetary balloon as a means for planetary exploration.

1. High-resolution observation of the planetary surface from altitudes as low as a few kilometers to a few dozen kilometers.
2. Exploration of a wide area of a planet by being carried on its winds.
3. Direct measurement of the composition and other properties of the atmosphere itself.
4. Direct measurement of the changes and distributions of wind speed and wind direction in the same manner as meteorological sondes.

From these characteristics, it is natural to attempt to use balloons to explore planets or satellites that have atmospheres.

As such, a planetary balloon has the advantages that it can perform observations at much closer distances than an orbiter can, its moving range is several orders of magnitude more extensive than that of a rover, and unlike an aircraft, it does not require a power supply to power its movement and it can thus continue to make observations for a much longer duration. It is thus an ideal vehicle for planetary

exploration. Balloons are able to make direct in-situ analysis of a planet's atmosphere, so that they can complement remote sensing from an orbiting satellite.

Although the flight path and speed are usually determined by winds and are consequently difficult to control, this approach has the double appeal that it is capable of performing wide-ranging observations and that the balloon can keep floating without doing anything. However, the technical difficulties are considerably greater than those encountered when flying a balloon over the earth.

4.2.2 History of Planetary Ballooning

Various plans for planetary balloons have been proposed and investigated since the 1960s at the initiative of Europe and US, but at the time of writing the only examples of actually flying planetary balloons are the two Venus balloons, Vega 1 and Vega 2, a joint mission by the former Soviet Union and France in 1985. As part of a Venus/Halley's Comet flyby mission, these balloons were deployed into the Venusian atmosphere when the exploratory spacecraft passed close to Venus. The mission succeeded in flying at an altitude of \sim 54 km for approximately two days. Details are presented in Sect. 4.3.1.

While there have so far been no subsequent missions, there have been all manner of proposals targeting various planets. The Jet Propulsion Laboratory (JPL), in particular, has been most active in grappling with the concept of planetary balloons. It coined the term "planetary aerobot" for a balloon having various capabilities, and it has researched and presented a variety of concepts.

4.2.3 Peculiarities of Planetary Balloons

A planetary balloon differs from a balloon on earth. A planetary balloon is transported by a spacecraft, and it enters the target atmosphere packed in a heat-resistant capsule. After the capsule has passed through the zone of maximum heating due to aerodynamic deceleration, the cover opens, the envelope of the balloon is extended, and it is inflated with lifting gas. Finally, unnecessary equipment such as the capsule and the decelerating system are jettisoned, and the balloon floats at the target altitude. These steps need to be executed autonomously.

The particular balloon envelope, balloon floating method, and lifting gas to be used should be selected by considering the atmospheric environment of each planet (its temperature, pressure, composition, etc.). Table 4.2 lists the lifting gases that can be used for planets and satellites where it is possible for a balloon to float. Because planetary exploration involves transporting the balloon a great distance, it is highly desirable to achieve a long flight of at least several weeks, something that is difficult to achieve even for a balloon on earth. Super-pressure balloons are the most suited for achieving this end.

Table 4.2 Molecular weight of planetary atmospheres and lifting gases that can be used in them

Planet/satellite	Atmospheric principal components	Average atmospheric molecular weight (kg/kmol)	Principal candidates for lifting gases
Venus	CO ₂	43.4	H ₂ /He/CH ₄ /NH ₃ /H ₂ O
Earth	N ₂ , O ₂	29.0	H ₂ /He
Mars	CO ₂	43.5	H ₂ /He
Titan	N ₂	28.6	H ₂ /He
Jupiter	H ₂	2.2	H ₂
Saturn	H ₂	2.1	H ₂
Uranus	H ₂	2.6	H ₂
Neptune	H ₂	2.6	H ₂

Hot-air type balloons are considered the most suitable balloons for atmospheres in which hydrogen is the principal component (such as Jovian planets). Since solar radiation is weak at such planets, the idea proposed is for the base of the balloon to thoroughly absorb the infrared radiation originating from the planet, and as much as possible, to avoid radiating heat into space by implementing some artifice on the upper outer surface of the balloon.

4.3 Examples of Planetary Balloons

4.3.1 Venus Balloons

Carbon dioxide is the principal component of Venus' atmosphere, and at the surface, the temperature, pressure, and density are 735 K, 9 MPa, and 65 kg/m³, respectively; at an altitude of 20 km, they are 580 K, 2.2 MPa, and 20 kg/m³; and at an altitude of 50 km, they are comparable with those at the Earth's surface being 350 K, 0.1 MPa, and 1.6 kg/m³ (Fig. 4.1). As described in Sect. 4.1.1.1, because easterly winds blow several tens of times faster than the rotational speed of Venus, a balloon flight can survey an extremely wide area in a short period of time.

In addition, because the atmosphere of Venus is much denser than that of Earth, sufficient buoyancy (i.e., sufficient capability to transport the observational equipment on board) can be obtained at low altitudes even for comparatively low-volume balloons. However, it is a high-temperature and high-pressure environment, so the balloon envelope must have a high heat resistance. Also, because of the presence of sulfuric-acid clouds, resistance to sulfuric acid must also be considered for long duration flights.

4.3.1.1 High-Altitude Inflatable Balloon (Vega)

Launched in December 1984, Vega 1 and Vega 2 entered the Venusian atmosphere in quick succession on 11 and 15 June 1985, respectively. After the balloons had separated from the lander, they were inflated with helium gas and floated in the vicinity of the equator (latitude 7.1° north and latitude 6.5° south, respectively) near the middle of the night. At an altitude of 54 km, the pressure was 540 hPa and the temperature was 305 K so that the environment resembled that at the surface of the Earth.

The two balloons were 3.4-m-diameter spherical super-pressure balloons made of Teflon, with a standard pressure differential of 30 hPa. The total mass of the balloon system was 21 kg, of which the mass of the gondola (which includes the observation equipment and the telemetry system) accounted for 6.5 kg. The gondola was suspended 13 m below the balloon, and it was about 1.3 m in height (Fig. 4.2) [2, 3]. In addition, Venus was approximately 0.7 AU (AU: astronomical unit; 1 AU = 1.5×10^{11} m) from the Earth at the time when the balloon entered the atmosphere.

The surrounding atmospheric pressure, temperature, and relative vertical wind speed were measured at intervals of 75 s. In addition, the brightness in the downward direction and the density of acid particulates within the cloud were measured using an illuminometer and a backscatter detector. Also, the presence of lightning was recorded.

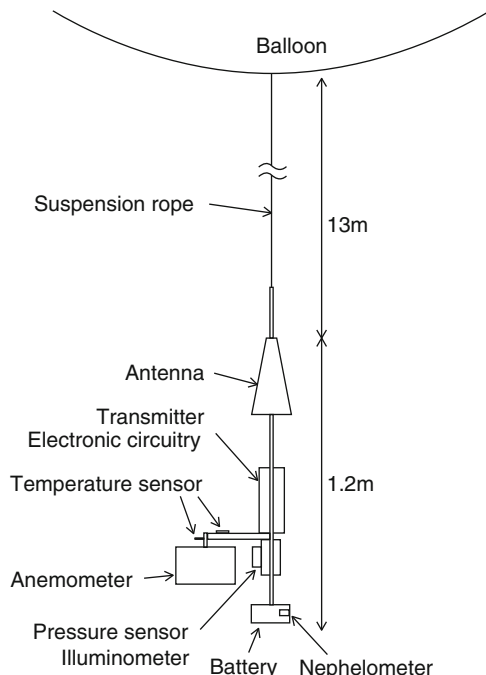


Fig. 4.2 Venus balloon "Vega"

The transmitter had a maximum output of 4.5 W, and it was used by automatically switching between data transmission mode and very long baseline interferometry (VLBI) mode for determining the balloon's position in accordance with a preprogrammed schedule. During telemeter mode, data were transmitted every 30 min to 2 h by compressing the data obtained in the previous 30 min to 852 bits. Data transmission required 332 s, which includes two 30-s periods before and after data transmission for just the carrier signal. The data rate at this time was approximately 4 bit/s.

Signals were received both by earth and by the flyby module. The speed and position of the balloon were determined by VLBI using 20 antennas at different locations on earth, and an average wind speed of 70 m/s was measured. Together with vertical wind measurements, measurements were made for the first time of the longitudinal or time variation of the 3D wind speeds in the equatorial upper troposphere.

The power source enabled a flight duration of 46.5 h and had an energy of 250 Wh by using 1 kg of lithium batteries, and the flight distance was 11,000 km (a third of the circumference of Venus). Of this, observations during the daytime amounted to 10 h. This period of observation far exceeds the total observation time of all the landers and probes that have explored Venus.

4.3.1.2 Mid-Altitude Inflatable Balloon

At altitudes of about 35 km (pressure: 0.58 MPa, temperature: 450 K), there are many heat-resistant films that can be used as the balloon film. As Fig. 4.3 shows, materials such as polyimide and liquid crystal polymers are capable of withstanding temperatures of 300°C and above [4, 5].

Since the balloon is below the cloud level, visible-spectrum and precise near-infrared measurements are also possible. The method of filling a high-pressure vessel with a lifting gas such as helium, transporting it, and then inflating the balloon

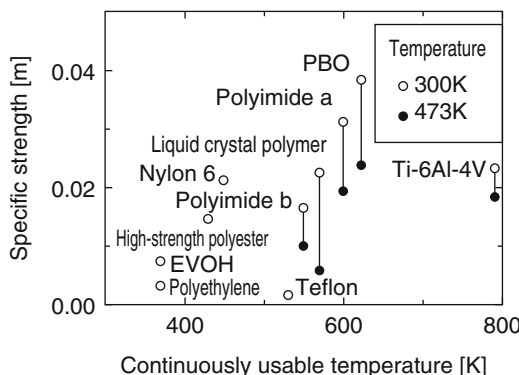


Fig. 4.3 Relationship between continuously usable temperature and strength of heat-resistant films

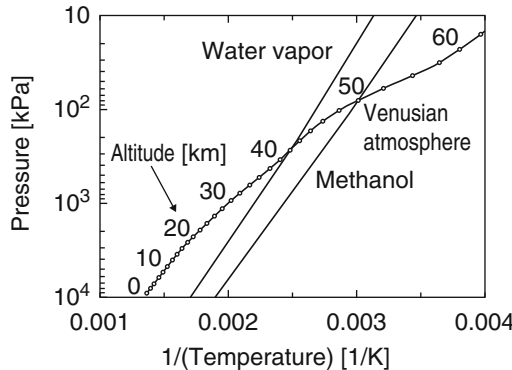


Fig. 4.4 Relationship between temperature and altitude in the Venusian atmosphere and the saturation vapor pressures of water and methanol. Water vapor becomes liquid at altitudes higher than 42 km, the intersection of the water-vapor line with the line for the Venusian atmosphere. Liquid water vaporizes at altitudes lower than 42 km

in the same manner as Vega has been considered. However, it is possible to use water as the lifting gas, since the saturated vapor pressure of water is higher than atmospheric pressure at altitudes below 42 km (Fig. 4.4).

The advantages of using water as the lifting gas are the following:

1. It has an extremely small volume during transport.
2. It does not require a high-pressure gas vessel, which increases the weight of the system.
3. By sealing water inside the balloon in advance, there is no need to use a gas injection device.

However, if the water does not completely vaporize during the brief parachute descent through the atmosphere, the balloon will descend lower than the target altitude to a region of high atmospheric temperature; hence, there is a risk of exceeding the heat resistance of either the balloon itself or of the on-board equipment.

For example, the amount of water required to float a balloon having a total floating mass of 10 kg to an altitude of 35 km is 4.4 kg. This water needs to vaporize within about an hour. In contrast to systems that use a heat exchanger, a system has been proposed in which water is allowed to adsorb onto a highly water-absorbent sheet that has been pasted on the inside of the balloon in advance. Such a system directly exploits the surrounding high-temperature atmosphere during descent [6].

The structure of a balloon employing this system is depicted in Fig. 4.5, and its deployment sequence is shown on the right side of Frontispiece 9. Using a cylindrical balloon having a large aspect ratio can increase the inflow of heat from the atmosphere because of its large surface area. Selection of a long cylindrical shape also has the advantage that the balloon can be stored efficiently in the entry capsule. The left side of Frontispiece 9 shows an artist's impression of such a balloon system.

When a polymeric film is used, the balloon's lifetime is determined by the gas barrier performance of the film. Since water vapor has a comparatively high perme-

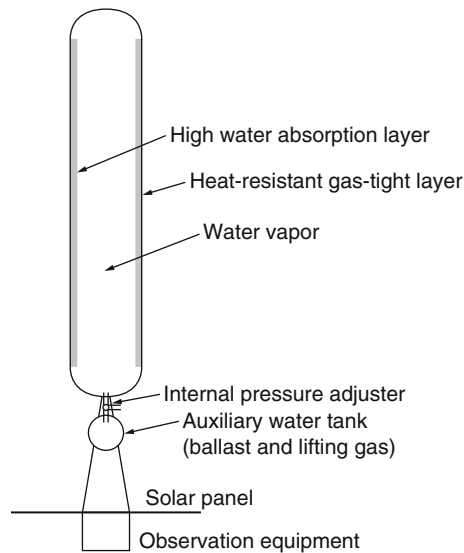


Fig. 4.5 Structure of inflatable balloon that utilizes water vapor

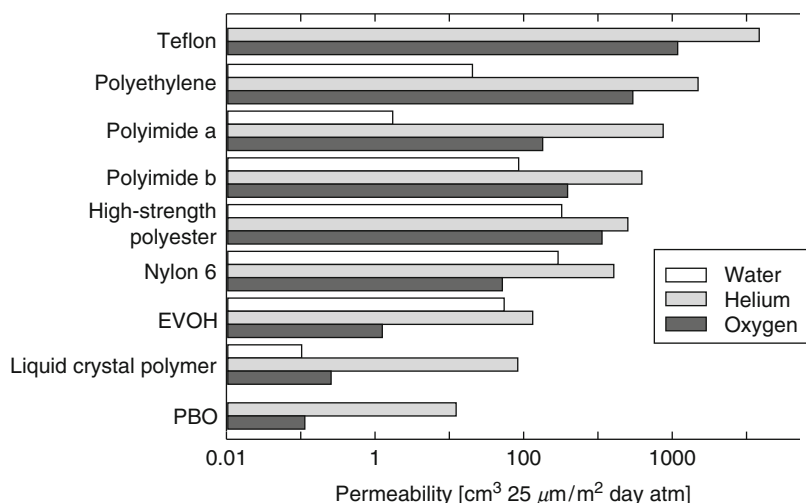


Fig. 4.6 Comparison of the gas barrier performances of heat-resistant films

ability (Fig. 4.6), measures such as employing a thin-film metallic coating should be used in conjunction with the use of materials that have a high water vapor barrier performance. As depicted in Fig. 4.5, water is carried on board as ballast, and flight durations could be dramatically extended if a method was adopted for supplying it as the lifting gas when the internal balloon pressure drops.

4.3.1.3 Variable Altitude System

For example, if water is used, it vaporizes at altitudes below 42 km (Fig. 4.4), and the buoyancy of the balloon increases; however, water liquefies at altitudes above 42 km, and buoyancy is lost. If such a property is exploited, it is possible to control the balloon's speed of ascent and descent by controlling liquefaction and vaporization through appropriate operation of the valve. For this reason, a liquid tank, a tube, and valve system plus a large, high-efficiency heat exchanger need to be carried on board. In addition, combinations of water and ammonia, helium and water, and ammonia or helium and methanol have been investigated [7].

In this manner, it should be possible to develop a balloon that can vary its altitude and that can over a few hours shuttle many times between the upper atmosphere and the planetary surface of Venus (Fig. 4.7) without expending any consumable materials (e.g., by venting lifting gas or dropping ballast). There are also proposals such as generating electricity by harnessing the energy expended by this vertical movement, and controlling the flight route to some extent in the latitudinal direction by generating horizontal thrust through the use of an airfoil when moving up and down [8].

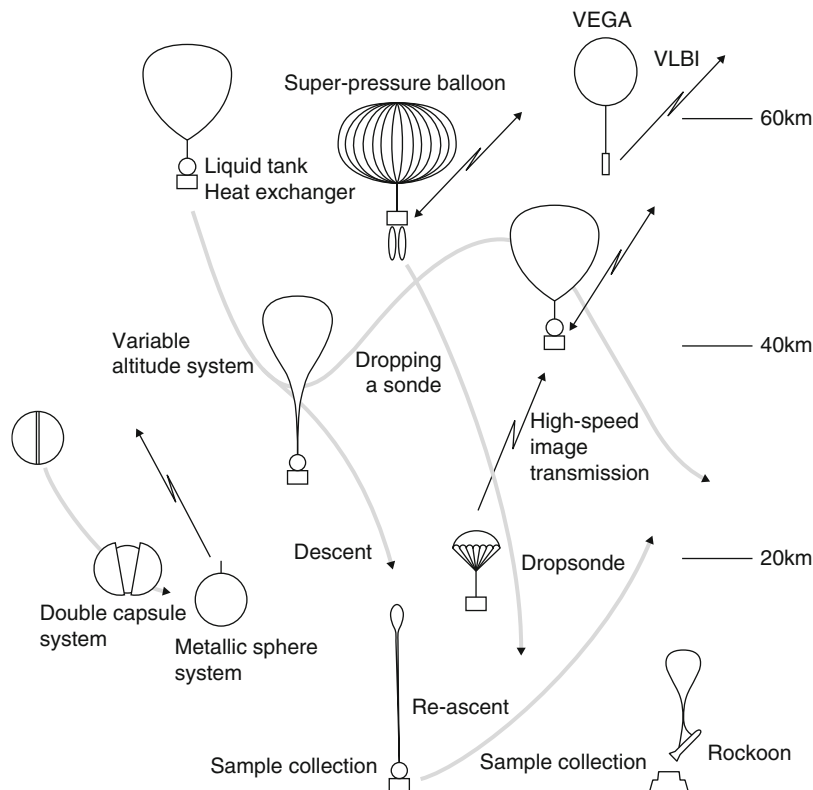


Fig. 4.7 Various Venus balloon missions that have been proposed

In addition, cooling of on-board equipment by using the phase changes of materials has been considered. More specifically, at low altitudes where it is hot, these solid materials would protect on-board equipment from melting and absorbing heat from the surrounding atmosphere. When the gondola returns to the upper layers of the atmosphere, the melted phase-change material solidifies by cooling the interior of the gondola by heat flow to the surrounding cool atmosphere via a heat pipe.

In addition, missions have been proposed to collect samples by descending to the surface of Venus with this system [8].

4.3.1.4 Dropsonde System

This is a system for dropping multiple dropsondes from a balloon floating at an altitude of 55–60 km [9]. When a balloon is used as a sonde platform, it simultaneously relays the signals between the sondes and earth. There are plans to take high-resolution photographs during descent while simultaneously collecting spectral data. As a sonde can only perform observations for a period of about an hour, one characteristic of such a system is that it has high-speed, high-capacity transmission between the sonde and the balloon, and that communication between the balloon and earth is conducted at low speeds and takes longer.

4.3.1.5 Low-Altitude Metallic Balloon System

As a consequence of the high density of Venus' atmosphere, a small balloon can obtain sufficient buoyancy at the high temperatures and pressures that exist at altitudes below 20 km. Instead of using inflatable balloons made from heat-resistant film, a system that transports a thin spherical metallic balloon in which lifting gas has been sealed at the outset could be feasible. Long duration flights are possible even under the high-temperature, sulfuric-acid atmospheric conditions, without needing to be concerned about the balloon strength and its gas barrier performance [10].

The most important aspect is the weight of the balloon itself. As the internal and external pressures of the balloon are approximately equal when floating above Venus, there is no particular requirement for strength. However, if it is decided to fill the balloon with lifting gas prior to launch, the balloon behaves as a pressure vessel when leaving the earth, and its shell will become thicker and heavier. On the basis of the volumes that can be conveyed by satellite and problems with manufacturing technology, a diameter of approximately 1–1.2 m is appropriate, but even if a titanium alloy of superior specific strength is used, it is difficult to generate sufficient surplus buoyancy. Single-layer balloons must be transported from the beginning as spherical high-pressure vessels, which increases the weight of the balloon body.

To substantially reduce this weight increase, a double-capsule balloon system has been proposed in which the balloon body is transported enclosed in a pressure-tight vessel for protection and it is released at the float altitude. More specifically, it is a system in which the shell has two layers, and the pressure-tight protective

case, which is required during transport, opens on descent to the float altitude, and is discarded (Fig. 4.7) [11].

For example, the strength of a 1-m-diameter titanium balloon is maintained at a thickness of approximately 0.1 mm, which results in a balloon weight of about 2 kg. If the float mass of the balloon is approximately 11 kg at an altitude of 20 km, the total floating mass will become 17 kg at an altitude of 13 km. Subtracting the mass of the balloon's body, structure, and lifting gas from this amount indicates that equipment equivalent to about half of the total floating mass may be carried on board.

If thin sheets are joined together to produce a large thin spherical shell, it is essential to use a bonding agent that maintains its strength at high temperatures and does not allow gas to leak. Alternative methods include titanium alloy diffusion bonding, electroforming, and using carbon fiber reinforced plastic (CFRP).

Figure 4.8 shows models that have been used for testing pressure proofing and airtightness. The model shown in Fig. 4.8a is made of a nickel–cobalt alloy manufactured by electroforming, and the model in Fig. 4.8b was formed by filament winding heat-resistant CFRP over a film liner to act as a gas barrier.

4.3.1.6 Returning of Samples

There is also a proposal to enable samples from Venus to be collected; it combines a lander and rockoon [12]. In this proposal, a lander from a satellite orbiting Venus is sent to land on Venus, and a balloon carrying the collected sample on board is launched. After floating at an altitude of about 60 km, the sample, which has been loaded into a rocket, is transported back to the orbiter. Plans have also been proposed to collect samples by descending to the surface of Venus by using the variable altitude system described in Sect. 4.3.1.3 (Fig. 4.7).

4.3.1.7 Hot-Air Balloons

At altitudes of 60–70 km, instead of helium gas balloon, a hot-air balloon system has been proposed that uses heat from the sun or from the surface of Venus [8].

4.3.1.8 Related Technology

In a high-temperature atmosphere like that of Venus, exceeding the operational temperature of the on-board electronics is a problem. Components have already been developed for deep underground exploration and for car electronics that can be used up to temperatures of approximately 220°C, and 8-bit computers and integrated circuits having a high degree of integration may also be used [13]. Cooling is essential for temperatures above this and when there are elements that cannot withstand high temperatures. Cooling can be achieved by using endothermic systems that use a material phase change, or by using electronic cooling. For example, in the case of a

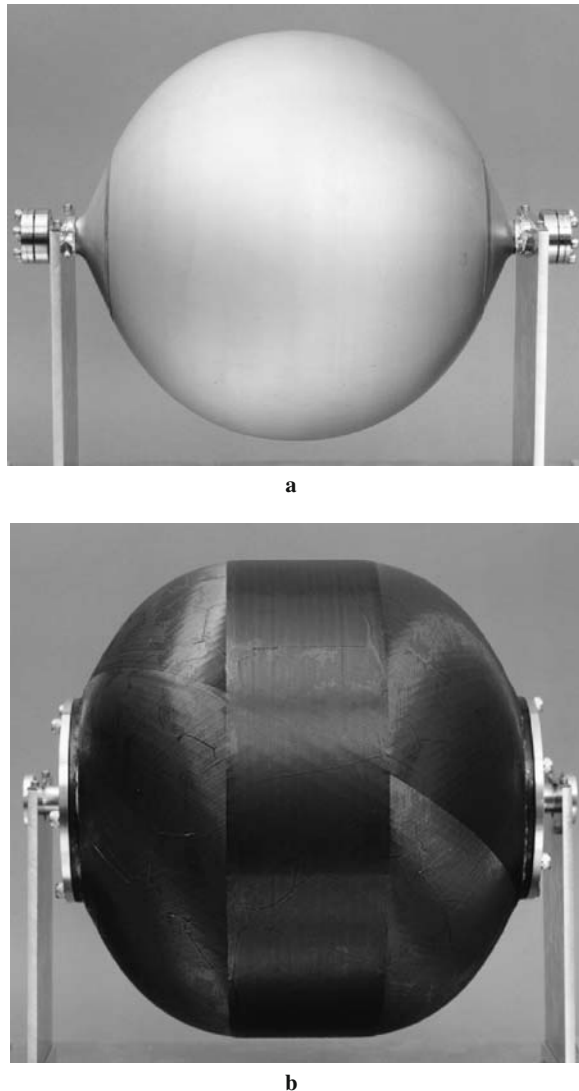


Fig. 4.8 Low-altitude Venus balloon models for testing pressure proofing and airtightness (thickness: 0.1 mm; diameter: 300 mm): **a** Nickel-cobalt; **b** CFRP

Venus balloon at an altitude of 20 km described in Sect. 4.3.1.5, it is optimal to use the heat of vaporization of ammonia. However, since ammonia can only be used once and must then be discarded, the amount of ammonia that is carried determines the lifetime of the balloon. Molten salt batteries, which operate above 300°C, may be used as the power source. In high-pressure environments, it may be necessary to protect components using pressure-tight vessels.

Solar cells are generally used as the power source for long-duration flights and observations. However, in addition to solar cells, wind-powered electrical generators that harness the vertical winds associated with changes in balloon altitude have been considered [14].

4.3.2 Mars Balloons

As shown in Fig. 4.1, the average pressure of the Martian atmosphere at the planetary surface is approximately 7 hPa, which corresponds to that at an altitude of 33.5 km on earth. The average temperature at the planetary surface is approximately 220 K, and diurnal temperature differences of 100 K occur. In addition, since the orbit of Mars is elliptical and its axis is tilted, there are large variations depending on its position and the season, and there can be differences as great as 160 K between summer daytime at the equator and winter nighttime in the polar region. Measurements that have been made by landers up until now indicate that normal winds are of the order of a few m/s, but wind speeds can reach over 100 m/s in the frequent sand storms that occur.

In the case of a Mars balloon, if a balloon designed for use in the Earth's stratosphere is used, its float altitude will merely be close to the Martian surface. Although it depends on the type of film used, the daytime gas temperature is thought to be about 30–60 K higher than that at night, and the diurnal gas temperature difference is predicted to be about 150 K. When this is converted to a pressure difference, it is equivalent to about 50% or more of the atmospheric pressure; this makes the use of zero-pressure balloon impractical, since the quantity of gas that would need to be vented would be too great.

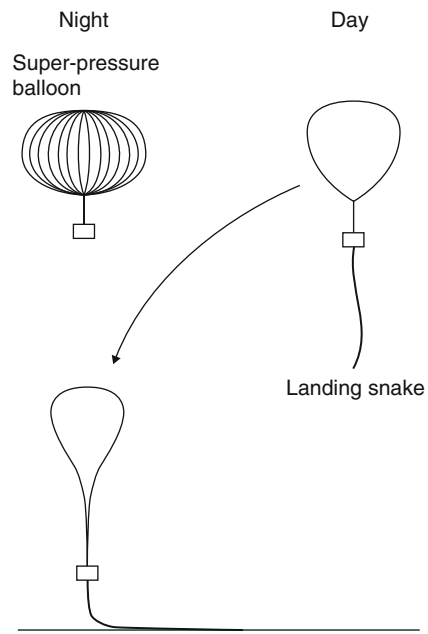
A lightweight super-pressure balloon is required that is able to withstand these pressure differences that are much more severe than those experienced by a super-pressure balloon on earth. In addition, it is desirable that the film's performance does not deteriorate over such a temperature range. To compound matters, there are mountains on Mars that have elevations of up to 25 km, making ballooning over such regions difficult.

4.3.2.1 Mars Balloon with Guide Rope

A balloon equipped with a guide rope (landing snake) has been proposed as a zero-pressure balloon capable of floating for long periods (Fig. 4.9) [15].

When the gas temperature falls and the balloon descends close to the surface, a long (a few tens of meters or longer) dangling guide rope (called a snake) makes contact with the surface first, and in doing so it offsets the drop in the buoyancy so that the balloon does not come in contact with the surface of Mars. When the gas temperature increases with the breaking of dawn, the balloon rises again, and the guide rope hangs down from the balloon. Consequently, it is a balloon that floats at

Fig. 4.9 Mars balloon with guide rope



an altitude of several kilometers in the daytime and that floats close to the ground at night (soft landing). This idea was first conceived by Charles Green, a British balloonist who was active in the first half of the 1800s. He performed a long distance flight from London to Germany in November 1836 by using a manned balloon that stabilized its flight altitude with this method.

4.3.2.2 Super-Pressure Mars Balloon

If a super-pressure balloon is used, the maximum pressure differential resulting from the diurnal temperature difference will be extremely large. However, if a super-pressure balloon is used that is based on the 3D gore design concept described in Sect. 2.2.3, a lightweight balloon can be realized that is capable of withstanding high pressure differentials.

For example, if floating at an altitude of 5 km (atmospheric pressure: 4.5 hPa; atmospheric density: 0.01 kg/m^3), the gas temperature at night is assumed to be 180 K, and the difference in gas temperatures between day and night is assumed to be 140 K. If we assume the pressure differential at night to be zero, the pressure differential inside and outside the balloon during the day will be approximately 3.5 hPa. According to 3D gore design concept, a balloon with a volume of $1,000 \text{ m}^3$ is feasible at a weight of about 6 kg. The total floating mass of the balloon is 10 kg, and a 2-kg gondola, excluding gas, can be suspended (Fig. 4.9).

4.3.2.3 Hot-Air Balloon

A hot-air balloon can be used on the daylight side [16]. Combination with a helium balloon has also been considered.

4.3.3 Other Balloons

4.3.3.1 Titan

On Titan, two approaches can be adopted: inflation of a balloon as it descends through the atmosphere (in the same manner as Vega) or inflation of a balloon that is on the surface of Titan, causing it to ascend (in the same manner as a balloon on Earth). It on a lander after descent may be adopted. A film having suitable low-temperature properties (e.g., Teflon) is required. A variable altitude system that uses helium and argon and a balloon with a guide rope have been proposed [8]. In addition, an air rover that is a hybrid of a balloon and a rover has been considered.

4.3.3.2 Jovian Planets

The principal component of Jovian atmospheres is hydrogen, and there is no lifting gas lighter than it. Consequently, systems that generate buoyancy through the heating of a lifting gas in the manner of hot-air balloons by carrying an oxidizing agent from earth and burning hydrogen and systems that ascend by the balloon film absorbing infrared rays from the planetary surface (infrared Montgolfiere balloon) have been considered (see Sect. 2.3.3.2).

For example, in the infrared absorption system of a JPL proposal [8], the balloon commences to expand at an altitude where the pressure is about 100 kPa, and by dropping a dropsonde at a minimum altitude of about 1 MPa, the balloon changes direction and ascends. The dropsonde falls to a maximum of 50 MPa (equivalent to an altitude of approximately 400 km) and transmits various data. After dropping the sonde, the temperature of the balloon's lifting gas gradually rises through the absorption of infrared rays, and the balloon relays data from the sonde as it ascends to an altitude of about 100 kPa.

4.4 Scientific Observations Through Planetary Ballooning

The followings have been set forth as highly significant scientific observations that justify the use of balloons on planets other than earth.

4.4.1 Photographic and Spectroscopic Observation of Planetary Surfaces

If a camera and a spectrometer are loaded on a balloon, higher resolution data can be obtained compared with that obtained by observing from an orbiting satellite, and moreover, unlike a lander, a broad area can be covered. In research of planetary surface topography, the extent to which new discoveries can be made by just improving the resolution of data has been demonstrated in the Martian explorations of recent years. Even in the case of obtaining spectrographic data, if a specific narrow range of terrain is captured with pinpoint accuracy, not only it is easy to infer the mineral composition, but also there is advantage of detecting geographically localized minerals. On planets with cloud cover such as Venus, there is also the advantage of getting under the clouds that obstruct observations made from above the atmosphere.

4.4.2 Meteorological Observation

To understand the mechanisms of planetary weather, it is necessary to detect atmospheric motions on various spatial and temporal scales. Balloons are well suited for performing these kinds of observations. For example, by tracking the trajectory of a balloon over a long period of time, large-scale circulatory patterns and the horizontal structures of atmospheric waves can be mapped out. In practice, the first measurement attempted when balloons enter planetary atmospheres will be to determine the horizontal wind speeds from the change in balloon's horizontal position over time. Even a balloon that is not loaded with any observational equipment can be useful for scientific observations provided its position can be determined thus enabling winds to be observed. In addition, by inferring the changes in vertical winds from data obtained from pressure sensors and temperature sensors loaded on the balloon, it will be possible to detect small-scale buoyancy waves and turbulence. It should be recalled that meteorological observations by balloons floating for long times have yielded significant results in researching the earth's weather in recent years.

4.4.3 Measurement of Atmospheric Components

By directly sampling the atmosphere, information pertaining to chemical reactions in the atmosphere or information pertaining to the origins of the planetary atmosphere such as isotopic ratios can be obtained. If the balloon essentially moves with the atmosphere, changes in the atmospheric composition measured by the balloon can be compared directly with laboratory results as compositional changes that occur in a specific air parcel. In addition, the eddy vertical transport of atmospheric

constituents by convection can be studied when floating at level flight in a region in which convective motion predominates, since sampling of upward and downward flows can be performed over time.

4.4.4 Measurement of Remnant Magnetism

When lava is ejected and solidifies on a planet having internal magnetism, the rock is magnetized in the direction of the magnetic field. Therefore, investigation of remnant magnetism distributed on the planetary surface provides clues about the geo-magnetic history and the crustal evolution of the planet. Since the strength of the magnetic field falls rapidly with distance from the magnetized rock, balloons can detect weak remnant magnetism that cannot be detected by orbiting satellites. In recent years, the Mars Global Surveyor of the US discovered remnant magnetism on Mars, and it has received a lot of attention. Detailed mapping of such regions using balloons would have great significance in elucidating the origins of remnant magnetism and the period in which it was created.

4.4.5 Observation of Lightning and Radar Exploration

Balloons float at altitudes lower than the ionosphere. This fact has advantages for detecting radio waves that are emitted from lightning discharges and for ground penetrating radar exploration. Because the ionosphere shields or modulates low-frequency electromagnetic waves, radio wave measurement and radar exploration from an orbiting satellite has to contend with a limited usable frequency range and difficulties in interpreting the data. These fundamental difficulties can be overcome by using a balloon that floats below the ionosphere. Moreover, in contrast with a lander, it can carry out this type of observation over a wide area.

References

1. Chamberlain, J.W., Hunten, D.M.: Theory of Planetary Atmospheres, an Introduction to Their Physics and Chemistry, Academic Press, Orlando, (1986)
2. Sagdeev, R.Z., et al.: The VEGA Venus Balloon Experiment, *Science*, Vol. 231, 1407–1408 (1986)
3. Kremnev, R.S.: VEGA Balloon System and Instrumentation, *Science*, Vol. 231, 1408–1411 (1986)
4. Lusignea, R.W.: Liquid Crystal Polymers: New Barrier Materials for Packaging, Proc. Future-PAK '96, (1996)
5. Rubin, S.: Liquid Crystalline Polymers Expand the Capabilities of Interplanetary Aerobots, AIAA Int. Balloon Technol. Conf., AIAA-99-3858, 44–60 (1999)

6. Izutsu, N., Yajima, N., Honda, H., Imamura, T.: Venus Balloons Using Water Vapor, *Adv. Space Res.*, Vol. 33, No. 10, 1831–1835 (2004)
7. Jones, J.A.: Reversible Fluid Balloon Altitude Control Concepts, AIAA-95-1621-CP, (1995)
8. Nock, K.T., et al.: Planetary Aerobots: A Program for Robotic Balloon Exploration, AIAA 34th Aerospace Sci. Meeting & Exhibit, AIAA-96-0355, (1996)
9. Cutts, J.A., et al.: Venus Aerobot Multisonde Mission, AIAA Int. Balloon Technol. Conf., AIAA-99-3857, 34–43 (1999)
10. Nishimura, J., et al.: Venus Balloon at low Altitude, AIAA Int. Balloon Technol. Conf., AIAA-91-3654-CP, 12–19 (1991)
11. Izutsu, N., et al.: Venus Balloons at Low Altitudes by Double Capsule System, *Adv. Space Res.*, Vol. 26, No. 9, 1373–1376 (2000)
12. Cutts, J.A., et al.: Venus Surface Sample Return: Role of Balloon Technology., AIAA Int. Balloon Technol. Conf., AIAA-99-3855, (1999)
13. Honeywell International Inc.: High Temperature Electronics Data Sheets, Honeywell International Inc
14. Bachelder, A., et al.: Venus Geoscience Aerobot Study (VEGAS), AIAA Int. Balloon Technol. Conf., AIAA Paper, 99-3856, 21–33 (1999)
15. Balamont, J.: Balloons for the Exploration of Mars, *Adv Space Res.*, Vol. 13, 137–144 (1992)
16. Jones, J., Wu, J.: Solar Montgolfiere Balloons for Mars, AIAA Int. Balloon Technol. Conf., AIAA-99-3852, 1–7 (1999)

Chapter 5

The Future of Scientific Ballooning

Abstract This chapter describes future aspects of scientific ballooning including technological progress and future application trends. The applicability of balloon technology to other fields is also mentioned.

5.1 Future Trends in Balloon Technology

5.1.1 *Payload Weight, Flight Duration, and Flight Altitude*

The payload capability of stratospheric balloons is already of the order of a few tons. Except for experiments in regions where people generally do not live, such as the polar regions, this payload weight is near the limit of mid-latitude balloon experiments in order to ensure flight safety. Also in regard to long-duration flights, the duration of flights in experiments in mid-latitude regions has increased, and has similarly neared its limit. Because of this, long-duration circular flights conducted in the Arctic and Antarctic Circles in summer (described in Sect. 3.4.6) are becoming increasingly important.

In missions to observe space, to exclude atmospheric effects, further increasing the altitude of flights is a subject that is expected to be grappled with in the future. However, even in cases where the payload weight is relatively small so that the weight of the balloon system is approximately equal to that of the balloon itself, to attain an altitude where the atmospheric density is smaller by a factor of $1/n$ requires increasing the balloon volume by a factor of n^3 . Accordingly, it is desirable to develop thin lightweight films in the future, but to reach an altitude of 60 km, the film thickness would have to be about $2 \mu\text{m}$, which is near the physical limit.

5.1.2 Long-Duration Balloon Flight Technology

Because recent research has established a rational design system for super-pressure balloons, which in principle places no limit on flight duration, practical applications of stratospheric ballooning using super-pressure balloons have increased [1,2]. However, the pressure required for maintaining shape at night depends on the diurnal temperature change of the lifting gas, and currently, resistance to a pressure differential of about 20% of the external pressure is necessary. To reduce this pressure differential, it is important to develop a balloon film that is capable of maintaining a small temperature difference between the gas and atmospheric during both the day and the night. A film is desired that has a high thermal conductivity and small external emission and absorption across all wavelength bands.

5.1.3 Control of Flight Path

If the direction of a balloon flight could be changed at will, it would greatly increase the usefulness of balloons. There have been many proposals of balloon systems that carry a propulsion device on board, which are referred to as powered balloons, but so far none have become practical realities.

One attempt in recent years is a system that uses a rope to lower a sail about 10 km down from a balloon flying at an altitude of 30 km or higher, and by positioning the rope in regions of different wind directions, it tries to acquire force to alter the course of the balloon [3]. Regarding other attempts, at ceiling altitudes near 20 km, there have been attempts to change course by changing the flight altitude itself [4]. Fundamentally, both fly by riding the winds in the predominant east-west direction but attempt to change flight course in the north-south direction. If super-pressure balloons are put to practical use and long-duration flights of several months become possible, the usefulness of such course changing capability will increase. Particularly in the Arctic and Antarctic in summer, a balloon that could approach the center of the vortex while flying by riding the circular winds would result in many applications.

5.1.4 Applications to Information Networks

Normally stratospheric balloons are in radio contact with the ground station at all times during the flight. If network capabilities are applied to the experiment, it is easy to extend this link from the base to any distant station [5]. If this is done, many students and researchers will be able to directly participate in balloon experiments, adding a sense of realism, by sitting in front of a computer terminal in a remote laboratory or other such location. This capability is an effective way to cultivate an interest in the next generation in space development and research, for which balloons have many advantages.

To expand such capabilities on a worldwide scale, it is desirable to introduce international standardized systems for balloon experiments, such as data formats for communicating with balloons. If internationalism can be expanded and common use of balloon test facilities can be devised, the usefulness of scientific ballooning will be advanced still further. The need to advance such international cooperation is particularly great in balloon experiments at special locations such as polar and equatorial regions.

5.1.5 *Planetary Balloons*

The field in which new technological trends are most reflected is planetary ballooning. The following three areas are the main focus for new technologies:

5.1.5.1 *Film Material Technology*

An advanced film technology that can be adapted to particular types of atmospheres, such as those having high temperatures and corrosive gases, are required. We can expect high-performance films from the significant achievements in polymer chemistry in recent years.

5.1.5.2 *Electronics Technology*

Semiconductor devices that are capable of operating at high temperatures above 200°C, other electronic devices such as passive elements, and mounting technology for these components are required for Venus balloons, which fly at low altitudes. Such technology forms a field that has recently become known as high-temperature electronics, and many achievements have been published that are not restricted to space applications [6, 7].

5.1.5.3 *Communications Technology*

Because only weak radio waves arrive from a balloon floating in a planetary atmosphere, ultra-long-range communications technology is required that has higher performance than communications between planetary exploration satellites and earth.

In addition to the basic technologies listed above, new ideas for balloon systems should be devised through the development of various individual technologies common to stratospheric balloons such as types of lifting gases, balloon inflation systems, and buoyancy control systems.

5.2 Future Trends in Balloon Applications

5.2.1 Increasing the Scale of Experimental and Observation Systems

In the era of the Space Shuttle and the Space Station, while the capability to carry large systems into space has progressed to the same or greater degree as the capabilities of balloons, the launch costs have become enormous. As a result, there are financial constraints that make it difficult to increase the number of large scientific missions. Consequently, attempts have been made to improve the capabilities of balloons and to actively cultivate observation by means of large systems that can operate even at balloon altitudes.

NASA's Ultra Long Duration Balloon (ULDB) project is an example of this [8]. This project, which has a symbolic target of 100-day-flight duration with a 1.5-ton payload at an altitude of 35 km by using a super-pressure balloon, shows a typical path for large scientific balloons of the future. However, since such balloons are subject to restrictions on flight areas as a result of the safety reasons mentioned in Sect. 5.1, this balloon experiment inevitably has its limitations.

5.2.2 The New Role of Balloons in the Satellite Era

In the fields of observations of the weather, atmospheric physics, and the earth's atmospheric environment, new roles are developing for balloons to complement the fact that satellite observations are able to cover the entire surface of the earth.

5.2.2.1 Changing Role in Aerological Observations

By combining meteorological observation data from satellites and numerical analysis using computers, it has become possible to prepare data on a 3D or 4D grid for the entire earth. However, satellites observe the portion of the earth's atmosphere from the earth's surface up to an altitude of about 60 km from a long distance of several hundred kilometers. On the one hand, because the atmosphere must be broken down into layers, a few kilometers thick, it is difficult to improve the absolute accuracy of these measurements.

On the other hand, because regular meteorological observations using rubber balloons are in-situ observations, they have a high absolute accuracy. Thus, calibrating certain 3D grid data through the use of the corresponding regular meteorological observation data facilitates improvements in accuracy. The results of this correction extend to adjacent grids.

Before the era of weather satellites, when meteorological observations were performed using rubber balloons, surface weather on a global scale is predicted just

using the data from these measurements and surface weather observations. As noted earlier, the use of aerological observation data today can be said to be a new role born out of the satellite era.

5.2.2.2 Construction of a Global-Scale Aerological Observation Network

As described earlier, if numerical analysis data are calibrated by aerological observation data, the accuracy of meteorological information for regions having a high density of observation stations will improve, but the accuracy for regions having few observation stations, such as wilderness areas and oceans will be low. Since meteorological phenomena shift their location and change with time, regions with poor accuracy will limit improvements in forecasting accuracy.

Thus, the SOPLEX project [9] planned by NCAR of the US in which a large number of balloons carrying multiple radiosondes on board are to be successively sent on transoceanic flights and meteorological observations are to be performed by periodically dropping sondes during the flight.

In the GAINS project [4] proposed by NOAA of the US, over 200 super-pressure balloons capable of long-duration flights are to be dispersed on a world-wide scale and a large number of sondes carried on board are to be successively dropped.

5.2.2.3 Balloon Observations for Validating Satellite Observations

As with the above-mentioned meteorological observations, correction and verification by balloon observation are also indispensable for sensors on satellites that observe the earth's atmosphere. An experiment having such an objective has already been carried out with the sensor known as the Improved Limb Atmospheric Spectrometer (ILAS), which measured minute components of the atmosphere such as the vertical profiles of ozone, methane, water vapor, nitrogen dioxide, nitric acid, and nitrous oxide. The sensor was carried on board the Advanced Earth Observing Satellite 1 (ADEOS 1) launched in 1996 by the National Space Development Agency (NASDA) of Japan. Furthermore, between January and March 1997, the National Institute for Environmental Studies conducted a large-scale atmospheric observation balloon project for validating the experiments of ILAS at the ES-RANGE (the space center of the Swedish Space Corporation, SSC) at Kiruna in the northern extremity of Sweden. In this balloon project, which was conducted in cooperation with CNES and SSC, more than 20 large balloons were launched in coordination with satellite overflights [10]. Each balloon observed one of the above-mentioned minor components using their own on-board instruments. The use of such balloon application is a new role for scientific balloons in the satellite era, and future developments are anticipated in this field.

5.3 Effects of Balloon Technology on Other Fields

5.3.1 *Linkage with Airship Technology*

Because the shape of a balloon generally has rotational symmetry about the perpendicular axis, its capability for supporting a load is excellent. However, on the one hand, free movement in the horizontal direction is practically impossible due to the large air resistance. On the other hand, if the capability to move in the horizontal direction is an important requirement, the result is the form of an airship. While an airship is advantageous for propulsion since it has a smaller air drag coefficient in the direction of movement, its ability to support a load is diminished. Hence, the weight of the main body is increased, and the feasibility of an airship reaching the stratosphere for practical applications is very remote.

Since the end of the 1990s, there have been attempts to reach the lower part of the stratosphere at altitudes of approximately 20 km by incorporating the advances in film materials and reexamining design concepts. A more ambitious project is the development of an airship that is capable of remaining in the same location by using a propulsive force (station keeping). This project is being promoted by NAL of Japan. If a balloon can be kept stationary over an urban airspace, it could be used for applications such as functioning as a communications relay station [11]. However, even if the altitude at which the average wind speed is weakest is selected, the propulsive force required to remain stationary is not small. In addition to the weight of the solar cell system required for providing this propulsive force, a storage system is needed to enable electrical power to be maintained during the night. This would result in an extremely large airship with a gross weight of 30–50 tons, and many problems would be encountered in developing such an airship.

For correcting the direction of travel by using a propulsive force while being carried along on the winds, by applying design concepts of stratospheric balloons, particularly the 3D gore design concept described in Sect. 2.2.3, more substantial weight reductions in airframes than those achieved in the past can be anticipated [12]. Such an airship would be considered to be suitable for an aerological observation network deployed on a global scale as described in Sect. 5.2.2.2.

5.3.2 *Applications to Space Structures*

Systems that can be transported as folded-up flexible structures and then expanded in a single stroke are effective for constructing large structures in space. Such systems have become a research topic in the field of space technology research. There is research into areas such as the formation of large-aperture parabolic antennas and the setting up of structures on lunar or planetary surfaces [12, 13]. The technology of stratospheric balloons, particularly super-pressure balloons, is highly suitable for such flexible space structures.

5.3.3 Applications to Ground Structures

It is possible to use the capability of a pressurized film to maintain structures in film structures for applications on the ground. Not necessarily in the form of a balloon, films can be used effectively even when they are partially incorporated into building structures such as when they are used in the ceilings of baseball stadiums and the like [14].

Table Talk 6: Where Research is Presented

No matter how influential it likes to think it is, the scientific ballooning community is small. If all the researchers in the world were assembled in one place, everyone could fit into a medium-sized conference room. The following introduces conferences and symposia at which research on balloon engineering is presented.

(1) Where Research is Presented Internationally

AIAA International Balloon Technology Conference

While sponsored by the American Institute of Aeronautics and Astronautics (AIAA), this conference takes pride in being an international conference, as indicated by its name. One major characteristic is that the conference title is specialized to balloon engineering. The authors of this book (Yajima et al.) presented research concerning the basic concepts of super-pressure balloons at the 1999 conference, and they were awarded the prize for the best research paper.

A fully-fledged academic journal that is the target of submissions is the Journal of Aircraft. If a paper on balloons passes the strict review by a number of referees, it will appear in the journal isolated from papers on fields such as fluid mechanics and structural dynamics pertaining to aircraft. Let us consider the rarity of papers on balloons not as an indication that they are out of place in the journal, but rather as a blessing in that they are more likely to be conspicuous.

COSPAR Scientific Assembly

COSPAR is the Committee on Space Research, and it is one of the historical comprehensive, huge scientific societies for international space relations. There is a Scientific Ballooning session within it. This session is not limited to balloon engineering, and it also attracts presenters of scientific observations that use balloons.

ESA Symposium on European Rocket and Balloon Program and Related Research

This is a society for sounding rockets and balloons sponsored by the European Space Agency (ESA), but it does not exclude participation from other regions, and it is essentially an international symposium.

(2) *Where Research is Presented in Japan*

Large Balloon Symposium

Sponsored by the ISAS, this is a symposium of interested parties. In addition to proceedings of presentations, a Large Balloon Special Edition of the ISAS Report is published as a collection of papers.

International Symposium on Space Technology and Science (ISTS)

This is an international conference focusing on space engineering that was established by senior researchers from the initial stages of Japan's space exploration to promote the internationalization of their efforts. It has now developed to a large scale, and includes a session called Space Science and Balloon.

Japan Society for Aeronautical and Space Sciences

There are various opportunities for presenting research, including the Space Sciences and Technology Conference cosponsored by other scientific societies. Submissions may be made in Japanese and English to various collections of papers. Incidentally, while this may be somewhat self-congratulatory, a research paper pertaining to the development and flight-testing of super-pressure balloons by the authors of this book (Izutsu et al.) was awarded the 2001 research paper prize.

References

1. Smith, Jr., I. S., Cutts, J. A.: Floating in Space, *Sci. Am.*, Nov. 74–79 (1999)
2. Yajima, N. Survey of Balloon Design Problems and Prospects for Large Super-Pressure Balloons in the Next Century, *Adv. Space Res.*, Vol. 30, No. 5, 1183–1192 (2002)
3. Aaron, K. M., Heun, M. K. T., Nock, K.: A Method for Balloon Trajectory Control, *Adv. Space. Res.*, Vol. 30, No. 5, 1227–1232 (2002)
4. Girz, C.M.I.R., et al.: GAINS - A Global Observing System, *Adv. Space Res.*, Vol. 30, No. 5, 1343–1348 (2002)

5. Cornier, C., Audoubert, J.: The Future Command-Control Architecture for Balloons over a TCP/IP Interconnection, Proceedings of the 15th ESA Symposium on European Rocket and Balloon Programs and Related Res., ESA SP-471, 535–540 (2001)
6. McCluskey, F. P., Grzybowski, R., Podlesak, T., (ed.): High Temperature Electronics, CRC Press, Boca Raton, (1997)
7. Tajima, M.: Perspective on High Temperature Electronics in Japan, Proceedings of the Third European Conference on High Temperature Electronics, IEEE Cat. No. 99EX372, 173–180 (1999)
8. Jones, V. W.: Current Status of the Long Duration Balloon Program, *Adv. Space Res.*, No.114, 191–200 (1994)
9. Cole, H. L., et al.: Development of an Advanced Balloon Platform and Dropsonde for Use in The Hemispheric Observing System Research and Predicability Experiment (THORPREX), NCAR, (2001)
10. Kanzawa, H., et al.: A plan for ILAS-II Correlative Measurements with Emphasis on a Validation Balloon Campaign at Kiruna-ESRANGE, Proceedings of the 15th ESA Symposium on European Rocket and Balloon Programs and Related Res., ESA SP-471, 305–308 (2001)
11. Maekawa, S., Nakadate, M., Takegaki, A.: On the Structures of the Low Altitude Stationary Flight Test Vehicle, *J. of Aircraft*, Vol. 44, No. 2, 882–666 (2007)
12. Jenkins, C.H.M. (ed): Gossamer Spacecraft, AIAA, Inc., Virginia, (2001)
13. Jenkins, C.H.M. (ed): Recent Advances in Gossamer Spacecraft, AIAA, Inc., Virginia, (2006)
14. Yajima, N., Izutsu, N., Honda, H.: Structure Variations of Pumpkin Balloon, *Adv. Space. Res.*, Vol. 33, No. 5, 1694–1699 (2002)

Appendices

Appendix 1 Standard atmosphere table (per JIS W 0201–1990)

Altitude (km)	Pressure (Pa)	Temperature (K)	Density (kgm^{-3})
0	101,325	288.150	1.22500
1	99,876.3	281.651	1.11166
2	79,501.4	275.154	1.00655
3	70,121.2	268.659	0.909254
4	61,660.4	262.166	0.819347
5	54,048.3	255.676	0.736429
6	47,217.6	249.187	0.660111
7	41,105.3	242.700	0.590018
8	35,651.6	236.215	0.525786
9	30,800.7	229.733	0.467063
10	26,499.9	223.252	0.413510
11	22,699.9	216.774	0.364801
12	19,399.4	216.650	0.311937
13	16,579.6	216.650	0.266595
14	14,170.3	216.650	0.227855
15	12,111.8	216.650	0.194755
16	10,352.8	216.650	0.166470
17	8,849.70	216.650	0.142301
18	7,565.21	216.650	0.121647
19	6,467.47	216.650	0.103995
20	5,529.29	216.650	0.0889097
21	4,728.92	217.581	0.0757146
22	4,047.48	218.574	0.0645096
23	3,466.85	219.567	0.0550055
24	2,971.74	220.560	0.0469377
25	2,549.21	221.552	0.0400837
26	2,188.37	222.544	0.0342565
27	1,879.97	223.536	0.0292982
28	1,616.19	224.527	0.0250762
29	1,390.42	225.518	0.0214783
30	1,197.03	226.509	0.0184101

Appendix 1 (Continued)

Altitude (km)	Pressure (Pa)	Temperature (K)	Density (kgm^{-3})
31	1,031.26	227.500	0.0157915
32	889.060	228.490	0.0135551
33	767.306	230.973	0.0115730
34	663.410	233.744	0.00988736
35	574.592	236.513	0.00846334
36	498.520	239.282	0.00725789
37	433.246	242.050	0.00623544
38	377.137	244.818	0.00536653
39	328.820	247.584	0.00462672
40	287.143	250.350	0.00399566
41	251.132	253.114	0.00345639
42	219.966	255.878	0.00299475
43	192.950	258.641	0.00259888
44	169.496	261.403	0.00225884
45	149.101	264.164	0.00196627
46	131.340	266.925	0.00171414
47	115.851	269.684	0.00149651
48	102.295	270.650	0.00131669
49	90.3363	270.650	0.00116277
50	79.7787	270.650	0.00102587
51	70.4576	270.650	0.000906897
52	62.2144	269.031	0.000805613
53	54.8734	266.277	0.000717904
54	48.3374	263.524	0.000639001
55	42.5249	260.771	0.000568096
56	37.3621	258.019	0.000504448
57	32.7818	255.268	0.000447377
58	28.7236	252.518	0.000396263
59	25.1323	249.769	0.000350535
60	21.9586	247.021	0.000309676

Appendix 2 Classification of unmanned free balloons (per Rules of the Air, Annex 2, the Convention on International Civil Aviation, Appendix 4. Unmanned Free Balloons, ICAO, Ninth Edition, 1990)

Characteristics	Payload mass (kg)					
	1	2	3	4	5	6 or more
Rope or other suspension						
230 Newtons or more						
Individual payload package						
Area density calculation	Area density more than 13g/cm ²					
Mass(g) Area of smallest surface (cm ²)	Area density less than 13g/cm ²					
Combined mass (if suspension or area density or mass of individual package are not factors)						

Appendix 3 Principal balloon specifications

Balloon volume ^a (m ³)	Film thickness ^b (μ m)	Balloon mass ^c (kg)	Representative value for payload mass ^c (kg)	Balloon diameter ^c (m)	Balloon length ^c (m)	Number of gores ^c	Attainable altitude ^d (km)
1,000	3.4	3	3	13.4	19.4	28	36.8
5,000	3.4	7	3	22.9	33.1	28	44.4
5,000	6	11	3	22.7	33.3	28	42.0
5,000	20	40	100	22.6	33.5	28	27.0
15,000	20	75	100	33.4	42.3	41	32.5
30,000	3.4	23	3	43.5	58.8	52	50.3
30,000	6	37	3	42.7	59.1	52	47.1
30,000	20	120	200	41.4	60.3	50	33.1
50,000	20	170	500	48.7	72.3	59	35.4
60,000	3.4	34	3	53.7	74.5	116	53.0
80,000	10	130	100	58.5	82.6	72	42.0
80,000	20	220	500	56.8	84.9	72	34.2
100,000	20	270	500	63.4	88.3	78	35.2
200,000	20	420	500	77.4	112.1	96	38.7
500,000	20	850	500	107.8	152.2	133	42.4
1,000,000	20	1700	1000	136.5	191.5	170	42.4

^aIndicates the expansion volume when loaded with the payload mass on the chart.

^bAssumed to be a balloon fitted with a double or triple film layer cap to increase strength at the top when both the balloon volume and payload mass are large (Sect. 3.5.4.). The increase in mass due to the cap is about 12–25% of the value noted.

^cEven for balloons of the same volume, the shape will differ depending on payload mass as shown in Fig. 2.9, and the design value will also change.

^dIndicates the float altitude when loaded with the payload mass indicated on the chart. The attainable altitude when the payload mass is changed is shown in Fig. 2.2.

Abbreviations

ADEOS	Advanced earth observing satellite
ATCRBC	Air Traffic Rader Beacon System
BADC	British Atmospheric Data Center
CMG	Control Moment Gyro
CNES	Center National d'Etudes Spatial (French Space Agency)
CSBF	Colombia Scientific Balloon Facility (USA)
DBC	Discrete beacon code
ECMWF	European Center for Medium-Range Weather Forecasts
ESRANGE	European sounding rocket range
EVOH	Ethylene vinyl alcohol
GPS	Global positioning system
GTS	Global telecommunication system
ICAO	International Civil Aviation Organization
IIS	Institute of Industrial Sciences (Japan)
IGY	International Geophysical Year
ILAS	Improved Lim atmospheric spectrometer
INPE	Instituto Nacional de Pesquisas (National Institute for Space Research (Brazil))
JPL	Jet Propulsion Laboratory (USA)
JSPS	Japan Society for the Promotion of Science
NASA	National Aeronautics and Space Administration (USA)
NCAR	National Center for Atmospheric Research (USA)
NCEP	National Center for Environmental Prediction (USA)
NIPR	National Institute of Polar Research (Japan)
NOAA	National Oceanic and Atmospheric Administration (USA)
NSBF	National Scientific Balloon Facility (USA)
NSF	National Scientific Foundation(USA)
SSC	Swedish Space Corporation
SSR	Secondary surveillance rader
TDRS	Tracking and data relay satellite
TIFR	TATA Institute of Fundamental Research (India)

UARS	Upper atmosphere research satellite
UKMO	United Kingdom Meteorological Office (The Met Office)
ULDB	Ultra-Long Duration Balloon
VLBI	Very long baseline interferometry
WFF	Wallop flight facility (USA)
WMO	World Meteorological Organization

Index

- 3D gore design concept, 24
Added mass, 57
Adiabatic expansion, 46, 58
Aerological data, 113
Aerological observation, 165
Airship, 200
Angular momentum, 102
ARGOS transmitter, 127
Ascent speed, 121
Assimilated data, 114
ATC transponder, 101
Atmospheric wave, 83
Attainable altitude, 17
Auxiliary balloon, 118

Ballast, 11
Ballast hopper, 92
Balloon destruct device, 92
Baroclinic wave, 88
Belt sealer, 142
Biaxial elongation, 41
Biaxial tension, 19
Boomerang Balloon, 133
Brittleness temperature, 137
Bulge, 35
Buoyant force, 10
Burst detector, 95

Ceiling altitude, 147
Circumpolar, 133
Cloud-top, 124
Command receiver, 99
Compound latex, 152
Control moment gyro, 102
Convective heat transfer, 68
Coriolis force, 83

Cosmic ray, 5
Cross parachute, 96
Crush pad, 97
Cycling Balloon, 133
Cylinder end, 33
Cylindrical balloon, 20

Density altitude, 64
Doppler lidar, 113
Doppler radar, 113
Doppler shift, 127
Doppler sodar, 113
Double cap, 146
Double-capsule, 185
Dropsonde, 113
Dynamic launching, 116

Effective absorptivity, 67
Effective emissivity, 67
Elastic deformation, 137
Elegant solution, 44
Envelope, 10
Equatorial region, 83
Ethylene vinyl alcohol, 134
Euler's elastica, 32
Exhaust valve, 3

Fiber reinforcement, 22
Flight control, 122
Flight safety, 128
Flow contraction coefficient, 58
Fluid dynamics, 15
Flyby, 178
Free lift, 10

GAINS project, 199
Galileo spacecraft, 177

- Geostrophic wind, 83, 85
- Geosynchronous orbit, 107
- Gimbal, 102
- Greenhouse effect, 78
- Heat balance, 66
- High-strength polyester film, 138
- Housekeeping, 112
- Hydrostatic equilibrium, 81
- Hypothetical, 61
- In-situ observation, 198
- Infrared absorptivity, 68
- Infrared emissivity, 67
- Infrared radiation, 124
- Infrared reflectivity, 68
- Infrared transmissivity, 68
- Injection, 119
- Inmarsat, 107
- Internal magnetism, 192
- Ionosphere, 192
- Iridium mobile satellite, 109
- Isobaric line, 83
- Isothermal density, 70
- Jet stream, 133
- Jovian planet, 176
- Jupiter, 176
- Lander, 180
- Launch, 104
- Level-flight, 147
- Lifting gas, 120
- Lighter than air, 10
- Line-of-sight distance, 105
- Load tape, 10
- Local curvature, 36
- Local radius, 35
- Long-duration balloon, 131
- Low-density polyethylene, 5
- Man-High project, 161
- Mars, 175
- Mars Global Surveyor, 192
- Maximum payload, 141
- Membrane, 3
- Mercury project, 162
- Meridional circulation, 83
- Mesosphere, 79
- Metallic balloon, 185
- Meteorological satellite, 113
- Minimum payload, 141
- MIR balloon, 53
- Momentum exchange device, 102
- Multilayer insulation, 103
- Natural convection, 68
- Natural rubber latex, 151
- Natural-shape balloon, 5
- Neptune, 176
- Numerical model, 113
- Numerical prediction, 163
- Nusselt number, 68
- Ozone, 153
- Ozonesonde, 163
- Parachute descent, 95
- Parachute drag, 96
- Pendulum motion, 101
- Photodissociation, 79
- Photoelectric absorption, 156
- Pibal observation, 153
- Pilot balloon, 151
- Planetary aerobot, 178
- Planetary balloon, 9
- Planetary wave, 88
- Plastic deformation, 137
- Pointing control, 101
- Polar front, 84
- Polyethylene film, 18
- polymer, 11
- Polyvinyl alcohol film, 138
- Positioning, 126
- Prandtl number, 69
- Pressure altitude, 63
- Primary cosmic ray, 159
- Principle of buoyancy, 15
- Pumpkin balloon, 31
- Radar-reflect, 93
- Radiative heat transfer, 67
- Radiosonde, 112
- Rawinsonde, 153
- Reaction wheel, 157
- Relay station, 107
- Remnant magnetism, 192
- Reynolds number, 56
- Rockoon, 6
- Roller vehicle, 116
- Rotational molding, 152
- Rubber balloon, 11
- Rupture strength, 146
- Saturn, 176
- Scale height, 81
- Secondary cosmic ray, 159
- Separation mechanism, 11
- Shape design, 19
- Shroud, 20
- Similarity parameter, 29

- Sky Anchor, 52
Slant range, 126
Slotted parachute, 96
Solar absorptivity, 68
Solar transmissivity, 68
Solstice, 82
SOPLEX project, 199
Specific strength, 38
Spherical balloon, 20
Stable Table, 144
Statically determinate, 29
Station keeping, 200
Strato-Lab project, 161
Stratopause, 79
Stratosphere, 78
Stratospheric balloon, 9
Structural mechanics, 29
subtropical jet, 84
Sulfuric-acid, 185
Sunset effect, 46
Super-pressure balloon, 11
Super-rotation, 175
Suspension system, 93

Taper-tangent, 33
Tear strength, 137
Temperature distribution, 82
Tetrahedral balloon, 21

Theodolite, 151
Thermal insulator, 103
Thermodynamics, 15
Titan, 176
Tropopause, 5
Troposphere, 78
Turn-around, 132
Two-axis tracking, 102

Ultra Long Duration Balloon, 198
Ultraviolet radiation, 79
Uniaxial tension, 35
Uranus, 176

Variational method, 43
Venting duct, 10
Venus, 173
Vernal and autumnal equinox, 82
Vertical air column, 79
Vulcanization, 11
Vulcanizing, 152

Weightlessness experiment, 162
Wind profiler, 110

Zero-pressure balloon, 5
Zonal wind, 84